

Smoothed Kalman Observer for Sensorless Field Oriented Control of Induction Motor

*A thesis
submitted in fulfillment of the requirements
for the award of the degree of*

Doctor of Philosophy

submitted by

Uma Syamkumar
(Reg. no. 5233/research-b-so/2014/CU)

Under the Supervision of

Prof. Jayanand B.

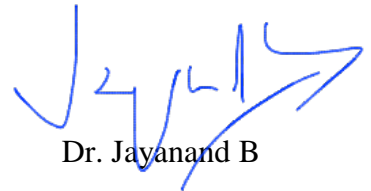


Department of Electrical Engineering
Government Engineering College, Trichur
Thrissur, Kerala, India-680009
(March, 2020)

Certificate

This is to certify that the thesis entitled “**Smoothed Kalman Observer for Sensorless Field Oriented Control of Induction motor**” is the record of bonafide research work done by Ms Uma Syamkumar under my supervision and guidance at Department of Electrical Engineering, Govt. Engineering College, Thrissur in partial fulfilment of the requirement for the Degree of Doctor of Philosophy under Faculty of Engineering, University of Calicut. The thesis incorporated all the necessary corrections/suggestions pointed by the adjudicators.

10th November 2020



Dr. Jayanand B

Professor and Head

Dept. of Electrical Engineering



Department of Electrical & Electronics Engineering
Government Engineering College, Trichur
Kerala, India-680009

Candidate's Declaration

I hereby declare that the work presented in the thesis entitled "**Smoothed Kalman Observer for Sensorless Field Oriented Control of Induction Motor**" in partial fulfillment of the requirements for the award of the Degree of **Doctor of Philosophy** and submitted in the Department of Electrical and Electronics Engineering of the Government Engineering College, Trichur is an authentic record of my own work carried out during a period from July, 2013 to December, 2019 under the supervision of **Prof.(Dr.) Jayanand B.**, Department of Electrical and Electronics Engineering, Government Engineering College, Trichur.

The matter presented in this thesis has not been submitted by me for the award of any other degree of this or any other Institute/University.

(Uma Syamkumar)
(Reg. no. 5233/research-b-so/2014/CU)

This is to certify that the above statement made by the candidate is true to the best of my knowledge and belief.

Place: Thrissur
Date:

(Dr. Jayanand B.)
Professor, EEE Department
GEC, Trichur

Dedicated to my family

ACKNOWLEDGMENTS

It is a great pleasure for me to express my respect and deep sense of gratitude to my Ph.D. supervisor [Dr. Jayanand B.](#), Professor, Department of Electrical Engineering, Government Engineering College, Trichur, for his wisdom, vision, expertise, guidance, enthusiastic involvement and persistent encouragement during the planning and development of this research work. I also gratefully acknowledge his painstaking efforts in thoroughly going through and improving the manuscripts without which this work could not have been completed.

I am highly obliged to [Dr. P. Reji](#), Head of the Department, Government Engineering College, Trichur, [Dr. M. Nandakumar](#), Head of the Department(Retd.), EEE and [Dr. A. Amar Dutt](#), Head of the Department(Retd.), EEE, for providing all the facilities, help and encouragement for carrying out the research work.

I sincerely acknowledge [Dr. Sheeba V. S.](#), Principal, GEC, Thrissur, [Dr. K. Vijayakumar](#) and [Dr. K. P. Indiradevi](#), former Principals of GEC, Thrissur, for their advice and suggestions.

Sincere acknowledgement goes to [Dr. Sasidharan Sreedharan](#), external expert from MES College of Engg., Kuttippuram and other internal doctoral committee members for the valuable time spared in the discussion of the present work and making innovative ideas for the future scope of my research work.

My thanks and appreciations go to my colleagues, [Dr. Suresh K. Damodaran](#) and [Dr. K. D. Joseph](#) for willingly helping me out with their abilities. I wish to express my appreciation to my colleagues [Miji Cherian](#), [Helen K. J.](#), [T. G. Sanish Kumar](#), [Dr. P. A. Abdul Samad](#), and [Dr. Ramesh Kumar P.](#) for their help and motivation throughout my research work. I also would like to express my deep and sincere thanks to my fellow research scholars, [Smrithi](#), [Harish](#), [Vishnu](#) and [Indu](#) for their constructive suggestions throughout my work.

I would also like to extend my special thanks to [Mr. Indukumar](#), [Mr. Nazar](#), [Mr. Roy](#) and other technical staff members of EEE Department, who had spent much time after regular working hours, during the experimentation work.

I am also thankful to the anonymous reviewers of my research publications. Their comments and suggestions were very helpful in shaping my research work.

I would also like to say a heartfelt thank you to my parents, [Mr. G. Syamkumar](#) and (late)[Mrs. N. T. Santhakumari](#) for their moral support, love, encouragement and blessings to complete this task. I am especially thankful to my husband, [Mr. Sathyadevan V. V.](#) who has been by my side throughout this journey, living every

single minute of it, and without whom, I would not have had the courage to embark on this journey in the first place. I am also indebted to my children, [Diya](#) and [Deepak](#) for standing by me throughout these years and helping me in whatever way they could, during this challenging period.

I gratefully acknowledge all other persons whose names do not appear here, for helping me either directly or indirectly in all even and odd times.

Finally, I am indebted and grateful to the Almighty for helping me in this endeavor.

(Uma Syamkumar)

ABSTRACT

Even though there are a number of electric motors available in the market, induction motors maintain their superiority over others due to their unique properties like low cost, ruggedness and reliability. But, the dynamic performance of induction machines is complex due to the coupling effect between stator and rotor fluxes. The performance can be improved by decoupling the torque and flux components of the stator current, which is the basic principle of field-oriented control(FOC) or vector control. Vector control needs the instantaneous rotor position for generating the control signal. This necessitates the mounting of speed sensors on the rotor. Mounting of speed sensors makes the entire system unreliable and deteriorates its dynamic behaviour. Also mounting of a rotational transducer is difficult in hostile environments and in high speed applications. In order to improve the ruggedness of the system, speed sensors are replaced with speed estimators or observers. Such systems are named sensorless drives.

The performance of a sensorless drive depends on the accuracy of the observer. The extended Kalman Filter(EKF) is an efficient algorithm for the state and parameter estimation of non-linear systems in the presence of noise and uncertainty. Kalman Filters are known to have a high convergence rate which can improve the transient performance of stochastic systems. Model uncertainties and non-linearities inherent in the induction motors are taken into account in Kalman filters. Due to these properties, they are widely used for the speed sensorless control of induction motors. The accuracy of an EKF based observer depends on the values of the process and measurement error covariance matrices. The choice of these matrices is crucial in the observer design using an EKF.

Smoothing is a process which helps to refine the estimated values of EKF using some of the measurements of future instants also. Since additional data is made use of, the estimates are bound to be better. A single-stage smoothing filter is used as an observer to estimate the rotor speed along with stator and rotor currents, using a fifth order model of the induction motor. Simulation studies are conducted with different reference speeds. The observer is implemented in real-time and results obtained, which are found to be better than those with a conventional extended Kalman filter(EKF).

The system with observer using a fifth order model is computationally intensive. Hence the observer is validated for a reduced order model of the system also.

Neural networks having the ability to mimic human brain can learn and process

information and can hence be used advantageously for speed estimation. A smoothing Kalman filter-trained real-time recurrent neural network is used as an observer to estimate the rotor speed and fluxes. The implementation results show the improvement in results compared to those with a conventional EKF-trained neural observer.

Contents

Certificate	iii
Dedication	vi
Acknowledgments	viii
Abstract	x
List of Figures	xix
List of Tables	xxi
List of Acronyms/Abbreviations	xxiv
List of Symbols	1
1 Introduction	1
1.1 Background	1
1.2 Motivation for the present research work	3
1.3 Objectives	4
1.4 Organization of the thesis	4
2 Literature review	7
2.1 Introduction	7
2.1.1 Literature Review on Sensorless Speed Control of Induction Motors using Extended Kalman Filter	9
2.1.2 Literature Review on Sensorless Speed Control of Induction Motors based on model reference adaptive systems	10
2.1.3 Literature Review on Sensorless Speed Control of Induction Motors using artificial neural networks	12
2.1.4 Summary	14
3 Smoothing Algorithms	15
3.1 Introduction	15
3.2 Estimation of data	16

3.2.1	Prediction	17
3.2.2	Filtering	19
3.3	Smoothing	20
3.3.1	Classification of Smoothing Algorithms	21
3.4	Single- Stage Smoothing	22
3.5	Summary	24
4	Full Order Smoothed Observer for Speed Estimation of Three Phase Induction Motor	25
4.1	Introduction	25
4.2	Mathematical Model of Induction Motor	26
4.3	Indirect field-oriented sensorless control of three-phase induction motor	29
4.4	Offline Estimation Results	31
4.4.1	Estimation using conventional extended Kalman observer . . .	32
4.4.2	Estimation using smoothed Kalman observer	38
4.5	Summary	46
5	Real-time implementation of the smoothed Kalman algorithm based full-order observer	47
5.1	Introduction	47
5.2	Experimental Setup	47
5.3	Experimental results of field-oriented control based on a fifth order smoothed Kalman observer	50
5.4	Experimental results of field-oriented control based on a fifth order conventional Kalman observer	57
5.5	Summary	64
6	Smoothed Observer for a reduced model of the induction motor	65
6.1	Introduction	65
6.2	Dynamic Model of the Induction Motor	66
6.3	Indirect field-oriented control of induction motor with a smoothed Kalman observer	66
6.4	Results of Offline Estimation	68
6.4.1	Speed and flux estimation using conventional Extended Kalman observer	68
6.4.2	Smoothed Kalman observer for a reduced model of three phase induction motor	73
6.5	Summary	78

7	Real-time implementation of the smoothed Kalman observer based on a reduced order model of induction motor	79
7.1	Introduction	79
7.2	Experimental Setup	79
7.3	Experimental results of field-oriented control based on a reduced order smoothed Kalman observer	80
7.4	Experimental results of field-oriented control based on a reduced order conventional Kalman observer	87
7.5	Summary	93
8	A Smoothed Kalman Filter-trained Recurrent Neural Network for Speed Estimation of Induction Motor	95
8.1	Introduction	95
8.2	A General Real-time Recurrent Neural Network	96
8.3	Parameter Based Smoothed Kalman Filter Algorithm for Training Recurrent Neural Network	98
8.4	Speed Estimation Using Real-Time Recurrent Neural Network	100
8.5	Offline estimation	103
8.5.1	Conventional EKF trained recurrent neural network observer	103
8.5.2	Smoothed Kalman filter trained recurrent neural network observer	108
8.6	Summary	113
9	Real-time implementation of the smoothed Kalman trained neural observer for IFOC of three phase induction motor	115
9.1	Introduction	115
9.2	Experimental Setup	115
9.3	Experimental results of field-oriented control based on smoothed Kalman filter trained recurrent neural network	116
9.4	Experimental results of field-oriented control based on conventional Kalman filter trained neural network	122
9.5	Summary	127
10	Conclusions and future directions	129
10.1	Conclusions	129
10.2	Scope for future study	130
	List of Publications	131
	Bibliography	133

List of Figures

1.1	Block diagram of direct vector control	2
1.2	Block diagram of indirect vector control	2
3.1	Flow Diagram of the smoothing algorithm	16
3.2	Block diagram of the dynamic system, S	16
3.3	Block diagram of Kalman filter	20
3.4	Block Diagram of Single- Stage Smoothing	24
4.1	Block diagram of the proposed drive system	30
4.2	The stator stationary axis components of measured stator voltages, v_{ds} and v_{qs}	31
4.3	The stator stationary axis components of measured stator currents i_{ds} and i_{qs}	31
4.4	Estimated and measured ω_r for a reference speed of 75 rad/s(mech.) at t=0s and with a conventional EKF observer	32
4.5	Estimated and measured i_{ds} for a reference speed of 75 rad/s(mech.) at t=0s and with a conventional EKF observer	33
4.6	Estimated and measured i_{qs} for a reference speed of 75 rad/s(mech.) at t=0s and with a conventional EKF observer	33
4.7	Estimated i_{dr} and i_{qr} for a reference speed of 75 rad/s(mech.) at t=0s and with a conventional EKF observer	33
4.8	Error between the measured and estimated values of a) ω_r b) I_{ds} and c) I_{qs} using conventional Kalman observer	34
4.9	Estimated and measured ω_r for reference speed of 20 rad/s(mech.) from 0s to 2s and 75 rad/s from t=2s to 4.5s and 50rad/s from t=4.5s to 7s with conventional EKF observer	35
4.10	Estimated and measured i_{ds} for reference speed of 20 rad/s(mech.) from 0s to 2s and 75 rad/s from t=2s to 4.5s and 50rad/s from t=4.5s to 7s with conventional EKF observer	35
4.11	Estimated and measured i_{qs} for reference speed of 20 rad/s(mech.) from 0s to 2s and 75 rad/s from t=2s to 4.5s and 50rad/s from t=4.5s to 7s with conventional EKF observer	36

4.12	Estimated i_{dr} and i_{qr} for reference speed of 20 rad/s(mech.) from 0s to 2s and 75 rad/s from t=2s to 4.5s and 50rad/s from t=4.5s to 7s with conventional EKF observer	36
4.13	Error between the measured and estimated values of a) ω_r b) I_{ds} and c) I_{qs} using conventional Kalman observer	37
4.14	Simulation results for a reference speed of 75 rad/s(mech.) at t=0s and with smoothed Kalman observer	38
4.15	Estimated and measured i_{ds} for a reference speed of 75 rad/s(mech.) at t=0s and with a smoothed Kalman observer	38
4.16	Estimated and measured i_{qs} for a reference speed of 75 rad/s(mech.) at t=0s and with a smoothed Kalman observer	39
4.17	Estimated i_{dr} and i_{qr} for a reference speed of 75 rad/s(mech.) at t=0s and with a smoothed Kalman observer	39
4.18	Error between the measured and estimated values of a) ω_r b) I_{ds} and c) I_{qs} using smoothed Kalman observer	40
4.19	Simulation Results for reference speed of 20 rad/s(mech.) from 0s to 2s and 75 rad/s from t=2s to 4.5s and 50rad/s from t=4.5s to 7s with smoothed Kalman observer	41
4.20	Estimated and measured i_{ds} for reference speed of 20 rad/s(mech.) from 0s to 2s and 75 rad/s from t=2s to 4.5s and 50rad/s from t=4.5s to 7s with smoothed Kalman observer	41
4.21	Estimated and measured i_{qs} for reference speed of 20 rad/s(mech.) from 0s to 2s and 75 rad/s from t=2s to 4.5s and 50rad/s from t=4.5s to 7s with smoothed Kalman observer	42
4.22	Estimated i_{dr} and i_{qr} for reference speed of 20 rad/s(mech.) from 0s to 2s and 75 rad/s from t=2s to 4.5s and 50rad/s from t=4.5s to 7s with smoothed Kalman observer	42
4.23	Error between the measured and estimated values of a) ω_r b) I_{ds} and c) I_{qs} using smoothed Kalman observer	43
4.24	Plot of the d and q axis components of rotor flux using smoothed Kalman observer	44
4.25	Simulation results for reference speed of 75 rad/s(mech.) with a torque applied at t= 3s a) conventional and b) smoothed Kalman Observer .	45
5.1	Block diagram of the experimental set up	48
5.2	Experimental set up	50

5.3	Experimental results for a reference speed of 75rad/s(mech.) a) Rotor speed, ω_r b) \hat{I}_{ds} & \hat{I}_{qs} c) \hat{I}_{dr} & \hat{I}_{qr}	51
5.4	Experimental results for a reference speed of 30rad/s(mech.)a) ω_r b) \hat{I}_{ds} & \hat{I}_{qs} c) \hat{I}_{dr} & \hat{I}_{qr}	52
5.5	Experimental results for a reference speed of 10rad/s(mech.)a) ω_r b) \hat{I}_{ds} & \hat{I}_{qs} c) \hat{I}_{dr} & \hat{I}_{qr}	53
5.6	Experimental results for a reference speed of 5 rad/s(mech.)a) ω_r b) \hat{I}_{ds} & \hat{I}_{qs} c) \hat{I}_{dr} & \hat{I}_{qr}	54
5.7	Experimental results for a reference speed which changes from 75rad/s(mech) to 30rad/s(mech) at 3s and then to 75rad/s(mech) at 6s a) ω_r b) \hat{I}_{ds} & \hat{I}_{qs} c) \hat{I}_{dr} & \hat{I}_{qr}	55
5.8	Experimental results for a reference speed which changes from 75rad/s(mech) to 0rad/s(mech) at 5s and continues at zero speed for 5s) a) ω_r b) \hat{I}_{ds} & \hat{I}_{qs} c) \hat{I}_{dr} & \hat{I}_{qr}	56
5.9	Experimental results for a reference speed of 75rad/s(mech.) a) Rotor speed, ω_r b) \hat{I}_{ds} & \hat{I}_{qs} c) \hat{I}_{dr} & \hat{I}_{qr}	58
5.10	Experimental results for a reference speed of 30rad/s(mech.)a) ω_r b) \hat{I}_{ds} & \hat{I}_{qs} c) \hat{I}_{dr} & \hat{I}_{qr}	59
5.11	Experimental results for a reference speed of 10rad/s(mech.) a) ω_r b) \hat{I}_{ds} & \hat{I}_{qs} c) \hat{I}_{dr} & \hat{I}_{qr}	60
5.12	Experimental results for a reference speed of 5 rad/s(mech.) a) ω_r b) \hat{I}_{ds} & \hat{I}_{qs} c) \hat{I}_{dr} & \hat{I}_{qr}	61
5.13	Experimental results for a reference speed which changes from 75rad/s(mech) to 30rad/s(mech) at 3s and then to 75rad/s(mech) at 6s) a) ω_r b) \hat{I}_{ds} & \hat{I}_{qs} c) \hat{I}_{dr} & \hat{I}_{qr}	62
5.14	Experimental results for a reference speed which changes from 75rad/s(mech) to 0rad/s(mech) at 5s and continues at zero speed for 5s) a) ω_r b) \hat{I}_{ds} & \hat{I}_{qs} c) \hat{I}_{dr} & \hat{I}_{qr}	63
6.1	Structure of the estimator using smoothed Kalman observer	67
6.2	Simulation results for a reference speed of 75 rad/s(mech.) at t=0s and with a conventional Kalman observer a) Estimated and measured ω_r ,Estimated and calculated values of rotor fluxes, b) ψ_{dr} & $\hat{\psi}_{dr}$ and c) ψ_{qr} & $\hat{\psi}_{qr}$	69
6.3	Error in estimation of a) ω_r b) ψ_{dr} c) ψ_{qr}	70
6.4	Estimated and measured values of a) rotor speed, ω_r ,rotor fluxes,b) ψ_{dr} & $\hat{\psi}_{dr}$ and c) ψ_{qr} & $\hat{\psi}_{qr}$	71

6.5	Error in estimation of a) ω_r b) ψ_{dr} c) ψ_{qr}	72
6.6	Estimated and measured values of rotor speed, ω_r , for a reference speed of 75rad/s	73
6.7	Estimated and calculated values of rotor fluxes a) ψ_{dr} and b) ψ_{qr}	74
6.8	Error in estimation of a) ω_r b) ψ_{dr} c) ψ_{qr}	75
6.9	Estimated and calculated values of a) rotor speed, ω_r and rotor fluxes, b) ψ_{dr} c) ψ_{qr}	76
6.10	Error in estimation of a) ω_r b) ψ_{dr} c) ψ_{qr}	77
7.1	Block diagram of the experimental set up	80
7.2	Experimental results for a reference speed of 75rad/s(mech.) a) ω_r b) ψ_{dr} c) ψ_{qr}	81
7.3	Experimental results for a reference speed of 30rad/s(mech.) a) ω_r b) ψ_{dr} c) ψ_{qr}	82
7.4	Experimental results for a reference speed of 10rad/s(mech.) a) ω_r b) ψ_{dr} c) ψ_{qr}	83
7.5	Experimental results for a reference speed of 5rad/s(mech.) a) ω_r b) ψ_{dr} c) ψ_{qr}	84
7.6	Experimental results for a reference speed of 75rad/s(mech) changes to 30 rad/s at 3s and back to 75 rad/s at 6s a) ω_r b) ψ_{dr} c) ψ_{qr}	85
7.7	Estimated Speed from the closed loop observer for a reference speed which changes from 75rad/s(mech) to 0rad/s(mech) at 5s and continues at zero speed for 5s a) ω_r b) ψ_{dr} c) ψ_{qr}	86
7.8	Experimental results for a reference speed of 75rad/s(mech.) a) ω_r b) ψ_{dr} c) ψ_{qr}	87
7.9	Experimental results for a reference speed of 30rad/s(mech.) a) ω_r b) ψ_{dr} c) ψ_{qr}	88
7.10	Experimental results for a reference speed of 10rad/s(mech.) a) ω_r b) ψ_{dr} c) ψ_{qr}	89
7.11	Experimental results for a reference speed of 5rad/s(mech.) a) ω_r b) ψ_{dr} c) ψ_{qr}	90
7.12	Experimental results for a reference speed of 75rad/s(mech) changes to 30 rad/s at 3s and back to 75 rad/s at 6s a) ω_r b) ψ_{dr} c) ψ_{qr}	91
7.13	Estimated Speed from the closed loop observer for a reference speed which changes from 75rad/s(mech) to 0rad/s(mech) at 5s and continues at zero speed for 5s a) ω_r b) ψ_{dr} c) ψ_{qr}	92
8.1	A Real-time Recurrent Neural Network	97

8.2	A real-time recurrent neural network without hidden neurons	98
8.3	Real-time Recurrent Neural Network for Speed Estimation	101
8.4	Estimation results with a conventional EKF trained recurrent neural network a) ω_r & $\hat{\omega}_r$ b) ψ_{dr} & $\hat{\psi}_{dr}$ c) ψ_{qr} & $\hat{\psi}_{qr}$	104
8.5	Error in estimation of a) ω_r b) ψ_{dr} and c) ψ_{qr}	105
8.6	Estimation results with a conventional EKF trained recurrent neural network a) ω_r & $\hat{\omega}_r$ b) ψ_{dr} & $\hat{\psi}_{dr}$ c) ψ_{qr} & $\hat{\psi}_{qr}$	106
8.7	Error in estimation of a) ω_r b) ψ_{dr} and c) ψ_{qr} with a varying reference speed	107
8.8	Estimation results with a smoothed EKF trained recurrent neural network a) ω_r & $\hat{\omega}_r$ b) ψ_{dr} & $\hat{\psi}_{dr}$ c) ψ_{qr} & $\hat{\psi}_{qr}$	108
8.9	Error in estimation of a) ω_r b) ψ_{dr} and c) ψ_{qr}	109
8.10	Estimation results with a smoothed EKF trained recurrent neural network a) ω_r & $\hat{\omega}_r$ b) ψ_{dr} & $\hat{\psi}_{dr}$ c) ψ_{qr} & $\hat{\psi}_{qr}$	110
8.11	Error in estimation of a) ω_r b) ψ_{dr} and c) ψ_{qr}	111
8.12	Speed estimation results when a load is applied at t=3s a)smoothed EKF trained RNN b) conventional EKF trained RNN	112
9.1	Block diagram of the experimental set up	116
9.2	Estimation results for a reference speed of 75rad/s a) ω_r b) ψ_{dr} c) ψ_{qr}	117
9.3	Estimation results for a reference speed of 30rad/s a) ω_r b) ψ_{dr} c) ψ_{qr}	118
9.4	Estimation results for a reference speed of 5rad/s a) ω_r b) ψ_{dr} c) ψ_{qr} .	119
9.5	Estimation results for a reference speed which changes from 75rad/s to 30rad/s at t=2.5s and then to 50rad/s at t=5s a) ω_r b) ψ_{dr} c) ψ_{qr} . .	120
9.6	Estimation results for a reference speed which changes from 75rad/s to 0 at t=4.5s and continues at zero speed till 7s a) ω_r b) ψ_{dr} c) ψ_{qr} . .	121
9.7	Estimation results for a reference speed of 75rad/s a) ω_r b) ψ_{dr} c) ψ_{qr}	122
9.8	Estimation results for a reference speed of 30rad/s a) ω_r b) ψ_{dr} c) ψ_{qr}	123
9.9	Estimation results for a reference speed of 5rad/s a) ω_r b) ψ_{dr} c) ψ_{qr} .	124
9.10	Estimation results for a reference speed which changes from 75rad/s to 30rad/s at t=2.5s and then to 50rad/s at t=5s a) ω_r b) ψ_{dr} c) ψ_{qr} . .	125
9.11	Estimation results for a reference speed which changes from 75rad/s to 0 at t=4.5s and continues at zero speed till 7s a) ω_r b) ψ_{dr} c) ψ_{qr} . .	126

List of Tables

4.1	Parameters of the Induction Motor	29
5.1	Mean Square Errors of estimation with and without smoothing (fifth order model of IM)	57
7.1	Comparison of estimation results using a smoothed and conventional EKF (reduced order model of motor)	93
9.1	Comparison of estimation results using a smoothed and conventional EKF - trained recurrent neural observer	127

List of Acronyms/Abbreviations

FOC	Field-oriented Control
EKF	Extended Kalman Filter
MRAS	Model Reference Adaptive System
MSE	Mean Squared Error
BIEKF	Bi Input Extended Kalman Filter
MPC	Model Predictive Control
IM	Induction Motor
ANN	Artificial Neural Network
PI	Proportional and Integral
THD	Total Harmonic Distortion
TMRAS	Torque Model Reference Adaptive System
FCS-MPC	Finite Control Set-Model Predictive Control
PID	Proportional, Integral and Derivative
HC	Hysteresis Controller
VSI	Voltage Source Inverter
CEKF	Conventional EKF
SKF	Smoothed Kalman Filter
IFOC	Indirect Field-Oriented Control

List of Symbols

i_{ds}	Stator direct-axis current
i_{qs}	Stator quadrature-axis current
i_{dr}	Rotor direct-axis current
i_{qr}	Rotor quadrature-axis current
v_{ds}	Stator direct-axis voltage
v_{qs}	Stator quadrature-axis voltage
R_s	Stator resistance
R_r	Rotor resistance
L_s	Stator inductance
L_r	Rotor inductance
L_m	Mutual inductance
ω_r	Rotor angular velocity
T_e	Electromagnetic Torque
J	Moment of Inertia
B	Coefficient of viscous friction
T_L	Load torque
w, v	Gaussian white noises
Q	covariance matrix of w
R	covariance matrix of v
P	Error covariance matrix
H	Output matrix
ϕ	State transition matrix
τ	Disturbance transition matrix
δ	Kronecker delta function
K	Kalman gain matrix
M	Smoothing filter gain matrix

E	Expectation
ψ_{dr}	Direct axis rotor flux
ψ_{qr}	Quadrature axis rotor flux
η	Learning rate of neural network
W	Weights of neural network
S	Non- negative definite weighting matrix
D	Desired output vector

Uma Syamkumar “Smoothed Kalman Observer for Sensorless Field Oriented Control of Induction Motor.” Thesis. Department of Electrical Engineering, Government Engineering College, Trichur, University of Calicut, , 2020.

Chapter 1

Introduction

This chapter provides a brief description of the background, motivation and objectives of this research work. An outline of this report is also presented.

1.1 Background

Even though there are a number of electric motors available in the market, induction motors maintain their superiority over others due to their unique properties like low cost, ruggedness and reliability. But, the dynamic performance of induction machines is complex due to the coupling effect between stator and rotor phases. In the case of a dc machine, flux axis and armature axis are inherently orthogonal due to the presence of commutator. The armature flux in no way affects the main flux in the case of an armature compensated machine. The dynamic behaviour of the machine can be controlled by keeping flux constant and controlling armature current. In contrast to dc machines, asynchronous machines require the control of stator voltages, their magnitude, phases and frequency, which is quite complex. The independent control of flux and torque in asynchronous machines can be made possible by resolving the stator current into two orthogonal components, one controlling the flux and the other controlling the torque [1]. One stator current component is resolved along the direction of rotor flux linkages, hence this component controls the flux. But, this requires the position of rotor flux at every instant. Thus, if this information is available, the ac machine can be controlled in the same way as a dc machine. This method of controlling an ac machine is called field oriented control(FOC) or vector control.

Depending on how the position of rotor flux linkages is obtained, vector control can be divided into direct vector control and indirect vector control. In direct vector control, rotor field position is calculated from terminal voltages and currents or by using Hall effect sensors or flux sensing windings. A block diagram representation of direct vector control is shown in Fig.1.1 [2].

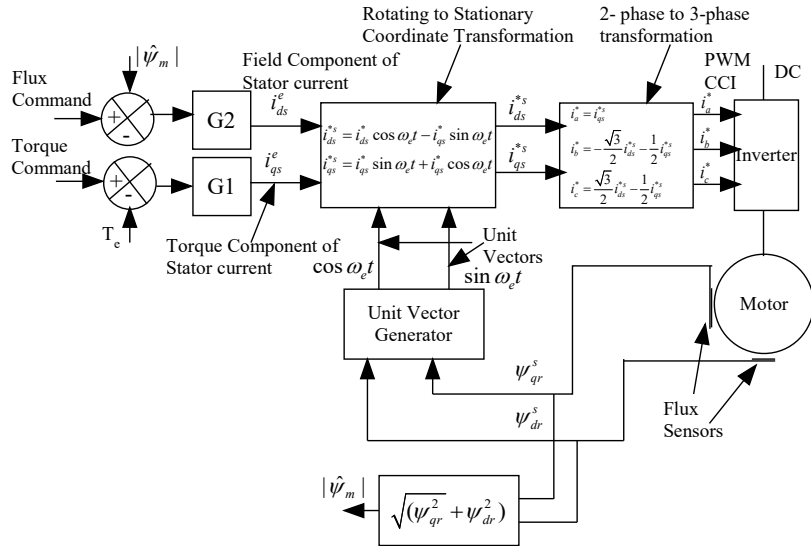


Figure 1.1: Block diagram of direct vector control

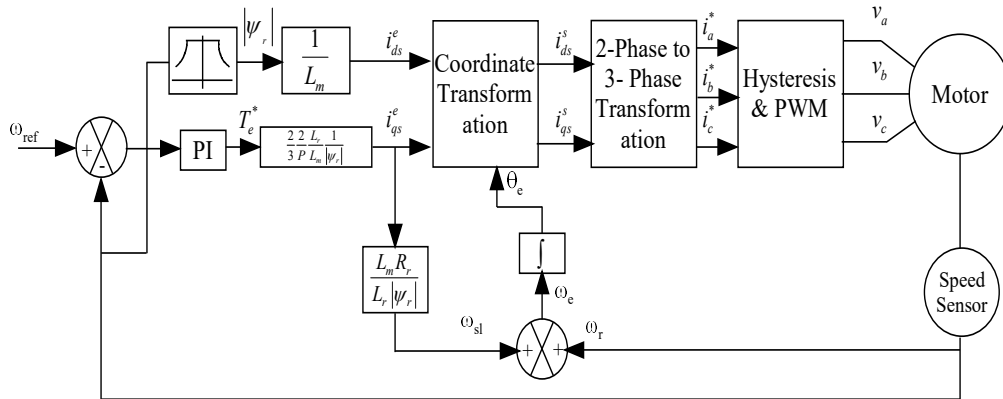


Figure 1.2: Block diagram of indirect vector control

Calculating the field angle from rotor position information along with partial estimation with machine parameters and not from any voltages and currents leads to another group of control called indirect vector control. A block diagram representation of indirect vector control is given in Fig.1.2

In indirect vector control methods, the instantaneous position of rotor flux is evaluated from the rotor speed and the required slip for a particular torque

requirement. Hence, the performance of the system highly depends on the accuracy of measurement of rotor speed. Speed sensors are mounted on the rotor to obtain the rotor speed, but this deteriorates the ruggedness of the system. Also mounting of a rotational transducer is difficult in hostile environments and high speed applications. In order to improve the ruggedness of the system, speed sensors are replaced with speed estimators or observers. Such systems are named as sensorless drives.

The performance of a sensorless drive depends on the accuracy of the observer. A very useful insight into the systems used in sensorless speed control of induction motors is obtained from [3]. A basic approach to sensorless speed control requires a speed estimation algorithm. Thus, several methods exploiting the fundamental model of the induction motor, such as open-loop estimators [4], model reference adaptive systems [5], sliding mode observers [6–8], artificial neural networks (ANNs) [9, 10], fuzzy logic [11, 12], Leunberger observer [13, 14] and extended Kalman filter [15] were developed.

The extended Kalman Filter (EKF) is an efficient algorithm for the state and parameter estimation of non-linear systems in the presence of noise and uncertainty. Kalman Filters are known to have a high convergence rate which can improve the transient performance of stochastic systems. Model uncertainties and non-linearities inherent in the induction motors are taken into account in Kalman filters. Due to these properties, they are widely used for the speed sensorless control of induction motors.

The accuracy of an EKF based observer depends on the values of the process and measurement error covariance matrices. The choice of these matrices is crucial in the observer design using an EKF.

1.2 Motivation for the present research work

The primary motivations for doing this research work are summarised as follows:

- Indirect vector control scheme is one of the significant methods used in industry for variation of speed in induction motors along with ac drives
- An accurate measurement of rotor speed is essential for closed loop vector control.
- Observers are one of the relevant speed estimation techniques for vector control of drives

- A reliable control signal is necessary for harmonic free, smooth operation of observer- based speed control of induction motor.
- Extended Kalman filter is a powerful algorithm which gives an accurate speed estimate in the presence of noise.

1.3 Objectives

The objectives of this work are to:

- Develop and implement a single- stage smoothing algorithm based extended Kalman filter for sensorless indirect field- oriented control of three- phase induction motor, which improves the performance in estimation of rotor speed.
- Compare the performance of the smoothed observer with those of a conventional EKF based observer, for the same values of process and measurement error covariance matrices.
- Develop and implement a smoothed EKF for speed estimation of the motor using a reduced mathematical model.
- Develop and implement a smoothed Kalman trained recurrent neural network observer to estimate speed of the motor.
- Study the performance of the observer at low and near zero speeds.

1.4 Organization of the thesis

The research work presented in the thesis is organized and structured in the form of ten chapters, which are briefly described as follows:

- i) **Chapter 1** gives a brief background of the research work. The motivation which led to this thesis and the objectives of this work are also presented.
- ii) **Chapter 2** provides a comprehensive review of literature on sensorless control of induction motor drives. The review is divided into three sections: sensorless control based on EKF, sensorless control based on model reference adaptive systems and those based on artificial intelligent techniques particularly, artificial neural networks.

- iii) **Chapter 3** elaborates the fundamentals of estimation of data. Here, the three steps in data estimation, namely, prediction, filtering and smoothing are discussed in detail. The three main smoothing algorithms are explained and the mathematics involved in single- stage smoothing algorithm is elaborated.
- iv) **Chapter 4** presents the development of an observer based on smoothed Kalman filter applied for sensorless control of an indirect vector controlled IM drive. Simulation studies are performed and results are presented.
- v) **Chapter 5** deals with a real-time implementation of the smoothed Kalman observer for speed control of induction motor. The estimated rotor speed from the observer is fed back to the system in closed- loop control. The system is tested for various reference speeds and the results are compared with those with a conventional EKF.
- vi) **Chapter 6** presents the development of an observer based on smoothed Kalman filter applied for sensorless control of an indirect vector controlled IM drive. A reduced order model of the induction motor is used. Simulation studies are performed and results are presented.
- vii) **Chapter 7** deals with the real-time implementation of the smoothed Kalman observer with the reduced order model of induction motor. The estimated rotor speed from the observer is fed back to the system in closed- loop control. The system is tested for various reference speeds and results are compared with those of a conventional EKF.
- viii) **Chapter 8** presents the development of a real-time recurrent neural network observer based on smoothed Kalman filter applied for sensorless control of an indirect vector controlled IM drive. A reduced model of the induction motor is used. Simulation studies are performed and results are presented.
- ix) **Chapter 9** deals with the real-time implementation of a smoothed Kalman filter trained recurrent neural network observer applied for sensorless control of an indirect vector controlled IM drive. The results for various reference speeds are compared with those of a conventional EKF trained recurrent neural network observer.
- x) **Chapter 10** concludes the thesis with overall discoveries of the present research work. The scope for future work is also mentioned.

Uma Syamkumar “Smoothed Kalman Observer for Sensorless Field Oriented Control of Induction Motor.” Thesis. Department of Electrical Engineering, Government Engineering College, Trichur, University of Calicut, , 2020.

Chapter 2

Literature review

This chapter presents a review of the literature available on speed control of three phase induction motors. Vector control of induction motors requires an accurate measurement of rotor speed. Mounting speed sensors on the rotor is a bad option in high speed and high risk applications. Hence sensorless speed control methods are gaining wide popularity.

2.1 Introduction

Induction motors are widely used in industry due to their advantageous properties like ruggedness, low cost and reliability compared to dc motors. Speed control of induction motors have attained greater attention of researchers with the advent of field oriented control(FOC). V/f control principle adjusts the stator voltage for a constant Volts/ Hertz ratio, by feedforward control. This method satisfies only moderate dynamic requirements of the machine, even though the method is simple. In order to improve the dynamic performance of the machine, field-oriented control or vector control is adopted. Vector control can be either direct or indirect. In direct vector control, the rotor flux is measured using Hall effect sensors and manipulated, whereas in indirect vector control, the rotor speed is measured or estimated and used to obtain the instantaneous rotor position, required for generating the unit vectors necessary for the coordinate transformation.

FOC requires the actual speed of the machine to be fed back, which necessitates the installation of speed sensors. This affects the robustness and reliability of the entire system. Hence research is focussed on development of speed sensorless methods for speed control, which has been a hot topic during the past three decades [16]. A very useful insight into the systems used in sensorless speed control of induction motors is obtained from [3]. Signal flow graphs of complex space vector quantities are used to study the various systems involved in sensorless control of induction motors in [3]. A basic approach to sensorless speed control requires a speed estimation algorithm. Speed sensorless control of induction motors is still an open area to research. Thus, several methods exploiting the fundamental model of the induction motor, such as

open-loop estimators [4], model reference adaptive systems [5], sliding mode observers [6–8], artificial neural networks (ANNs) [9, 10], fuzzy logic [11, 12], Leunberger observer [13, 14] and extended Kalman filter [15] were developed.

In [17], a method of simultaneously estimating the stator and rotor resistances and rotor speed is presented and verified experimentally. But the method is validated only for high speeds. In [9, 10], a novel method for parameter identification of induction motors with ANNs is presented and good results are obtained than those using classical ones. An observer which estimates the speed, based on fuzzy logic is developed in [11] and is validated using numerical examples, whereas a type-2 fuzzy model replaces the PI controller in a speed sensorless direct vector control scheme based on MRAS in [12]. A fuzzy model is found to be robust to load as well as speed uncertainties. A model reference adaptive system is used for field oriented control of induction motors in [5]. The problem with these observers is that they fail to be effective at low speeds, giving results which are inaccurate at these speeds. A Leunberger observer, used in [13, 14] is a deterministic one, which fails to act under circumstances of load disturbances or parameter variations or internal noise in the system.

Even though speed sensorless drives are well established in industry, the operation at low and persistent zero speeds are still a challenge [18]. This is due to parameter uncertainties, signal acquisition error, and noise at very low speeds. At zero speed, the problem encountered is because of the fact that stator current ceases to send information on rotor angular velocity [3, 18]. Model-based methods using the state equations of the machine and signal injection methods are used for speed estimation at low and zero speeds [19]. Speed injection methods are capable of persistent low/zero speed operation but they are highly sophisticated and computationally intensive [18]. Model-based estimation methods as in [20]- [21] have been proposed specifically to deal with low and zero-speed operation of induction motors. In [3], a stator flux estimator for low and persistent zero speed is designed. The time-variable dc offset voltage is estimated from the flux drift in a parallel stator model and used to eliminate the offset by feedforward control. Residual high-frequency disturbances are compensated by feedback flux amplitude control. The total leakage inductance as seen from the stator windings is exploited to extract the rotor position angle and the rotor speed in [22]. This method is found to provide accurate speed estimates even at standstill. [7, 8] presents a sliding mode observer for sensorless speed control of induction motor. A stator current observer based on sliding mode principles is used to estimate speed over a wide range, including above rated speed. Even though

the dynamic performance is improved, chattering is found to affect the estimates. A review of sensorless estimation methods for induction motor drives is presented in [23].

2.1.1 Literature Review on Sensorless Speed Control of Induction Motors using Extended Kalman Filter

Unlike other methods, extended Kalman filters are stochastic observers which take into account the process and measurement noises, such that estimation is done even if the plant is non- linear or noisy [24]. It provides optimal filtering of noises in measurement and process, provided the covariance matrices of these noises are known [25]. EKF has a high convergence rate which is capable of improving the transient performance. EKFs take into account, the uncertainties in the system model as well as the non- linearities inherent in it. These properties make the EKF widely acceptable in sensorless speed control applications of induction motors. An overview of the applications of Kalman filter is presented in [26]. [24] uses EKF to estimate the speed of an induction motor with a fourth order model of the motor. The rotor speed is considered a constant. A reduced order EKF [27] is also mentioned so as to reduce the computational complexity of a fifth order mathematical model. A speed and flux observer based on extended Kalman filter is presented in [28]. The speed observer is shown to present accurate results over a wide speed range. Moreover, it is shown to be robust to machine parameter variations [29]. In [15], an EKF based observer is used to estimate rotor speed in addition to stator currents and rotor fluxes. Rotor speed is considered as a slow-varying state variable and hence assumed constant between adjacent time- intervals. An EKF which estimates load torque in addition to rotor speed, rotor fluxes and stator currents is presented in [30]. Here, rotor speed is not treated as a constant, but is dependent on the load torque via the mechanical equation of the motor. This makes estimation at low speeds possible. In this paper, estimated rotor speed is not used as a feedback in the closed loop system. A BI- EKF is presented in [31], where two extended induction motor models are used, with a single EKF for simultaneous estimation of stator and rotor resistances along with other state variables. A modification of this bi- input EKF is presented by the same authors in [32]. A robust estimation of flux and speed of an induction motor is carried out in [33–35], which uses a fourth- order system to estimate the rotor flux and rotor speed is estimated using a recursive least squares algorithm. A finite state-predictive torque controller uses measured stator currents, estimated rotor speed, stator and rotor

fluxes in the predictive model. Noisy estimates deteriorate the quality of steady state performance in terms of THD, torque ripple and flux ripple. Hence EKF is used for estimation in [36] to eliminate noise from estimates.

Recently, EKF has been researched upon widely as a result of which there are many variations in the conventional EKF. Unscented Kalman filters in [37] are used for speed estimation, where the unscented transforms are non-linear so that the non-linear behavior of the system is captured.

The determination of the error covariance matrices has a significant effect on estimation with EKF. Trial and error method is usually used for assuming these covariance matrices. This method being a time-consuming method, researches are proceeding in a direction so as to obtain an optimum value for these matrices. As a result, there are papers in which optimized values of these matrices are obtained using genetic algorithms [38] and differential evolution algorithm [39]. However, optimization methods are to be done offline and are often time-consuming. In [40], an adaptive fading EKF is designed wherein a fading factor is applied to the estimated covariance matrix in order to increase the variance of its estimated state vector. The authors claim an improved performance of the observer compared to the standard EKF algorithm, with a slight increase in the computational burden. But the real-time implementation is yet to be done. In [41], an adaptive EKF is used for speed sensorless control of induction motors. In this algorithm, the covariance matrix of the output noise is assumed to be known and the covariance matrix of the system noise is estimated.

2.1.2 Literature Review on Sensorless Speed Control of Induction Motors based on model reference adaptive systems

Of the various methods developed in the recent past for speed sensorless IM drives, model reference adaptive system(MRAS) has gained wide popularity, since they are simple and easy to implement. Extensive studies on rotor-flux based MRAS has shown that they can give excellent performance upto 5% of the rated speed [5, 42]. Rotor flux based MRAS suffer from problems due to machine parameter variations, inverter non-linearity, pure integration effects etc. These problems become dominant at low speeds. A model based on counter electromotive force, instead of rotor flux is used in [43]. The authors claim the method to be independent of changes in stator resistance. A stator current based MRAS estimator is presented in [44–47]. A reduced order flux observer [48] with stator resistance adaptation is presented

in [49]. A stator- flux based MRAS presented in [50] incorporates a dc offset compensator structure in closed loop, so that the problems associated with exiting stator flux estimators are overcome. Active power, reactive power and two fictitious quantities are made use of to estimate rotor speed in [51, 52]. This method has the advantage that no parameters other than the rotor resistance are involved in the process. In [53], an MRAS which makes use of the error in rotor fluxes of the two models in addition to the error in electromagnetic torque is described. The observed rotor speed is used in the sensorless vector control using a sliding mode controller. A torque model reference adaptive system(TMRAS) is studied in [54] which claims to give good performance in low and zero speeds. In [55], a Luenberger load torque estimator based on MRAS is presented. The torque observer is interconnected with the speed estimator, so as to obtain a robust high performance indirect field oriented control system. Instability issues associated with adaptive flux observers, especially in the low speed regions are addressed in [56]. A detailed stability analysis is presented in the regenerative low speed regions, while using stator resistance and speed estimators simultaneously.

In almost all these works, a proportional- integral(PI) controller is used as the adaptation mechanism of the MRAS for speed estimation. Ability of the PI controller to perform over a wide range of speeds and its simplicity contribute to its wide usage. But at low speeds, machine parameter variations and inverter non-linearities give rise to errors. Hence the constant- gain PI controller may not be able to provide a satisfactory performance. Moreover, tuning of PI controllers itself is a tedious task. Various approaches to the adaptation mechanism of MRAS estimators are available in literature. Thus the fixed-gain PI controller is replaced by various advanced algorithms.

Instead of a PI controller as in classical MRAS, a sliding mode observer is used to estimate the speed of the motor in [57–63]. Two sliding mode MRAS speed observers are presented in [61]. The voltage model of the induction motor is used to generate the reference rotor fluxes and current model is used as the adaptive model. A sliding- mode pseudo- MRAS observer which estimates the torque and speed of a three phase induction motor is presented in [63]. Even though this method improves the dynamic response of the drive system, an intolerable amount of chattering is produced in the estimates.

Another solution to PI controller is provided in [62, 64], where a fuzzy logic controller replaces a PI controller. Fuzzy logic controller shows improvement in the estimator dynamic performance but computational complexity is a major drawback of this scheme.

In order to resolve the issues connected with adaptation mechanism, a finite control set-model predictive control(FCS-MPC) is introduced in [65]. The FCS-MPC is based on an optimization problem whose objective is to minimize the error signal, which is used to tune the MRAS estimator. This same method has been applied to the controller side of sensorless vector control of IM in [66, 67]. [68] presents a method for estimating the load torque of an indirect vector controlled induction motor drive, based on MRAS technique. The load torque is estimated using a Luenberger observer. The MRAS estimation is used to estimate the parameters of the motor as presented in [69]. Rotor resistance and mutual inductance are estimated, since they tend to change with changes in temperature and flux level.

A novel hybrid estimator consisting of an extended Kalman filter and an active power based MRAS is presented in [70], which estimates the stator currents and flux, rotor speed, load torque and rotor resistance. An improved rotor flux space vector based MRAS is presented in [71]. This improved performance is obtained by using a stator voltage reference vector instead of the actual voltage vector. The reference vector is generated from the errors in the reference and measured current vectors.

[72] gives a review of various model reference adaptive systems based sensorless speed control of induction motors.

2.1.3 Literature Review on Sensorless Speed Control of Induction Motors using artificial neural networks

Neural networks have grown to be a well established methodology in solving very difficult problems in engineering. They are widely used in identification and control of nonlinear dynamic systems [73–76] because of their ability to approximate a wide variety of nonlinear functions to any desired degree of accuracy. They also have the added advantages of fast parallel computation, immunity from harmonic ripples and fault tolerance. There are investigations going on in extending the application of neural networks to identification and control of induction motor drives [20, 77–79]. State estimation using neural networks is also an interesting topic, which has been studied lately [80, 81]. ANNs are used to replace the PID controller in the vector controlled IM drive in [82].

Neural network observers have emerged as a promising method, in situations where the plant dynamics are unknown [83–85]. In most of these a multi-layer neural network is trained offline using backpropagation algorithm. This gave good

results in estimation and was robust to parameter variations. But, the network has to be trained with enough samples. In [86], a neural network speed observer is presented, where the speed estimation is done online. The network is trained using the backpropagation algorithm and is shown to give fairly good results with estimation under load and speed variations. A multilayer neural network for speed estimation in a rotor flux based MRAS system is proposed in [87, 88]. In [89], the speed and flux estimation is performed using a multilayer ANN, which is trained offline using experimental measurements based on current model alone, avoiding the voltage model. All drive non-linearities are considered and satisfactory performance results are obtained for low and zero speed operation. But the training of ANN is computationally intensive and offline also. The structure of the network is chosen by trial and error considering computational complexity and accuracy. A similar work involving training of a multilayer neural network using experimental data before using it online is presented in [90]. [91] presents a rotor speed observer which works online on least square algorithm implemented by an original neuron. Rotor resistance and stator resistance for indirect vector controlled IM drive are estimated using an ANN and fuzzy logic observer in [92–94]

Recurrent neural networks have superior capabilities over multilayer networks in dynamic system identification [95, 96]. They can be trained online whereas multilayer networks have to be trained offline with sufficient samples [97, 98]. In [10], two neural networks are used to estimate the speed of an induction motor. The speed estimated by a multilayer perceptron is corrected using an Elman recurrent network. In [99], ANN based parameter estimation is performed. ANNs, including multilayer and recurrent, are used to estimate various parameters of the induction machine, and is used as a memory to estimate the value during transients. In [100, 101], a neuro- fuzzy hybrid controller is used as a controller instead of conventional PI controller and performance compared. The hybrid controller is found to give better and robust performances compared to conventional and neural or fuzzy controllers. [102] presents a robust speed estimation and control of an induction motor based on ANNs. The controller is based on sliding mode principles and the speed estimator is based on ANN. The rotor speed is derived to be a non-linear mapping of motor stator voltages and currents. The ANN is trained to reproduce this mapping.

2.1.4 Summary

This chapter gives a brief idea about the various observers used in sensorless drives, their pros and cons. The observers based on extended Kalman filter algorithm is studied specifically and it is seen that the process and measurement error covariance matrices play a significant role in the accuracy of the observer. Moreover, these observers fail to give accurate results in low and zero speeds. It is also noted that, while using extended Kalman filter algorithm, the covariance matrices vary for different reference speeds.

The focus of this research work is to incorporate smoothing to the filtering algorithm, so that the performance of the observer is improved. The covariance matrices are kept constant for different reference speeds, thus analyzing the effect of these matrices on estimation.

Uma Syamkumar “Smoothed Kalman Observer for Sensorless Field Oriented Control of Induction Motor.” Thesis. Department of Electrical Engineering, Government Engineering College, Trichur, University of Calicut, , 2020.

Chapter 3

Smoothing Algorithms

This chapter briefly explains the theory behind Kalman filter algorithm and the different smoothing algorithms. Estimation of data consists of three stages- prediction, filtering and smoothing. Here, the difference between each stage is elaborated.

3.1 Introduction

Estimation using extended Kalman filters depends very largely on the values of process and measurement error covariances. These covariance matrices are usually obtained by trial and error method, which is very time- consuming. Moreover, filtering operates on measurements upto the current time. An improved estimation performance can be obtained through the use of smoothers if some processing delay can be tolerated. Smoothing is a process which helps to refine the estimated values of EKF using some of the measurements of future instants also. Since additional data is made use of, the estimates are bound to be better. The problem of smoothing deals with estimates of the system's state, which are of the form,

$$\hat{x}(k|j) = \phi_k[y(i), i = 1, 2, \dots, j] \quad (3.1.1)$$

where $j > k$, that is, the time at which the estimate is made lies to the left of the time of last measurement, $y(j)$, on the time scale [103]. Fig.3.1 shows the flow of the process involved in smoothing.

In this chapter, the three stages in estimation of data are discussed in section 3.2, smoothing and the three different types of smoothing algorithms are discussed in section 3.3. In section 3.4, the single-stage smoothing algorithm is derived and explained. Section 3.5 concludes the chapter.

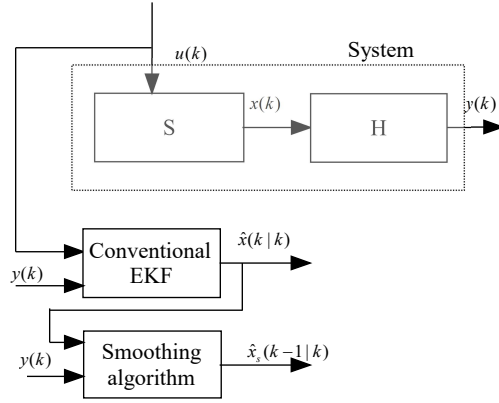


Figure 3.1: Flow Diagram of the smoothing algorithm

3.2 Estimation of data

A dynamic system, S , is considered, whose state is a discrete-time random process of dimension, $n, |x(k), k \in I|$, where $I = k : k = 0, 1, \dots, N$. $x(k)$ is a function of time. $x(k)$ for some fixed value of k is to be estimated, assuming that $x(k)$ is not accessible for direct measurement. But, $x(k)$ is assumed to be causally related to a sequence of measurements, $y(1), y(2), \dots, y(j)$. A measurement system, H relates $y(i)$ to $x(k)$, as shown in Fig.3.2. $y(i), i = 1, 2, \dots, j$ is assumed to be an m -dimensional, discrete-time random process.

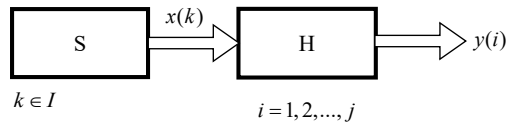


Figure 3.2: Block diagram of the dynamic system, S

$x(k)$ is to be estimated based only on the measurements $y(i)$. Hence, it can be denoted as $\hat{x}(k|j)$ and can be defined as an n -dimensional function, ϕ_k of the

measurements, i.e

$$\hat{x}(k|j) = \phi_k[y(i), i = 1, 2, \dots, j] \quad (3.2.1)$$

Thus, estimation is a process of determining ϕ_k in some rational and meaningful manner. If $k > j$, the problem is one of *prediction*, if $k = j$, one of *filtering*, and if $k < j$, one of *smoothing* or *interpolation*.

3.2.1 Prediction

Consider the system,

$$x(k+1) = \phi(k+1, k)x(k) + \Gamma(k+1, k)w(k) \quad (3.2.2)$$

$$y(k+1) = H(k+1)x(k+1) + v(k+1) \quad (3.2.3)$$

where x is an n -vector, the state; w is a p -vector, the disturbance; y is an m -vector, the measurement(system output); v is an m -vector, the measurement error; and $k = 0, 1, \dots$, is the discrete time index. Also, ϕ is an $n \times n$ state transition matrix, Γ is an $n \times p$ disturbance transition matrix; and H is an $m \times n$ measurement matrix. The process $w(k), k = 0, 1, \dots$ is a p -dimensional Gaussian white sequence for which

$$E[w(k)] = 0$$

for all $k = 0, 1, \dots$, and

$$E[w(j)w'(k)] = Q(k)\delta_{jk}$$

for all $j, k = 0, 1, \dots$, where $Q(k)$ is a positive semi-definite $p \times p$ matrix.

The process $v(k+1), k = 0, 1, \dots$ is a m -dimensional Gaussian white sequence for which

$$E[v(k+1)] = 0$$

for all $k = 0, 1, \dots$, and

$$E[v(j+1)v'(k+1)] = R(k+1)\delta_{jk}$$

for all $j, k = 0, 1, \dots$, where $R(k+1)$ is a positive semi-definite $m \times m$ matrix. The random processes, w and v are non-correlated, so that

$$E[v(j)w'(k)] = 0 \quad (3.2.4)$$

for all $j = 1, 2, \dots$, and $k = 0, 1, \dots$. The initial state, $x(0)$ is a Gaussian random n -vector with mean

$$E[x(0)] = 0$$

and covariance,

$$E[x(0)x'(0)] = P(0)$$

where, $P(0)$ is an $n \times n$ positive semi-definite matrix. Now the algorithm for optimal predicted estimate, $\hat{x}(k|j)$, $k > j$, $j = 0, 1, \dots$, can be developed. It is assumed that the optimal filtered estimate, $\hat{x}(j|j)$ and the $n \times n$ covariance matrix, $E[\tilde{x}(j|j)\tilde{x}'(j|j)] = P(j|j)$ is available for some $j = 0, 1, \dots$ [103]. Now,

$$\hat{x}(j|j) = E[x(j)|y(1), \dots, y(j)] \quad (3.2.5)$$

is the optimal filtered estimate $x(j)$ for $j = 1, 2, \dots$. For $j = 0$, we have no measurements, and it follows that

$$\hat{x}(0|0) = E[x(0)] = 0 \quad (3.2.6)$$

Thus, $\hat{x}(j|j)$ is a Gaussian with zero mean. Also, the filtering error,

$$\tilde{x}(j|j) = x(j) - \hat{x}(j|j) \quad (3.2.7)$$

is a zero mean Gaussian random vector whose covariance matrix, $P(j|j)$ is assumed to be known. For $j = 0$, we have

$$\tilde{x}(0|0) = x(0) - \hat{x}(0) = x(0) \quad (3.2.8)$$

so that

$$P(0|0) = E[\tilde{x}(0|0)\tilde{x}'(0|0)] = E[x(0)x'(0)] \quad (3.2.9)$$

or

$$P(0|0) = P(0) \quad (3.2.10)$$

The optimal predicted estimate for all $k > j$ can be given by,

$$\hat{x}(k|j) = \phi(k, j)\hat{x}(j|j) \quad (3.2.11)$$

From this equation, the single stage optimal predicted estimate is given by the expression,

$$\hat{x}(k+1|k) = \phi(k+1, k)\hat{x}(k|k) \quad (3.2.12)$$

$\tilde{x}(k+1|k) = x(k+1) - \hat{x}(k+1|k)$ is the single-stage prediction error. $\tilde{x}(k+1|k)$ has a covariance matrix, given by

$$P(k+1|k) = \phi(k+1, k)P(k|k)\phi'(k+1, k) + \Gamma(k+1, k)Q(k)\Gamma'(k+1, k) \quad (3.2.13)$$

3.2.2 Filtering

The filtering algorithm for the system given by eqns.(3.2.2) and (3.2.3) are developed based on the following assumptions:

- the initial estimate, $\hat{x}(0|0) = 0$
- the covariance matrix of the filtering error at the initial time,

$$P(0|0) = E[\tilde{x}(0|0)\tilde{x}'(0|0)] = E[x(0)x'(0)] = P(0) \quad (3.2.14)$$

- the set of measurements, $y(1), \dots, y(k), y(k+1)$, k is a non-negative integer.

The optimal estimate of the filter, $\hat{x}(k+1|k+1)$ is given by the recursive relation [?],

$$\hat{x}(k+1|k+1) = \phi(k+1, k)\hat{x}(k|k) + K(k+1)[y(k+1) - H(k+1)\phi(k+1, k)\hat{x}(k|k)] \quad (3.2.15)$$

for $k = 0, 1, \dots$ where $\hat{x}(0|0) = 0$. $K(k+1)$ is an $n \times m$ matrix which can be described by the equations,

$$K(k+1) = P(k+1)H'(k+1)[H(k+1)P(k+1|k)H'(k+1) + R(k+1)]^{-1} \quad (3.2.16)$$

$$P(k+1|k) = \phi(k+1, k)P(k|k)\phi'(k+1, k) + \Gamma(k+1, k)Q(k)\Gamma'(k+1, k) \quad (3.2.17)$$

$$P(k+1|k+1) = [I - K(k+1)H(k+1)]P(k+1|k) \quad (3.2.18)$$

for $k = 0, 1, \dots$, where I is the $n \times n$ identity matrix and $P(0|0) = P(0)$ is the initial condition for eqn.(3.2.17).

The algorithm for recursive filtering, described by eqns.(3.2.15) to (3.2.18) is called the *Kalman filter*.

The recursive nature of Kalman filter, makes it possible to process measurements

to obtain the optimal filtered estimate. The information flow in the filter can be represented in a simple form using the block diagram of Fig.3.3.

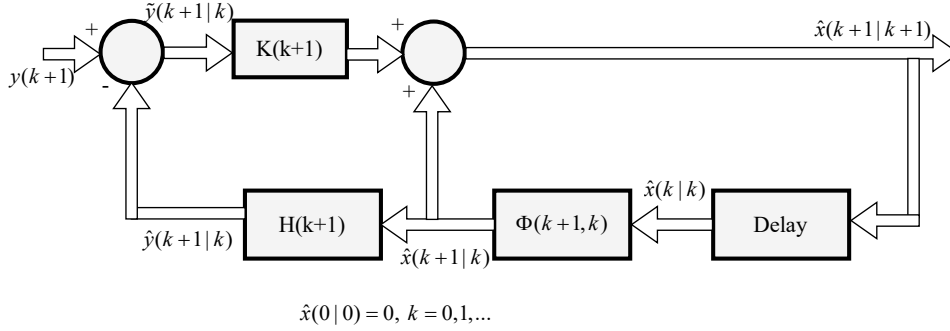


Figure 3.3: Block diagram of Kalman filter

The estimate, $\hat{x}(k|k)$ is premultiplied by the state transition matrix, $\phi(k+1, k)$. This gives the predicted estimate, $\hat{x}(k+1|k)$. Premultiplying $\hat{x}(k|k)$ by $H(k+1)$, gives $\hat{y}(k+1)$. This, when subtracted from $y(k+1)$, the actual measurement, gives the measurement residual, $\tilde{z}(k+1|k)$. $\hat{x}(k+1|k+1)$ is obtained by adding $K(k+1)$ times this residual to $\hat{x}(k+1|k)$. $\hat{x}(k+1|k+1)$ is stored till the next measurement, and the cycle is repeated.

The correction term, $K(k+1)\tilde{y}(k+1|k)$ is added to the predicted estimate, $\hat{x}(k+1|k)$, to determine the filtered estimate. The correction term involves a weighting of the measurement residual by the matrix, $K(k+1)$. This weighting matrix is referred to as the *Kalman gain matrix*.

3.3 Smoothing

Smoothing deals with estimates of the system's state, which are of the form,

$$\hat{x}(k|j) = \phi_k[y(i), i = 1, \dots, j] \quad (3.3.1)$$

where $j > k$; that is, the time at which it is desired to estimate the state lies behind the time of last measurement, $y(j)$, on the time scale. The optimal smoothed estimate is given by

$$\hat{x}(k|j) = E[x(k)|y(1), \dots, y(j)] \quad (3.3.2)$$

3.3.1 Classification of Smoothing Algorithms

The three main classes of smoothing algorithms of the states of a system are:

1. Fixed- Interval Smoothed Estimate: $\hat{x}(k|N)$, $k = 0, 1, \dots, N - 1$, where N is a fixed positive integer.
2. Fixed- Point Smoothed Estimate: $\hat{x}(k|j)$, $j = k + 1, k + 2, \dots$, where k is a fixed positive integer. Also termed as single- point smoothed estimate.
3. Fixed- Lag Smoothed Estimate: $\hat{x}(k|k + N)$, $k = 0, 1, \dots$, where N is a fixed positive integer.

Fixed- Interval Smoothing

This algorithm is for retrospective data analysis, where measurements recorded over an interval, $(0, N)$ are used to obtain the improved estimates. The smoothed estimate is expressed as:

$$\hat{x}(k|N) = E[x(k)|y(1), y(2), \dots, y(N)] \quad (3.3.3)$$

where, $k = 0, 1, 2, \dots, N$.

In eqn(3.3.3), only the filtered estimate, $\hat{x}(N|N)$ is available from EKF. Hence, this forms the starting point of the algorithm and it is backward recursive in time and can be used only for offline estimation problems where a set of measurement data is available a priori.

Fixed- Point Smoothing

This algorithm gives an estimate of the system states at a fixed point in time, which is based not only on measurements upto that time, but also on measurements taken beyond it. Mathematically, the fixed- point smoothed estimate can be expressed as:

$$\hat{x}(k|j) = E[x(k)|y(1), y(2), \dots, y(j)] \quad (3.3.4)$$

for some fixed k , with $j > k$.

Fixed- Lag Smoothing

In this algorithm, the time- point at which the smoothed estimate of the system state is required, lags behind the time point of the most recent measurement by a fixed interval of time, N , that is, $t_{k+N} - t_k = \text{a constant}$, for all $k = 0, 1, 2, \dots$. The optimal

fixed- lag smoothed estimates are given by the relation,

$$\hat{x}(k|k+N) = E[x(k)|y(1), y(2), \dots, y(k), y(k+1), \dots, y(k+N)] \quad (3.3.5)$$

A forward- time recursive algorithm can be obtained for optimal fixed- lag smoothing. This algorithm can be obtained online in estimation problems, where a lag between measurements and estimations is permissible. The fixed- lag smoothed estimate can be considered as an extension of the optimal filtered estimate, $\hat{x}(k|k)$, where the time at which estimate of the state is desired is same as the time of most recent measurement.

3.4 Single- Stage Smoothing

In fixed- lag smoothing algorithm, if the lag is just one time instant, we can name it as single- stage smoothing. In this case, the estimate of interest will be expressed as $\hat{x}(k|k+1)$, for every $k = 0, 1, 2, \dots$. To derive the algorithm, we take the measurements, $y(1), y(2), \dots, y(k), \tilde{y}(k+1|k)$. Now,

$$\begin{aligned} \tilde{y}(k+1|k) &= y(k+1) - \hat{y}(k+1|k) \\ &= y(k+1) - H(k+1)\hat{x}(k+1|k) \\ &= H(k+1)\tilde{x}(k+1|k) + v(k+1) \end{aligned} \quad (3.4.1)$$

$\tilde{y}(k+1|k)$ is independent of the set of measurements $[y(1), y(2), \dots, y(k)]$. Hence,

$$\begin{aligned} \hat{x}(k|k+1) &= E[x(k)|y(1), y(2), \dots, y(k), \tilde{y}(k+1|k)] \\ &= E[x(k)|y(1), y(2), \dots, y(k)] + E[x(k)|\tilde{y}(k+1|k)] \end{aligned} \quad (3.4.2)$$

The first term on the RHS of this equation is $\hat{x}(k|k)$, while the second term is $P_{y\tilde{y}}P_{\tilde{y}\tilde{y}^{-1}}(\tilde{y}(k+1|k))$. This follows because $x(k)$ and $\tilde{y}(k+1|k)$ are jointly Gaussian, each with zero mean. $P_{y\tilde{y}} = E[x(k)\tilde{y}'(k+1|k)]$ and $P_{\tilde{y}\tilde{y}} = E[\tilde{y}(k+1|k)\tilde{y}'(k+1|k)]$. Hence,

$$\hat{x}(k|k+1) = \hat{x}(k|k) + P_{y\tilde{y}}M_{\tilde{y}\tilde{y}^{-1}}\tilde{y}(k+1|k) \quad (3.4.3)$$

It can be shown that

$$P_{y\tilde{y}} = E[x(k)\tilde{x}'(k|k)]\phi'(k+1, k)H'(k+1) \quad (3.4.4)$$

Since $x(k) = \tilde{x}(k|k) + \hat{x}(k|k)$, eqn.3.4.4 reduces to

$$P_{y\tilde{y}} = E[\tilde{x}(k|k)\tilde{x}'(k|k)]\phi'(k+1, k)H'(k+1) = P(k|k)\phi'(k+1, k)H'(k+1) \quad (3.4.5)$$

where $P(k|k)$ is the optimal filtering error covariance matrix. Also,

$$P_{\tilde{y}\tilde{y}} = E[\tilde{y}(k+1|k)\tilde{y}'(k+1|k)] = H(k+1)P(k+1|k)H'(k+1) + R(k+1) \quad (3.4.6)$$

where $P(k+1|k)$ is the optimal prediction error covariance matrix. The smoothing filter gain matrix, $P_{y\tilde{y}}P_{\tilde{y}\tilde{y}}^{-1}$, can be denoted as $M(k|k+1)$, where the two time instants represent the estimate and measurement time instants respectively. This gain can be shown to be equal to

$$M(k|k+1) = P(k|k)\phi'(k+1, k)H'(k+1)[H(k+1)P(k+1|k)H'(k+1) + R(k+1)]^{-1} \quad (3.4.7)$$

Now eqn.(3.4.3) can be written as:

$$\hat{x}(k|k+1) = \hat{x}(k|k) + M(k|k+1)[y(k+1) - H(k+1)\phi(k+1, k)\hat{x}(k|k)] \quad (3.4.8)$$

for $k = 0, 1, 2, \dots$, with $\hat{x}(0|0) = \tilde{x}(0) = 0$, as the initial condition. Eqn.(3.4.8) is the optimal single-stage smoothing algorithm. Here, the correction term is added to the corrected(filtered) estimate instead of to the predicted estimate as in KF. The gain matrix, $M(k|k+1)$ is different from the Kalman gain, $K(k+1)$. It can be shown that $K(k+1)$ is a factor of $M(k|k+1)$. From eqn.(3.4.8), it is clear that $\hat{x}(k|k)$ is an input of the smoothing filter at each instant. also, the computation of $M(k|k+1)$ requires $P(k|k)$ and $P(k+1|k)$ from the optimal Kalman filter. Hence, single-stage smoothing has to be accompanied by optimal filtering algorithm. Upon simplification, eqn.(3.4.7) can be expressed as

$$M(k|k+1) = A(k)K(k+1) \quad (3.4.9)$$

where,

$$A(k) = P(k|k)\phi'(k+1, k)P^{-1}(k+1|k) \quad (3.4.10)$$

It is obvious from eqn. (3.4.9) that $K(k+1)$ is a factor of $M(k|k+1)$. From eqns. (3.4.9) and (3.4.8), we can write

$$\hat{x}(k|k+1) = \hat{x}(k|k) + A(k)K(k+1)[y(k+1) - H(k+1)\phi(k+1, k)\hat{x}(k|k)] \quad (3.4.11)$$

$K(k + 1)[y(k + 1) - H(k + 1)\phi(k + 1, k)\hat{x}(k|k)]$ can be directly obtained from the optimal filter. A block diagram representing the single- stage smoothing algorithm is shown in Fig.3.4.

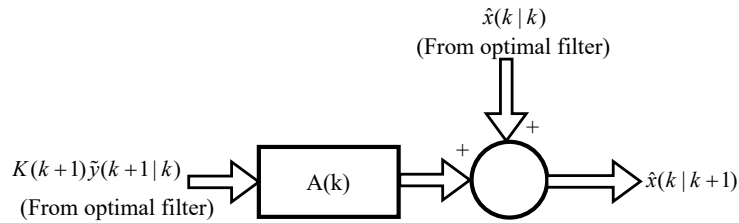


Figure 3.4: Block Diagram of Single- Stage Smoothing

3.5 Summary

In this chapter, a brief description of the three stages of estimation, namely, prediction, filtering and smoothing is given. The different types of smoothed estimates are outlined. Single-stage smoothing, which is the algorithm used in this thesis work is explained in the latter section of this chapter.

Uma Syamkumar “Smoothed Kalman Observer for Sensorless Field Oriented Control of Induction Motor.” Thesis. Department of Electrical Engineering, Government Engineering College, Trichur, University of Calicut, , 2020.

Chapter 4

Full Order Smoothed Observer for Speed Estimation of Three Phase Induction Motor

This chapter explains the speed estimation of the three phase induction motor using a full order observer. The observer is based on a smoothed Kalman filter. A fourth order model of the induction motor is used for this purpose. The stator currents and rotor currents in the dq reference frame are also estimated along with the rotor speed. The estimation results are compared with those obtained without smoothing.

4.1 Introduction

The dynamic performance of an induction motor can be improved by field- oriented control. By this method, the three phase induction machine is made to behave as a separately excited dc motor. The basic idea is to decompose the three phase voltage and current components into two phase quantities, thus reducing the number of voltages and currents to be controlled to four. The two stator current components are phase shifted by 90° and hence decoupled control is possible. Moreover, one component aligned along the d- axis(flux axis) controls the flux and the other aligned along the q-axis(torque axis) controls the torque.

Based on these transformations, a mathematical model of the machine can be obtained in the stator reference frame. This is suitable when the analysis of the machine fed from an inverter is to be carried out. In this model, the stator and rotor voltages are expressed in terms of the stator and rotor currents.

Observers are essential in field- oriented control of induction machines. This is because mounting of speed sensors on the rotor makes the system unreliable and unstable. Moreover, it is not advisable in high speed and high risk applications. A full- order observer estimates all the states of the system irrespective of whether it is measurable or not.

This chapter presents a full order observer for indirect field oriented control of induction motor. The observer is based on smoothed Kalman filter algorithm and

the simulation results are compared with those obtained with conventional extended Kalman filter.

The chapter is organised as follows: Section 4.2 elaborates the mathematical model of the three phase induction motor, section 4.3 explains the indirect field oriented control of induction motor using the full-order model of the machine, section 4.4 illustrates the estimation results which are obtained offline, using the conventional extended Kalman filter algorithm (section 4.4.1) and smoothed Kalman filter algorithm (section 4.4.2). Section 4.5 summarises the chapter.

4.2 Mathematical Model of Induction Motor

To begin with, the fourth order mathematical model of induction motor in the dq reference frame is considered. This model has four state variables, which are

- d - axis stator current, i_{ds}
- q - axis stator current, i_{qs}
- d - axis rotor current, i_{dr}
- q - axis rotor current, i_{qr}

The basic equation representing this model is given in eqn.(4.2.4). The stator voltage components are the inputs and the stator current components are the outputs.

$$x = \begin{bmatrix} i_{ds} & i_{qs} & i_{dr} & i_{qr} \end{bmatrix} \quad (4.2.1)$$

$$u = \begin{bmatrix} v_{ds} & v_{qs} \end{bmatrix} \quad (4.2.2)$$

$$y = \begin{bmatrix} i_{ds} & i_{qs} \end{bmatrix} \quad (4.2.3)$$

$$\dot{x} = \frac{1}{L_s L_r - L_m^2} * \begin{bmatrix} -R_s L_r & L_m^2 \omega_r & L_m R_r & L_m L_r \omega_r \\ -L_m^2 \omega_r & -R_s L_r & -L_m L_r \omega_r & L_m R_r \\ -L_m R_s & -L_m L_s \omega_r & -L_s R_r & -L_s L_r \omega_r \\ L_m L_s \omega_r & L_m R_s & L_s L_r \omega_r & -L_s R_r \end{bmatrix} * x$$

$$+ \frac{1}{L_s L_r - L_m^2} * \begin{bmatrix} L_r & 0 \\ 0 & L_r \\ -L_m & 0 \\ 0 & -L_m \end{bmatrix} * u$$
(4.2.4)

and

$$y = \begin{bmatrix} 1 & 0 & 0 & 0 \\ 0 & 1 & 0 & 0 \end{bmatrix} * x$$
(4.2.5)

To this fourth order system, the rotor speed, ω_r is added as a fifth state variable, thus making the system fifth order. The rotor speed is not considered as a constant, instead it is governed by the mechanical equation of the motor, given by

$$T_e = J \frac{d\omega_r}{dt} + B\omega_r + T_L$$
(4.2.6)

where, J is the moment of inertia, B is the viscous friction coefficient and T_L is the load torque. Addition of ω_r to the state matrix, gives rise to a system matrix involving multiplication of states, which makes the system non-linear. This model can now be converted into a discrete time-varying model as given in eqns. (4.2.7) and (4.2.8) [24].

$$x(k+1) = f(x(k), u(k))$$

$$= \mathbf{f}(x(k))x(k) + \mathbf{g}u(k)$$
(4.2.7)

$$y(k) = h(x(k))x(k)$$

$$= \mathbf{H}x(k)$$
(4.2.8)

where

$$x(k) = \begin{bmatrix} i_{ds}(k) & i_{qs}(k) & i_{dr}(k) & i_{qr}(k) & \omega_r(k) \end{bmatrix}$$
(4.2.9)

$$u(k) = \begin{bmatrix} v_{ds}(k) & v_{qs}(k) \end{bmatrix}$$
(4.2.10)

$$y(k) = \begin{bmatrix} i_{ds}(k) & i_{qs}(k) \end{bmatrix} \quad (4.2.11)$$

$$\underbrace{\begin{bmatrix} i_{ds}(k+1) \\ i_{qs}(k+1) \\ i_{dr}(k+1) \\ i_{qr}(k+1) \\ \omega_r(k+1) \end{bmatrix}}_{\mathbf{x}(k+1)} = \underbrace{\begin{bmatrix} a_{11} & a_{12}\omega_r(k) & a_{13} & a_{14}\omega_r(k) & 0 \\ a_{21}\omega_r(k) & a_{22} & -a_{23}\omega_r(k) & a_{24} & 0 \\ a_{31} & -a_{32}\omega_r(k) & a_{33} & -a_{34}\omega_r(k) & 0 \\ a_{41}\omega_r(k) & a_{42} & a_{43}\omega_r(k) & a_{44} & 0 \\ -a_{51}i_{qr}(k) & 0 & a_{51}i_{qs}(k) & 0 & 1 \end{bmatrix}}_{\mathbf{f}(\mathbf{x}(k))} \underbrace{\begin{bmatrix} i_{ds}(k) \\ i_{qs}(k) \\ i_{dr}(k) \\ i_{qr}(k) \\ \omega_r(k) \end{bmatrix}}_{\mathbf{x}(k)} + \underbrace{\begin{bmatrix} a_{15} & 0 & a_{35} & 0 & 0 \\ 0 & a_{25} & 0 & a_{45} & 0 \end{bmatrix}^T}_{\mathbf{B}} \underbrace{\begin{bmatrix} v_{ds}(k) \\ v_{qs}(k) \end{bmatrix}}_{\mathbf{u}(k)} + \mathbf{w}(k) \quad (4.2.12)$$

$$\underbrace{\begin{bmatrix} i_{ds}(k) \\ i_{qs}(k) \end{bmatrix}}_{\mathbf{y}(k)} = \underbrace{\begin{bmatrix} 1 & 0 & 0 & 0 & 0 \\ 0 & 1 & 0 & 0 & 0 \end{bmatrix}}_{\mathbf{H}} \mathbf{x}(k) + \mathbf{v}(k) \quad (4.2.13)$$

$$\begin{aligned} a_{11} &= 1 - \frac{R_s L_r t_s}{a_0}; & a_{12} &= \frac{L_m^2 t_s}{a_0}; & a_{13} &= \frac{R_r L_m t_s}{a_0}; & a_{14} &= \frac{-L_s L_m t_s}{a_0}; & a_{15} &= \frac{L_r t_s}{a_0}; \\ a_{21} &= \frac{-L_m^2 t_s}{a_0}; & a_{22} &= 1 - \frac{R_s L_r t_s}{a_0}; & a_{23} &= \frac{-L_m L_r t_s}{a_0}; & a_{24} &= a_{13}; & a_{25} &= a_{15}; \\ a_{31} &= \frac{L_m R_s t_s}{a_0}; & a_{32} &= \frac{-L_m L_s t_s}{a_0}; & a_{33} &= 1 - \frac{-L_s R_r t_s}{a_0}; & a_{34} &= \frac{-L_s L_r t_s}{a_0}; & a_{35} &= \frac{-L_m t_s}{a_0}; \\ a_{41} &= -a_{32}; & a_{42} &= a_{31}; & a_{43} &= -a_{34}; & a_{44} &= a_{33}; & a_{45} &= -a_{35}; \\ a_{51} &= \frac{3P}{2} \frac{L_m}{J} t_s; & a_0 &= L_s L_r - L_m^2 \end{aligned}$$

Since $i_{ds}(k)$ and $i_{qs}(k)$ are the output variables, the matrix, H is,

$$H = \begin{bmatrix} 1 & 0 & 0 & 0 & 0 \\ 0 & 1 & 0 & 0 & 0 \end{bmatrix} \quad (4.2.14)$$

R_s , R_r and L_s , L_r are the resistances and inductances of the stator and rotor respectively. L_m is the mutual inductance, ω_r is the rotor speed in rad/sec and t_s is the sampling time in seconds. The parameters of the induction motor used in the experimental work are given in Table. 4.1.

Table 4.1: Parameters of the Induction Motor

Parameter	Value
Power	0.75KW
Rated Speed, N	1390 rpm
Stator Resistance, R_1	10.5 Ω
Rotor Resistance, R_2	10.03 Ω
Stator Inductance, L_1	0.5926mH
Rotor Inductance, L_2	0.5863mH
Mutual Inductance, L_m	0.5495mH
Moment of Inertia, J	0.0013kgm ²
Number of poles, P	4
Frequency, f	50Hz

4.3 Indirect field-oriented sensorless control of three-phase induction motor

The sensorless control of three phase induction motor is accomplished using an observer. Extended Kalman filters are very advantageous in estimation, especially in the presence of noise. The induction motor is prone to noise in the form of measurement noise and process noise. This is taken into account while modelling the machine. The process noise and measurement noise are added to the mathematical equation of the motor as shown in equation 4.3.1 and 4.3.2, thus making the model stochastic.

$$\begin{aligned} x(k+1) &= f(x(k), u(k)) + w(k) \\ &= \mathbf{f}(x(k))x(k) + \mathbf{g}u(k) + w(k) \end{aligned} \quad (4.3.1)$$

$$\begin{aligned} y(k) &= h(x(k))x(k) + v(k) \\ &= \mathbf{H}x(k) + v(k) \end{aligned} \quad (4.3.2)$$

$w(k)$ and $v(k)$ are Gaussian white noises having \mathbf{Q} and \mathbf{R} as the covariance matrices, which are characterized by

$$E(w(i)) = 0 \quad (4.3.3a)$$

$$E(v(i)) = 0 \quad (4.3.3b)$$

$$E(w(i)w(j)^T) = Q\delta(i, j) \quad (4.3.3c)$$

$$E(v(i)w(j)^T) = R\delta(i, j) \quad (4.3.3d)$$

A block diagram of the proposed drive system is shown in Fig.4.1. The reference speed is compared with the actual speed of the machine. This error drives a speed controller, which generates the reference torque. The reference q -axis stator current is calculated from the reference torque using the relation,

$$I_{qs}^* = \frac{2}{3} \frac{2}{P} \frac{L_r}{L_m} * T_e \quad (4.3.4)$$

The reference d and q axes stator currents are converted to three phase abc reference currents, using the 2-3-phase transformation and fed to a hysteresis current controller. The hysteresis current controller compares the reference currents with the actual currents of the motor and generate the gate signals for the inverter.

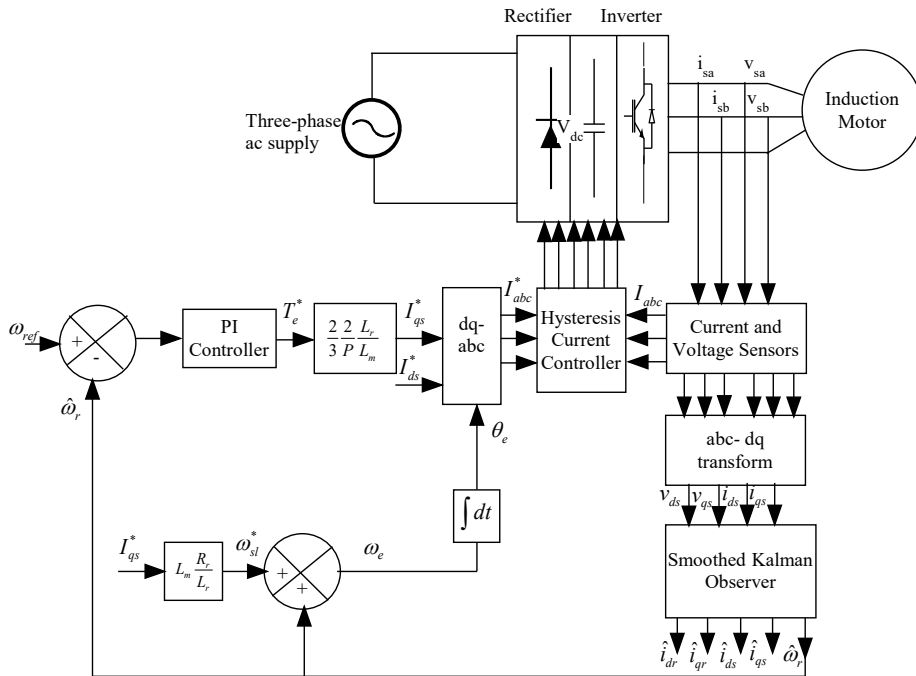


Figure 4.1: Block diagram of the proposed drive system

4.4 Offline Estimation Results

In the offline analysis, the induction machine is made to run in indirect vector control mode and the stator voltages, currents and rotor speed are measured. Fig.4.2 shows the d and q axis components of the measured stator voltage for a small period of time.

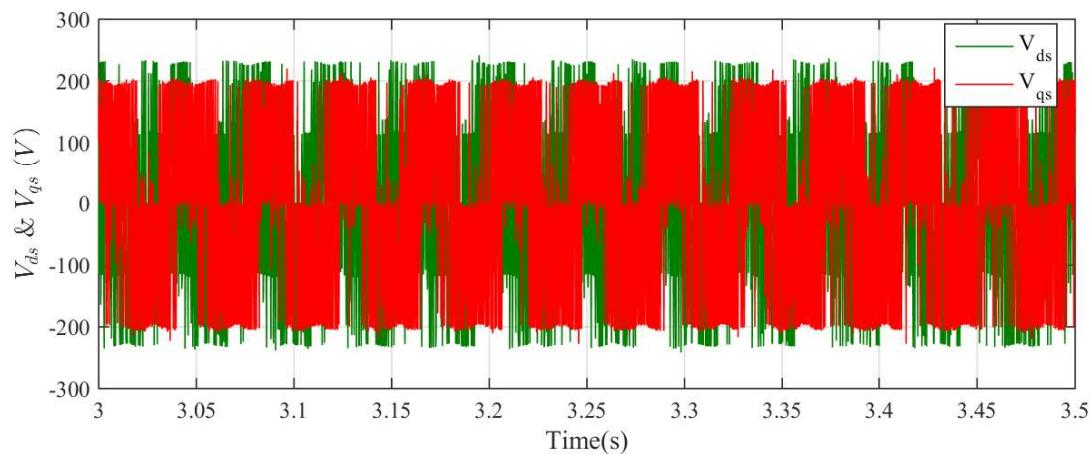


Figure 4.2: The stator stationary axis components of measured stator voltages, v_{ds} and v_{qs}

Fig.4.3 shows the corresponding d and q axis components of stator currents for the same time period.

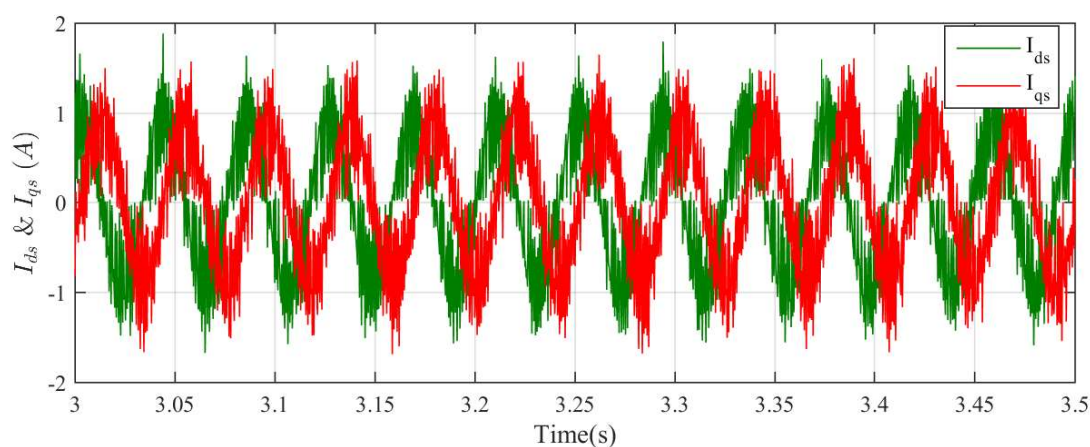


Figure 4.3: The stator stationary axis components of measured stator currents i_{ds} and i_{qs}

4.4.1 Estimation using conventional extended Kalman observer

The stator voltages and currents measured from the indirect vector controlled IM drive are given as inputs to the observer based on conventional extended Kalman filter algorithm and all the state variables are estimated. The algorithm is tested for two different reference rotor angular velocities- one, a step reference of magnitude 75rad/s at t=0 and the second one a step whose magnitude changes from 20rad/s to 75rad/s at t=2s and then to 50rad/s at t=4.5s. The estimation results with the conventional EKF observer for the first reference speed are shown in Figs.4.4- 4.7. Fig.4.4 shows the estimated and measured rotor speed. It can be seen that even though the observer is tracking the measured speed in steady state, the estimation in the transient region is erroneous.

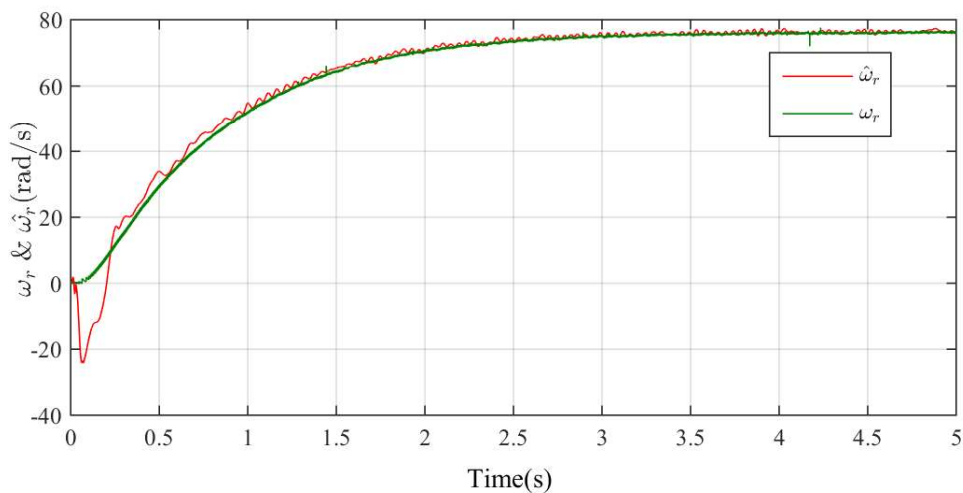


Figure 4.4: Estimated and measured ω_r for a reference speed of 75 rad/s(mech.) at t=0s and with a conventional EKF observer

Figs.4.5 and 4.6 depicts the estimated and measured stator current components at this reference speed.

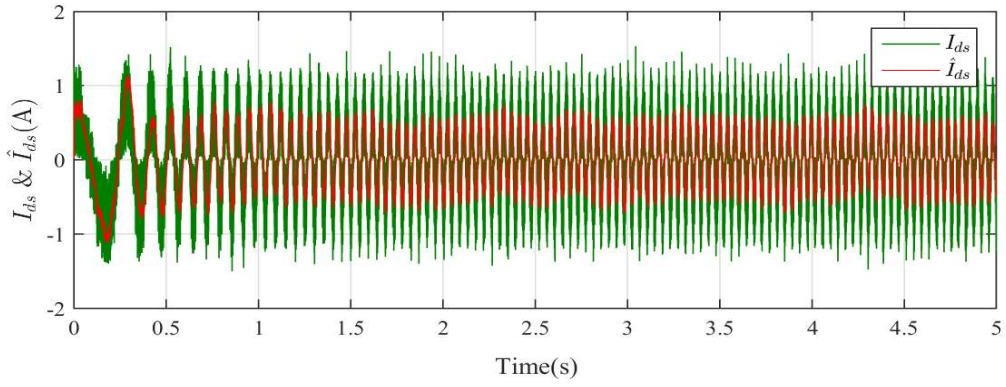


Figure 4.5: Estimated and measured i_{ds} for a reference speed of 75 rad/s(mech.) at $t=0$ s and with a conventional EKF observer

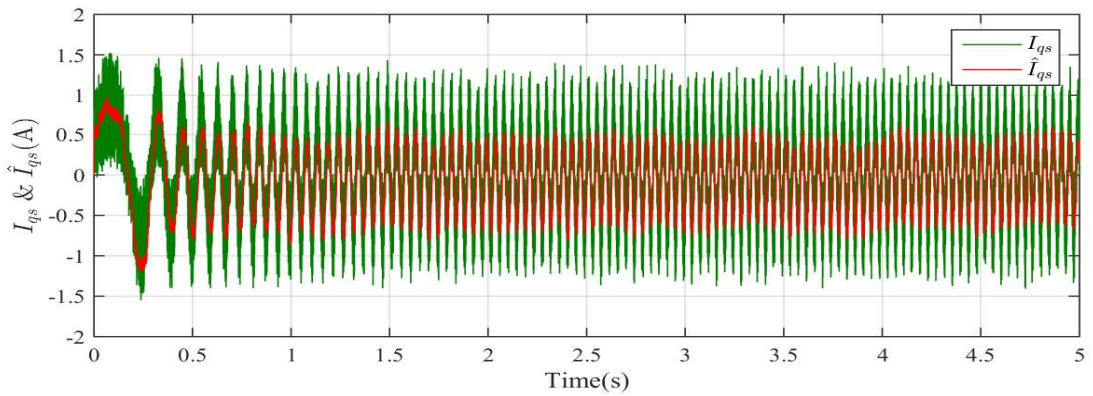


Figure 4.6: Estimated and measured i_{qs} for a reference speed of 75 rad/s(mech.) at $t=0$ s and with a conventional EKF observer

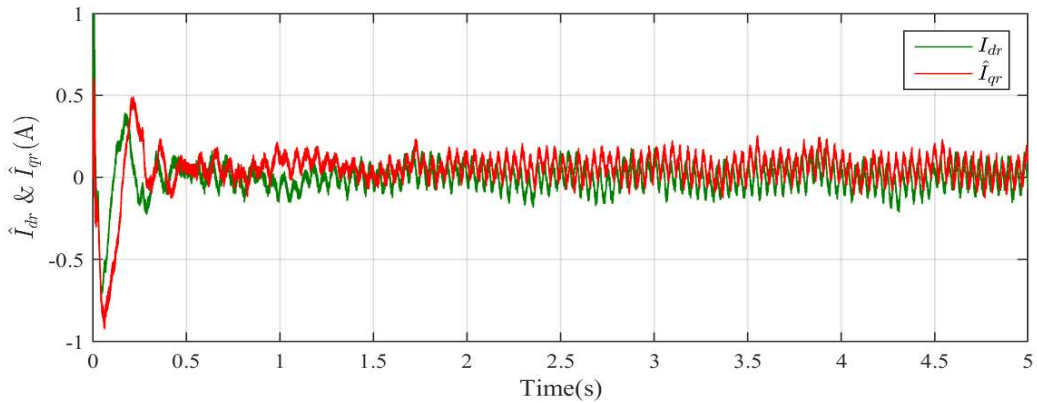
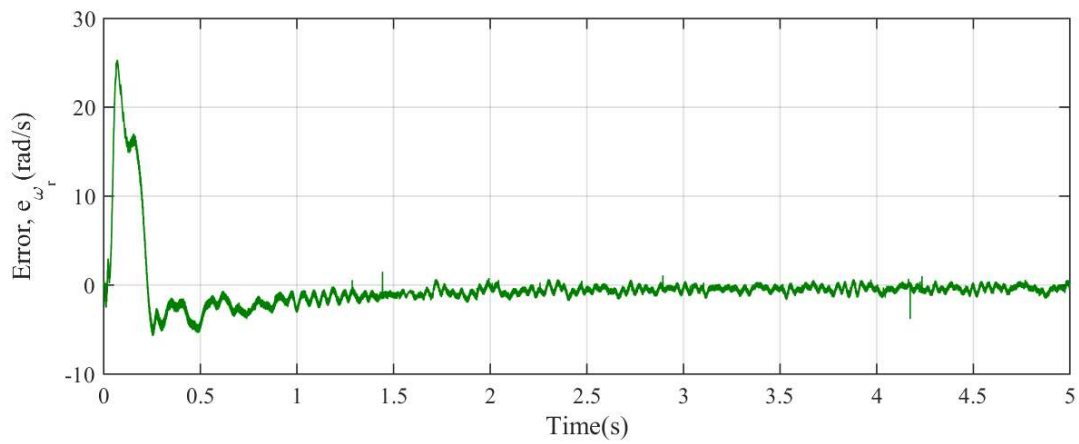


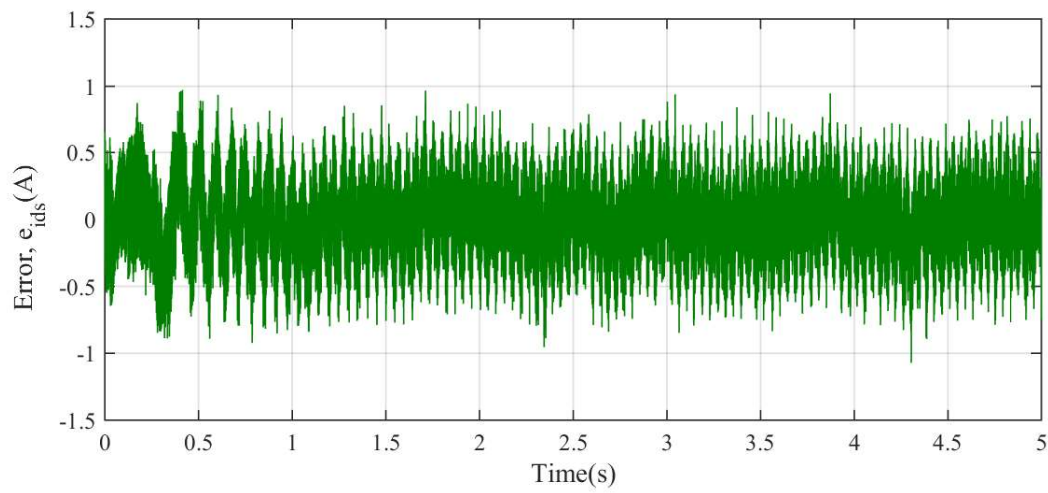
Figure 4.7: Estimated i_{dr} and i_{qr} for a reference speed of 75 rad/s(mech.) at $t=0$ s and with a conventional EKF observer

Fig.4.7 shows the observed values of rotor currents, as obtained from the observer. The error between the measured and estimated values of rotor speed and stator d and q axes components of currents are shown in Figs.4.8a,4.8b and 4.8c

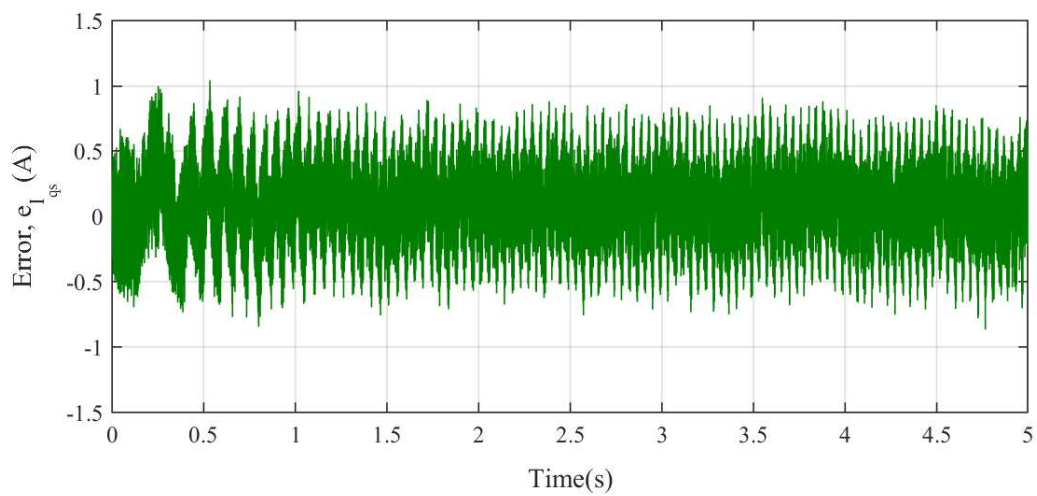
respectively.



(a)



(b)



(c)

Figure 4.8: Error between the measured and estimated values of a) ω_r b) I_{ds} and c) I_{qs} using conventional Kalman observer

As a second experiment, a time- varying reference speed is applied. Figs.4.9, 4.10,4.11, 4.12 show the estimated and measured values of ω_r , the d and q axes stator currents and the d and q axes rotor currents, respectively.

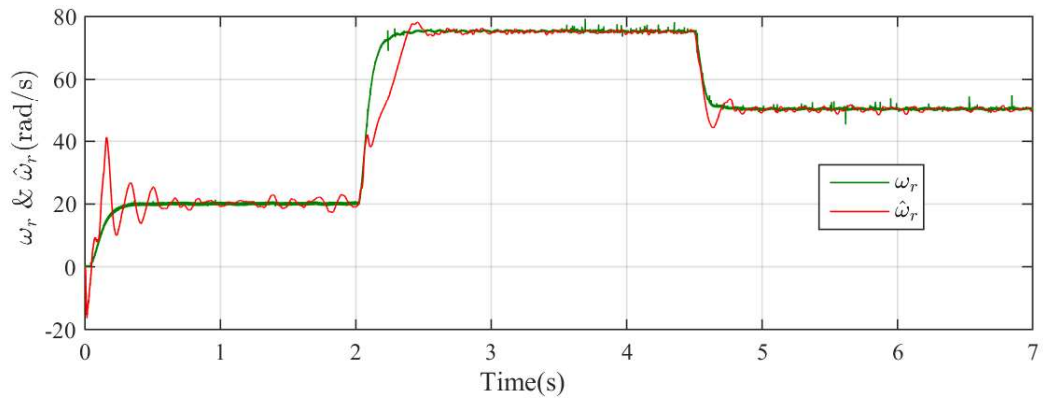


Figure 4.9: Estimated and measured ω_r for reference speed of 20 rad/s(mech.) from 0s to 2s and 75 rad/s from t=2s to 4.5s and 50rad/s from t=4.5s to 7s with conventional EKF observer

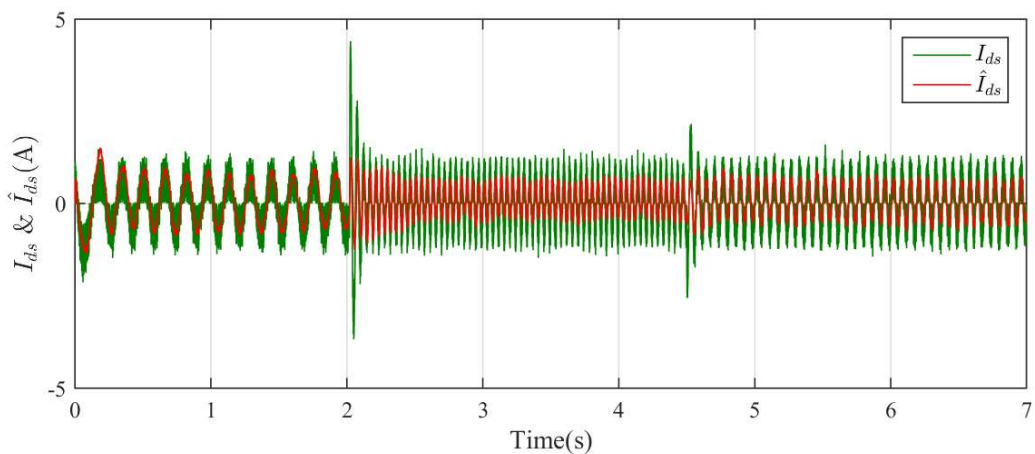


Figure 4.10: Estimated and measured i_{ds} for reference speed of 20 rad/s(mech.) from 0s to 2s and 75 rad/s from t=2s to 4.5s and 50rad/s from t=4.5s to 7s with conventional EKF observer

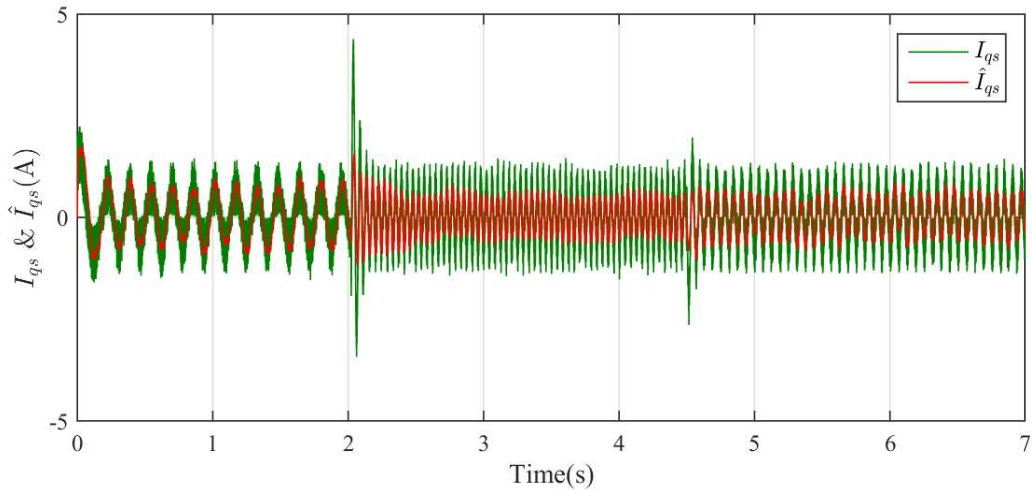


Figure 4.11: Estimated and measured i_{qs} for reference speed of 20 rad/s(mech.) from 0s to 2s and 75 rad/s from t=2s to 4.5s and 50rad/s from t=4.5s to 7s with conventional EKF observer

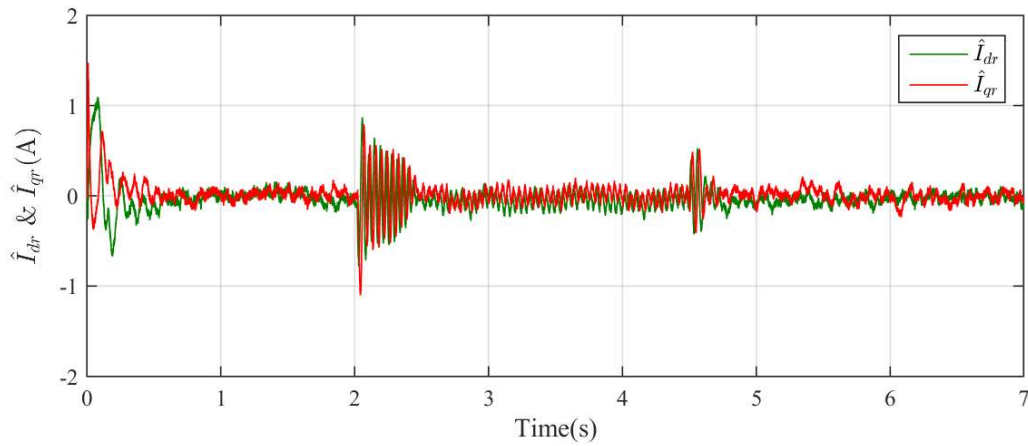
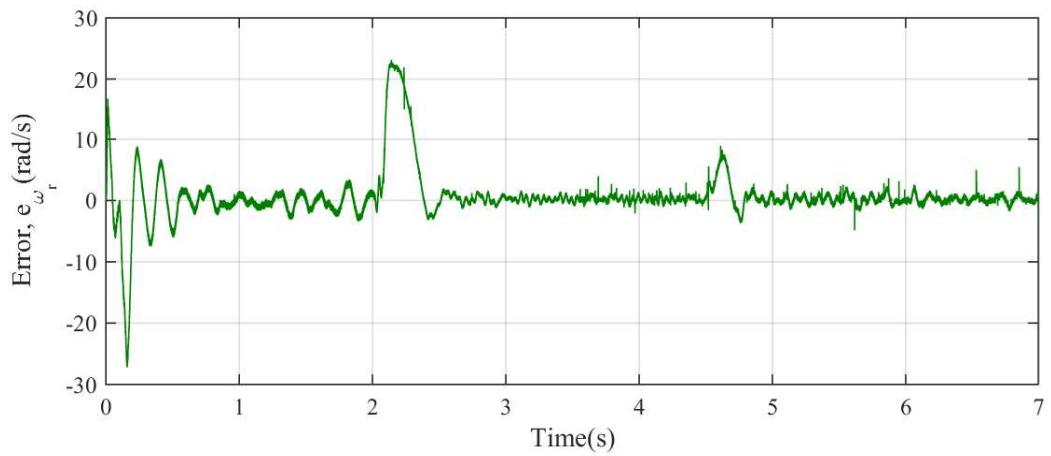
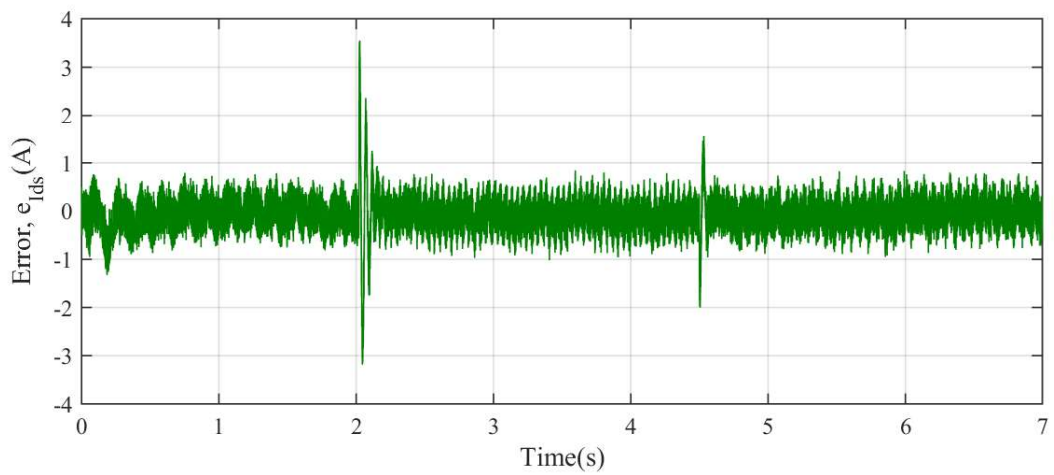


Figure 4.12: Estimated i_{dr} and i_{qr} for reference speed of 20 rad/s(mech.) from 0s to 2s and 75 rad/s from t=2s to 4.5s and 50rad/s from t=4.5s to 7s with conventional EKF observer

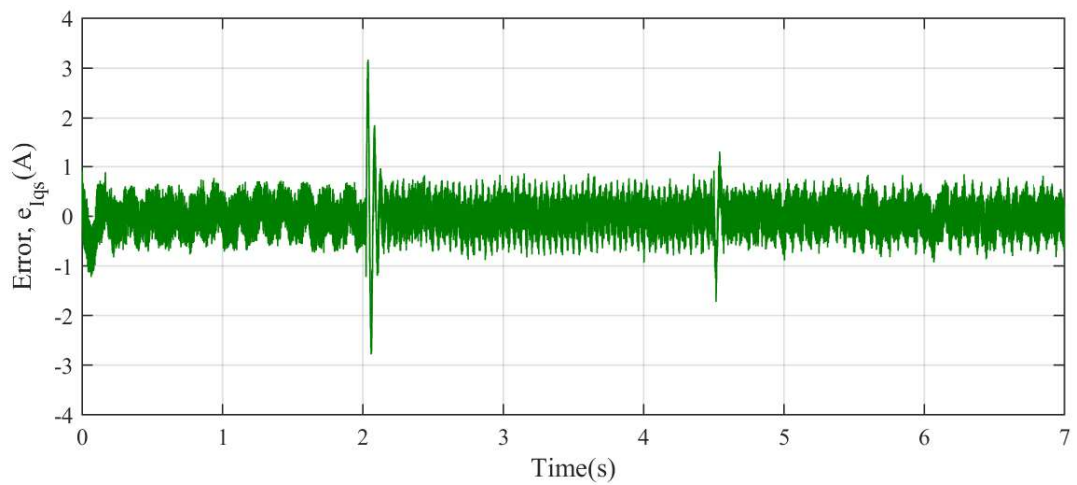
The error between the measured and estimated values of rotor speed and stator d and q axes components are shown in Figs.4.13a,4.13b and 4.13c.



(a)



(b)



(c)

Figure 4.13: Error between the measured and estimated values of a) ω_r , b) I_{ds} and c) I_{qs} using conventional Kalman observer

4.4.2 Estimation using smoothed Kalman observer

Estimation is done using the smoothed Kalman observer, with the same values of process and measurement noise covariance matrices. Fig.4.14 shows the measured and estimated values of rotor speed. The estimated and measured stator currents as well as the estimated rotor currents are shown in Figs.4.15,4.16 and 4.17 respectively. The results show a noticeable improvement in the estimates using the smoothed algorithm, which is prominent in the transient region.

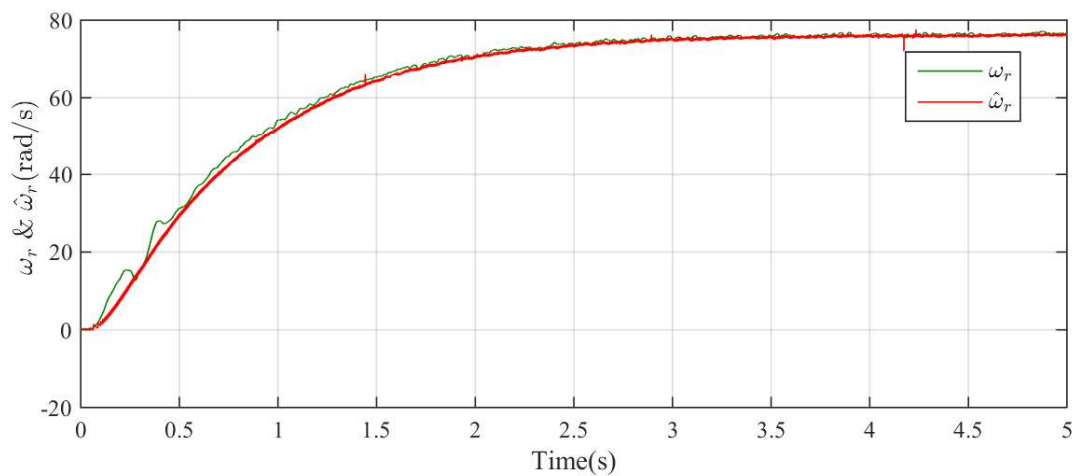


Figure 4.14: Simulation results for a reference speed of 75 rad/s(mech.) at t=0s and with smoothed Kalman observer

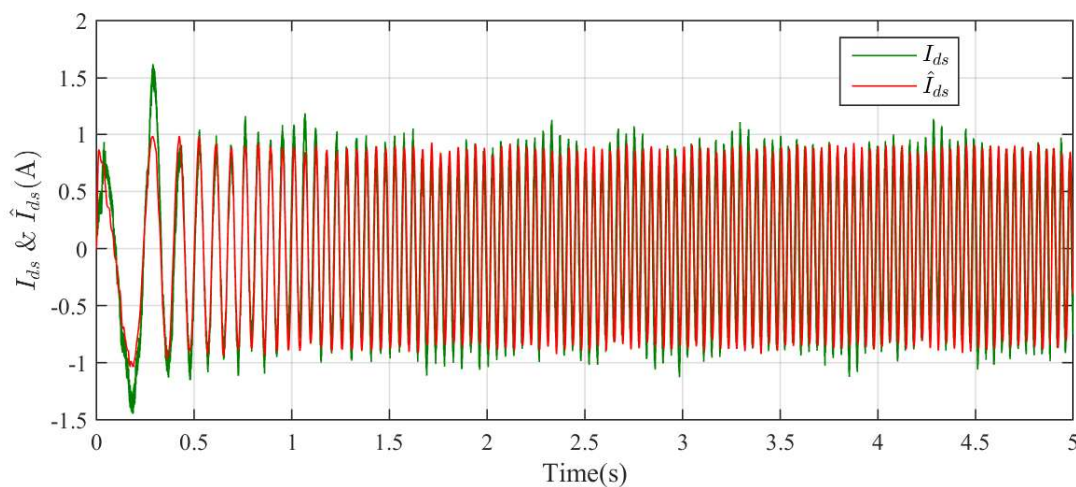


Figure 4.15: Estimated and measured i_{ds} for a reference speed of 75 rad/s(mech.) at t=0s and with a smoothed Kalman observer

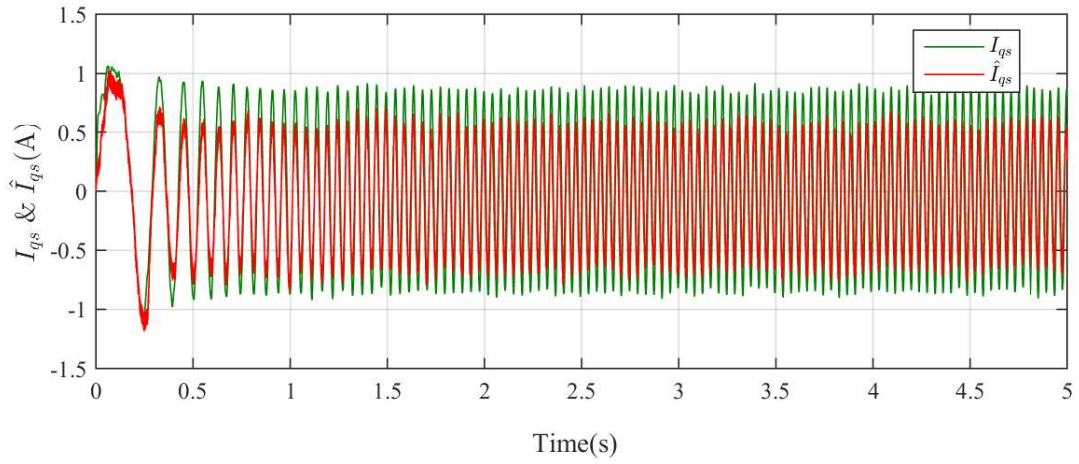


Figure 4.16: Estimated and measured i_{qs} for a reference speed of 75 rad/s(mech.) at $t=0$ s and with a smoothed Kalman observer

Fig.4.17 shows the estimates of rotor currents as obtained from the observer.

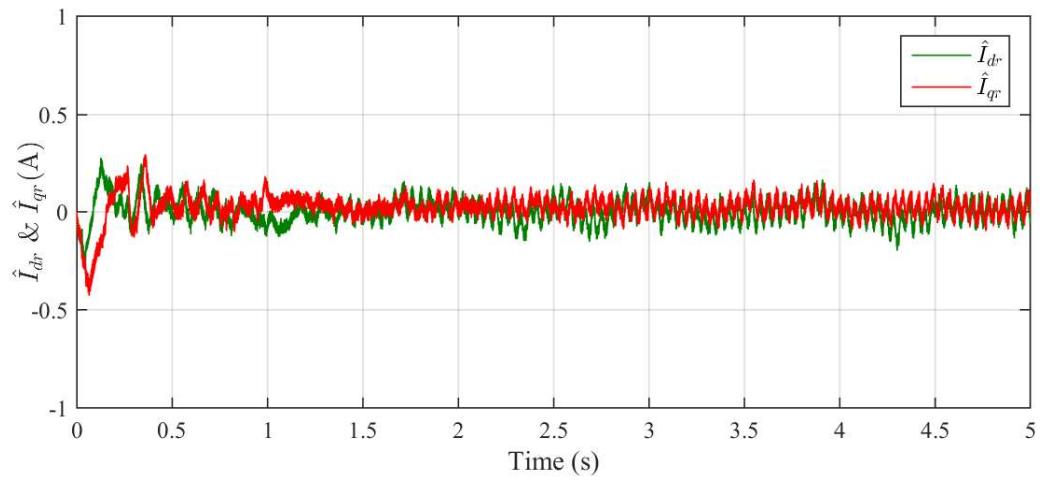
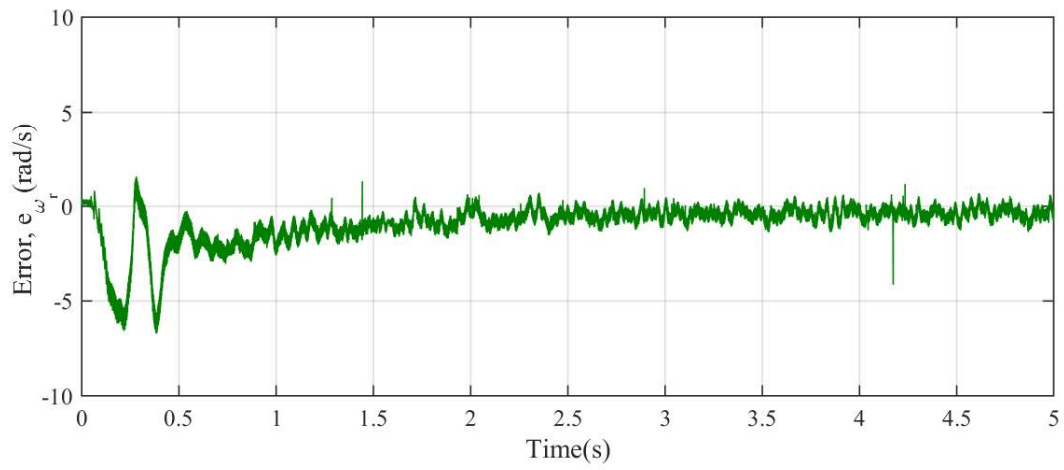
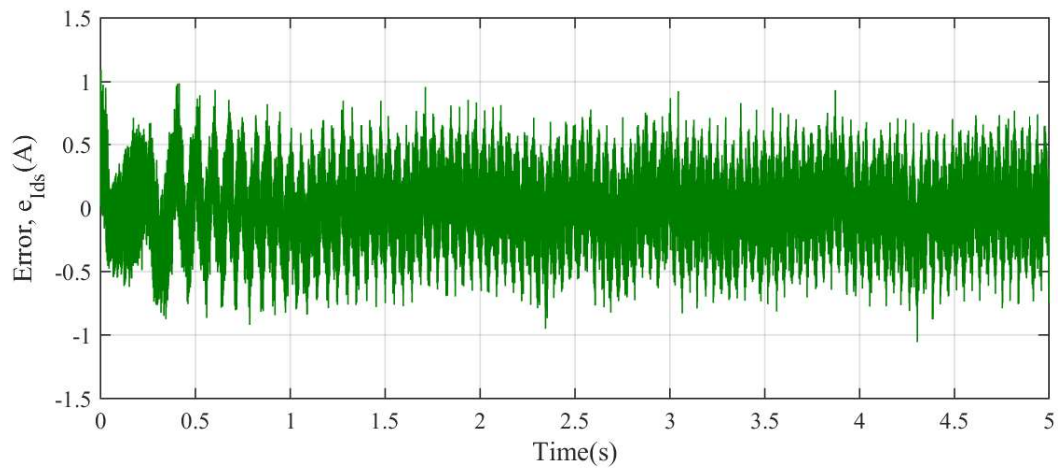


Figure 4.17: Estimated i_{dr} and i_{qr} for a reference speed of 75 rad/s(mech.) at $t=0$ s and with a smoothed Kalman observer

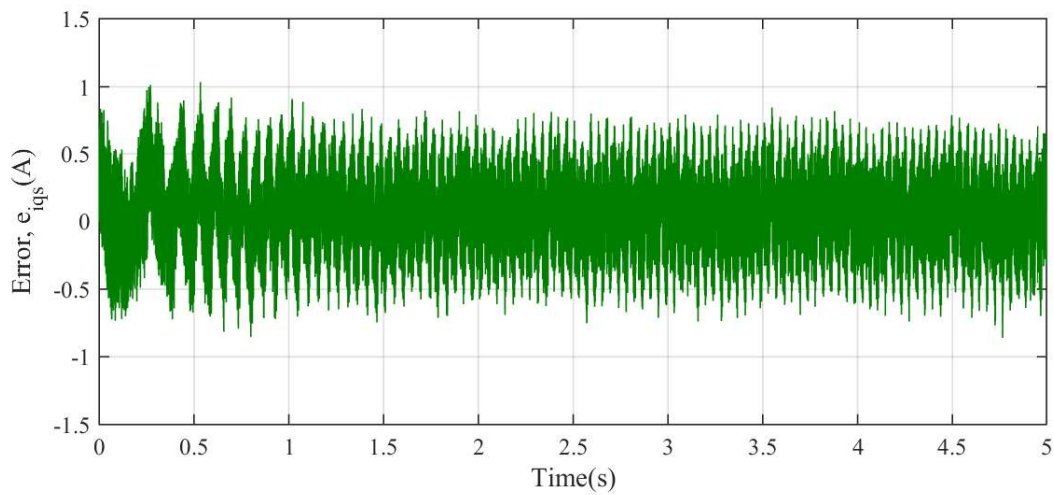
The error between the measured and estimated values of rotor speed and stator d and q axes components are shown in Figs.4.18a,4.18b and 4.18c.



(a)



(b)



(c)

Figure 4.18: Error between the measured and estimated values of a) ω_r b) I_{ds} and c) I_{qs} using smoothed Kalman observer

Figs.4.19 shows the speed estimates for a varying reference speed. The corresponding stator and rotor current estimates are shown in Fig.4.20,4.21,4.22 respectively.

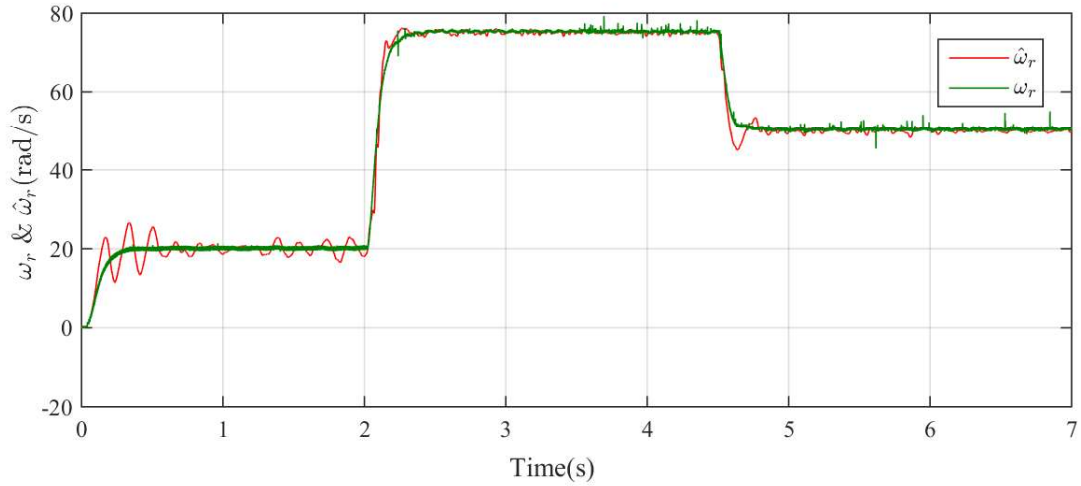


Figure 4.19: Simulation Results for reference speed of 20 rad/s(mech.) from 0s to 2s and 75 rad/s from t=2s to 4.5s and 50rad/s from t=4.5s to 7s with smoothed Kalman observer

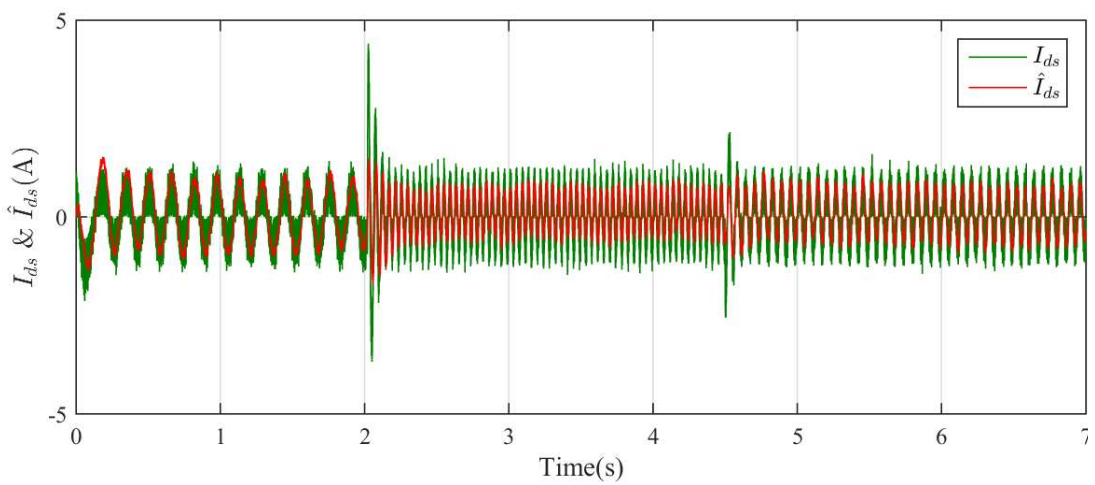


Figure 4.20: Estimated and measured i_{ds} for reference speed of 20 rad/s(mech.) from 0s to 2s and 75 rad/s from t=2s to 4.5s and 50rad/s from t=4.5s to 7s with smoothed Kalman observer

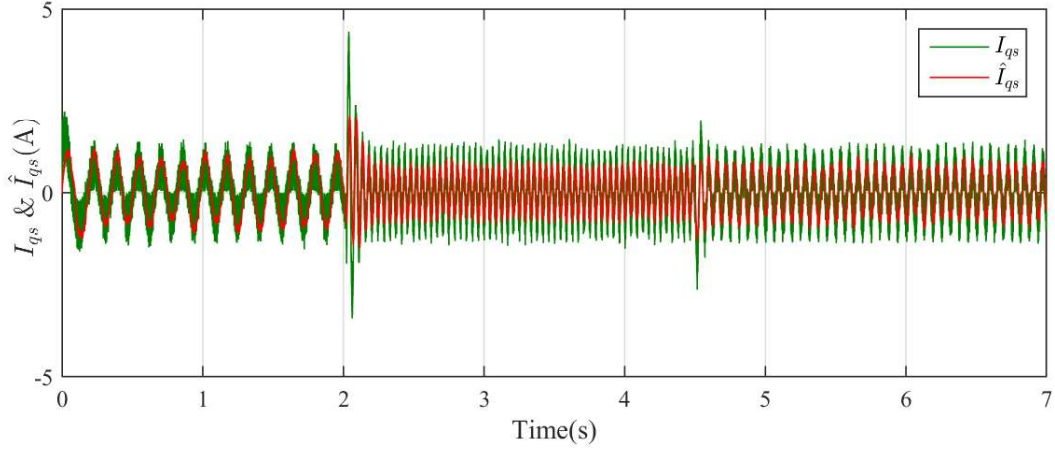


Figure 4.21: Estimated and measured i_{qs} for reference speed of 20 rad/s(mech.) from 0s to 2s and 75 rad/s from t=2s to 4.5s and 50rad/s from t=4.5s to 7s with smoothed Kalman observer

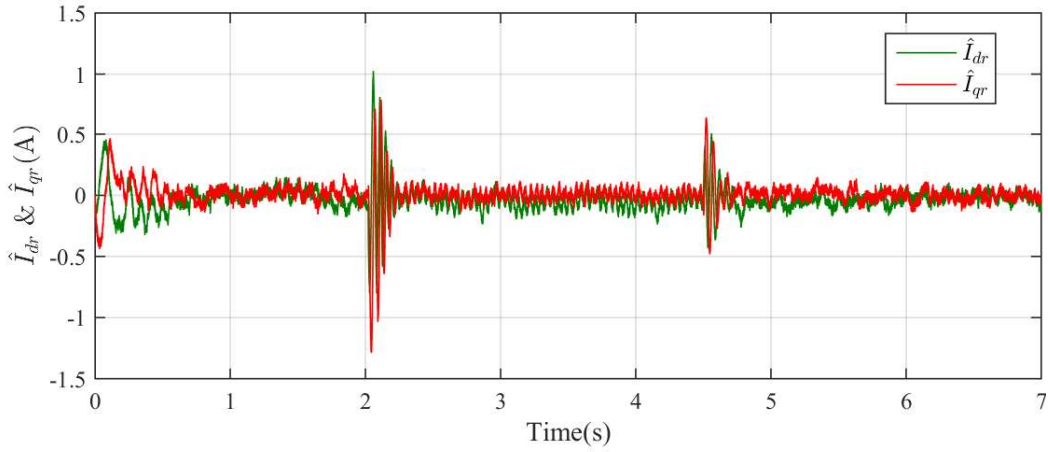
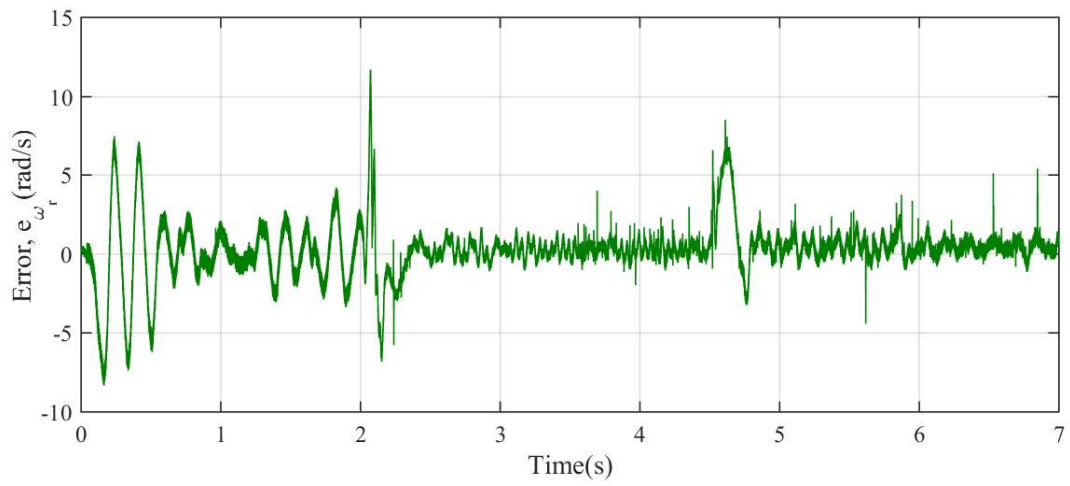
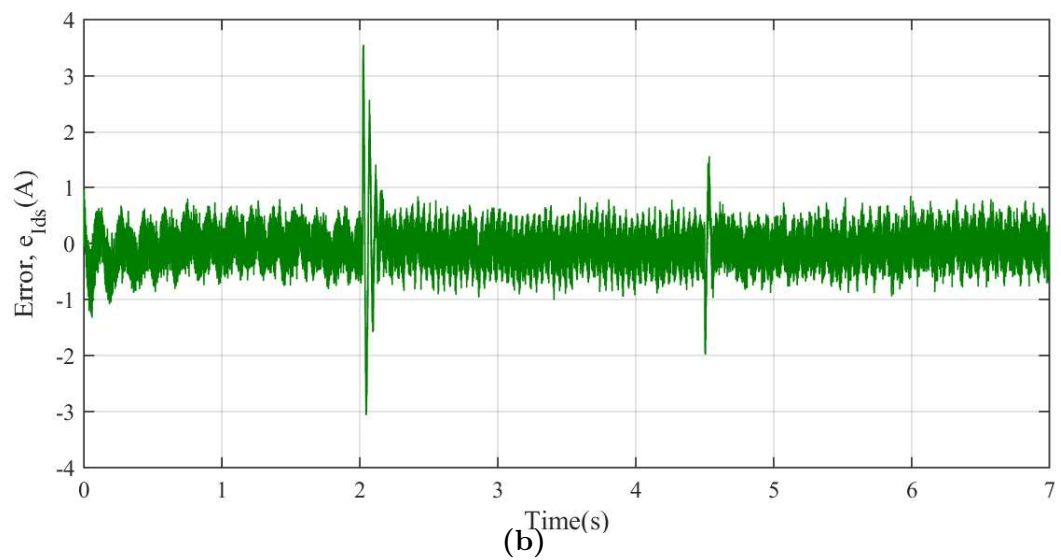


Figure 4.22: Estimated i_{dr} and i_{qr} for reference speed of 20 rad/s(mech.) from 0s to 2s and 75 rad/s from t=2s to 4.5s and 50rad/s from t=4.5s to 7s with smoothed Kalman observer

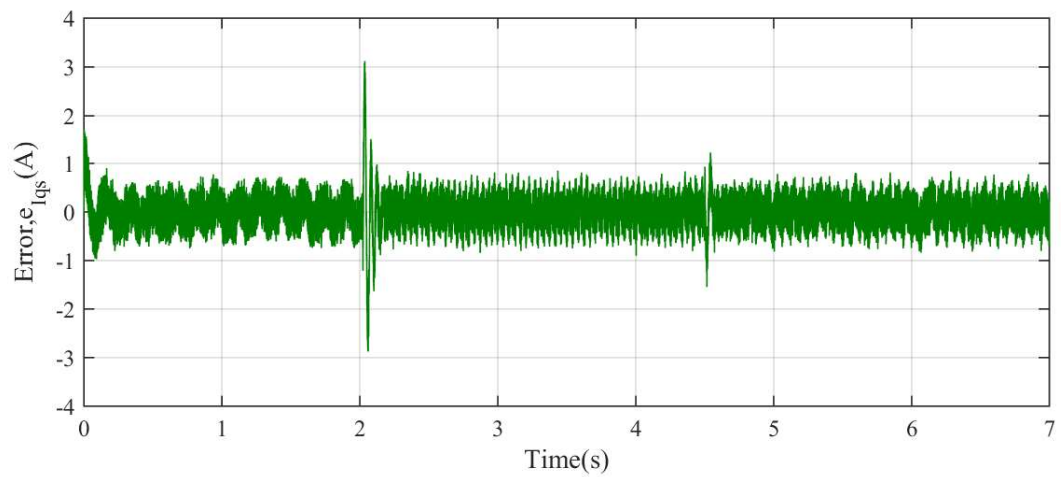
The error between the measured and estimated values of rotor speed and stator d and q axes components are shown in Figs.4.23a,4.23b and 4.23c.



(a)



(b)



(c)

Figure 4.23: Error between the measured and estimated values of a) ω_r , b) I_{ds} and c) I_{qs} using smoothed Kalman observer

A plot of the rotor flux estimate is shown in Fig. 4.24.

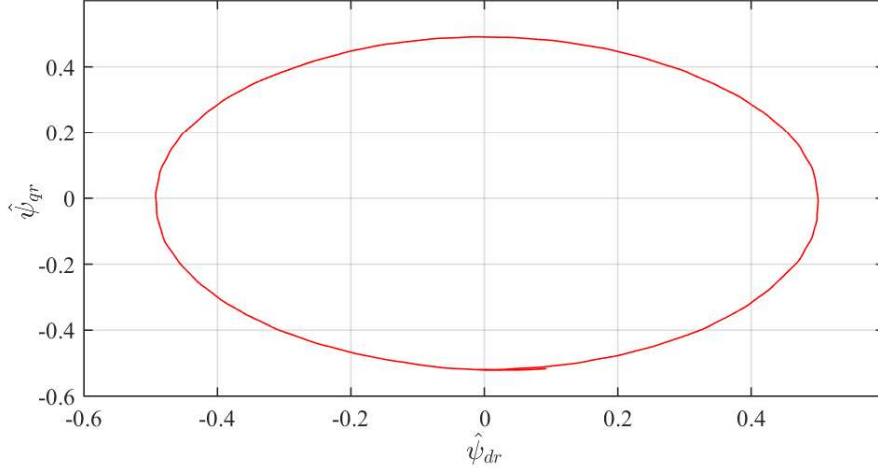


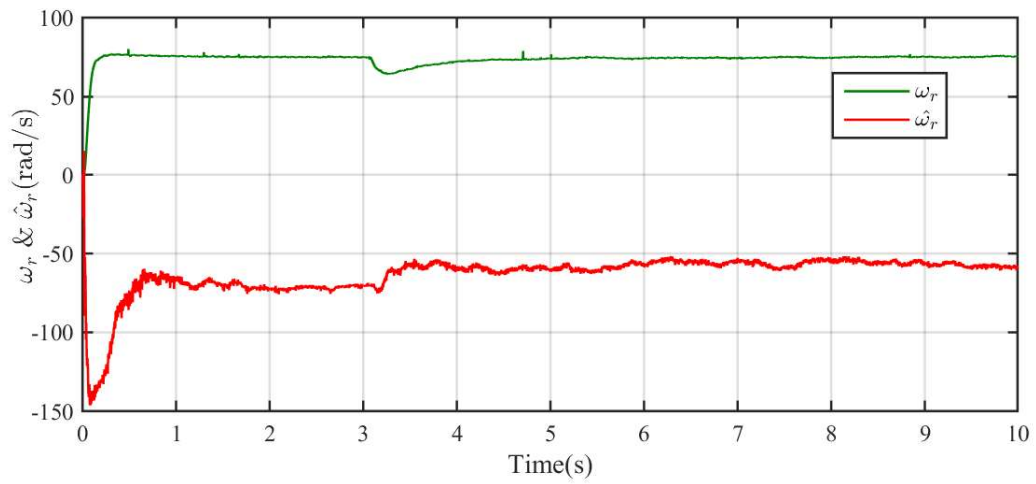
Figure 4.24: Plot of the d and q axis components of rotor flux using smoothed Kalman observer

A load was applied to the machine through a resistive load connected to the dc generator coupled to the induction motor. A resistor connected to the terminals of the dc machine armature is used to vary the load torque applied to the induction motor, based on $T_L = \frac{K_t^2 \omega}{R}$, where K_t is the torque constant of the dc machine, ω is the angular velocity and R is the total resistance. The induction motor is run in closed loop with a reference speed of 75rad/s and a load torque of 4Nm was applied at 3s. The stator currents measured in this context were applied offline to the conventional and smoothed Kalman observers for speed estimation. Fig.4.25a shows the estimation performance with a conventional Kalman observer and Fig.4.25b shows the improvement in the estimate with a smoothed Kalman observer. As can be seen, the speed estimate with the conventional observer shows a reversal of speed, whereas the smoothed estimate is found to track the measured speed except for an initial overshoot. Here also, the covariance matrices are maintained the same. The values of the noise covariance matrices used throughout the simulation are:

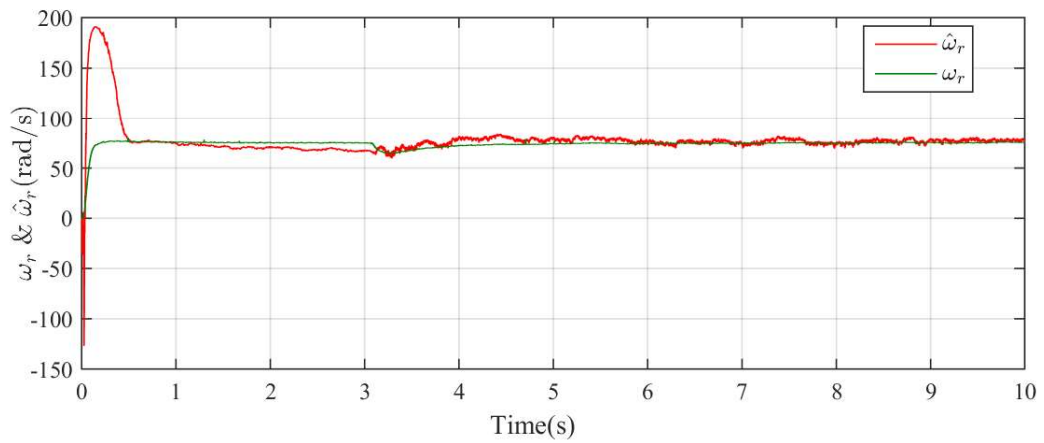
$$\mathbf{Q} = \begin{bmatrix} 10^{-8} & 0 & 0 & 0 & 0 \\ 0 & 10^{-8} & 0 & 0 & 0 \\ 0 & 0 & 10^{-8} & 0 & 0 \\ 0 & 0 & 0 & 10^{-8} & 0 \\ 0 & 0 & 0 & 0 & 10^{-8} \end{bmatrix}$$

and

$$\mathbf{R} = \begin{bmatrix} 300 & 0 \\ 0 & 300 \end{bmatrix}$$



(a)



(b)

Figure 4.25: Simulation results for reference speed of 75 rad/s(mech.) with a torque applied at $t= 3s$ a) conventional and b) smoothed Kalman Observer

4.5 Summary

This chapter presents a smoothed Kalman observer for estimating the rotor speed of a three phase induction motor. A fifth order mathematical model of the motor is used. The rotor speed, ω_r is considered as a state variable and is governed by the mechanical equation of the motor, rather than a constant. Single- stage smoothing is applied to the extended Kalman filter algorithm and is used as an observer for estimation of all the state variables. The stator currents, which are the output variables are also observed, thus making the observer full- order.

The estimation results obtained with the smoothed Kalman observer are compared with those obtained with a conventional extended Kalman observer. Estimation results for two different reference speeds are presented. On comparison of figures, 4.4 and 4.14, it can be seen that the speed estimation has improved on incorporating smoothing. Smoothing has also given a better result in estimation of the stator currents, i_{ds} and i_{qs} also. This is evident from the error curves of Fig. 4.8a-4.8c and Fig. 4.18a-4.18c. Similar betterment is obtained for a varying reference speed also. The improvement in the speed estimation is mainly in the transient region of response, thus improving the dynamic response of the system.

Uma Syamkumar “Smoothed Kalman Observer for Sensorless Field Oriented Control of Induction Motor.” Thesis. Department of Electrical Engineering, Government Engineering College, Trichur, University of Calicut, , 2020.

Chapter 5

Real-time implementation of the smoothed Kalman algorithm based full-order observer

This chapter presents the real-time implementation of the smoothed Kalman filter based observer for indirect field-oriented control of three-phase induction motor. The closed loop observer based system is implemented using the full-order model of the machine. The results are compared with those of a conventional EKF based observer.

5.1 Introduction

The simulation studies performed in the previous chapter are validated experimentally. The real-time implementations are performed with the help of a data acquisition card of National Instruments. The full-order observer algorithm is tested for indirect field-oriented control of induction motor in closed loop. The efficacy of the algorithm is confirmed for various reference speeds, including low and zero speeds.

This chapter is organised as follows: Section 5.2 explains the hardware set up of the system, section 5.3 shows the results of closed loop performance of the system with a smoothed Kalman based observer. The performance of the system with a conventional EKF based observer is elaborated in section 5.4. Section 5.5 summarises the chapter.

5.2 Experimental Setup

For the experimental validation of the offline estimation results, the speed estimate given by the observer is used as feedback in the indirect field-oriented control of the motor. A block diagram of the experimental set up is shown in Fig.5.1.

- a level- shifter board
- INST 2IV- sensor board is used for measuring the stator currents and voltages.
- a voltage source inverter stack of Semikron.
- a tachogenerator with 15V/1500rpm, measures the rotor speed, which is used only to confirm the estimations.

The control and estimation algorithms are implemented using Real- Time Windows Target of Matlab/ Simulink. An INST 2IV- sensor board of Entuple Technologies is used to measure the instantaneous values of stator voltages and currents of the motor. These analog voltages and currents are converted into digital form and fed to the computer via the NI PCIe- 6351 X- Series card. The rotor speed estimate from the observer is fed back to the FOC closed loop system, after converting to digital form. The error between the reference and actual speed is given to PI controller and is used to generate the q- axis component of stator current. The d-axis component is kept constant proportional to the motor rated flux. These currents are converted into stationary *abc* reference frame by the *dq- abc* block. The error between these reference stator currents and the actual measured currents is given to a hysteresis current controller (HC) which generates the firing pulses for the voltage source inverter (VSI), which drives the motor. The actual test bed is displayed in Fig.5.2.

Experiments are conducted with various reference speeds, ranging from high to very low, including persistent zero speed. The estimates obtained from the observer based on smoothed Kalman filter algorithm and conventional Kalman filter algorithm are discussed in sections 5.3 and 5.4.

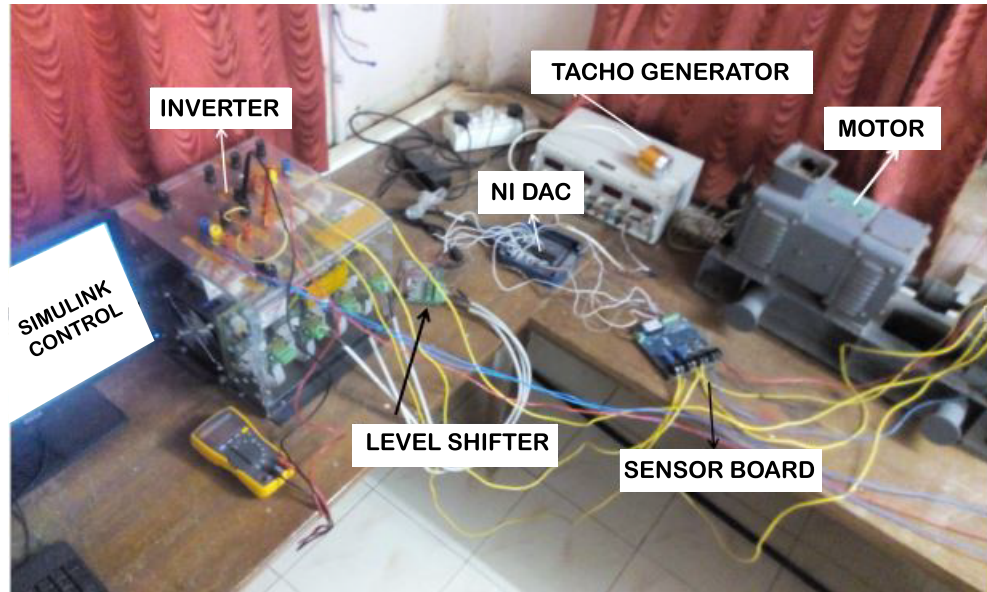
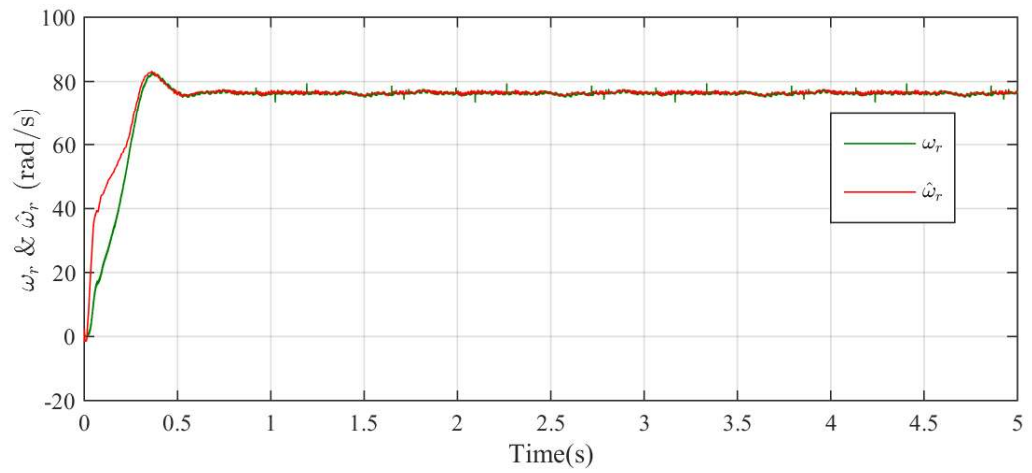


Figure 5.2: Experimental set up

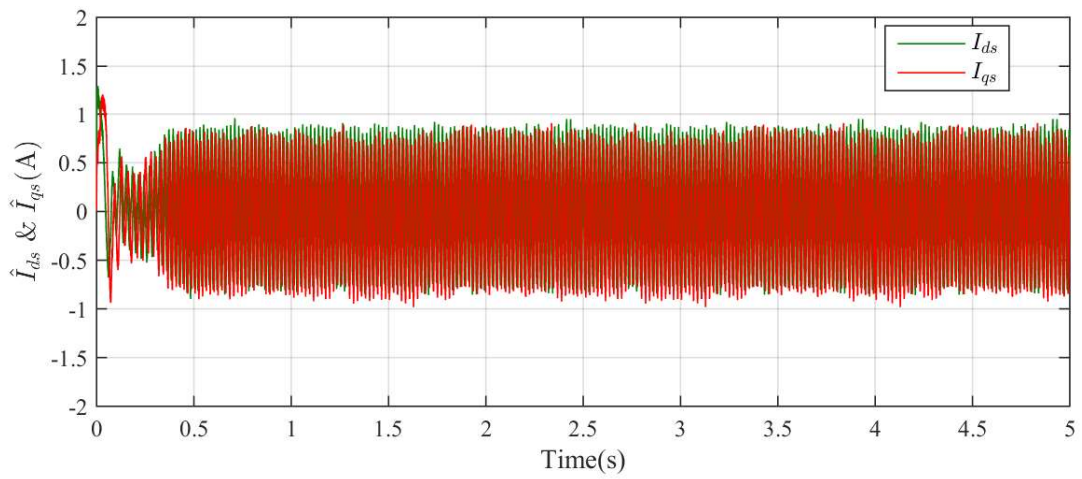
5.3 Experimental results of field-oriented control based on a fifth order smoothed Kalman observer

The full order observer based on smoothed Kalman filter algorithm is tested online for an indirect field-oriented control of induction motor. The closed loop system is checked for various reference speeds. A tacho-generator measures the actual speed of the machine, which is used for comparison purpose only. Figs.5.3- 5.8 show the rotor speed estimated using the proposed observer for different reference speeds.

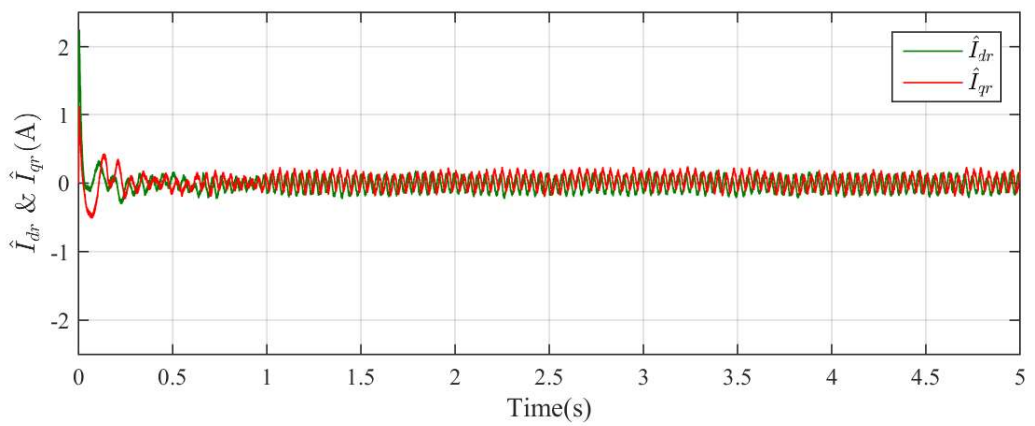
In Fig.5.3, the estimates of rotor speed, ω_r , and stator currents, I_{ds} , I_{qs} are shown. Fig.5.3c shows a plot of the rotor fluxes, ψ_{dr} and ψ_{qr} .



(a)

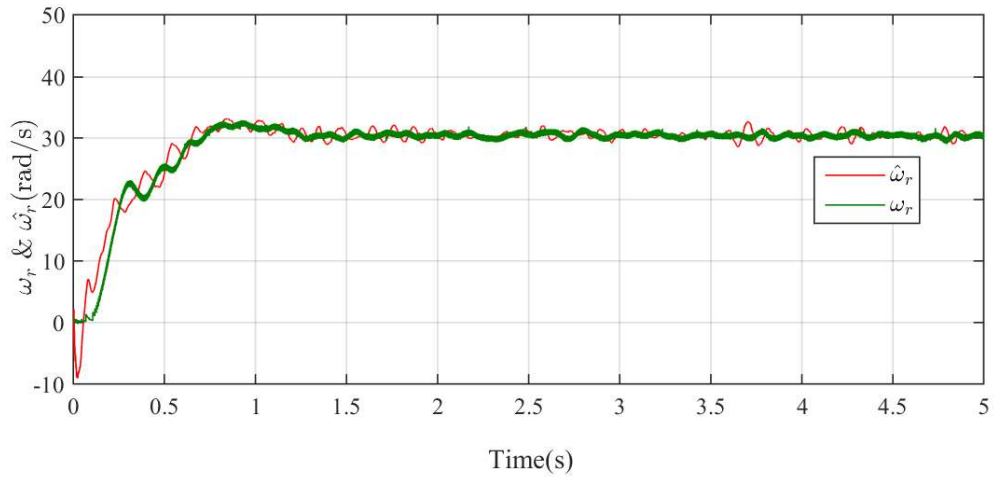


(b)

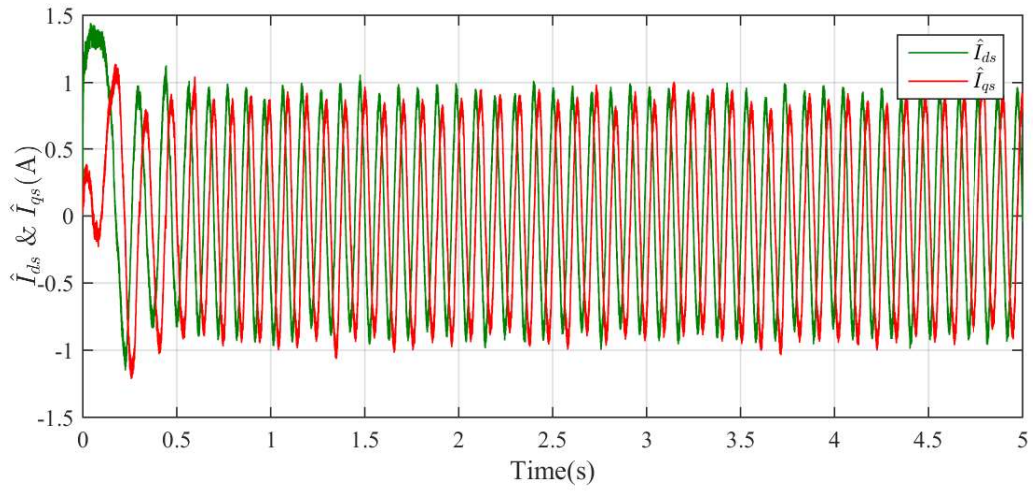


(c)

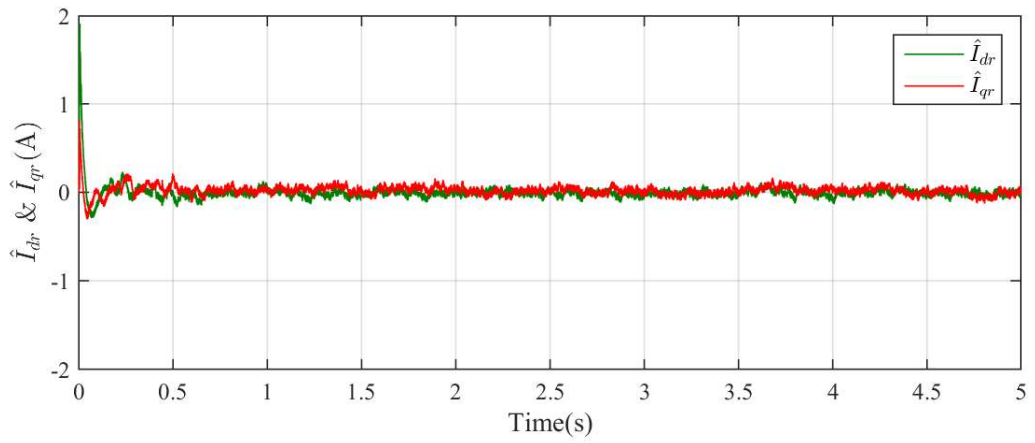
Figure 5.3: Experimental results for a reference speed of 75rad/s(mech.) a) Rotor speed, ω_r b) \hat{I}_{ds} & \hat{I}_{qs} c) \hat{I}_{dr} & \hat{I}_{qr}



(a)

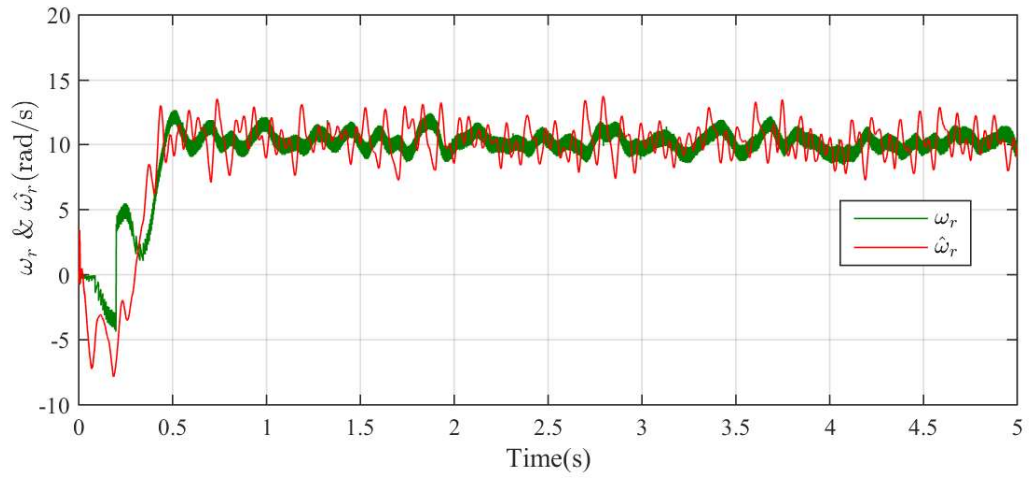


(b)

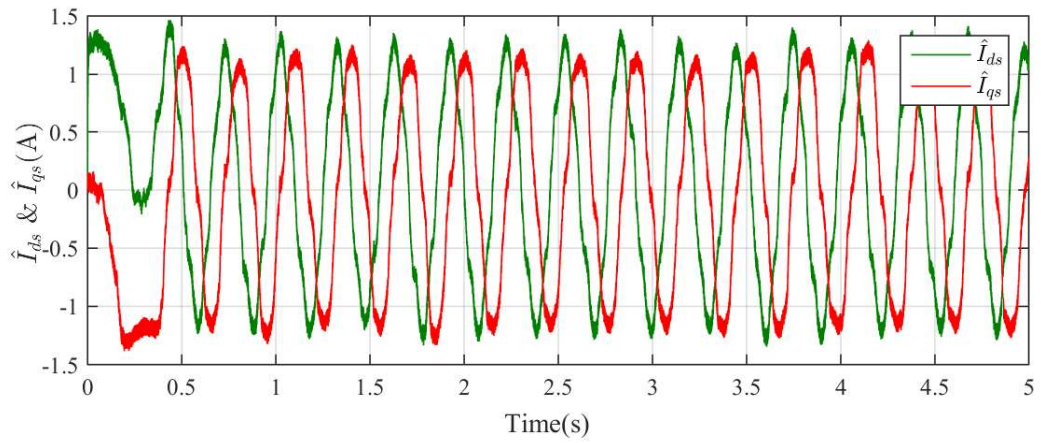


(c)

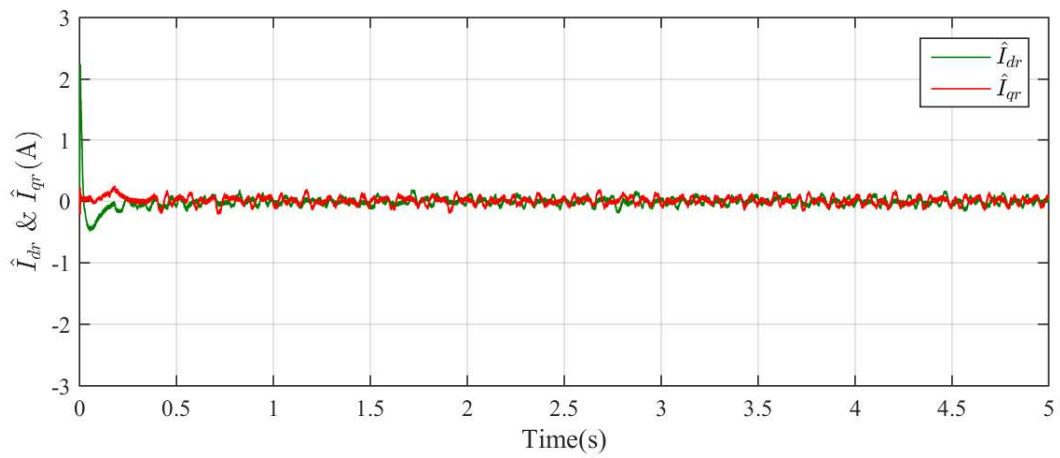
Figure 5.4: Experimental results for a reference speed of 30rad/s(mech.) a) ω_r b) \hat{I}_{ds} & \hat{I}_{qs} c) \hat{I}_{dr} & \hat{I}_{qr}



(a)

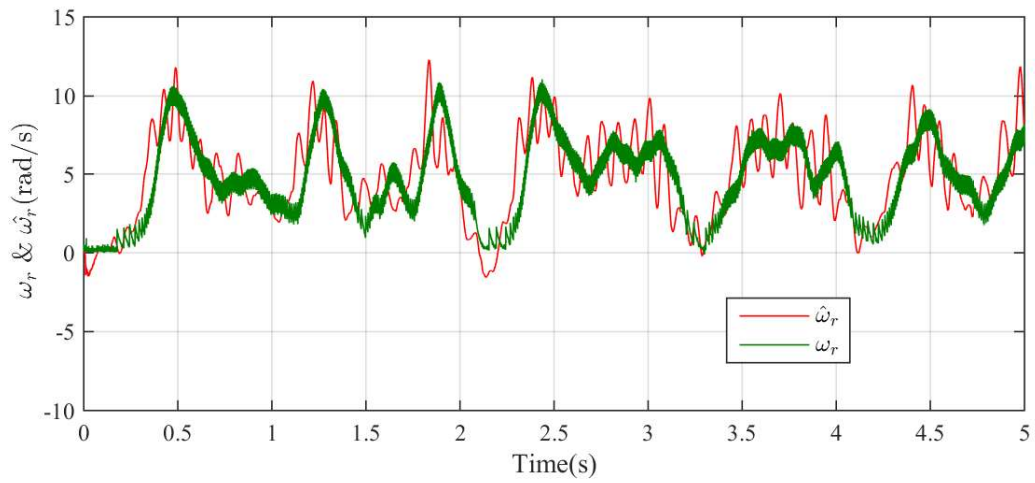


(b)

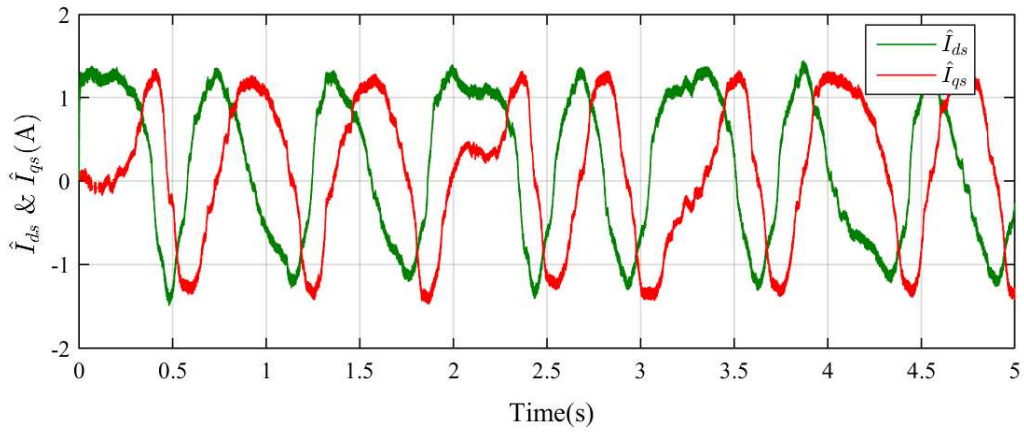


(c)

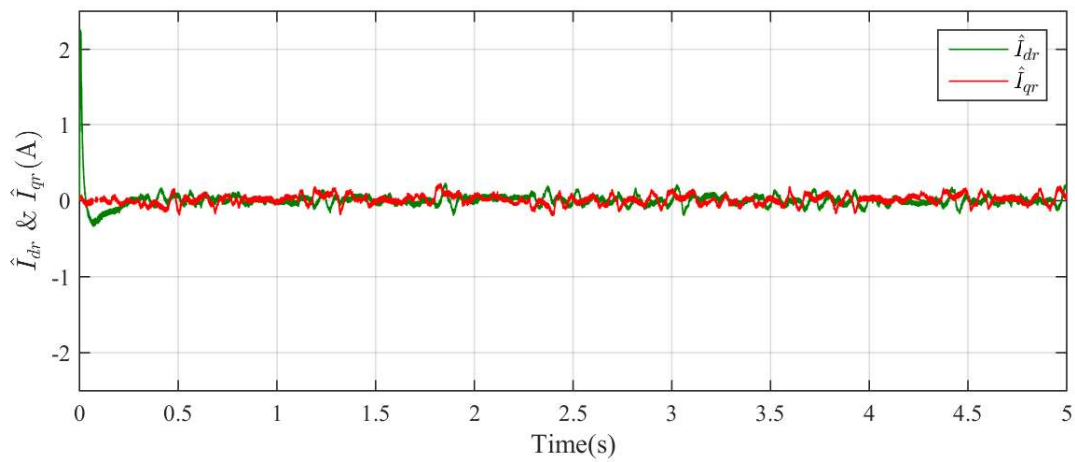
Figure 5.5: Experimental results for a reference speed of 10rad/s(mech.) a) ω_r b) \hat{I}_{ds} & \hat{I}_{qs} c) \hat{I}_{dr} & \hat{I}_{qr}



(a)

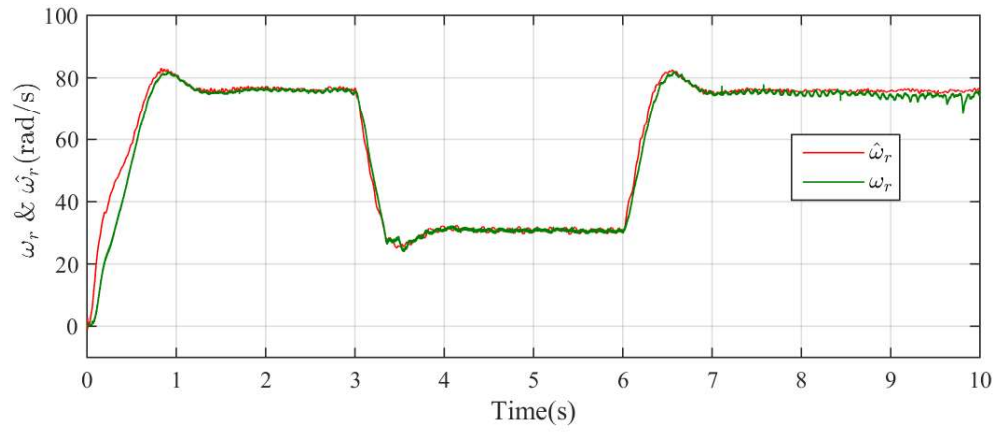


(b)

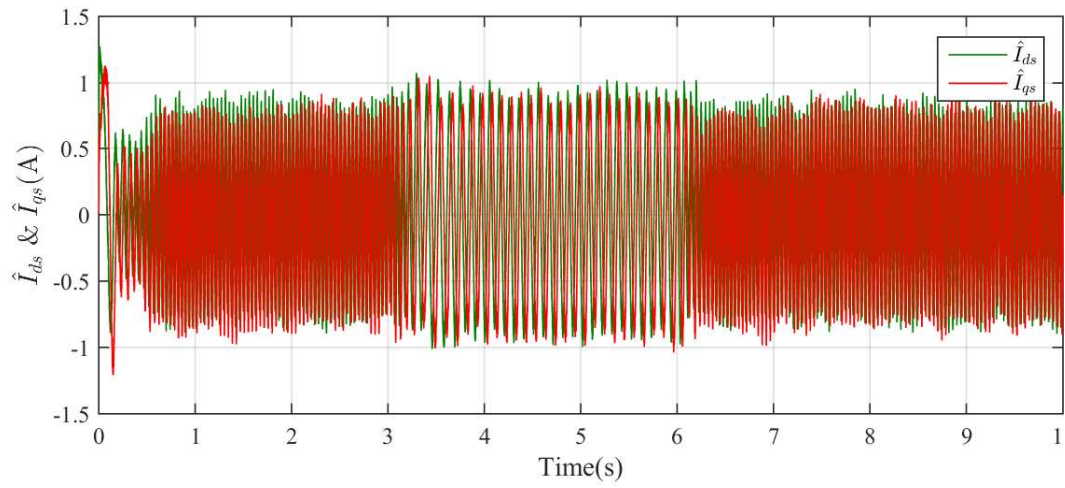


(c)

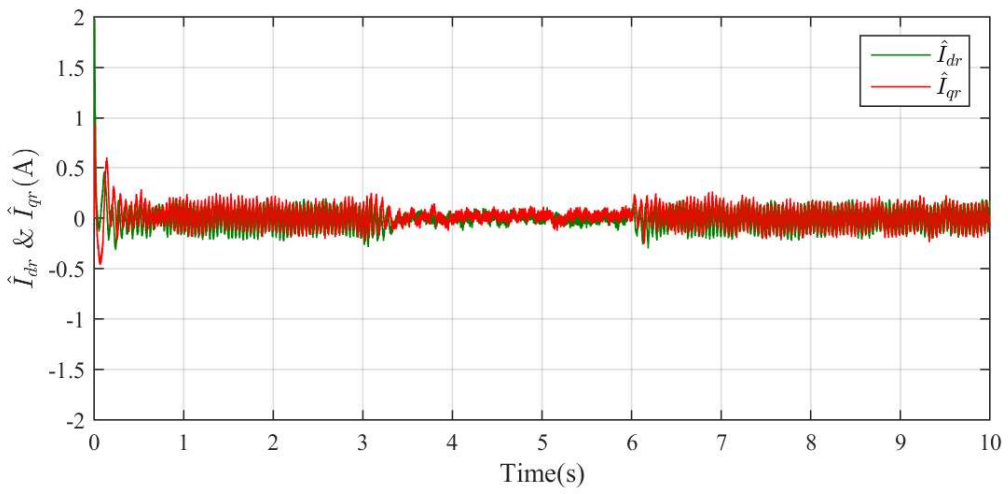
Figure 5.6: Experimental results for a reference speed of 5 rad/s(mech.) a) ω_r b) \hat{I}_{ds} & \hat{I}_{qs} c) \hat{I}_{dr} & \hat{I}_{qr}



(a)

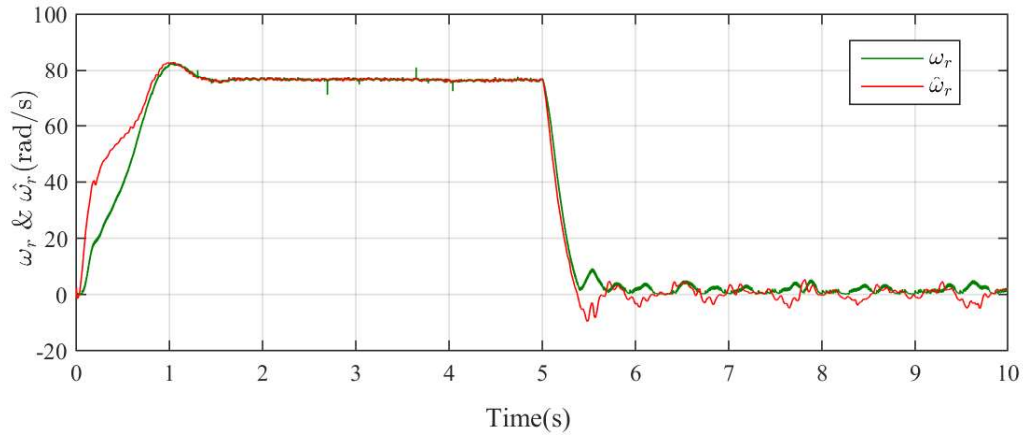


(b)

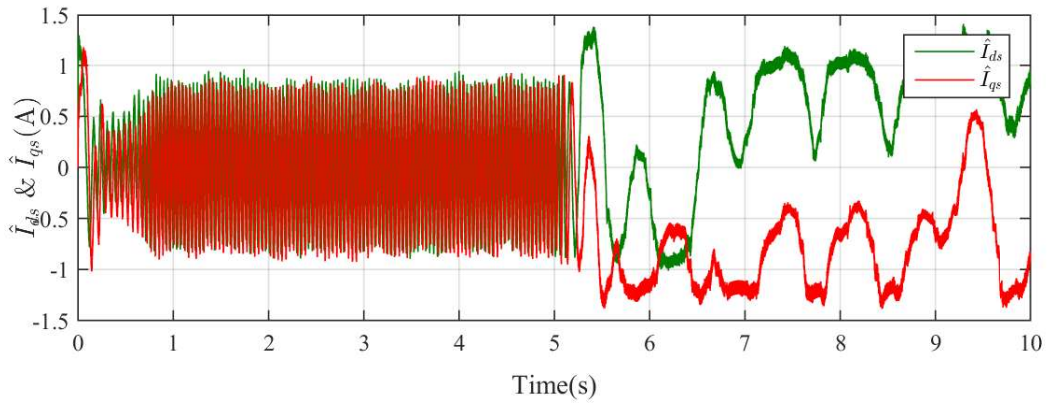


(c)

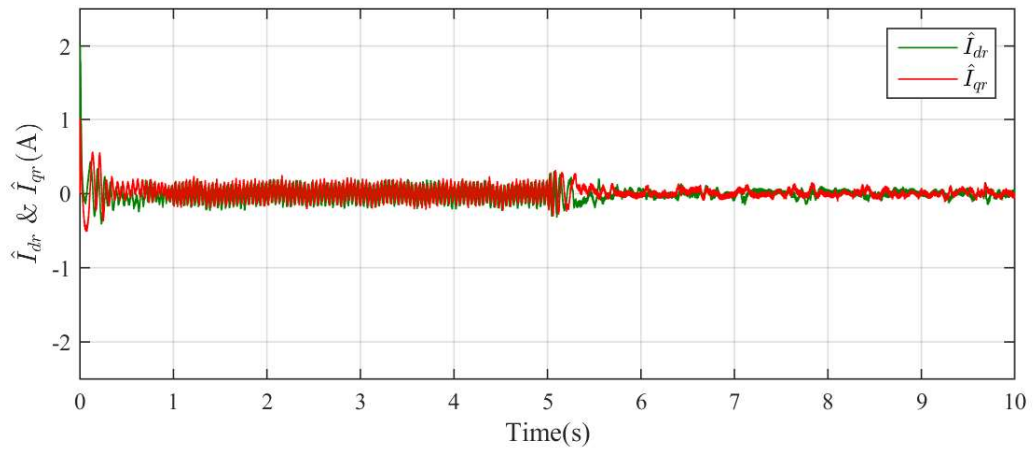
Figure 5.7: Experimental results for a reference speed which changes from 75rad/s(mech) to 30rad/s(mech) at 3s and then to 75rad/s(mech) at 6s a) ω_r b) \hat{I}_{ds} & \hat{I}_{qs} c) \hat{I}_{dr} & \hat{I}_{qr}



(a)



(b)



(c)

Figure 5.8: Experimental results for a reference speed which changes from 75rad/s(mech) to 0rad/s(mech) at 5s and continues at zero speed for 5s a) ω_r b) \hat{I}_{ds} & \hat{I}_{qs} c) \hat{I}_{dr} & \hat{I}_{qr}

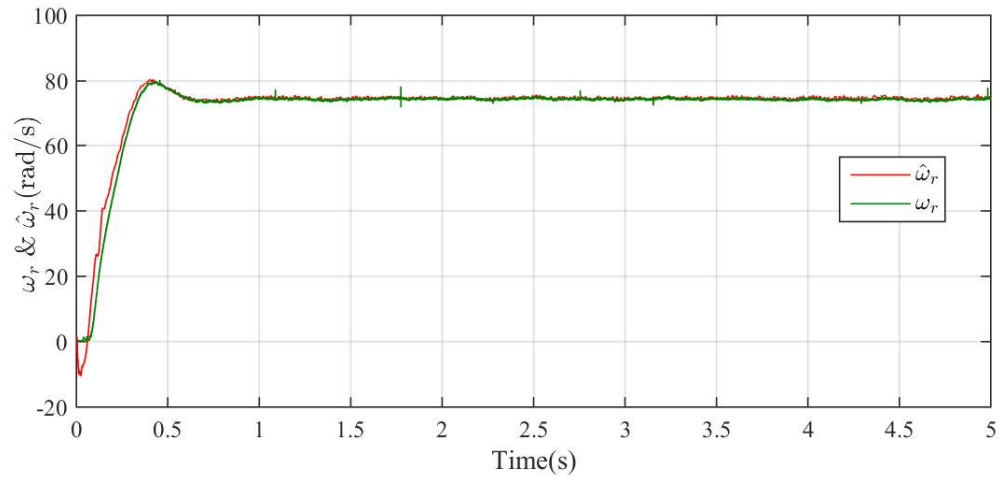
5.4 Experimental results of field-oriented control based on a fifth order conventional Kalman observer

The same experiment is conducted with a conventional EKF based observer and results are obtained. The conventional EKF has stages of prediction and filtering only. Thus the outputs till the present instant of time only are utilized for estimation. The estimation results are compared with those obtained with the proposed smoothed Kalman observer. The estimation with conventional EKF is done with the same process and measurement error covariance matrices as is used with the proposed observer. The results for the same reference speeds are depicted in Figs.5.9-5.14. It can be seen that the estimation is better with the smoothed observer and the improvement is prominent in the transient region. The steady state results are more or less the same.

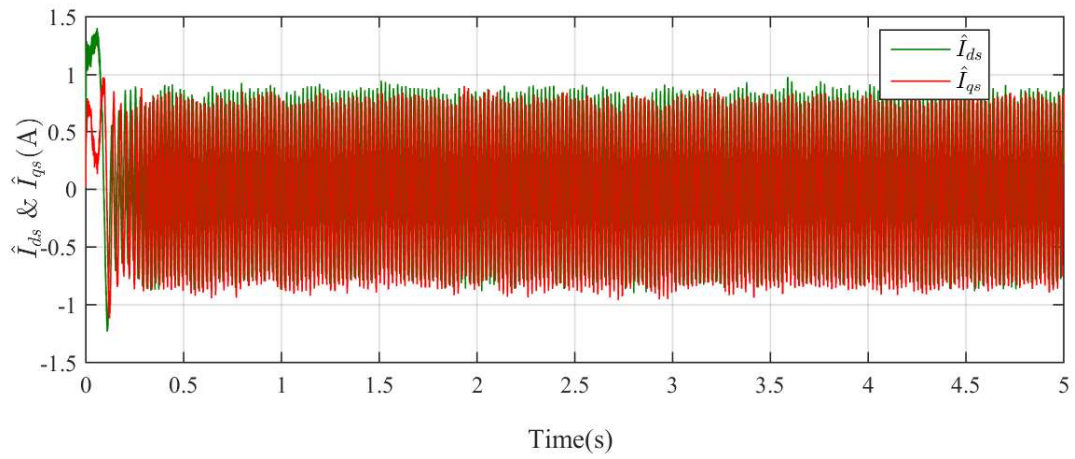
To validate the superiority of the smoothed Kalman observer, the mean square errors in both the cases are calculated and compared. Table 5.1 consolidates the mean squared errors(MSE) of these estimations.

Table 5.1: Mean Square Errors of estimation with and without smoothing (fifth order model of IM)

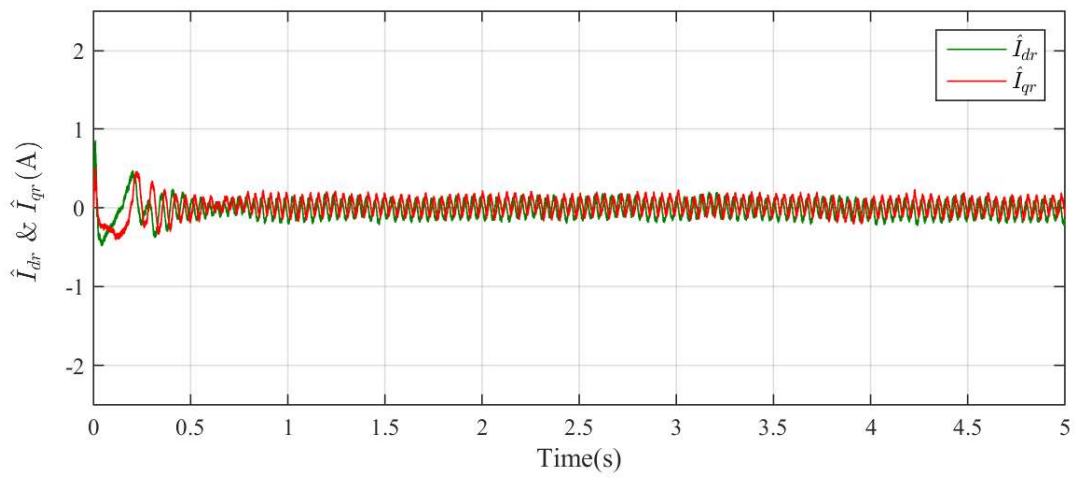
Ref.Speed(rad/s)	Mean Squared Error(rad/s)		% Decrease
	CEKF	SKF	
75	85.74	31.51	63.2%
30	57.55	5.086	91.1%
10	10.21	5.541	45.72%
5	10.01	7.719	22.70%
75- 0	101.6	85.36	15.9%
75-30-75	36.56	24.9	11.66%



(a)

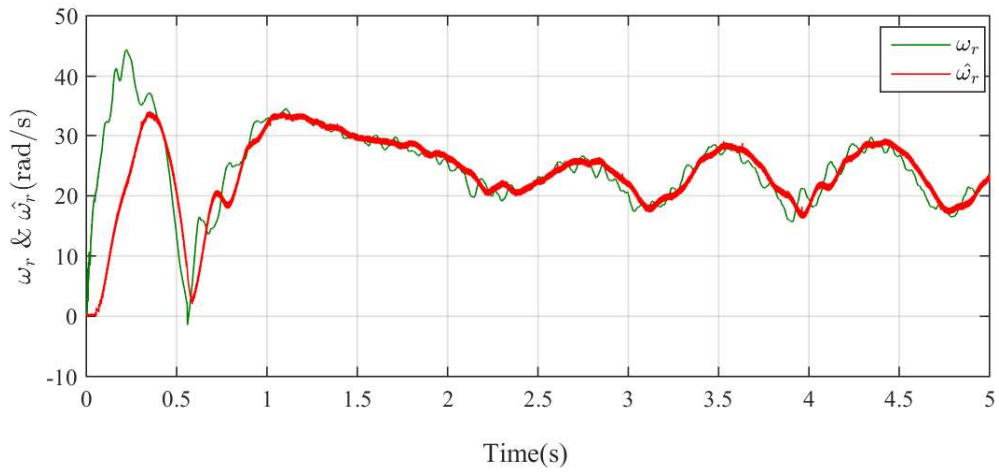


(b)

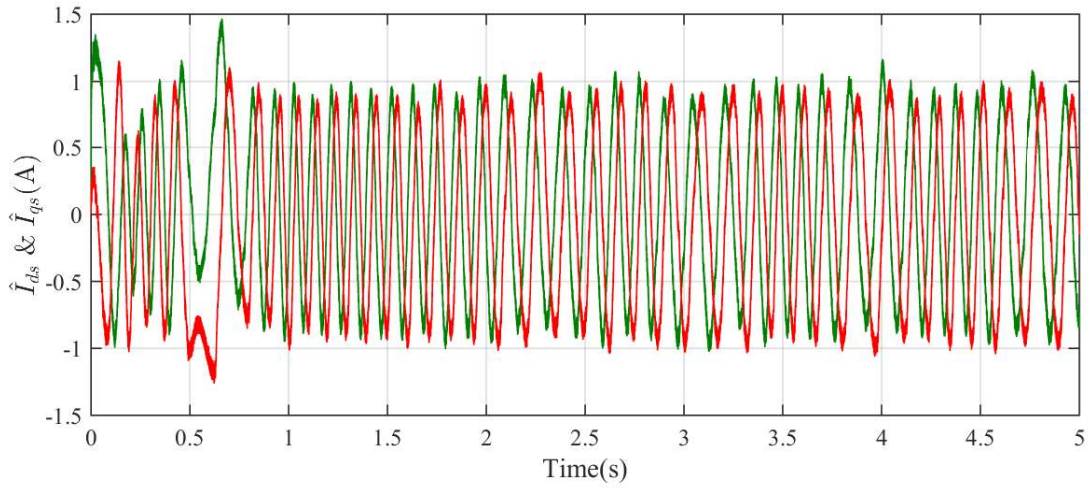


(c)

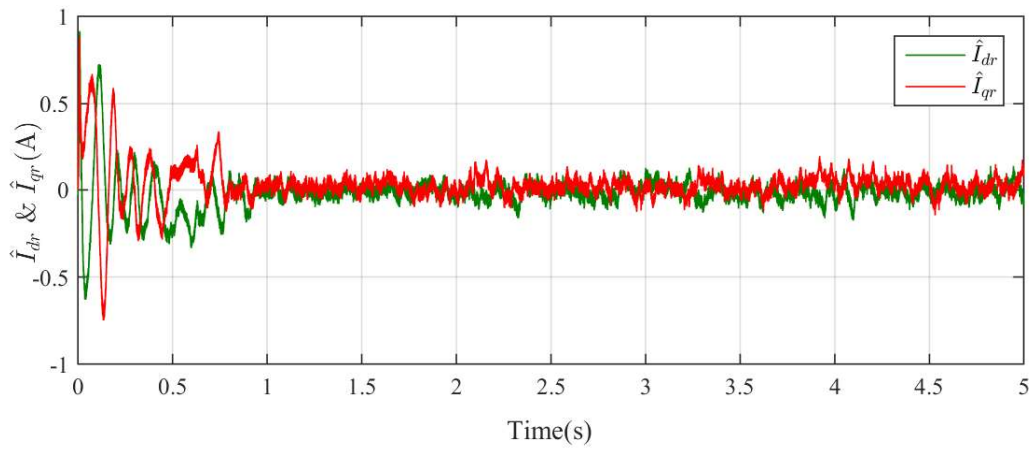
Figure 5.9: Experimental results for a reference speed of 75rad/s(mech.) a) Rotor speed, ω_r b) \hat{I}_{ds} & \hat{I}_{qs} c) \hat{I}_{dr} & \hat{I}_{qr}



(a)

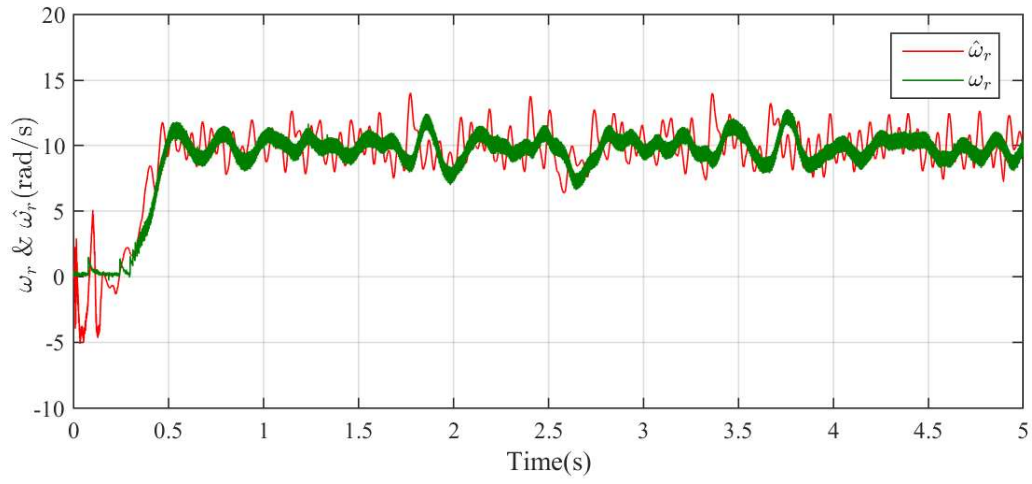


(b)

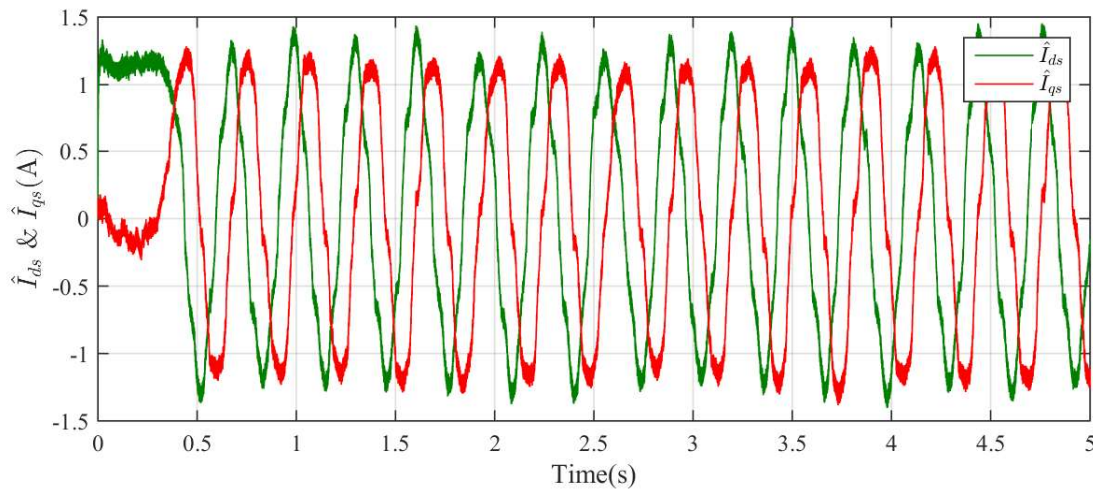


(c)

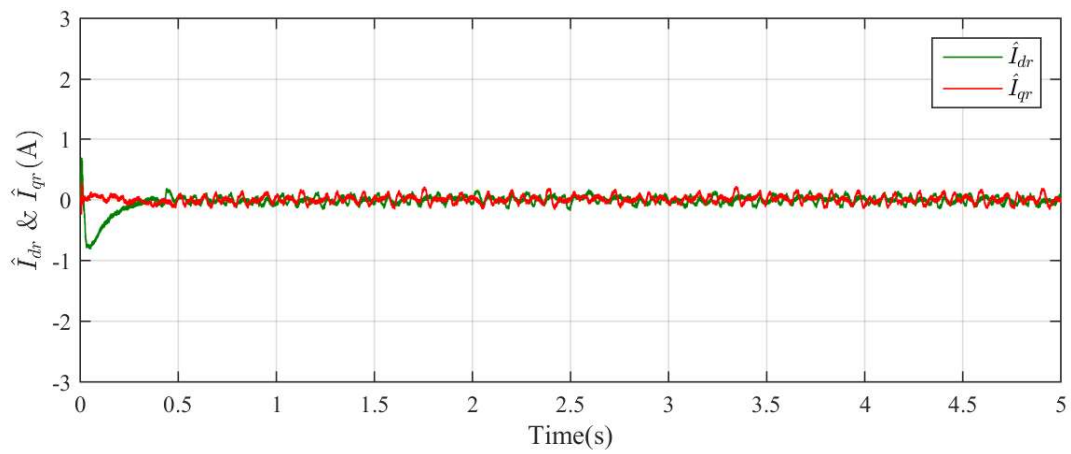
Figure 5.10: Experimental results for a reference speed of 30rad/s(mech.) a) ω_r b) \hat{I}_{ds} & \hat{I}_{qs} c) \hat{I}_{dr} & \hat{I}_{qr}



(a)



(b)



(c)

Figure 5.11: Experimental results for a reference speed of 10rad/s(mech.) a) ω_r
 b) \hat{I}_{ds} & \hat{I}_{qs} c) \hat{I}_{dr} & \hat{I}_{qr}

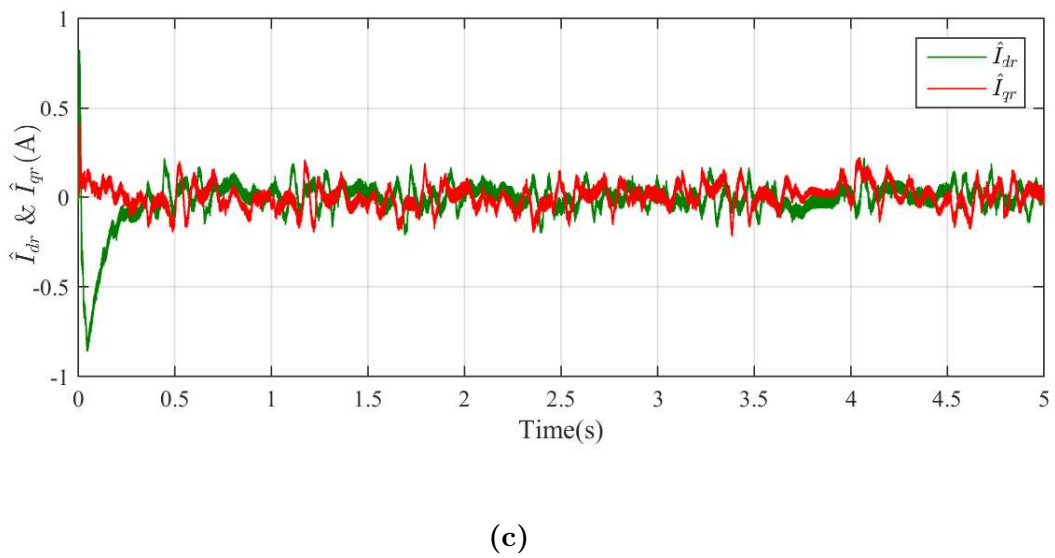
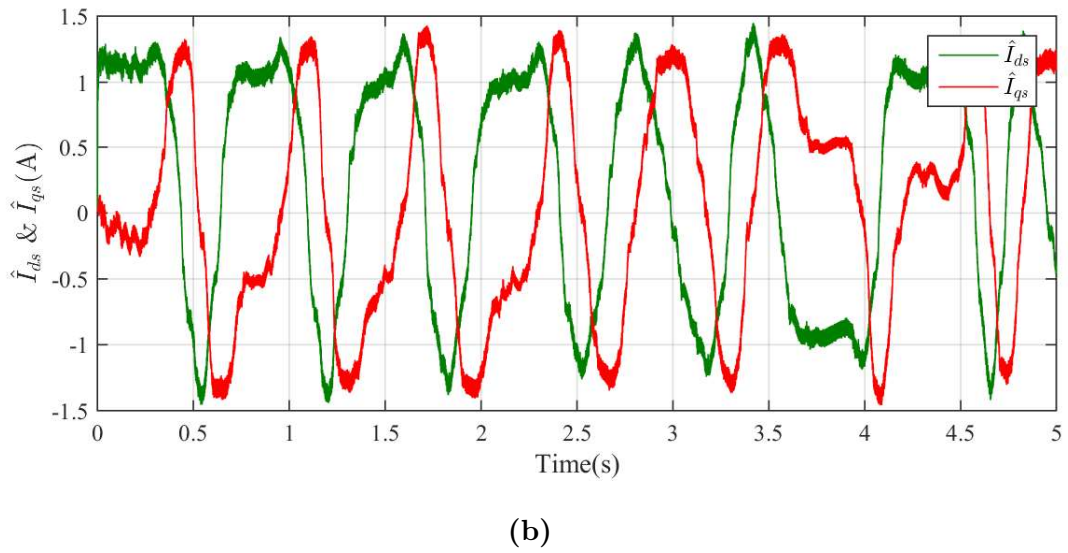
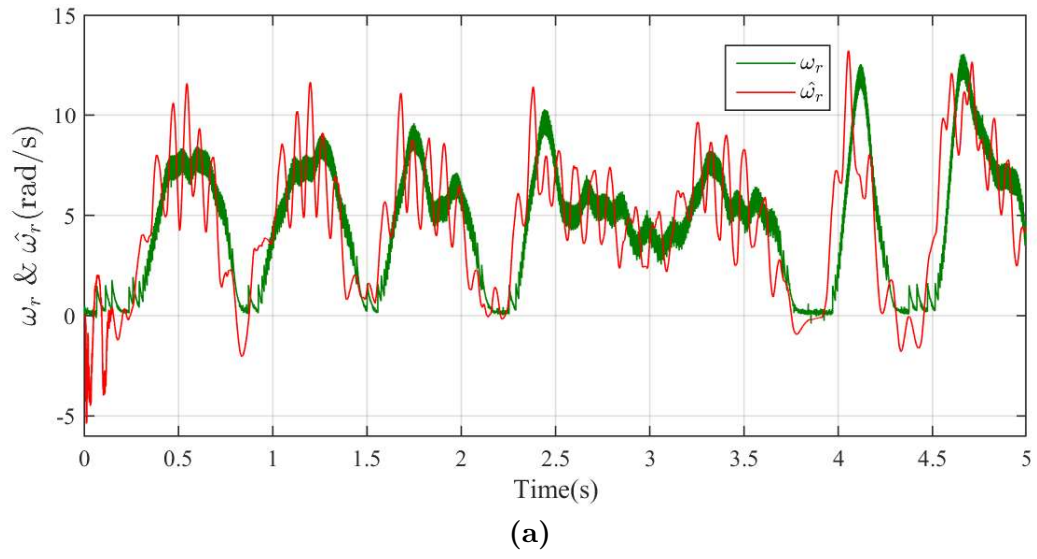
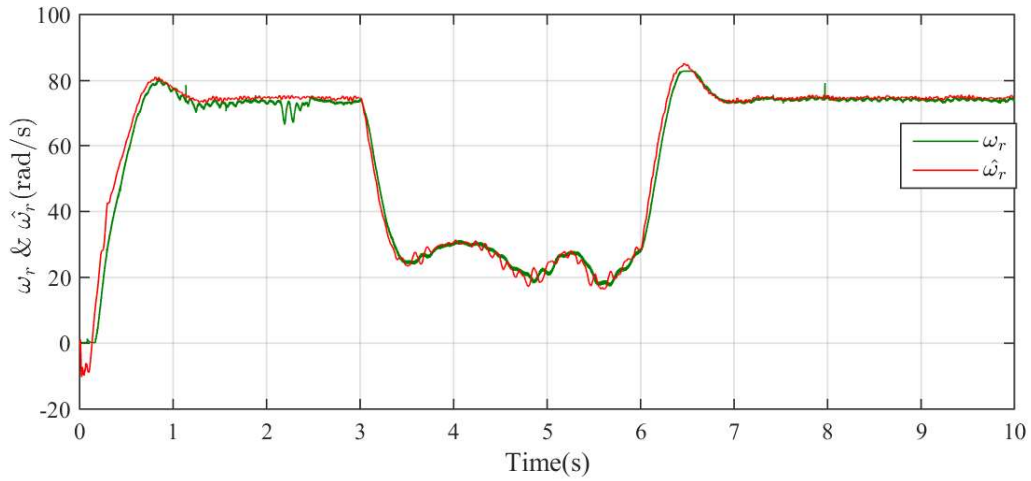
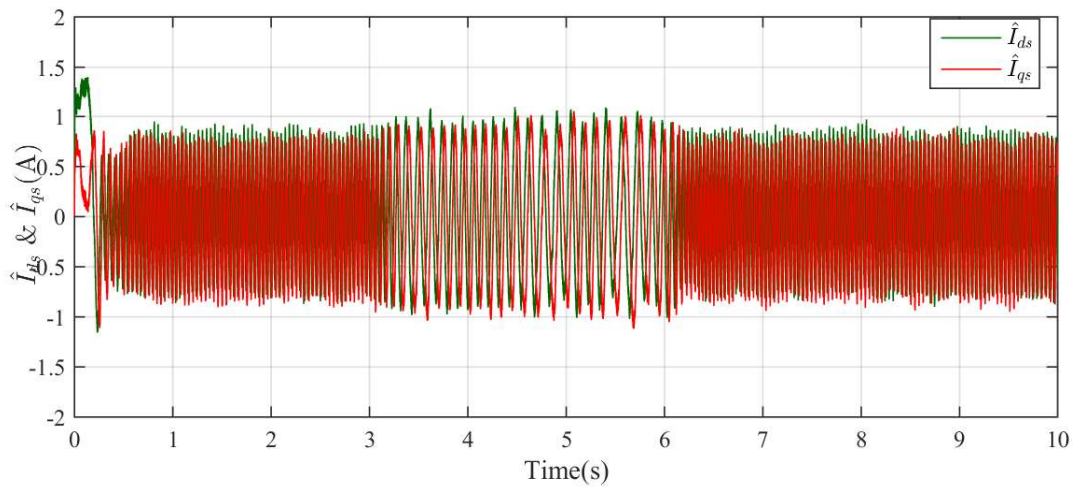


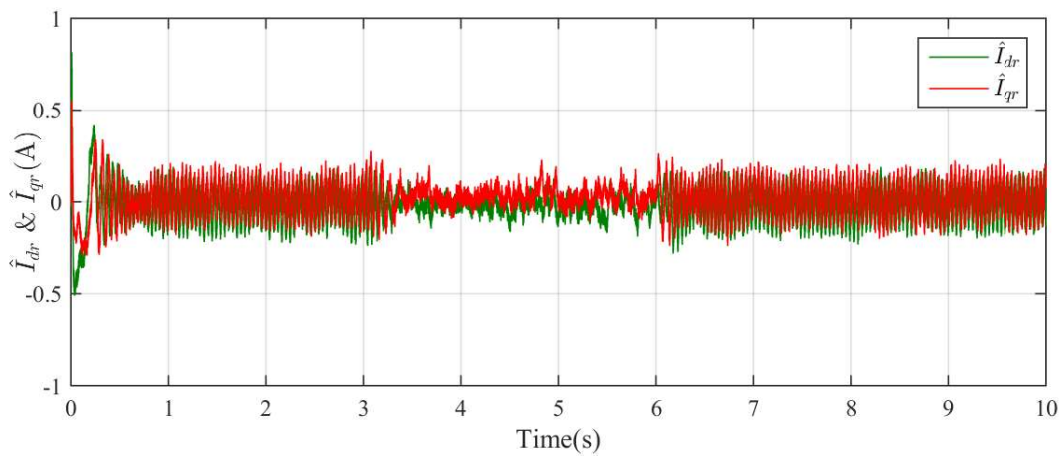
Figure 5.12: Experimental results for a reference speed of 5 rad/s(mech.) a) ω_r b) \hat{I}_{ds} & \hat{I}_{qs} c) \hat{I}_{dr} & \hat{I}_{qr}



(a)

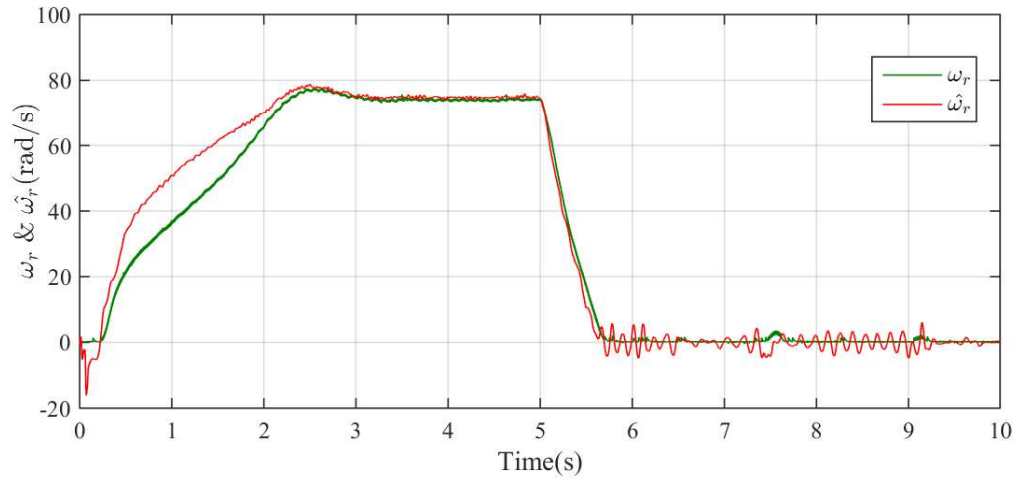


(b)

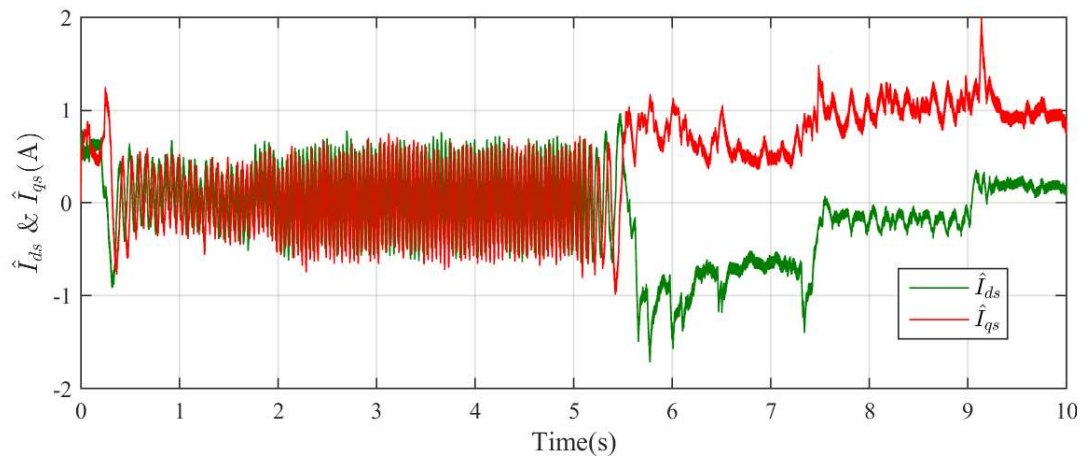


(c)

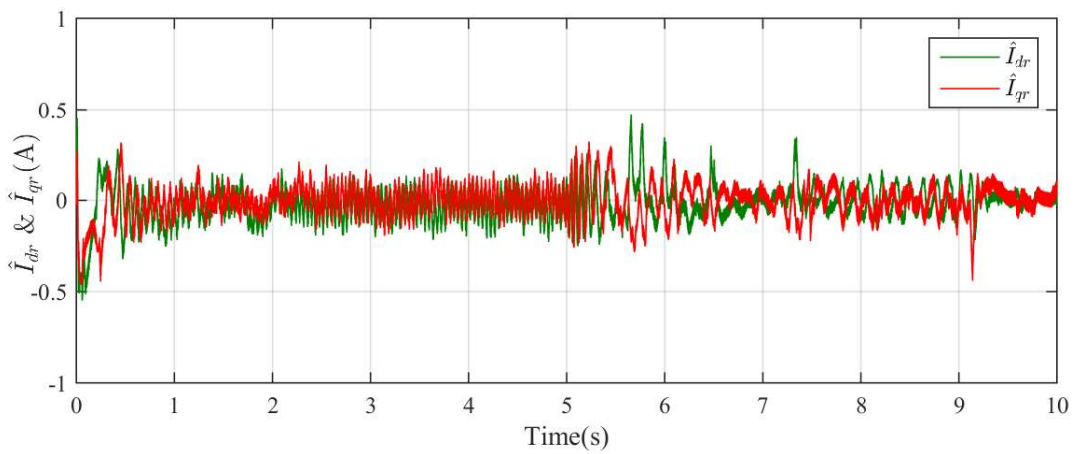
Figure 5.13: Experimental results for a reference speed which changes from 75rad/s(mech) to 30rad/s(mech) at 3s and then to 75rad/s(mech) at 6s a) ω_r b) \hat{I}_{ds} & \hat{I}_{qs} c) \hat{I}_{dr} & \hat{I}_{qr}



(a)



(b)



(c)

Figure 5.14: Experimental results for a reference speed which changes from 75rad/s(mech) to 0rad/s(mech) at 5s and continues at zero speed for 5s a) ω_r b) \hat{I}_{ds} & \hat{I}_{qs} c) \hat{I}_{dr} & \hat{I}_{qr}

5.5 Summary

This chapter presents the results of real-time implementation of a smoothed Kalman observer based indirect field-oriented control of induction motor. The results obtained are compared with those obtained with a conventional EKF based observer. Table 5.1 consolidates the mean squared errors(MSE) of these estimations. Considering the performances of the two observers- one, based on conventional EKF and the second one which incorporates a single-stage smoothing algorithm, the following comments can be made:

- The performances of estimation at steady-state of both the algorithms are close to each other.
- The goodness of the smoothing algorithm over the conventional one is evident during the transient states, such as a sudden change in reference speed.
- The measurement and process error covariances used throughout the experiments are the same. Hence the improvement in estimation is solely due to the additional data included in the smoothing algorithm.
- Improved results are obtained at low and zero- speeds.

Uma Syamkumar “Smoothed Kalman Observer for Sensorless Field Oriented Control of Induction Motor.” Thesis. Department of Electrical Engineering, Government Engineering College, Trichur, University of Calicut, , 2020.

Chapter 6

Smoothed Observer for a reduced model of the induction motor

This chapter explores the application of the smoothed Kalman observer algorithm for a reduced order model of the induction motor. The full- order observer presented in chapter 4 is of fifth order and hence the complete closed loop system implementation is computationally intensive. Hence a reduced order system is used here, which is of third order.

6.1 Introduction

An accurate information of rotor speed is desired for operation of vector controlled induction motor drive. The rotor speed can be estimated using voltage and current signals. One of the popular model- based estimation methods is the model reference adaptive system(MRAS). Numerous MRAS methods based on rotor flux, back emf and reactive power [5, 43, 104–106] are proposed in literature. However, the rotor-flux MRAS introduced by Schauder [5] remains the most popular and a lot of work is focussed on improvement of its performance. Parameter sensitivity and pure integration problems limit its performance at low and zero speed.

Extended Kalman filter(EKF) filters the system from noise and uncertainties. MRAS with EKF is found to give a high dynamic response in the presence of noise and parameter variations. Two mathematical models of the induction motor are used to estimate the flux and speed of the rotor. Both the models are of second order, making computation easy. The first model, which is called the voltage model, is independent of the rotor speed. Hence, this model is used as the reference model from which the reference values of rotor fluxes are calculated using the stator voltages and currents. The current model is dependent on rotor speed, which makes it apt to be used as the observer. This second order model is made third order and non- linear, by choosing the rotor speed also as a state variable. The smoothed Kalman algorithm is used to estimate the rotor fluxes and speed.

This chapter is organized as follows: Section 6.2 explains the dynamic model of the

induction motor, section 6.3 elaborates the application of the smoothed Kalman observer in indirect field oriented control of induction motor. Section 6.4 gives the offline estimation results of the extended Kalman-MRAS system for various reference speeds, using the conventional method (6.4.1) and with smoothing incorporated (6.4.2). Section 6.5 concludes the chapter.

6.2 Dynamic Model of the Induction Motor

The voltage model of the induction motor given in eqn(6.2.1) [86], being independent of rotor speed, is used to generate the reference fluxes of the machine. The current model(eqn.6.2.2) is dependent on the rotor speed. Hence this model is used to estimate the rotor fluxes and speed.

$$\begin{bmatrix} p\psi_{dr}^s \\ p\psi_{qr}^s \end{bmatrix} = \frac{L_r}{L_m} \left[\begin{bmatrix} v_{ds}^s \\ v_{qs}^s \end{bmatrix} - \begin{bmatrix} R_s + \sigma L_s p & 0 \\ 0 & R_s + \sigma L_s p \end{bmatrix} \begin{bmatrix} i_{ds}^s \\ i_{qs}^s \end{bmatrix} \right] \quad (6.2.1)$$

$$\begin{bmatrix} p\psi_{dr}^s \\ p\psi_{qr}^s \end{bmatrix} = \frac{L_r}{L_m} \begin{bmatrix} \frac{-1}{T_r} & -\omega_r \\ \omega_r & \frac{-1}{T_r} \end{bmatrix} \begin{bmatrix} \psi_{dr}^s \\ \psi_{qr}^s \end{bmatrix} + \frac{L_m}{T_r} \begin{bmatrix} i_{ds}^s \\ i_{qs}^s \end{bmatrix} \quad (6.2.2)$$

(6.2.2) is extended to include ω_r also as a state variable, thus making the system third order. These models are discretized using Euler's backward formula,

$$\frac{x(k+1) - x(k)}{t_s} = \dot{x}(t) \quad (6.2.3)$$

The discretised augmented state model is given in (6.2.4).

$$\begin{bmatrix} \psi_{dr}^s(k+1) \\ \psi_{qr}^s(k+1) \\ \omega_r(k+1) \end{bmatrix} = \begin{bmatrix} 1 - \frac{R_r T_s}{L_r} & -\omega_r T_s & 0 \\ \omega_r T_s & 1 - \frac{R_r T_s}{L_r} & 0 \\ K_t i_{qs} & -K_t i_{ds} & 1 \end{bmatrix} \begin{bmatrix} \psi_{dr}^s(k) \\ \psi_{qr}^s(k) \\ \omega_r(k) \end{bmatrix} + \begin{bmatrix} \frac{L_m R_r T_s}{L_r} & 0 \\ 0 & \frac{L_m R_r T_s}{L_r} \\ 0 & 0 \end{bmatrix} \begin{bmatrix} i_{ds}^s(k) \\ i_{qs}^s(k) \end{bmatrix} \quad (6.2.4)$$

6.3 Indirect field-oriented control of induction motor with a smoothed Kalman observer

A stochastic model is used to consider the uncertainties and noise involved in a practical machine. w and v in eqns. 6.3.1 and 6.3.2 are the Gaussian white noises

added to accomplish this.

$$x(k+1) = f(x(k), u(k)) + w(i) \quad (6.3.1)$$

$$y(k) = H(x(k)) + v(k) \quad (6.3.2)$$

$w(k)$ and $v(k)$ have covariance matrices, \mathbf{Q} and \mathbf{R} which are characterised by

$$E(w(i)) = 0 \quad (6.3.3a)$$

$$E(v(k)) = 0 \quad (6.3.3b)$$

$$E(w(i)w(j)^T) = Q\delta(i, j) \quad (6.3.3c)$$

$$E(v(i)v(j)^T) = R\delta(i, j) \quad (6.3.3d)$$

The rotor fluxes calculated from the voltage model in equation (6.2.1) are taken as the reference fluxes. The third-order current model (eq.6.2.4) is the adjustable model, since it is dependent on rotor angular velocity, ω_r . Since reference values of the rotor fluxes are available, they are chosen as outputs of the system. The direct and quadrature axis rotor fluxes, ψ_{dr} and ψ_{qr} are the outputs. Hence the output matrix, H is

$$H = \begin{bmatrix} 1 & 0 & 0 \\ 0 & 1 & 0 \end{bmatrix}$$

The error between the reference and actual fluxes are used in the implementation of the extended Kalman filter algorithm. Fig.6.1 illustrates the structure of the proposed speed estimator using smoothed Kalman observer.

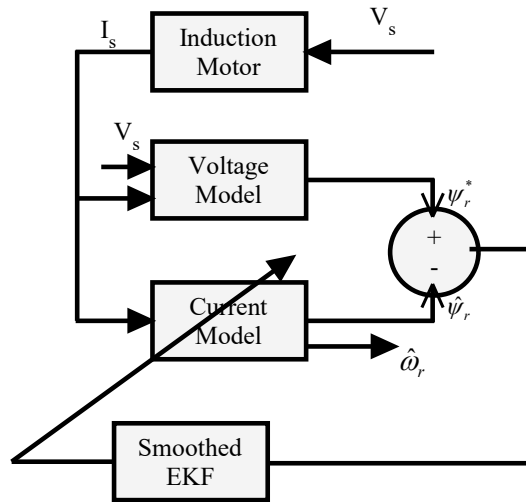


Figure 6.1: Structure of the estimator using smoothed Kalman observer

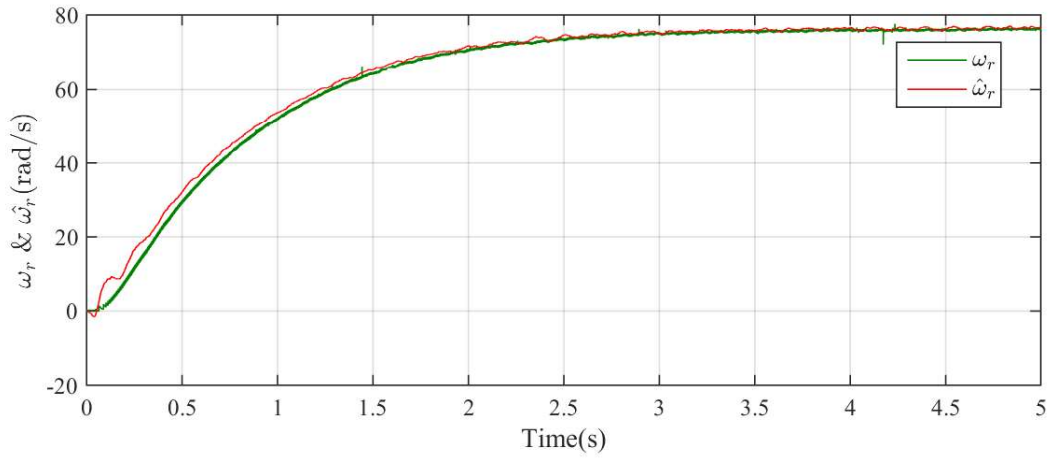
In Fig.6.1, voltage equations and current equations are as defined in equations 6.2.1 and 6.2.2 respectively.

6.4 Results of Offline Estimation

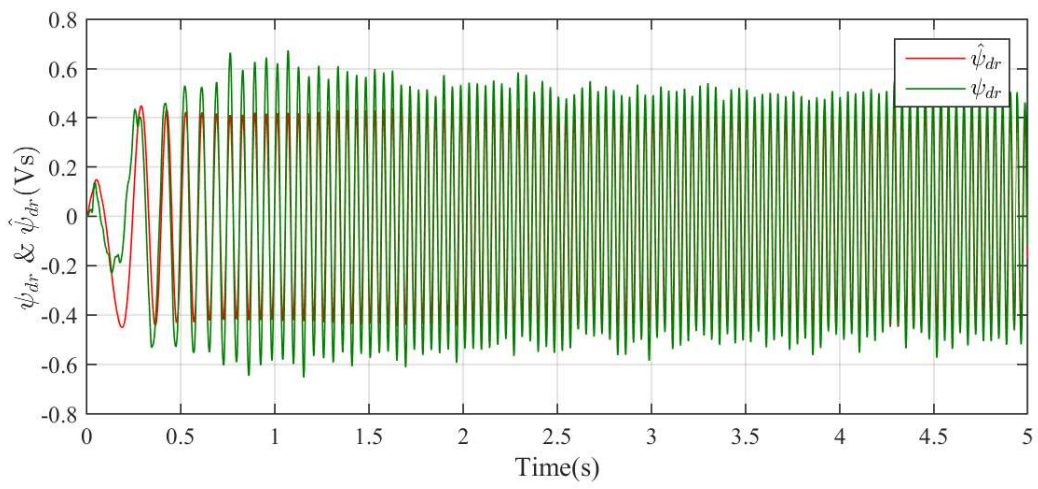
In the offline estimation, the machine runs in vector control mode without the observer and the stator voltages, currents and rotor speed are measured. The measured stator voltages and currents are given as inputs to the observers using conventional EKF and EKF with smoothing algorithm. The estimated rotor speed in both cases are compared with the measured speed. The comparison is done for two different reference speeds. Speed estimates for these reference speeds with the conventional EKF algorithm and the smoothed EKF, along with the estimated and calculated rotor fluxes are given in sections 6.4.1 and 6.4.2 respectively.

6.4.1 Speed and flux estimation using conventional Extended Kalman observer

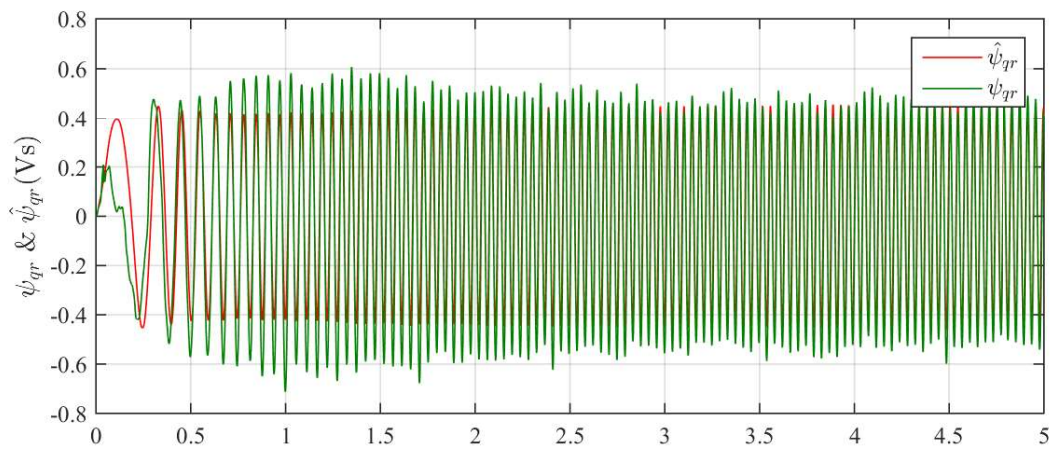
During the offline estimation process, the motor is subjected to two different reference speeds- one, a step reference of magnitude 75rad/s at $t=0$ and the second one a step whose magnitude changes from 20rad/s to 75rad/s at $t=2$ s and then to 50rad/s at $t=4.5$ s. The rotor speed to be fed back in the closed loop indirect FOC is estimated using a conventional EKF. This involves only the prediction and filtering stages. The process and measurement error covariance matrices are selected to be diagonal to simplify the determination process. Estimation is done with two different reference speeds. The estimated rotor speed and measured speed for a reference speed of 75rad/s., using the conventional Kalman observer are shown in Fig.6.2a. The d and q -axes components of the rotor fluxes as observed from the extended Kalman observer are compared with those calculated from the voltage model of the machine (equation 6.2.1). The corresponding results are shown in Figs. 6.2b and 6.2c.



(a)



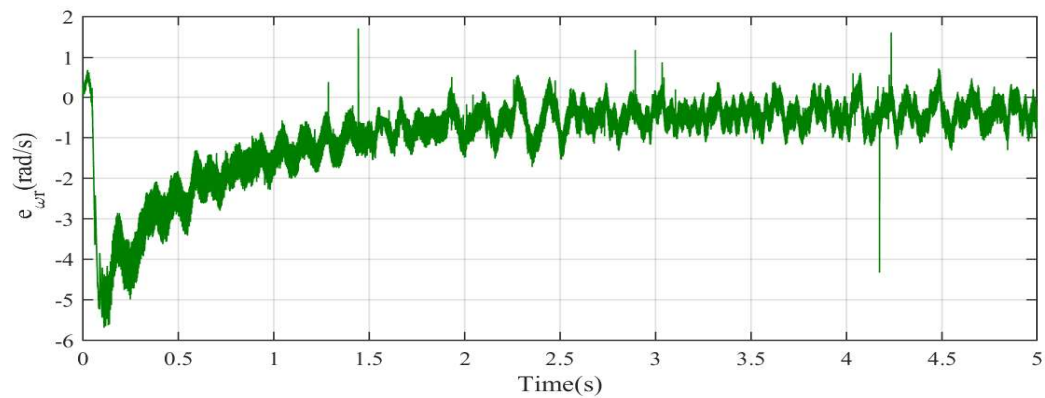
(b)



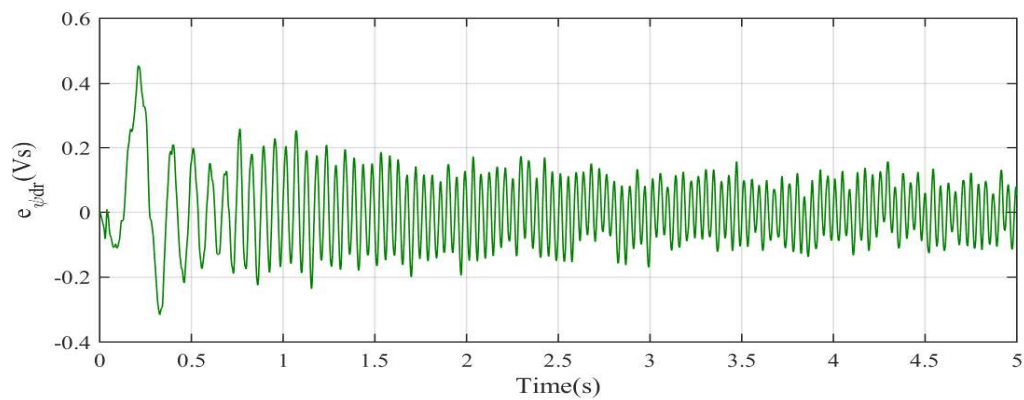
(c)

Figure 6.2: Simulation results for a reference speed of 75 rad/s(mech.) at $t=0s$ and with a conventional Kalman observer a) Estimated and measured ω_r ,Estimated and calculated values of rotor fluxes, b) ψ_{dr} & $\hat{\psi}_{dr}$ and c) ψ_{qr} & $\hat{\psi}_{qr}$

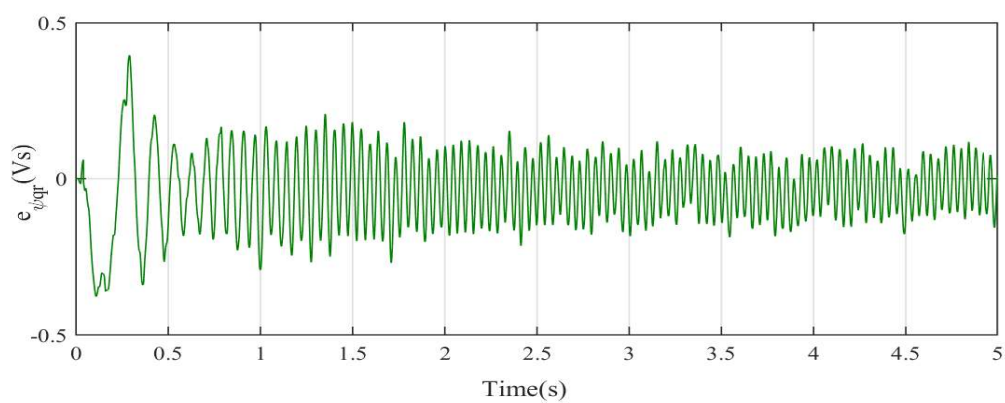
The error in estimation of rotor speed and the d and q - axis rotor fluxes are shown in Fig.6.3



(a)



(b)

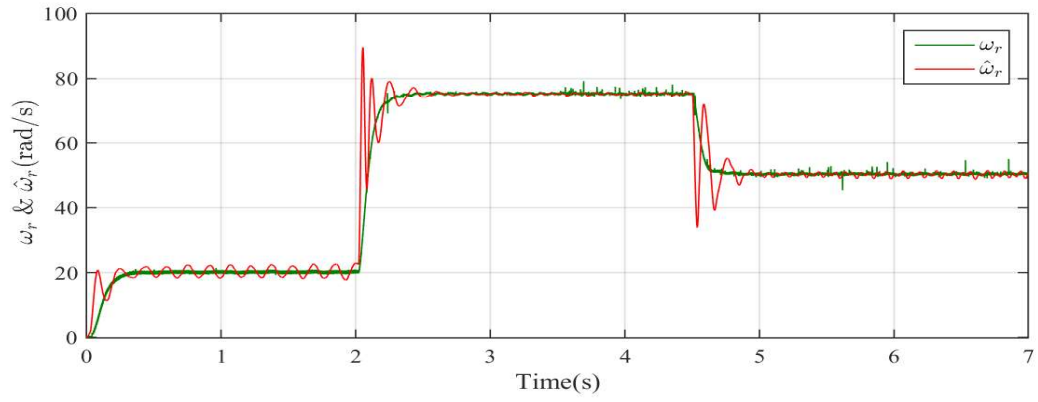


(c)

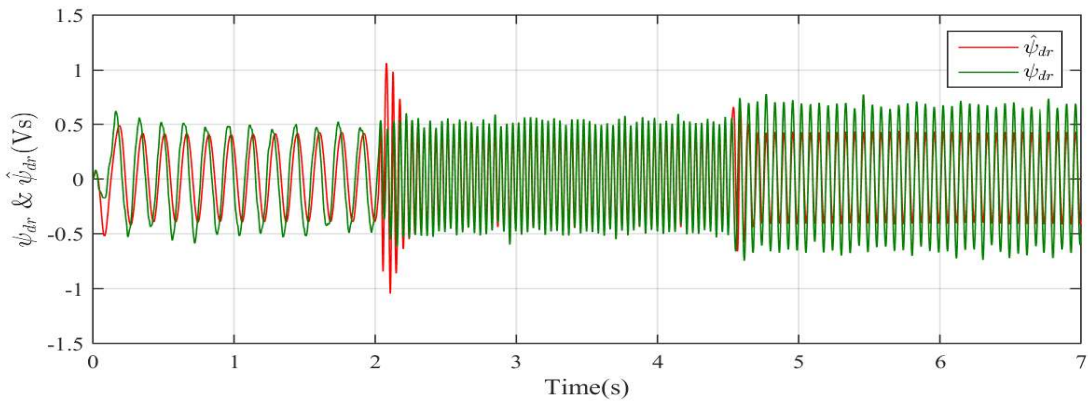
Figure 6.3: Error in estimation of a) ω_r b) ψ_{dr} c) ψ_{qr}

Estimation with the conventional EKF at a changing reference speed is performed

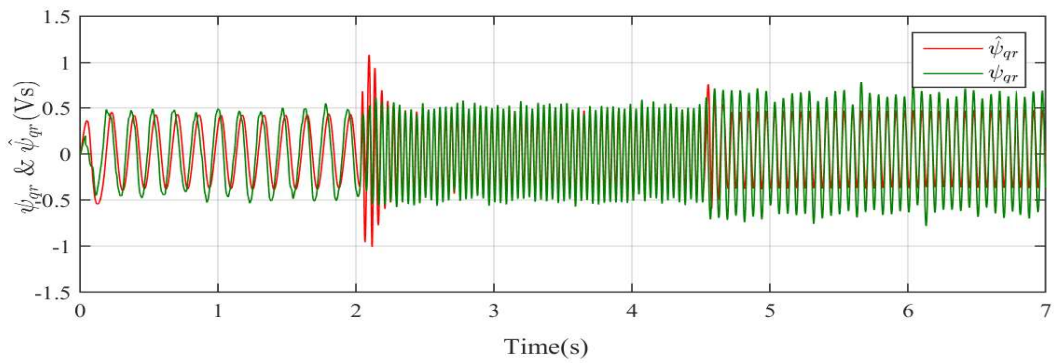
next. This is a varying reference speed- a step whose magnitude changes from 20rad/s to 75rad/s at $t=2s$ and then to 50rad/s at $t=4.5s$. The observations are depicted in figures 6.4a, 6.4b and 6.4c.



(a)



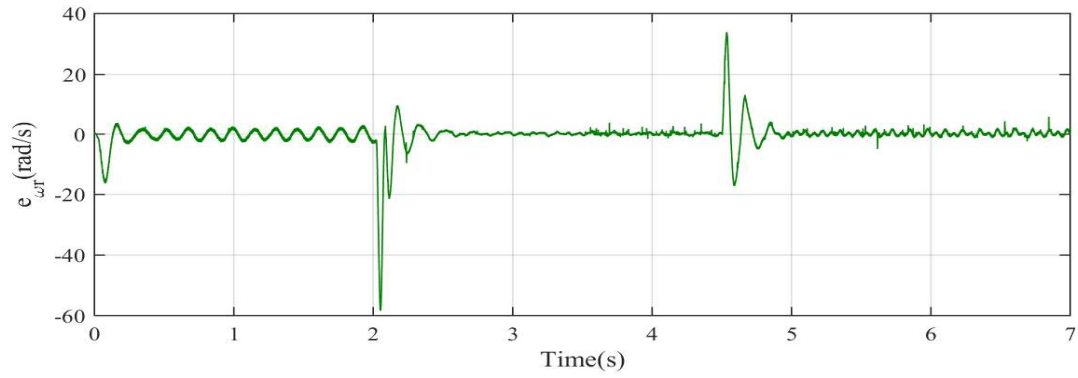
(b)



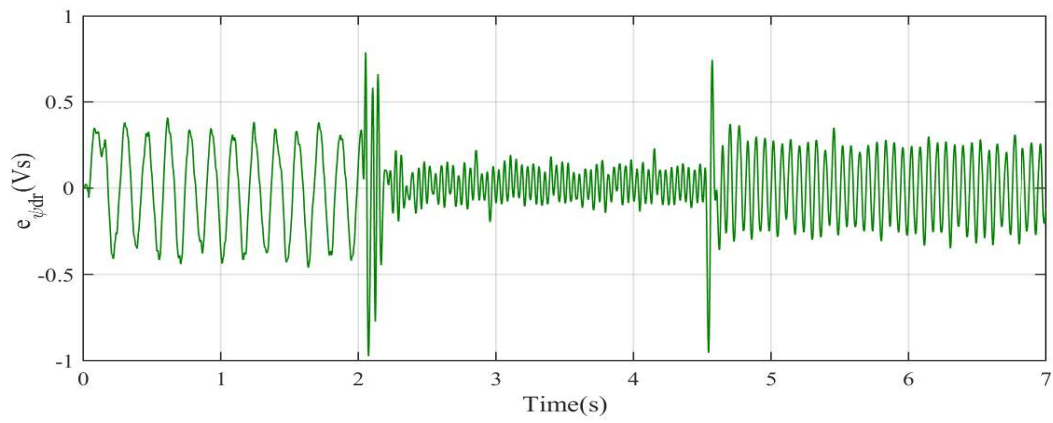
(c)

Figure 6.4: Estimated and measured values of a) rotor speed, ω_r , rotor fluxes, b) ψ_{dr} & $\hat{\psi}_{dr}$ and c) ψ_{qr} & $\hat{\psi}_{qr}$

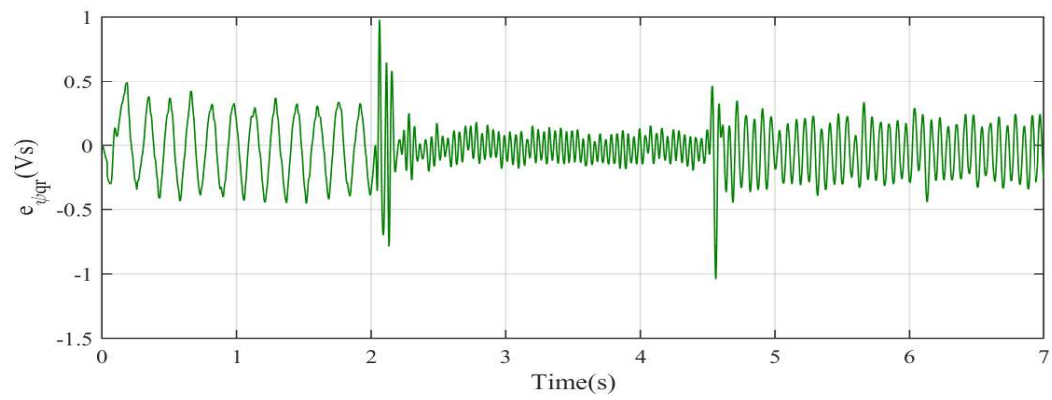
The errors in estimation are shown in Fig.6.5.



(a)



(b)



(c)

Figure 6.5: Error in estimation of a) ω_r b) ψ_{dr} c) ψ_{qr}

The process and noise covariance matrices used for estimation are

$$\mathbf{Q} = \begin{bmatrix} 0.0000001 & 0 & 0 \\ 0 & 0.0000001 & 0 \\ 0 & 0 & 0.0000001 \end{bmatrix} \quad (6.4.1)$$

$$\mathbf{R} = \begin{bmatrix} 150 & 0 \\ 0 & 150 \end{bmatrix} \quad (6.4.2)$$

These matrices are used in estimation with smoothed Kalman observer also.

6.4.2 Smoothed Kalman observer for a reduced model of three phase induction motor

A smoothed Kalman filter based observer is used to estimate the states of the motor. Smoothing is performed with one stage of output. The outputs at the $(k+1)^{st}$ instant are used to smooth those at the k^{th} instant. Here also, the simulation is conducted for the same sets of reference speed and the same voltage and current measurements used with the conventional EKF. The values of the process and measurement noise covariance matrices are the same as those used in section 6.4.1. The estimated value of rotor speed, ω_r for a reference speed of 75rad/s is shown in Fig. 6.6. The estimated and calculated rotor fluxes, ψ_{dr} and ψ_{qr} for this reference speed are shown in figures 6.7a and 6.7b.

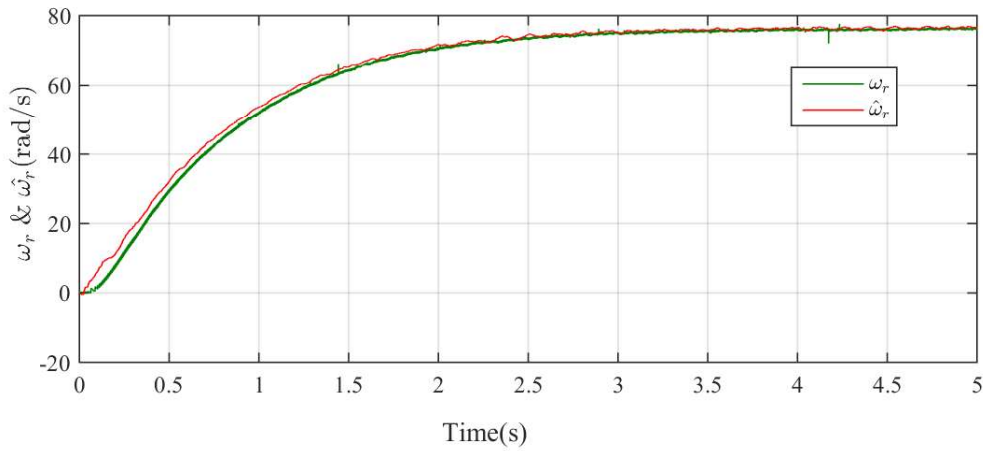
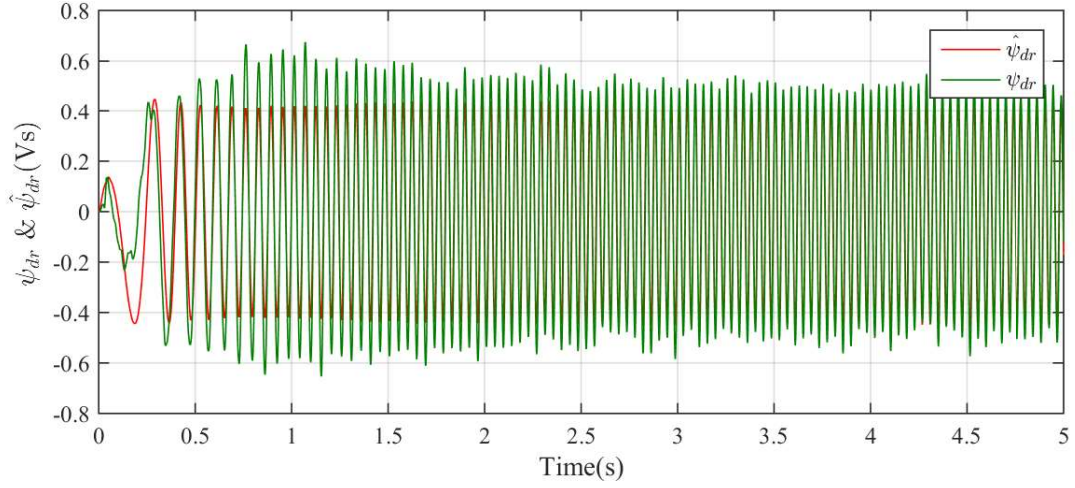
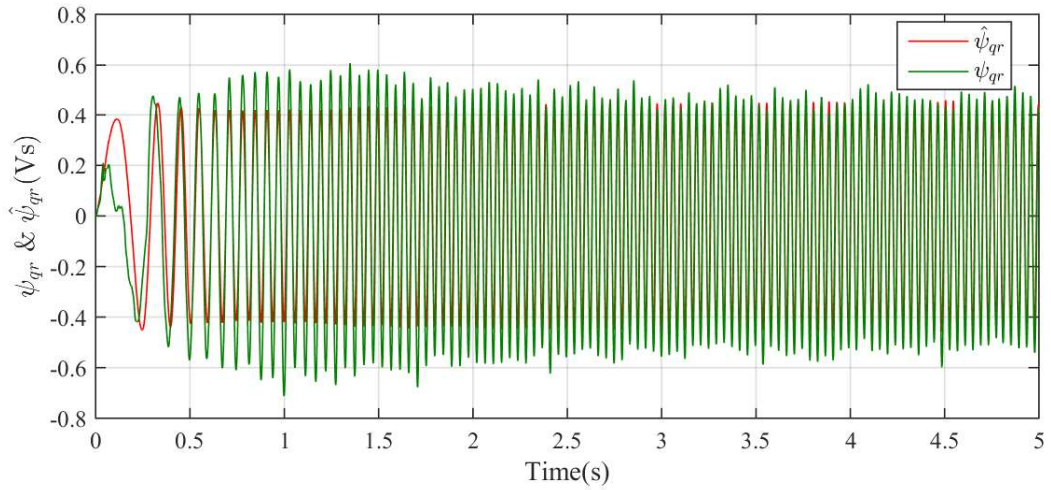


Figure 6.6: Estimated and measured values of rotor speed, ω_r , for a reference speed of 75rad/s



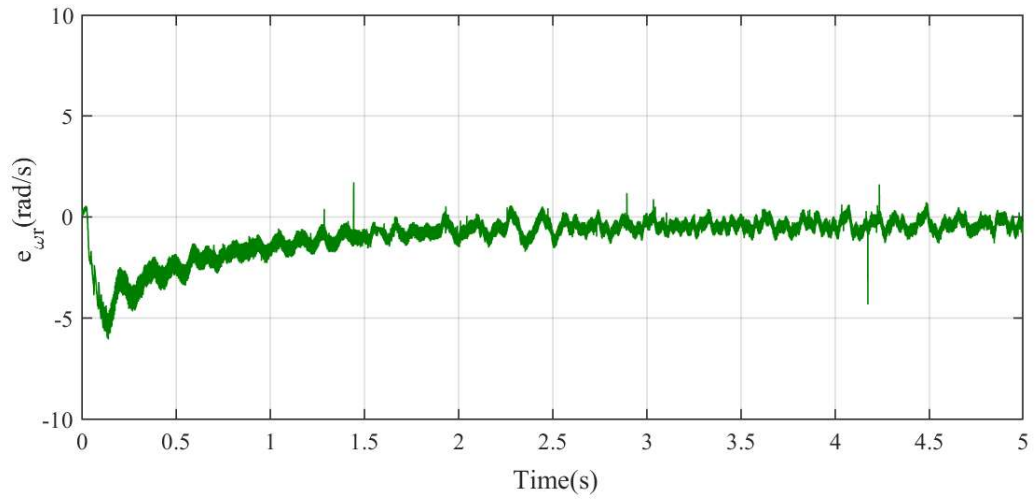
(a)



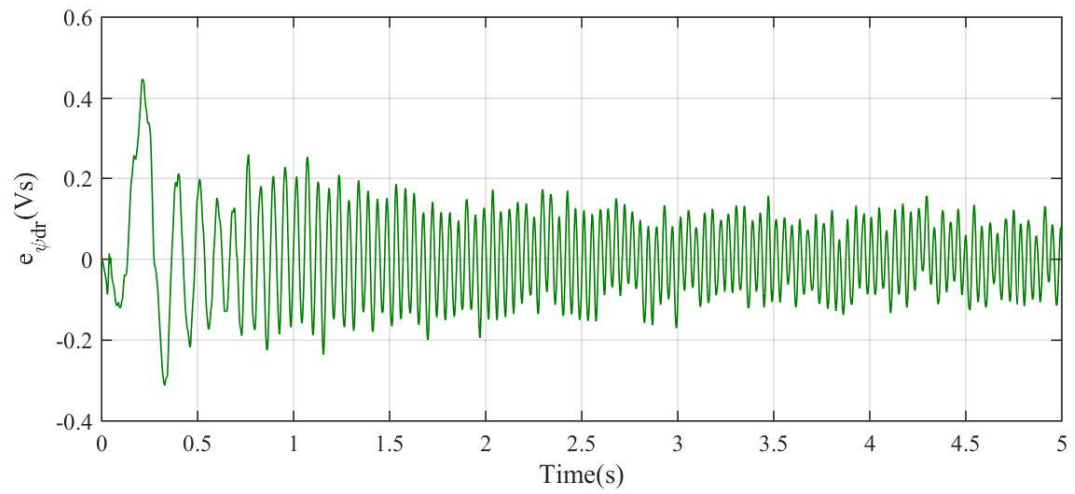
(b)

Figure 6.7: Estimated and calculated values of rotor fluxes a) ψ_{dr} and b) ψ_{gr}

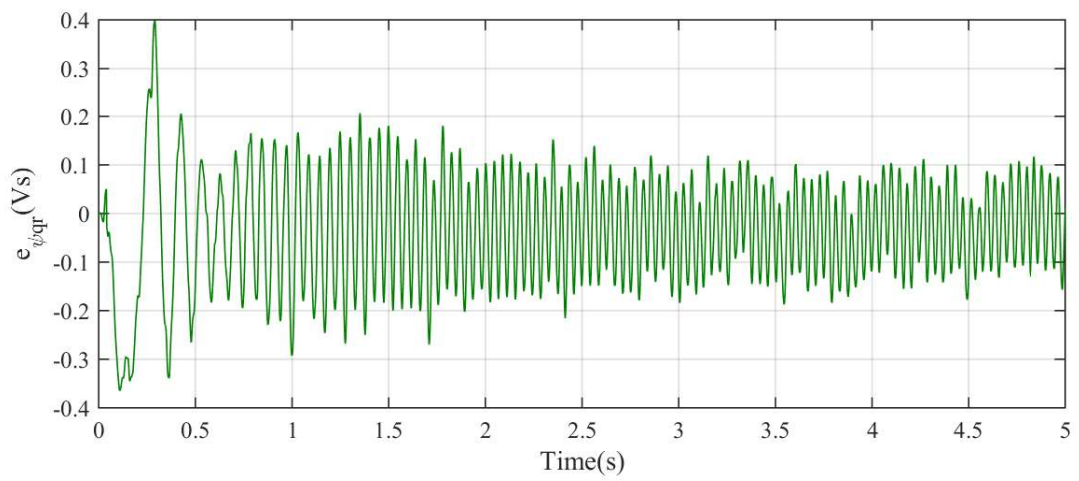
The corresponding error in estimation is shown in Fig. 6.8. It is clear from the error graphs that the errors with a smoothed Kalman observer are less compared to that with a conventional EKF. Since all other parameters are maintained constant, this improvement in estimation is due to the additional data made use of in smoothing.



(a)



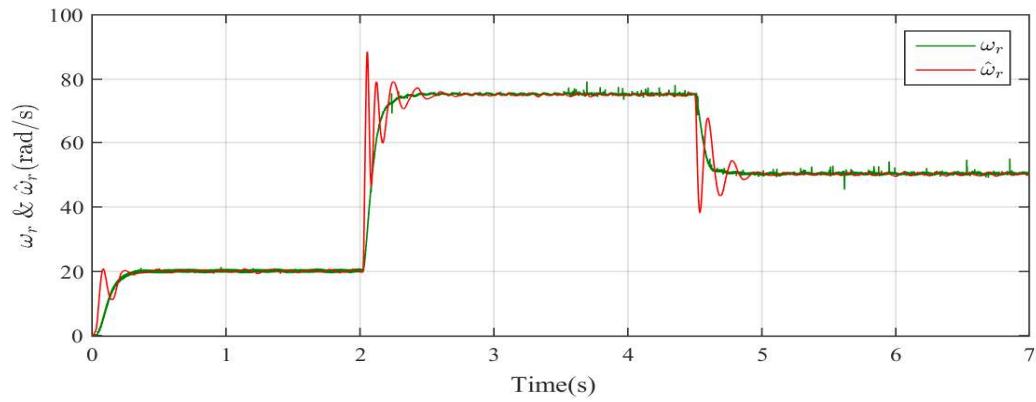
(b)



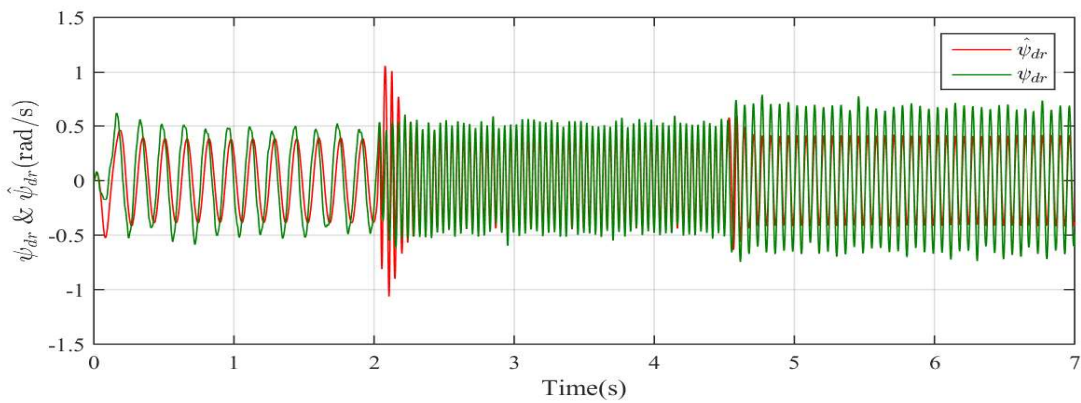
(c)

Figure 6.8: Error in estimation of a) ω_r b) ψ_{dr} c) ψ_{qr}

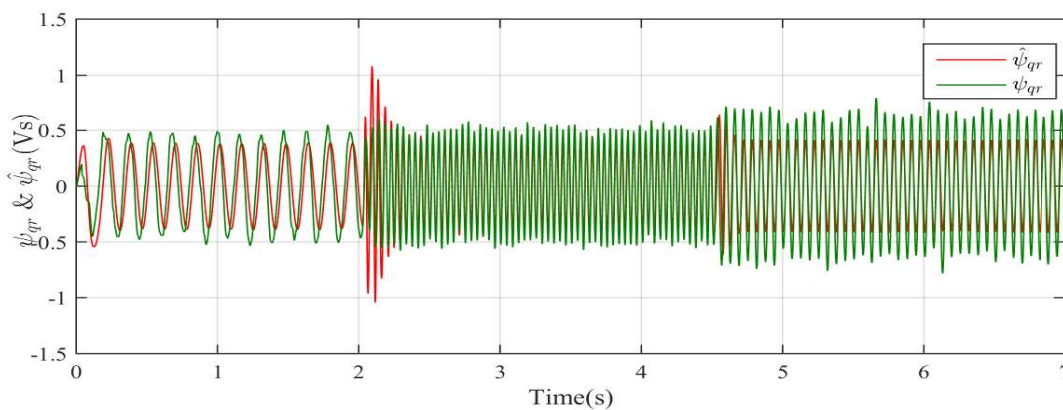
The simulation with a different reference speed was done with the smoothed Kalman observer also. The results of estimation are shown in figures 6.9a, 6.9b and 6.9c.



(a)



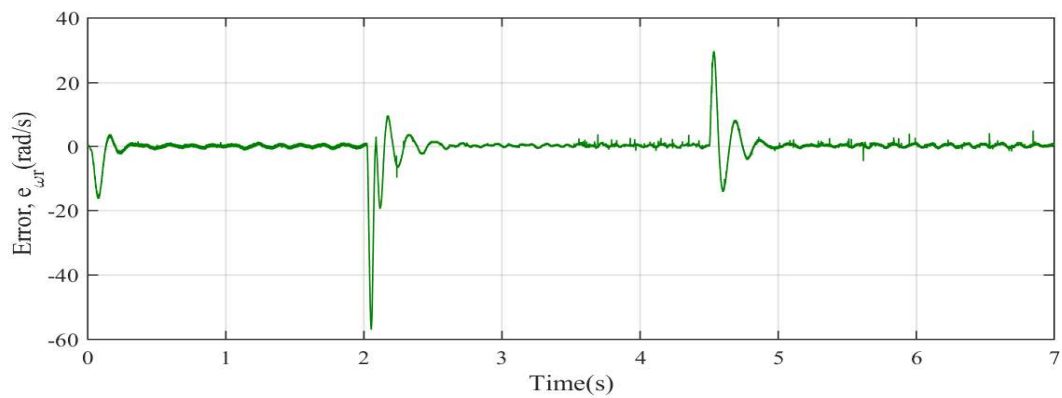
(b)



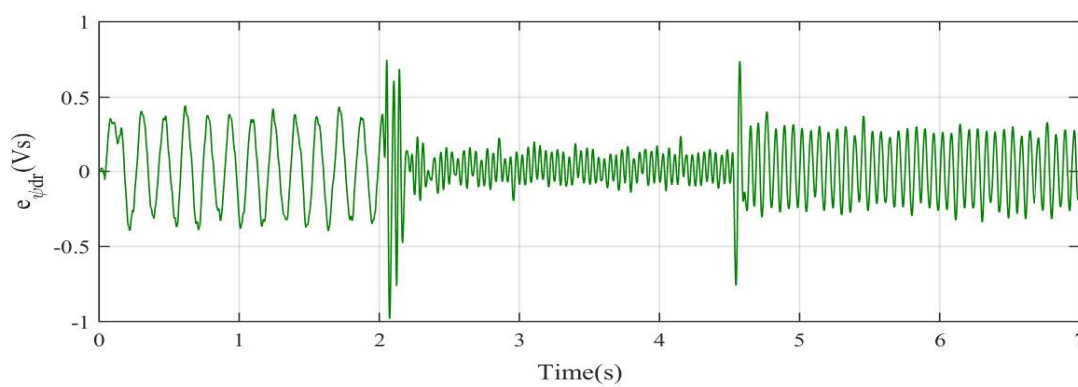
(c)

Figure 6.9: Estimated and calculated values of a) rotor speed, ω_r and rotor fluxes, b) ψ_{dr} c) ψ_{qr}

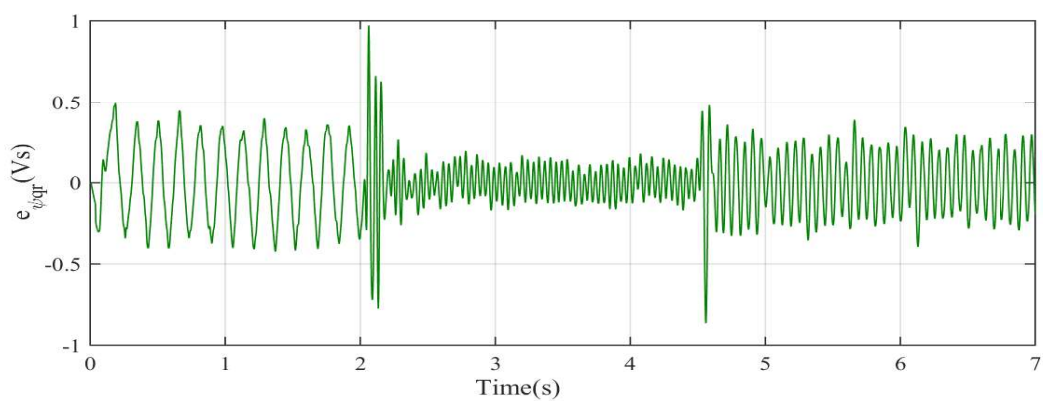
The corresponding errors are shown in Fig.6.10.



(a)



(b)



(c)

Figure 6.10: Error in estimation of a) ω_r b) ψ_{dr} c) ψ_{qr}

6.5 Summary

This chapter presents the offline estimation performances of an indirect vector controlled induction motor drive using observers based on conventional EKF and smoothing based Kalman algorithm. The observer is based on a reduced order mathematical model of the induction motor. The results obtained show an improvement in the estimation with smoothing algorithm. The improvement is prominent in the transient region. Since the error covariance matrices are kept constant, the betterment is due to the additional data considered for smoothing.

Uma Syamkumar “Smoothed Kalman Observer for Sensorless Field Oriented Control of Induction Motor.” Thesis. Department of Electrical Engineering, Government Engineering College, Trichur, University of Calicut, , 2020.

Chapter 7

Real-time implementation of the smoothed Kalman observer based on a reduced order model of induction motor

This chapter presents the real-time implementation of the smoothed Kalman filter based observer for indirect field-oriented control of three-phase induction motor. The closed loop observer based system is implemented using the reduced-order model of the machine. The results are compared with those of a conventional EKF based observer.

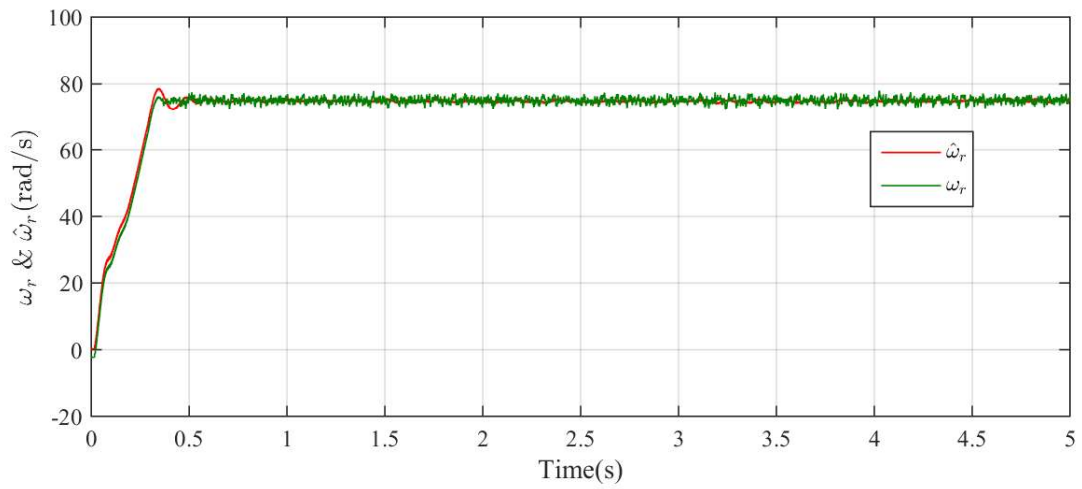
7.1 Introduction

The experimental validation of the simulation studies performed in the previous chapter (chapter 6) is done. The experimental set up of the previous experiment itself is used here also. The use of a reduced model of the induction motor alleviates the computational complexity of a fifth order system. The efficiency of the algorithm is confirmed for various reference speeds, including low and zero speeds.

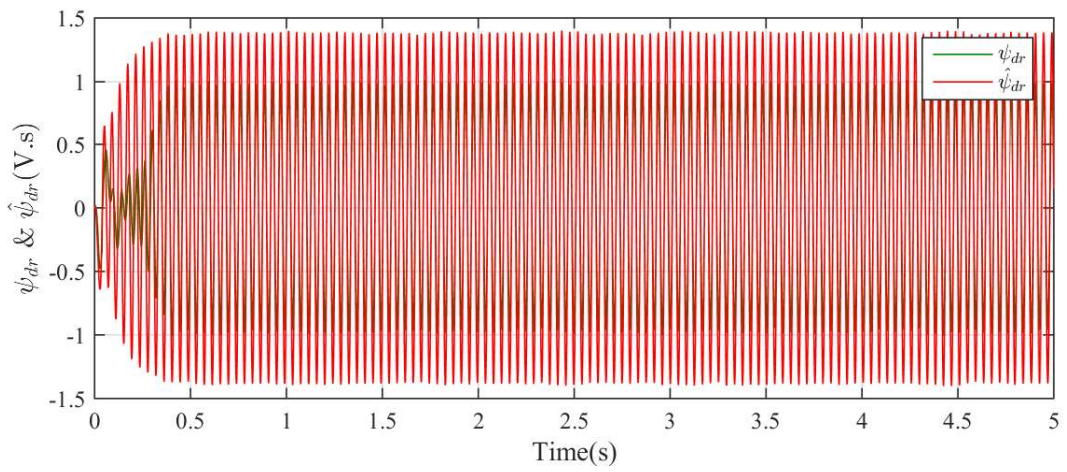
This chapter is organised as follows: Section 7.2 explains the hardware set up of the system and section 7.3 shows the results of closed loop performance of the system with a smoothed Kalman based observer. The performance of the system with a conventional EKF based observer is elaborated in section 7.4. Section 7.5 summarises the chapter.

7.2 Experimental Setup

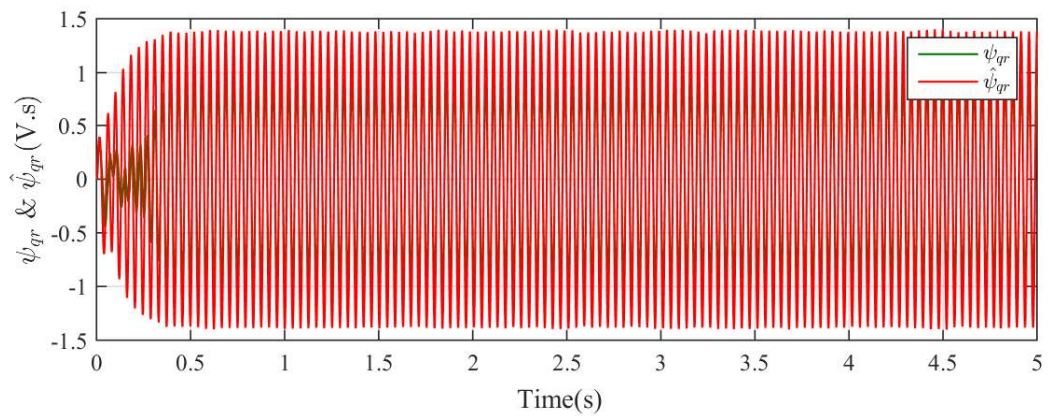
A block diagram of the experimental set up is shown in Fig.7.1. The hardware setup is the same as that used for validating the fifth order observer in chapter 5.



(a)

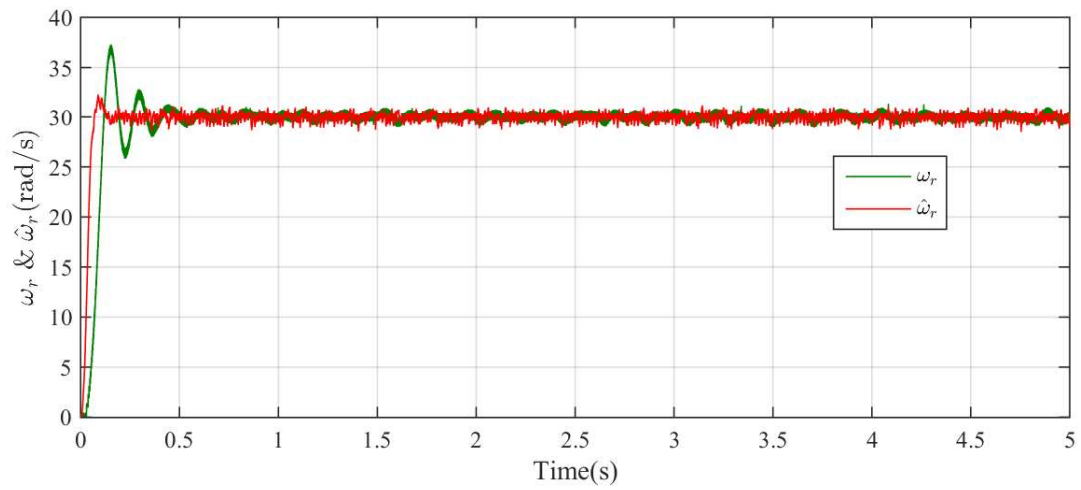


(b)

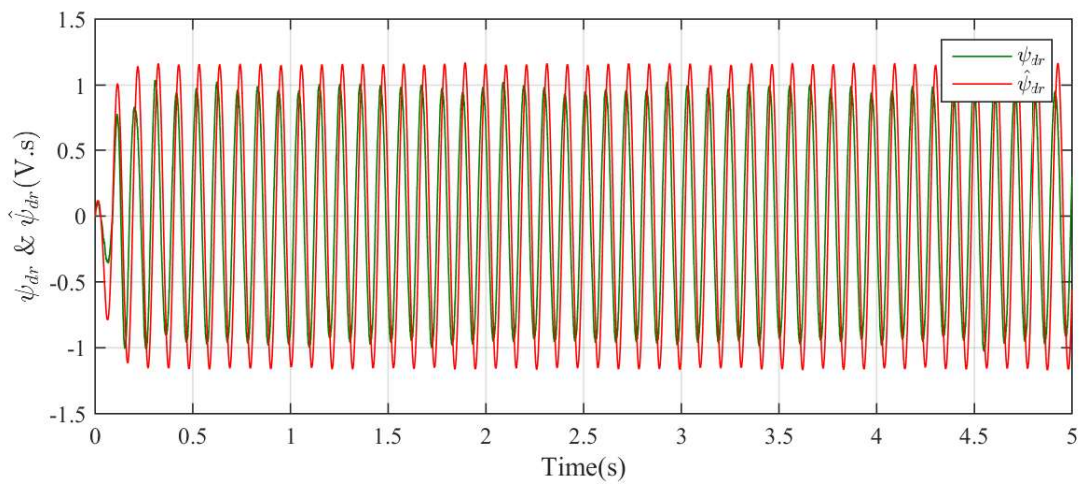


(c)

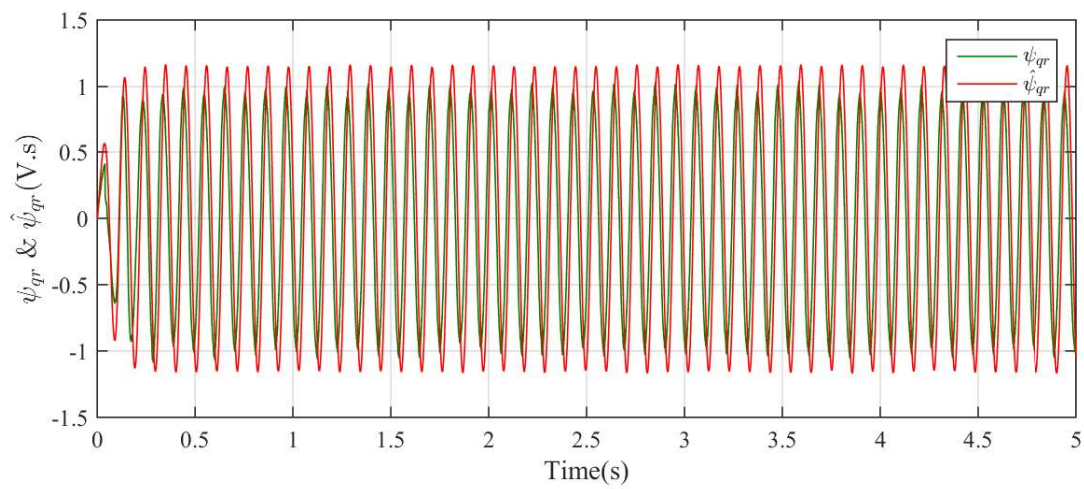
Figure 7.2: Experimental results for a reference speed of 75rad/s(mech.) a) ω_r b) ψ_{dr} c) ψ_{qr}



(a)

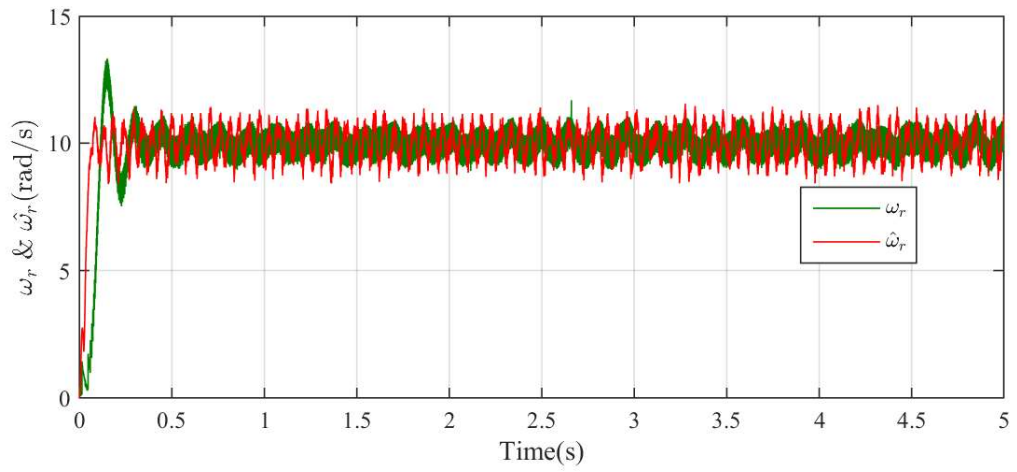


(b)

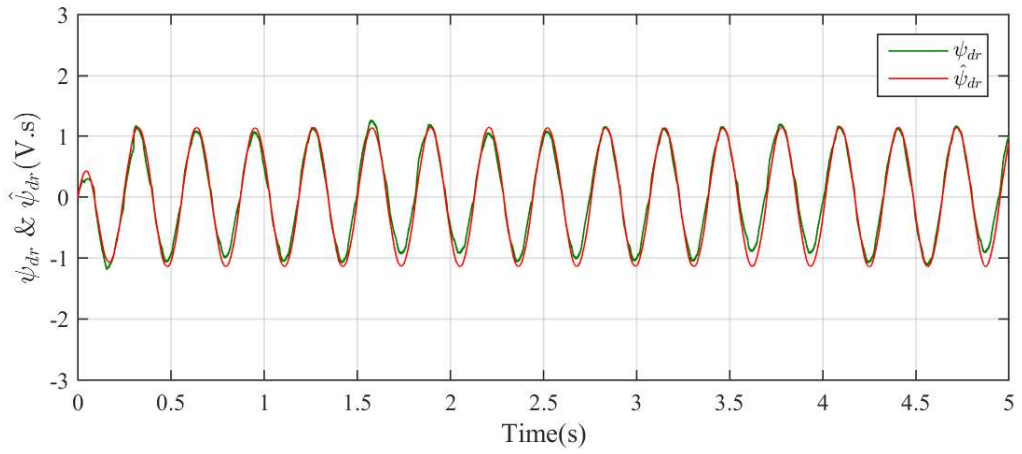


(c)

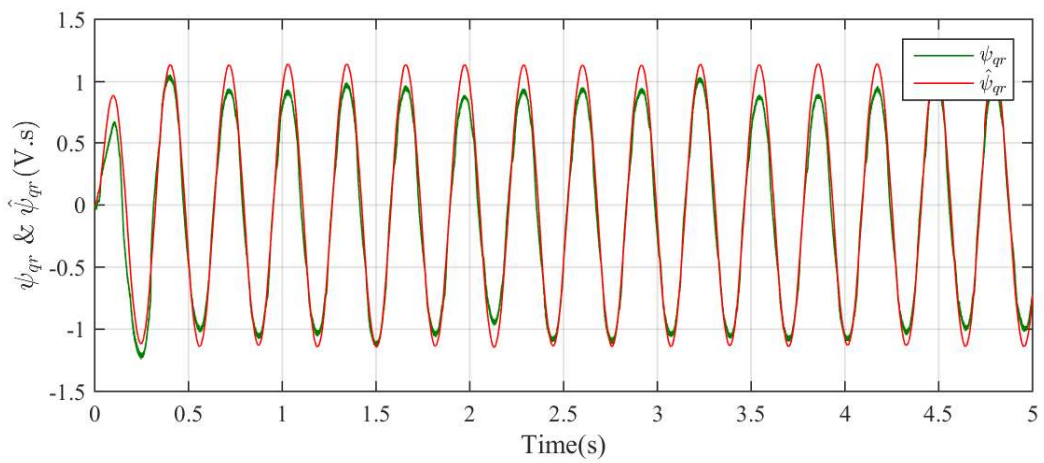
Figure 7.3: Experimental results for a reference speed of 30rad/s(mech.) a) ω_r b) ψ_{dr} c) ψ_{qr}



(a)

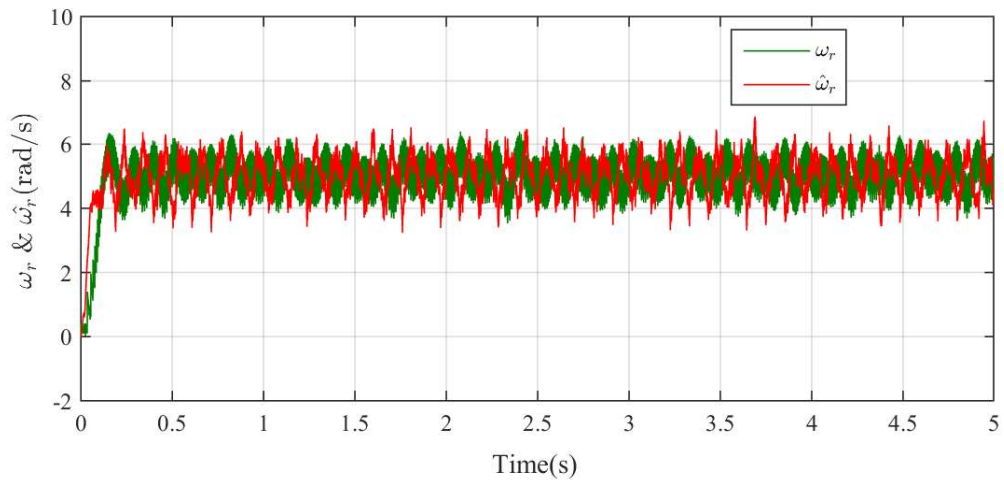


(b)

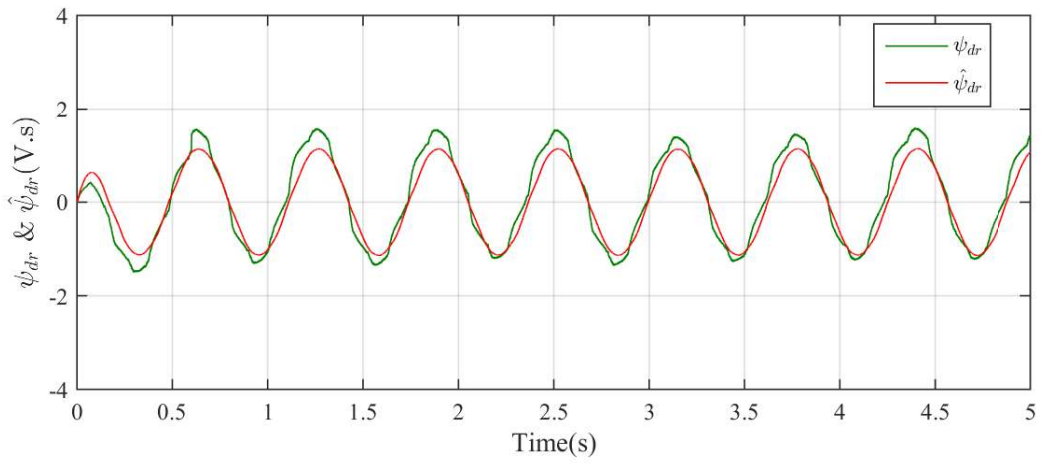


(c)

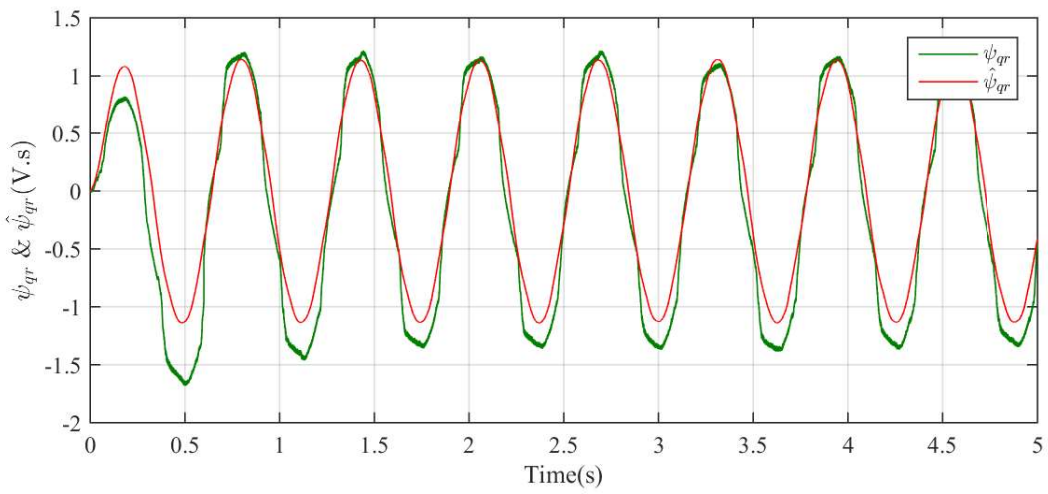
Figure 7.4: Experimental results for a reference speed of 10rad/s(mech.) a) ω_r b) ψ_{dr} c) ψ_{qr}



(a)

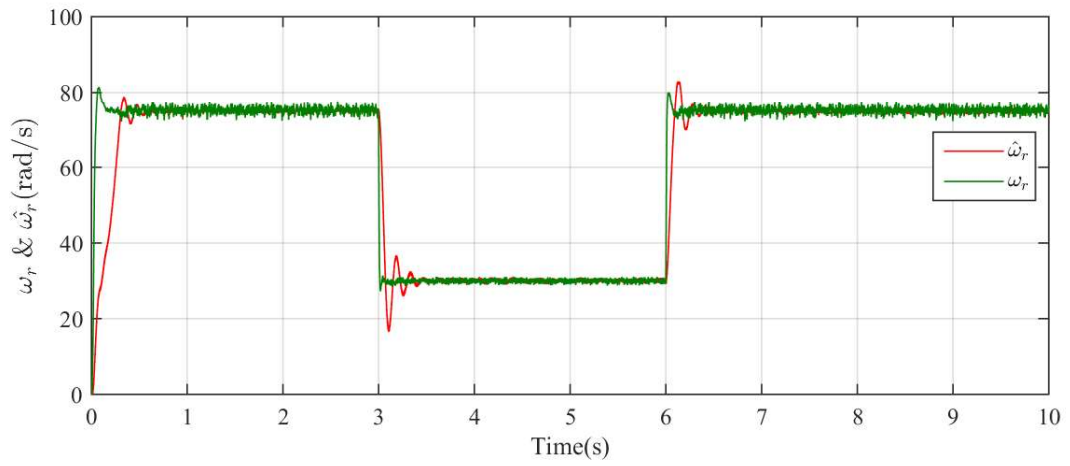


(b)

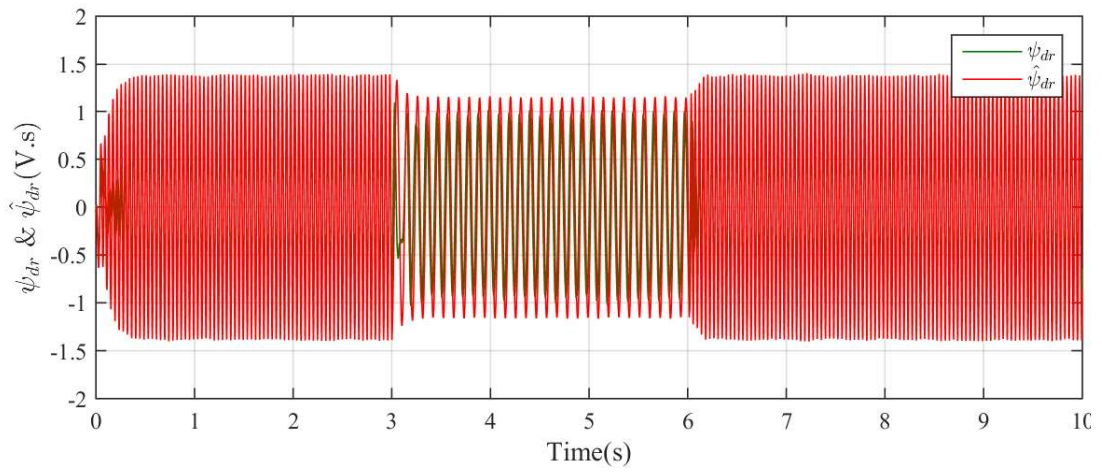


(c)

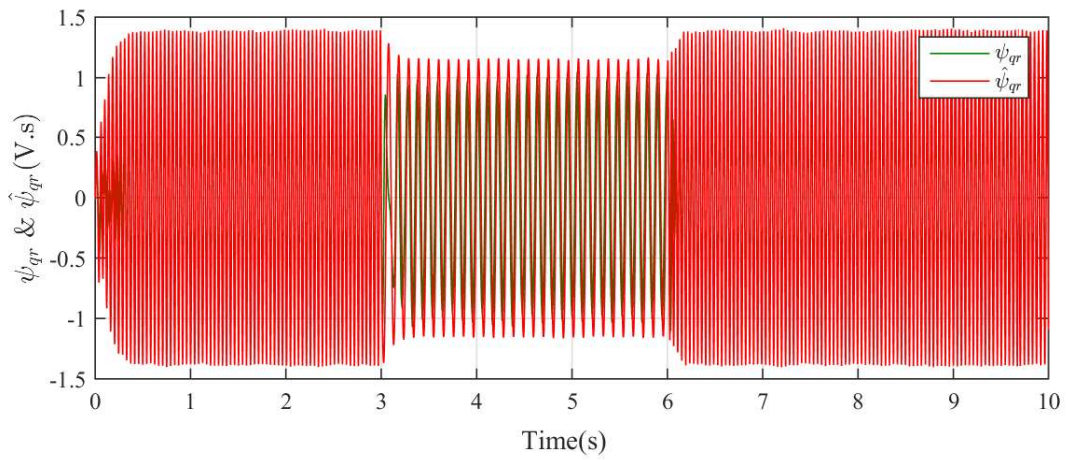
Figure 7.5: Experimental results for a reference speed of 5rad/s(mech.) a) ω_r b) ψ_{dr} c) ψ_{qr}



(a)

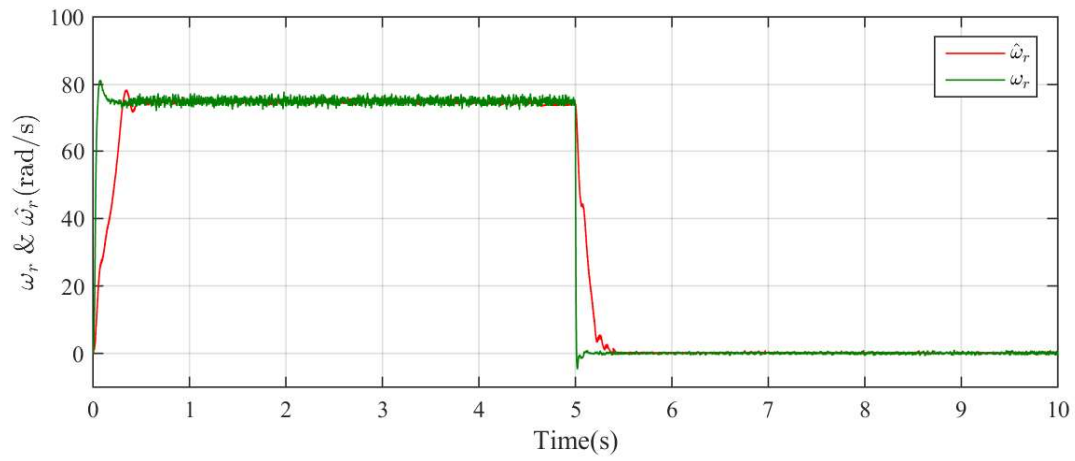


(b)

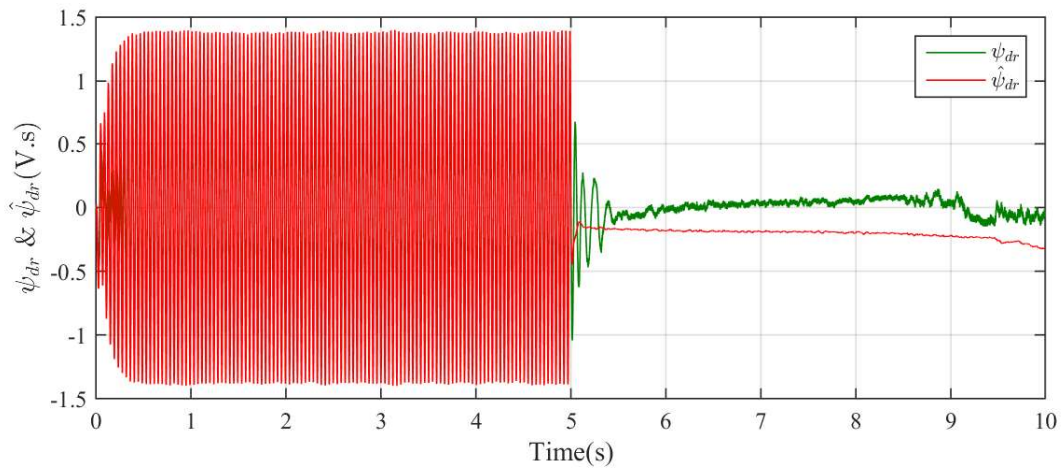


(c)

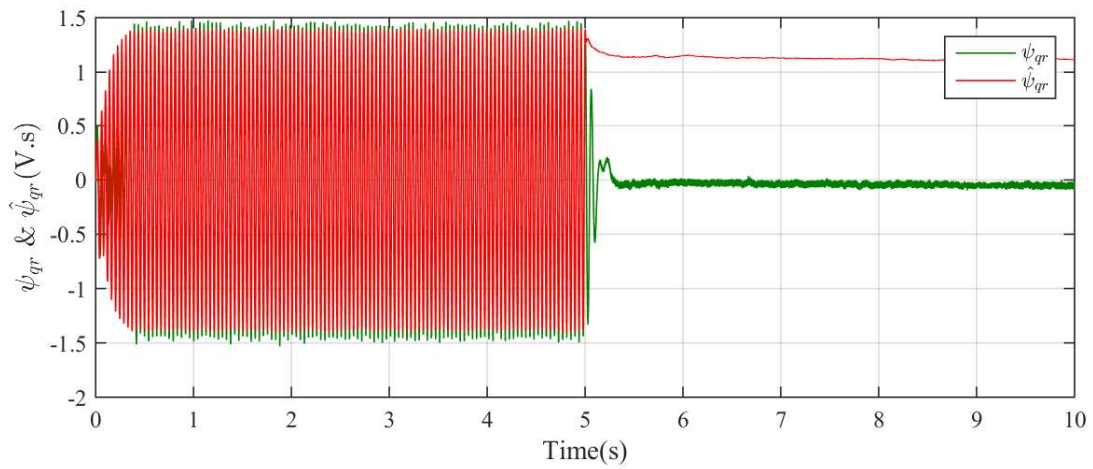
Figure 7.6: Experimental results for a reference speed of 75rad/s(mech) changes to 30 rad/s at 3s and back to 75 rad/s at 6s a) ω_r b) ψ_{dr} c) ψ_{qr}



(a)



(b)



(c)

Figure 7.7: Estimated Speed from the closed loop observer for a reference speed which changes from 75rad/s(mech) to 0rad/s(mech) at 5s and continues at zero speed for 5s a) ω_r b) ψ_{dr} c) ψ_{qr}

7.4 Experimental results of field-oriented control based on a reduced order conventional Kalman observer

A comparison of the results obtained with smoothed Kalman observer is done with those obtained with a conventional Kalman observer. The experiments are conducted

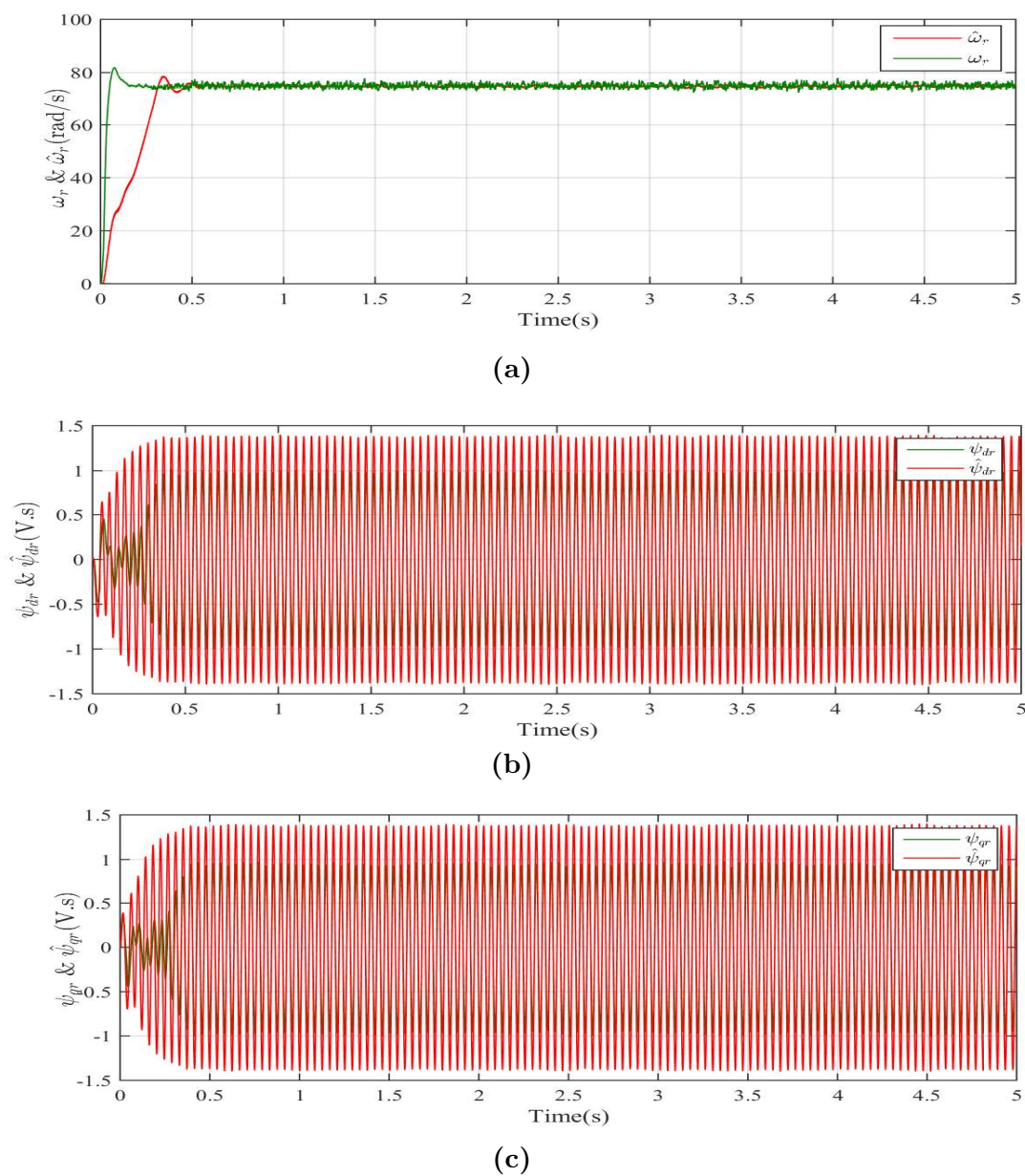
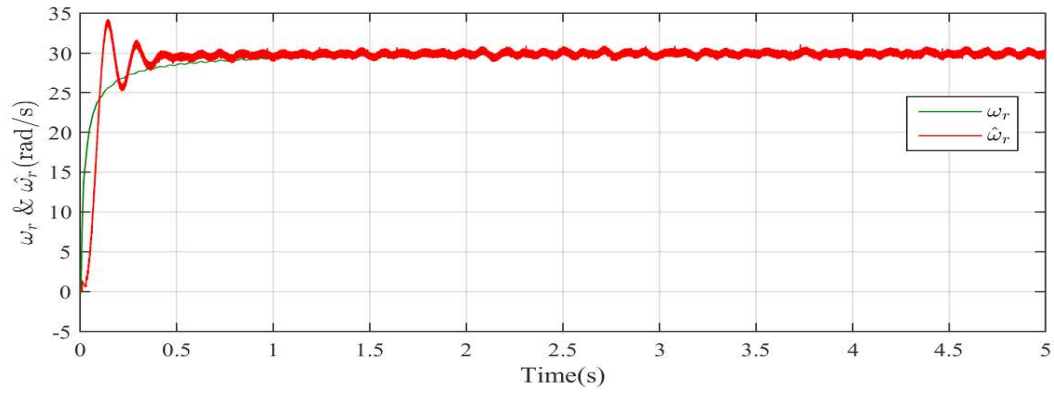
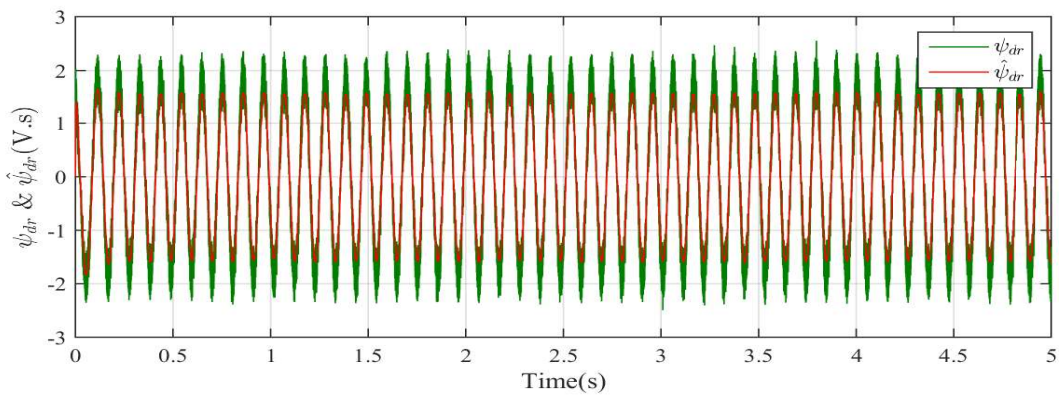


Figure 7.8: Experimental results for a reference speed of 75rad/s(mech.) a) ω_r b) ψ_{dr} c) ψ_{gr}

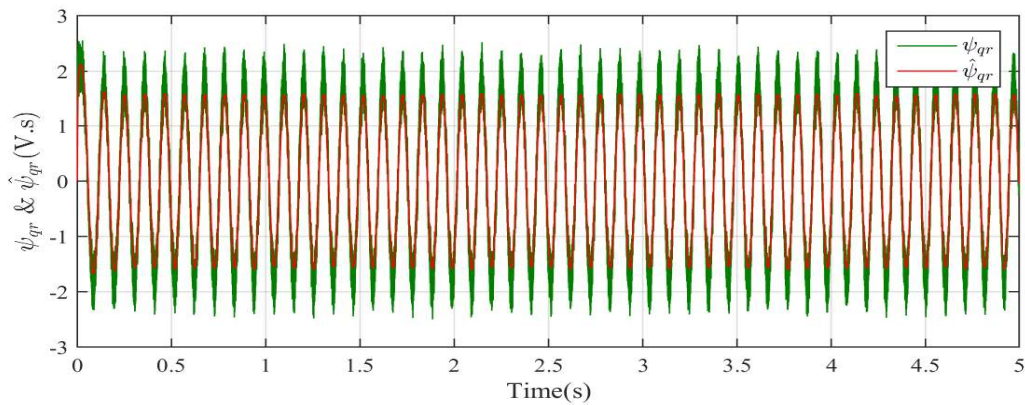
for the same reference speeds and same values of process and measurement noise covariance matrices. The results obtained are depicted in Figs. 7.8-7.13.



(a)

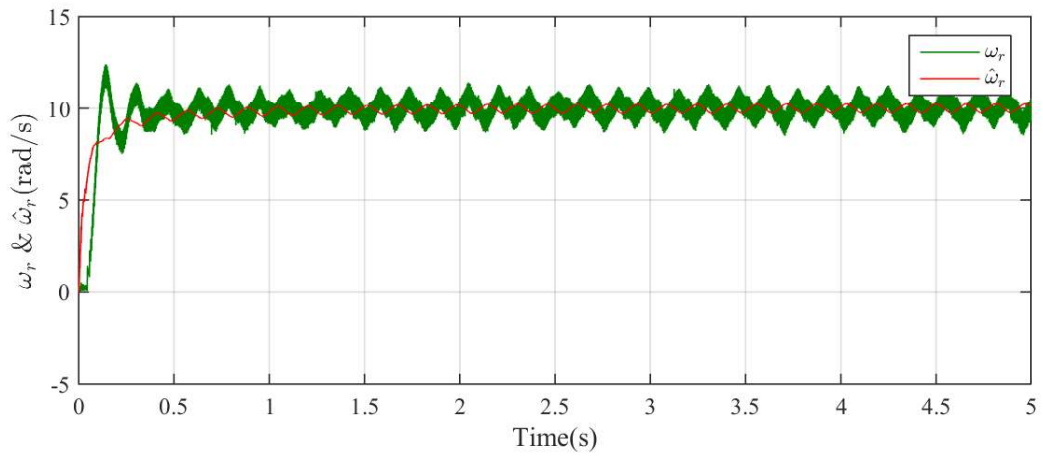


(b)

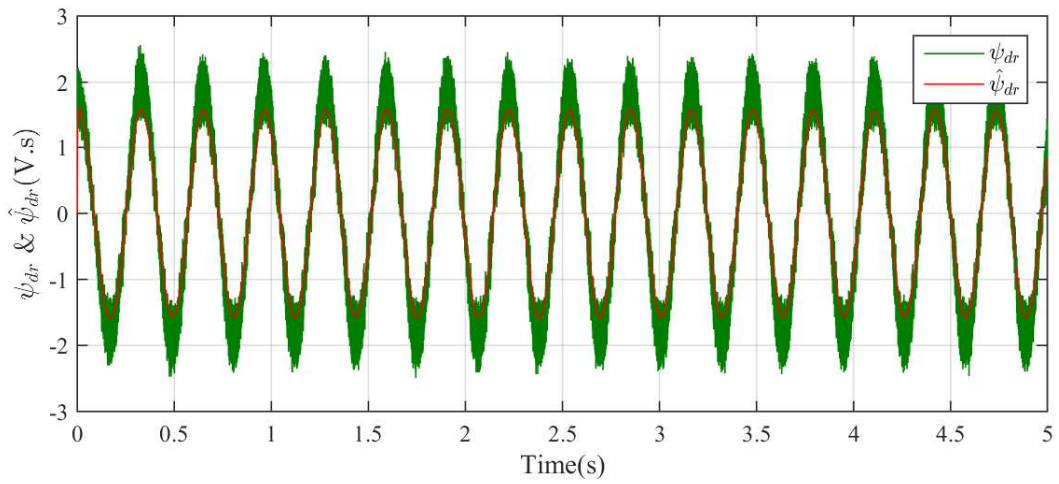


(c)

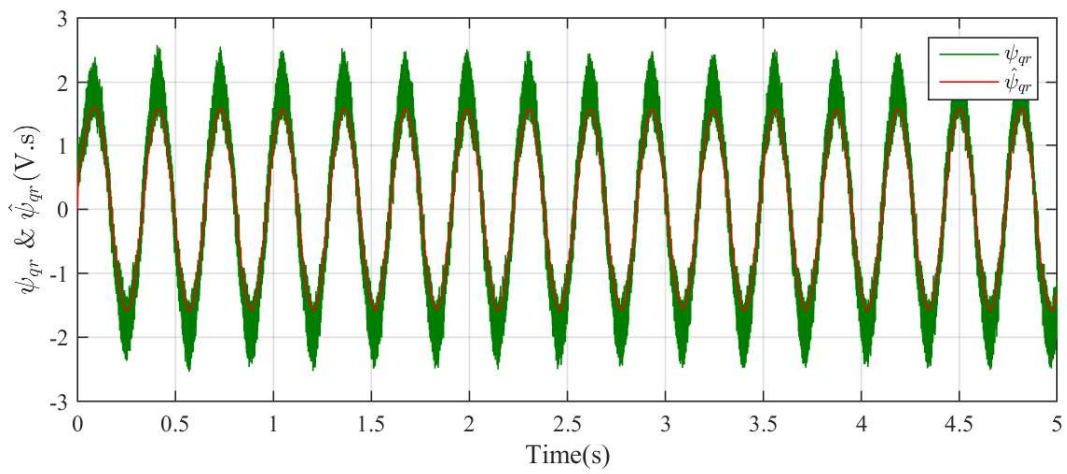
Figure 7.9: Experimental results for a reference speed of 30rad/s(mech.) a) ω_r b) ψ_{dr} c) ψ_{qr}



(a)

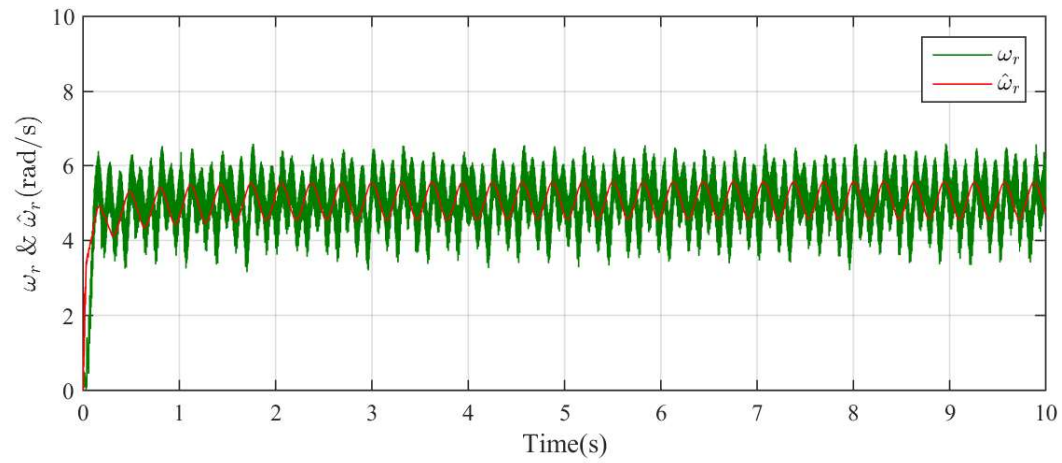


(b)

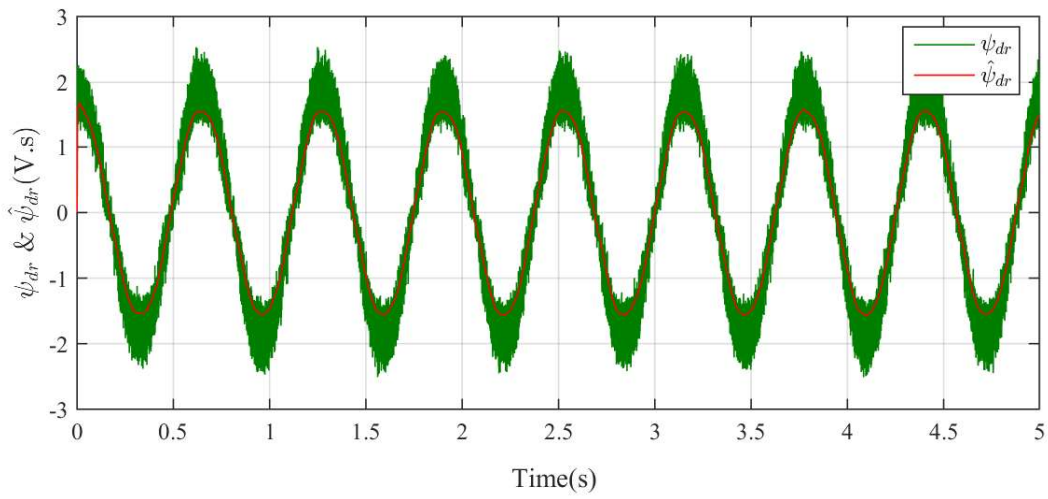


(c)

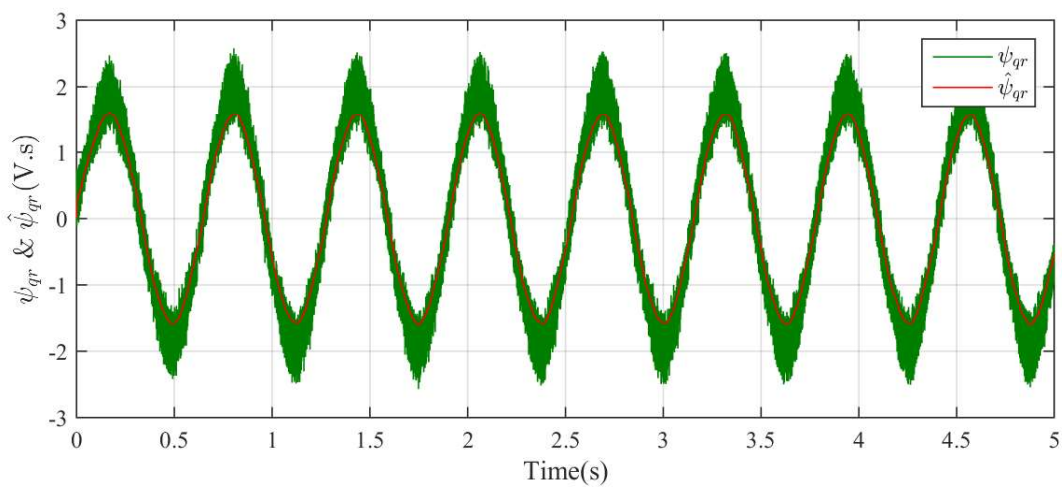
Figure 7.10: Experimental results for a reference speed of 10rad/s(mech.) a) ω_r b) ψ_{dr} c) ψ_{qr}



(a)

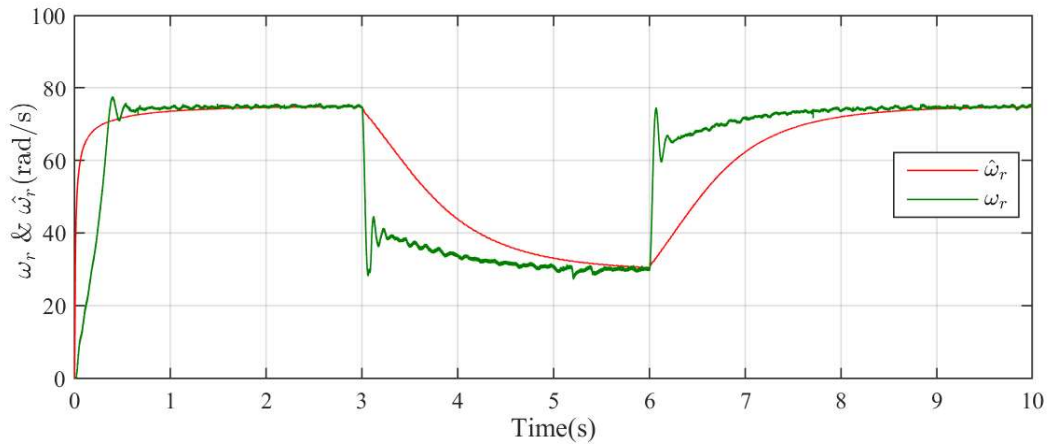


(b)

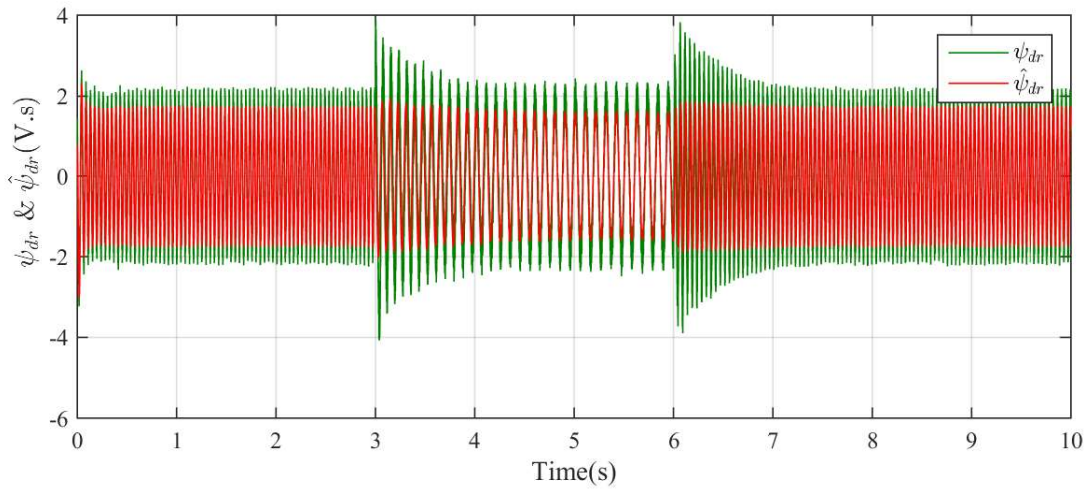


(c)

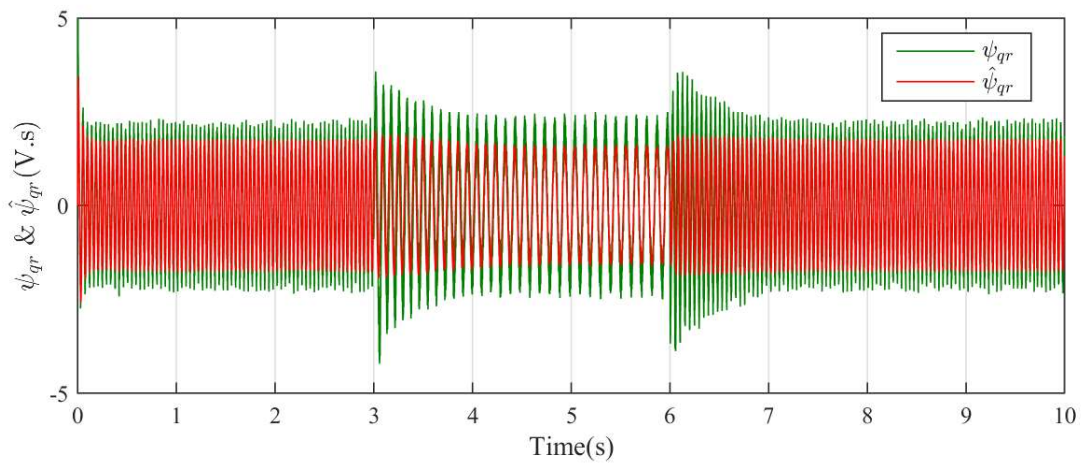
Figure 7.11: Experimental results for a reference speed of 5rad/s(mech.) a) ω_r b) ψ_{dr} c) ψ_{qr}



(a)

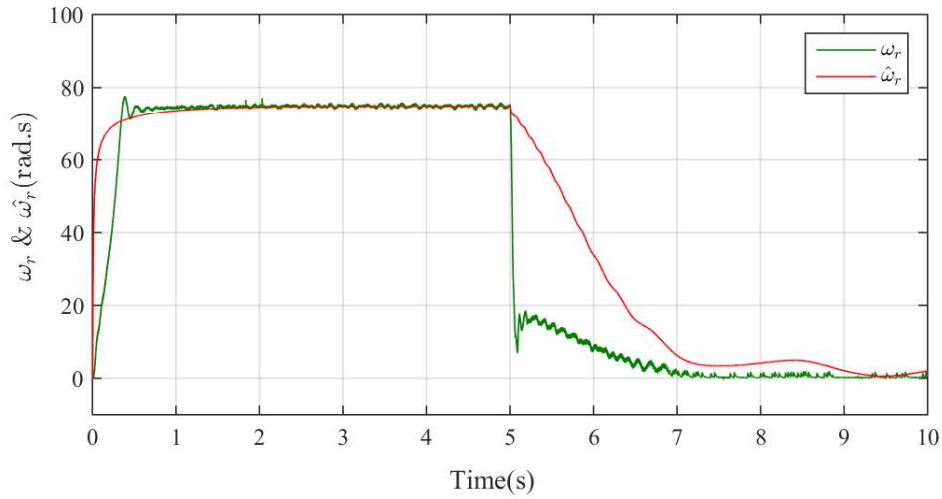


(b)

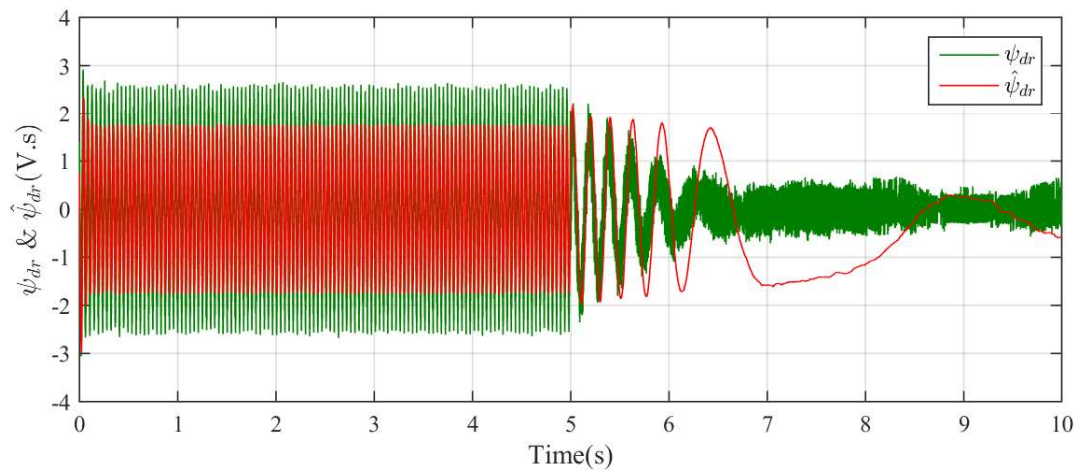


(c)

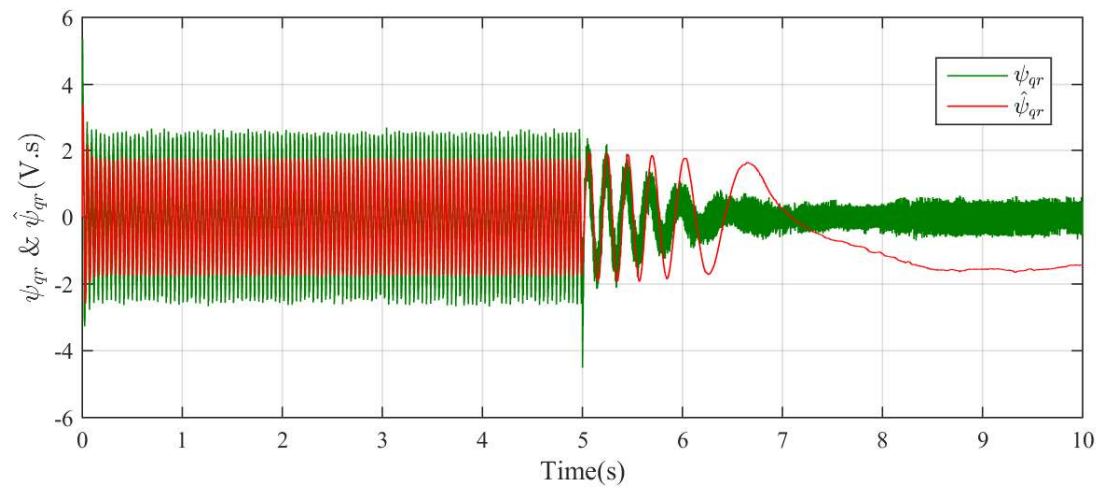
Figure 7.12: Experimental results for a reference speed of 75rad/s(mech) changes to 30 rad/s at 3s and back to 75 rad/s at 6s a) ω_r b) ψ_{dr} c) ψ_{qr}



(a)



(b)



(c)

Figure 7.13: Estimated Speed from the closed loop observer for a reference speed which changes from 75rad/s(mech) to 0rad/s(mech) at 5s and continues at zero speed for 5s a) ω_r b) ψ_{dr} c) ψ_{qr}

7.5 Summary

In this chapter, a smoothed Kalman observer for indirect field-oriented control of three phase induction motor, based on a reduced order model is discussed. The results obtained are compared with those obtained with a conventional Kalman filter. The comparison is done from the mean squared errors obtained in both the cases. The mean squared errors for various reference speeds are shown in table 7.1. Since the \mathbf{Q} and \mathbf{R} values are same in both SKF and CEKF, the steady state performances are more or less same, but there is prominent improvement in the transient response.

Table 7.1: Comparison of estimation results using a smoothed and conventional EKF (reduced order model of motor)

Ref. Speed(rad/s)	Mean Squared Error(rad/s)		% decrease
	CEKF	SKF	
75rad/s	341.7	5.53	98.3%
30rad/s	22.13	15.03	32.1%
10rad/s	6.25	3.41	45.44%
5rad/s	4.12	2.13	48.3%
75- 0	974.36	300.98	69.2%
75-30-75	573.15	241.08	57.93%

Uma Syamkumar “Smoothed Kalman Observer for Sensorless Field Oriented Control of Induction Motor.” Thesis. Department of Electrical Engineering, Government Engineering College, Trichur, University of Calicut, , 2020.

Chapter 8

A Smoothed Kalman Filter-trained Recurrent Neural Network for Speed Estimation of Induction Motor

This chapter explores the application of a smoothed Kalman-trained neural network observer for a reduced order model of the induction motor. The recurrent neural network, unlike feedforward neural networks, has at least one feedback loop, which makes it suitable for systems which are time-varying. The recurrent neural-network gets trained continuously, making the system real-time.

8.1 Introduction

Neural networks having the ability to mimic human brain can learn and process information and can hence be used advantageously for speed estimation. Different types of neural networks in a variety of configurations are available in the literature [107]. Most widely used classes of networks in the area of identification are i) multilayer networks and ii) recurrent networks. Multilayer networks, in which information flow in the forward direction only are successful in pattern recognition problems while recurrent networks have been useful in associative memories as well as for solutions of optimisation problems. Multilayer networks represent static nonlinear maps whereas recurrent networks represent nonlinear dynamic feedback systems. A multilayer neural network will have an input layer, a hidden layer and an output layer. The neurons in all these layers are interconnected by means of weights, which are measures of the information flowing through the network. All neurons except those in the input layer will have an activation function, like a sigmoidal function. The weights of the networks are adjusted to minimise a suitable function of the error between the actual output and the desired output. This results in a mapping function between the outputs and inputs. Hence, multilayer networks provide versatile input-output maps with the elements of the weight matrices as parameters.

Recurrent neural networks, on the other hand, are not feedforward networks. They

will have atleast one feedback loop. These networks have the ability to deal with time-varying input or output through its own temporal operation [95, 96]. A recurrent neural network, with its training operation running continuously is called a real-time recurrent neural network.

A smoothed Kalman filter based algorithm is used here to train the recurrent neural network for speed and flux estimation of three phase induction motor. The learning process starts at the onset of estimation process and the duration of training in every step is definite, which is equal to the duration of execution of training algorithm, once. This makes the estimation process feasible with real-time applications.

This chapter is organized as follows: Section 8.2 explains the structure of a general real-time recurrent neural network. The training algorithm is explained in section 8.3. Section 8.4 explains the application of the proposed training algorithm on the three phase induction motor model. Section 8.5 elaborates the offline estimation results with a conventional EKF algorithm (8.5.1) and the proposed algorithm(8.5.2). Section 8.6 concludes the chapter.

8.2 A General Real-time Recurrent Neural Network

The structure of a real-time recurrent neural network is depicted in Fig.8.1. This network has a total of \mathbf{N} neurons. The outputs of these \mathbf{N} neurons are fed back with a unit time-delay. In addition, there are \mathbf{M} external inputs. Thus, there are $(\mathbf{M}+\mathbf{N})$ inputs to the network. Out of the total \mathbf{N} neurons, \mathbf{P} neurons may be considered as output neurons and the remaining $(\mathbf{N}-\mathbf{P})$ neurons act as hidden neurons.

$X(k)$ denotes the $M \times 1$ external input vector applied to the network at the k^{th} discrete instant and $Y(k+1)$ denotes the corresponding output vector produced one time-step later, at the time instant, $(k+1)$. The external input vector, $X(k)$ and the one time-step delayed output vector together form the $(M+N) \times 1$ input vector, $U(k)$. Thus,

$$U(k) = \left[Y_1(k) Y_2(k) \dots Y_n(k) X_1(k) X_2(k) \dots X_M(k) \right]^T$$

The output of any neuron, j at a discrete time, $(k+1)$ is given by

$$Y_j(k+1) = f(\text{net}_j(k)) \quad (8.2.1)$$

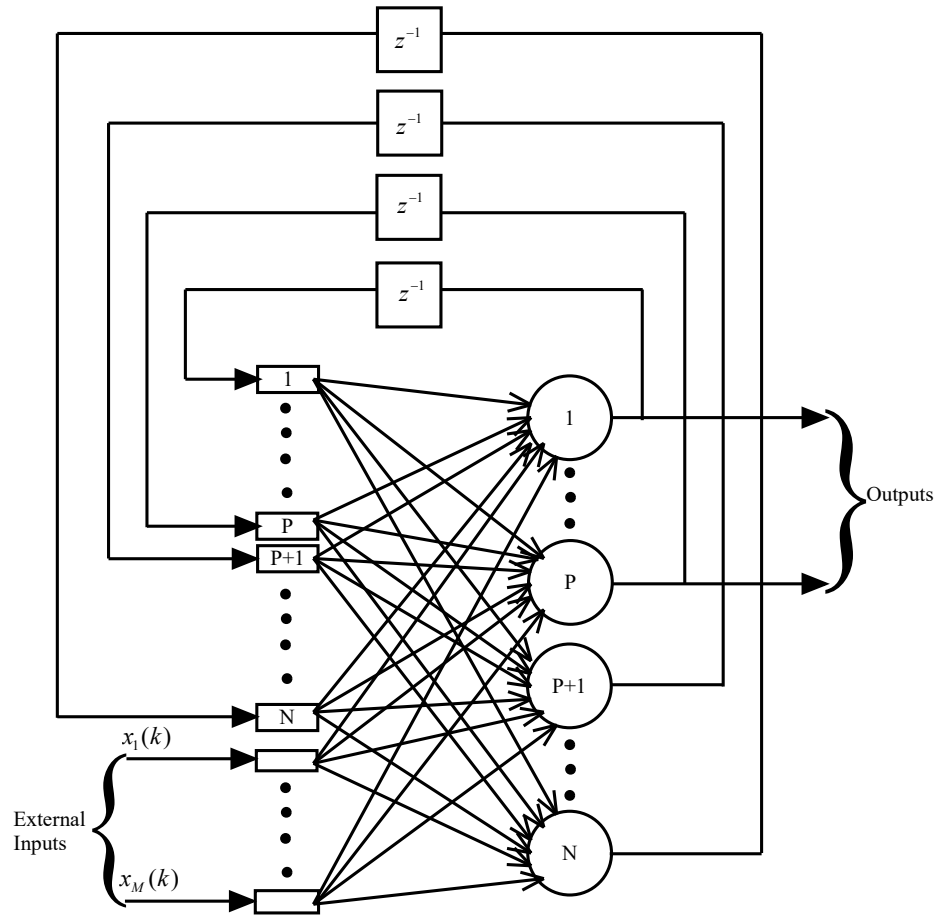


Figure 8.1: A Real-time Recurrent Neural Network

where, $f(\cdot)$ is the activation function of the neuron and

$$net_j(k) = \sum_{i=1}^{(M+N)} w_{ji} U_i(k) \quad (8.2.2)$$

denotes the net input into the j^{th} neuron. These two equations together constitute the entire dynamics of the network.

8.3 Parameter Based Smoothed Kalman Filter Algorithm for Training Recurrent Neural Network

A parameter estimation problem is similar to training a neural network where the error between the actual and the desired outputs are minimised, based on some error function.

Consider a real-time recurrent neural network, without any hidden neurons as shown in Fig. 8.2.

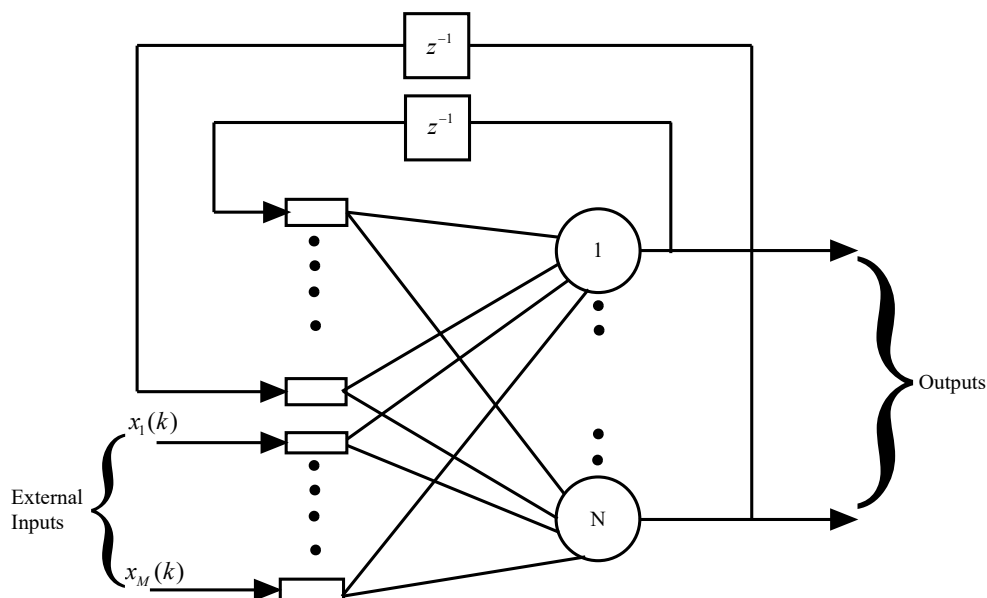


Figure 8.2: A real-time recurrent neural network without hidden neurons

The desired values of the output at the k^{th} instant is given by a column vector,

$$d(k) = [d_1(k) \ d_2(k) \ \dots \ d_N(k)]^T \quad (8.3.1)$$

$$f(k) = [f_1(net_1) \ f_2(net_2) \ \dots \ f_N(net_N)]^T \quad (8.3.2)$$

denotes a vector of outputs of the neurons. Error vector can be written as

$$e(k) = f(k) - d(k) \quad (8.3.3)$$

This error can be minimised by defining a training cost function, defined by

$$E(k) = \frac{1}{2}e(k)^T S(k)e(k) \quad (8.3.4)$$

where $S(k)$ is a user specified non- negative definite weighting matrix. $W(k)$ represents the weights of the network which can be trained, and is of dimension, M . The updated estimate of the weight vector at instant, k is denoted by $\hat{W}(k)$. $P(k)$, the error covariance matrix is updated at each step and stored. This covariance matrix is made use of to model the interaction among weights in the network. $P(k)$ at the onset of training procedure is set as $P(0)$, which is diagonal. Training algorithm consists of the following steps:

1. At the k^{th} step, the inputs and outputs of recurrent nodes are transmitted through the network and $f(k)$ is computed.
2. $e(k)$, the error vector, is computed and the dynamic derivatives of each component of $f(k)$, with respect to the current weight estimate, $\hat{w}(k)$ are evaluated.
3. These derivatives are arranged into an $M \times N$ matrix, $H(k)$ as

$$H(k) = \begin{bmatrix} \frac{\delta f_1(net_1)}{\delta W_1} & \dots & \frac{\delta f_n(net_n)}{\delta W_1} \\ & \cdot & \\ & \cdot & \\ & \cdot & \\ & \cdot & \\ \frac{\delta f_1(net_1)}{\delta W_m} & \dots & \frac{\delta f_n(net_n)}{\delta W_m} \end{bmatrix} \quad (8.3.5)$$

4. The updated weights, $\hat{w}(k)$ and error covariance matrix, $P(k)$ are obtained by the recursive Kalman filter algorithm:

$$A(k) = [\eta(k)S(k)^{-1} + H(k)^T P(k)H(k)]^{-1} \quad (8.3.6)$$

$$K(k) = P(k)H(k)A(k) \quad (8.3.7)$$

$$\hat{W}(k+1) = \hat{W}(k) + K(k)e(k) \quad (8.3.8)$$

$$P(k+1) = P(k) - K(k)H(k)^T P(k) + Q(k) \quad (8.3.9)$$

$\eta(k)$ is the learning rate of the neural network.

5. The weights updated using EKF are refined using the smoothing algorithm. The smoothed estimate of weight is obtained using the following equations:

$$M(k) = P(k)H^T P^{-1} \quad (8.3.10)$$

$$\hat{W}_s(k) = \hat{W}(k) + M(k)(\hat{W}(k) - W(k)) \quad (8.3.11)$$

where $M(k)$ is the smoothing gain matrix.

8.4 Speed Estimation Using Real-Time Recurrent Neural Network

Speed estimation makes use of two mathematical models for rotor flux calculation. First one relates rotor flux to terminal voltages and current and is independent of speed. The second one represents the rotor as a state space model and contains rotor speed variable. These two models are:

$$\begin{bmatrix} p\psi_{dr}^s \\ p\psi_{qr}^s \end{bmatrix} = \frac{L_r}{L_m} \begin{bmatrix} v_{ds}^s \\ v_{qs}^s \end{bmatrix} - \begin{bmatrix} R_s + \sigma L_s p & 0 \\ 0 & R_s + \sigma L_s p \end{bmatrix} \begin{bmatrix} i_{ds}^s \\ i_{qs}^s \end{bmatrix} \quad (8.4.1)$$

$$\begin{bmatrix} p\psi_{dr}^s \\ p\psi_{qr}^s \end{bmatrix} = \frac{L_r}{L_m} \begin{bmatrix} \frac{-1}{T_r} & -\omega_r \\ \omega_r & \frac{-1}{T_r} \end{bmatrix} \begin{bmatrix} \psi_{dr}^s \\ \psi_{qr}^s \end{bmatrix} + \frac{L_m}{T_r} \begin{bmatrix} i_{ds}^s \\ i_{qs}^s \end{bmatrix} \quad (8.4.2)$$

ψ_{dr} and ψ_{qr} at any instant can be calculated from the first model. The second model will give the same values of ψ_{dr} and ψ_{qr} , only if ω_r is the actual speed of the machine. The actual speed of the machine can be obtained by adjusting the value of ω_r , until the two fluxes become equal. This is accomplished by discretizing eqn(8.4.2) and representing it as a real-time recurrent network. The outputs of the network are the fluxes calculated using eqn(8.4.2) and the reference outputs are the fluxes computed using eqn(8.4.1). Discretization of eqn(8.4.2) yields

$$\begin{bmatrix} \psi_{dr}(k+1) \\ \psi_{qr}(k+1) \end{bmatrix} = \begin{bmatrix} 1 - \frac{R_1 t_s}{L_r} & -\omega_r t_s \\ \omega_r t_s & 1 - \frac{R_1 t_s}{L_r} \end{bmatrix} \begin{bmatrix} \psi_{dr}(k) \\ \psi_{qr}(k) \end{bmatrix} + \begin{bmatrix} \frac{R_r L_m t_s}{L_r} & 0 \\ 0 & \frac{R_r L_m t_s}{L_r} \end{bmatrix} \begin{bmatrix} i_{ds}(k) \\ i_{qs}(k) \end{bmatrix} \quad (8.4.3)$$

A recurrent neural network for this system will have the structure given in Fig.8.3. There are two neurons, whose outputs are time-delayed and fed back as inputs, along with two external inputs. The external inputs are the stator currents, i_{ds} and i_{qs} . The

outputs of the network are the rotor fluxes, ψ_{dr} and ψ_{qr} . The weights of the network are identified from eqn(8.4.3) and are shown in Fig.8.3.

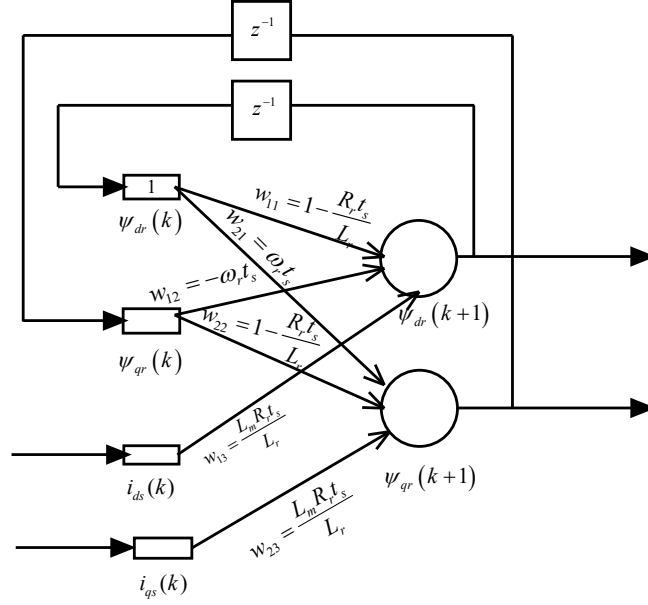


Figure 8.3: Real-time Recurrent Neural Network for Speed Estimation

The outputs of the network can be expressed as

$$y_1(k+1) = \psi_{dr}(k+1) = f_1(net_1) \quad (8.4.4)$$

$$y_2(k+1) = \psi_{qr}(k+1) = f_2(net_2) \quad (8.4.5)$$

where,

$$net_1 = w_{11}\psi_{dr}(k) + w_{12}\psi_{qr}(k) + w_{13}i_{ds}(k) \quad (8.4.6)$$

$$net_2 = w_{21}\psi_{dr}(k) + w_{22}\psi_{qr}(k) + w_{23}i_{qs}(k) \quad (8.4.7)$$

f_1 and f_2 are the non-linear activation functions, which in this case are taken as linear functions with unity gain. Thus, the output vector can be written as,

$$Y(k+1) = \begin{bmatrix} y_1(k+1) & y_2(k+1) \end{bmatrix}^T \quad (8.4.8)$$

The desired output vector can be identified as

$$D(k+1) = \left[\psi_{dr}(k+1) \ \psi_{qr}(k+1) \right]^T \quad (8.4.9)$$

from eqn.8.4.1. Error vector,

$$e(k) = Y(k) - D(k) \quad (8.4.10)$$

Among the six weights involved, only two are dependent on speed and hence only these two weights need to be considered as trainable, keeping the other weights constant, during the estimation process. The weight matrix is

$$w(k) = \left[w_{11}(k) \ w_{12}(k) \ w_{13}(k) \ w_{21}(k) \ w_{22}(k) \ w_{23}(k) \right]^T \quad (8.4.11)$$

The dynamic derivative matrix is

$$H(k) = \begin{bmatrix} \frac{\delta y_1}{\delta w_{11}} & 0 \\ \frac{\delta y_1}{\delta w_{12}} & 0 \\ \frac{\delta y_1}{\delta w_{13}} & 0 \\ 0 & \frac{\delta y_2}{\delta w_{21}} \\ 0 & \frac{\delta y_2}{\delta w_{22}} \\ 0 & \frac{\delta y_2}{\delta w_{23}} \end{bmatrix} \quad (8.4.12)$$

where,

$$\frac{\delta y_1}{\delta w_{11}} = \frac{\delta f_1(net_1)}{\delta net_1} \cdot \frac{\delta net_1}{\delta w_{11}} = \psi_{dr}(k) \quad (8.4.13)$$

$$\frac{\delta y_1}{\delta w_{12}} = \frac{\delta f_1(net_1)}{\delta net_1} \cdot \frac{\delta net_1}{\delta w_{12}} = \psi_{qr}(k) \quad (8.4.14)$$

$$\frac{\delta y_1}{\delta w_{13}} = \frac{\delta f_1(net_1)}{\delta net_1} \cdot \frac{\delta net_1}{\delta w_{13}} = i_{ds}(k) \quad (8.4.15)$$

$$\frac{\delta y_2}{\delta w_{21}} = \frac{\delta f_2(net_2)}{\delta net_2} \cdot \frac{\delta net_2}{\delta w_{21}} = \psi_{dr}(k) \quad (8.4.16)$$

$$\frac{\delta y_2}{\delta w_{22}} = \frac{\delta f_2(net_2)}{\delta net_2} \cdot \frac{\delta net_2}{\delta w_{22}} = \psi_{qr}(k) \quad (8.4.17)$$

$$\frac{\delta y_2}{\delta w_{23}} = \frac{\delta f_2(net_2)}{\delta net_2} \cdot \frac{\delta net_2}{\delta w_{23}} = i_{qs}(k) \quad (8.4.18)$$

Now, rotor speed can be estimated as

$$\omega_r(k+1) = \frac{w_{21}(k+1)}{t_s} \quad (8.4.19)$$

8.5 Offline estimation

To test the observer, the voltages and currents measured from the indirect field-oriented controlled induction motor are used. These voltages and currents are the inputs to the observer. As in the previous studies, two different reference voltages are used for testing- one, a step speed of 75rad/s at t=0, and a second one which is 20rad/s till t=2s, then changes to 75rad/s and then jumps to 50rad/s at t=4.5s. Initially, the results with a conventional EKF trained recurrent neural network is observed. The change in estimation when smoothing is incorporated is then observed. The values of the process and measurement noise covariance matrices, \mathbf{Q} and \mathbf{R} , used are

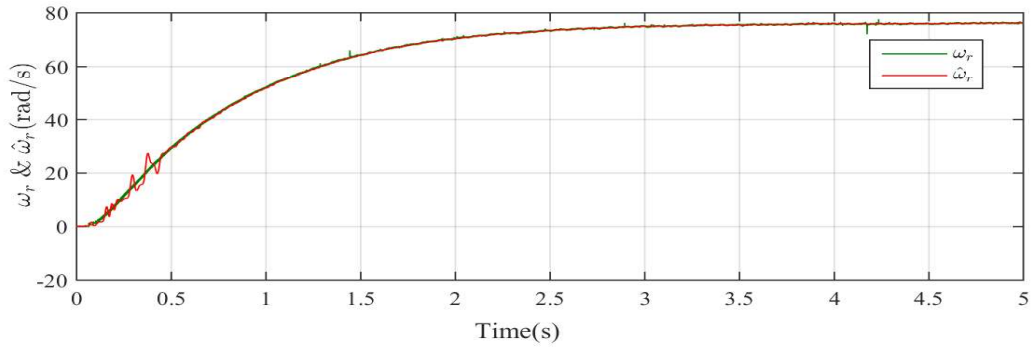
$$\mathbf{Q} = \begin{bmatrix} 10^{-6} & 0 \\ 0 & 10^{-6} \end{bmatrix}$$

and

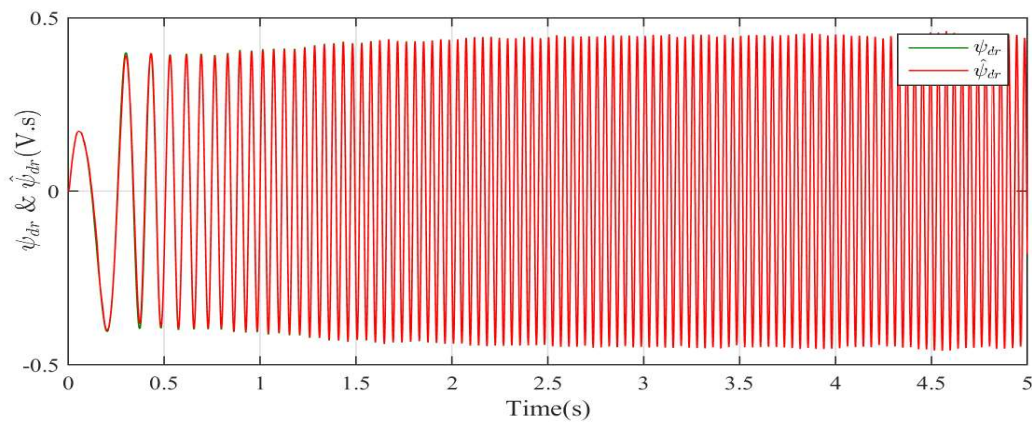
$$\mathbf{R} = \begin{bmatrix} 150 & 0 \\ 0 & 150 \end{bmatrix}$$

8.5.1 Conventional EKF trained recurrent neural network observer

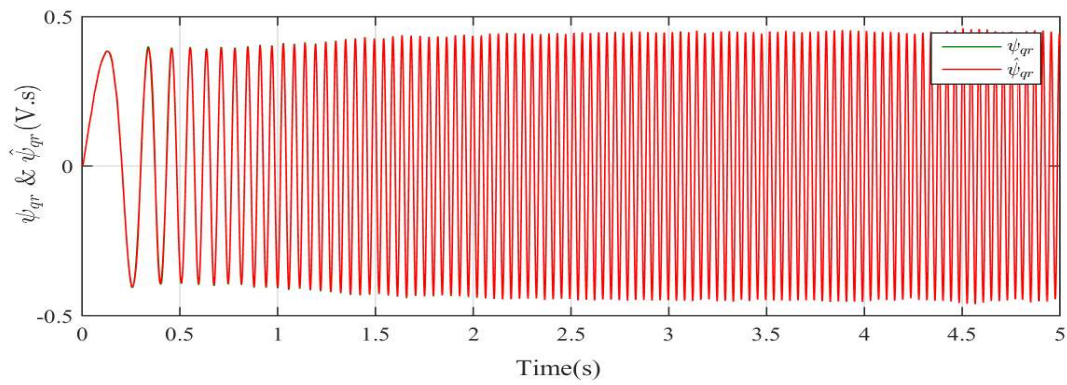
Here, a conventional EKF algorithm is used to train the recurrent neural network. The updation of weights is done according to equations 8.3.6 - 8.3.9. The results obtained for a step reference speed of 75rad/s are shown in Fig.8.4.



(a)



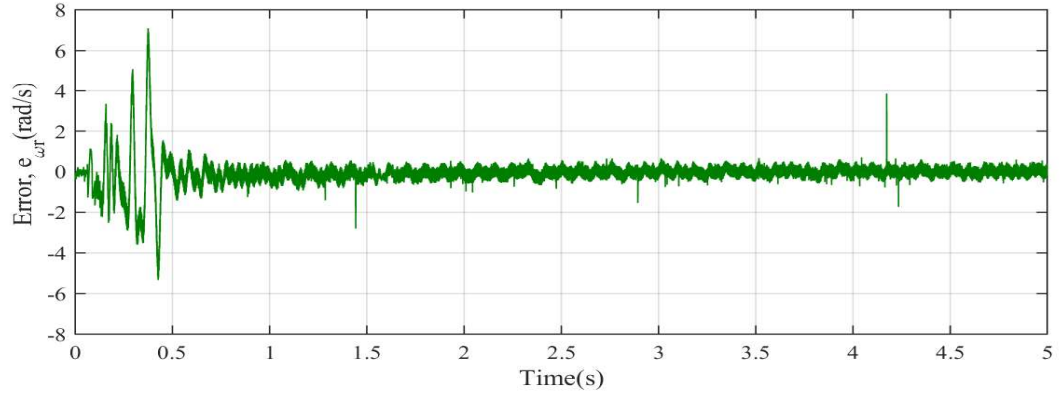
(b)



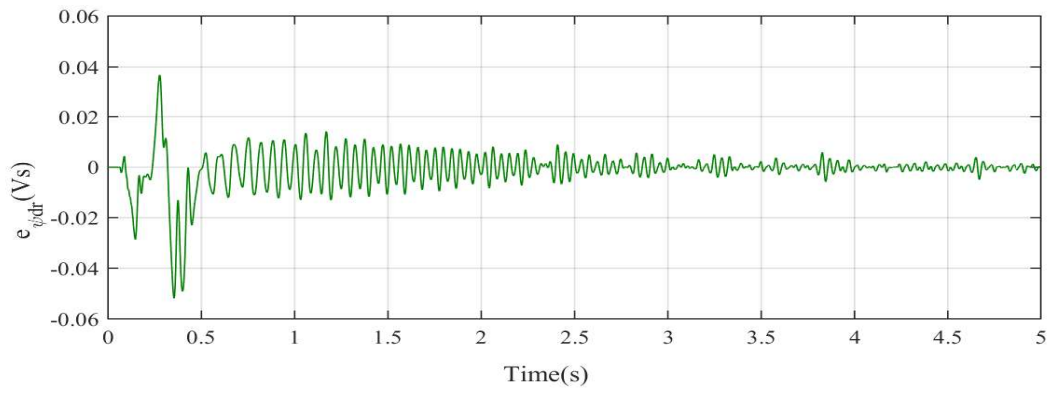
(c)

Figure 8.4: Estimation results with a conventional EKF trained recurrent neural network a) ω_r & $\hat{\omega}_r$ b) ψ_{dr} & $\hat{\psi}_{dr}$ c) ψ_{qr} & $\hat{\psi}_{qr}$

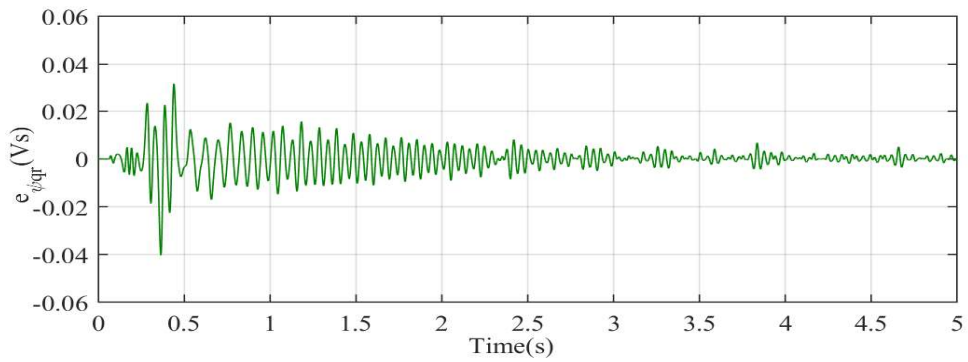
The errors in estimation of rotor speed, ω_r , d and q axis rotor fluxes, ψ_{dr} and ψ_{qr} are shown in Figs.8.5a, 8.5b and 8.5c respectively.



(a)



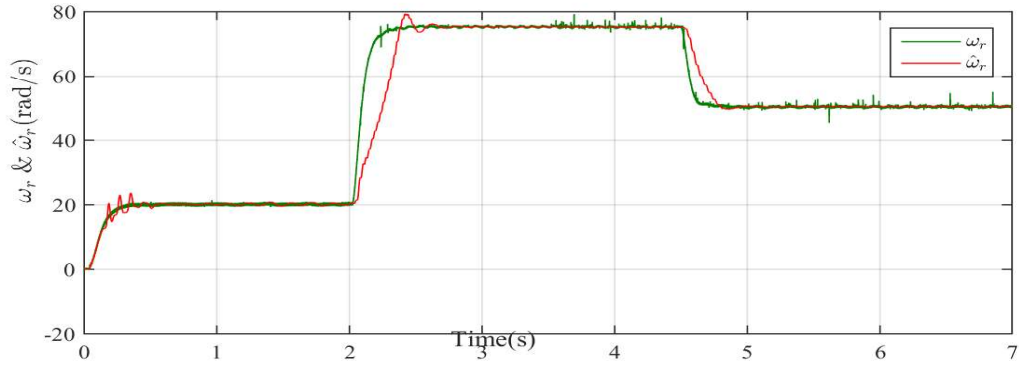
(b)



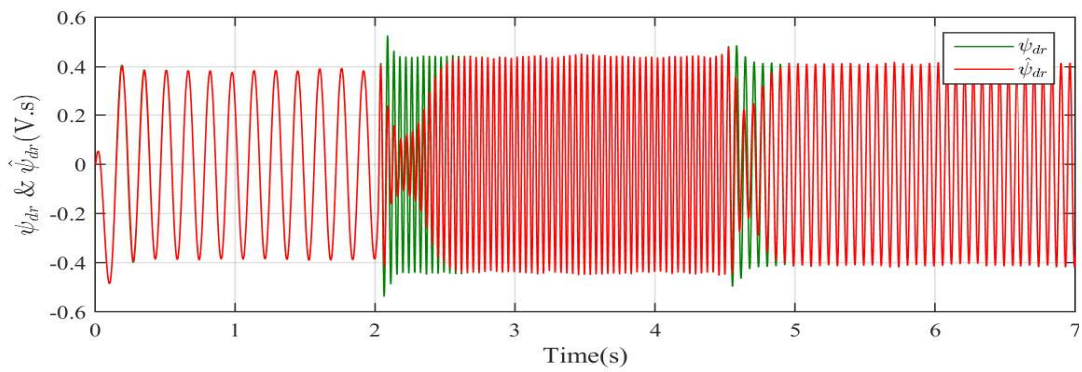
(c)

Figure 8.5: Error in estimation of a) ω_r , b) ψ_{dr} and c) ψ_{qr}

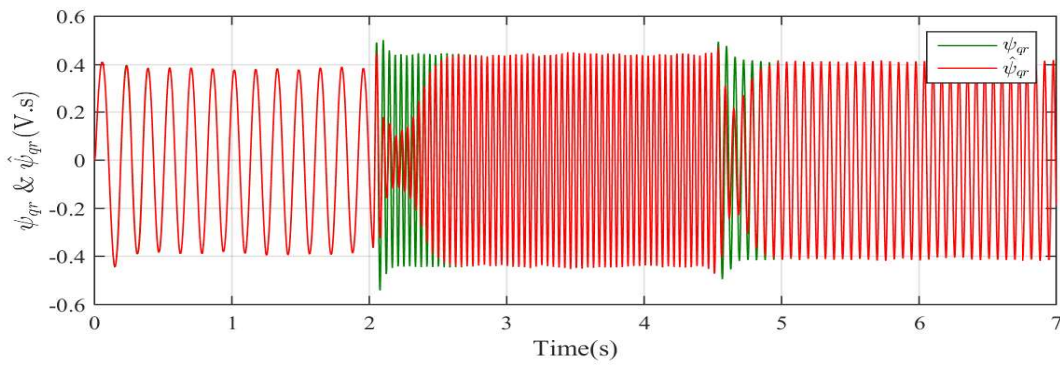
The algorithm is tested for a varying reference speed, which changes from 20rad/s to 75 rad/s at $t=2.5s$, and then to 50rad/s at $t=4.5s$. The estimation results are shown in Figs. 8.6a, 8.6b and 8.6c.



(a)



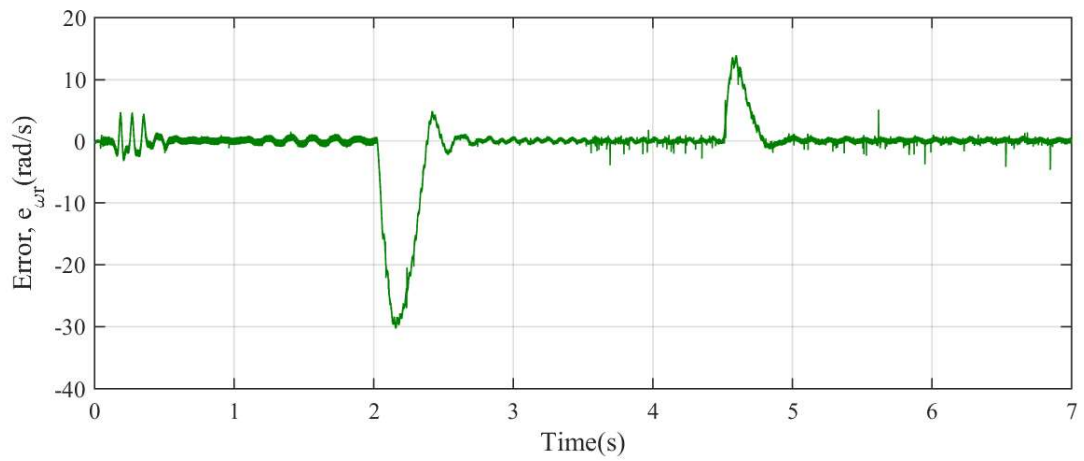
(b)



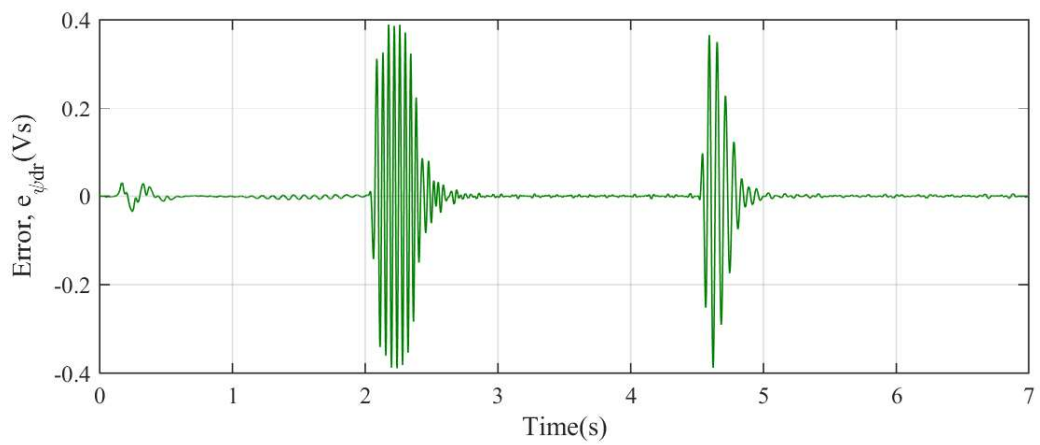
(c)

Figure 8.6: Estimation results with a conventional EKF trained recurrent neural network a) ω_r & $\hat{\omega}_r$ b) ψ_{dr} & $\hat{\psi}_{dr}$ c) ψ_{qr} & $\hat{\psi}_{qr}$

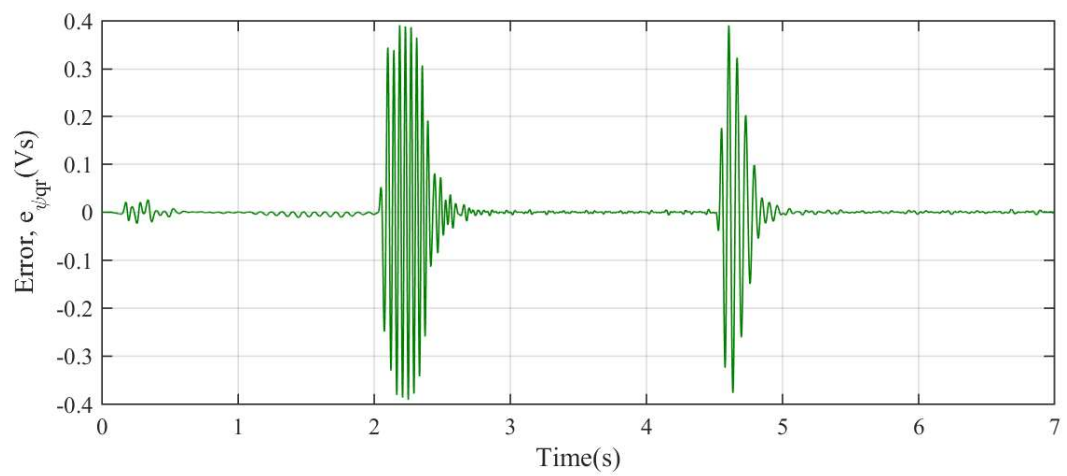
The error in estimation of the three quantities are shown in Figs.8.7a, 8.7b and 8.7c.



(a)



(b)



(c)

Figure 8.7: Error in estimation of a) ω_r b) ψ_{dr} and c) ψ_{qr} with a varying reference speed

8.5.2 Smoothed Kalman filter trained recurrent neural network observer

The recurrent neural network is trained by incorporating single-stage smoothing into the EKF algorithm. This is based on the equations, 8.3.10- 8.3.11. The output measurement of the present instant is used to smooth the estimation of the previous instant. This additional data involved is bound to make the estimate better. This can be verified from the estimation results as well as the error.

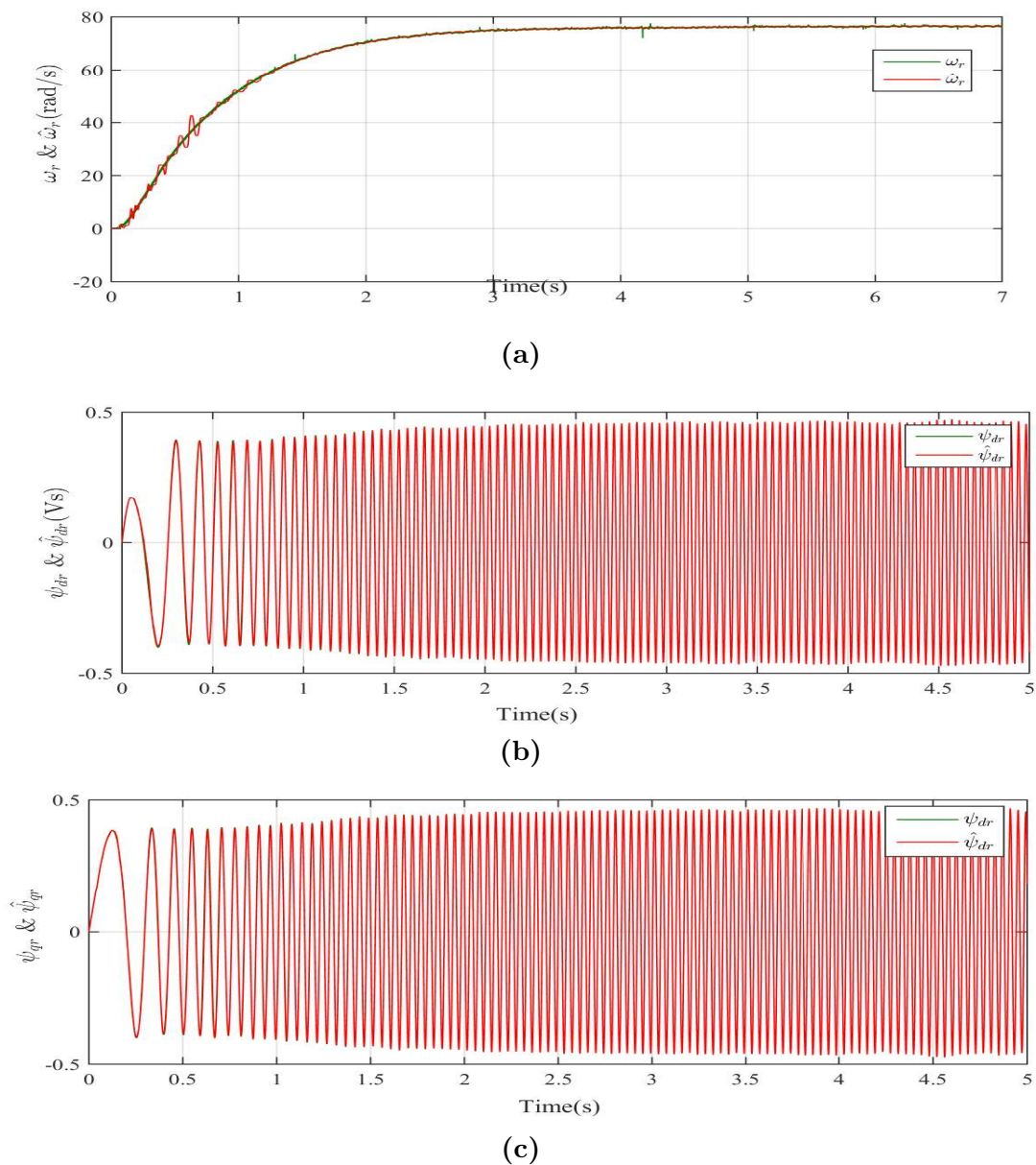
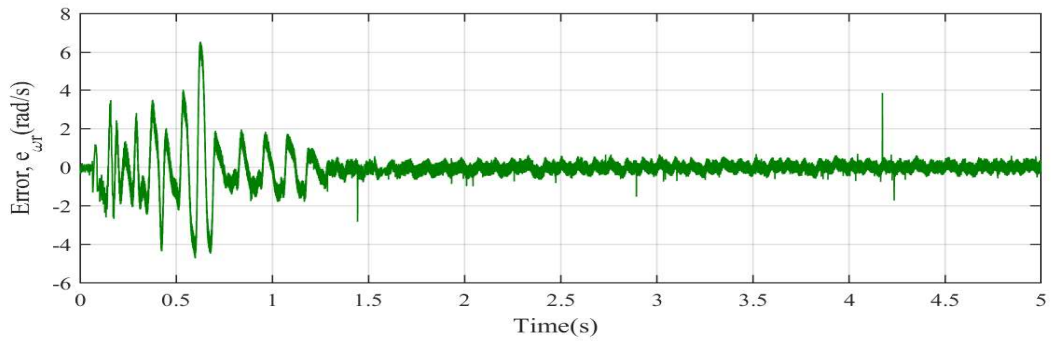


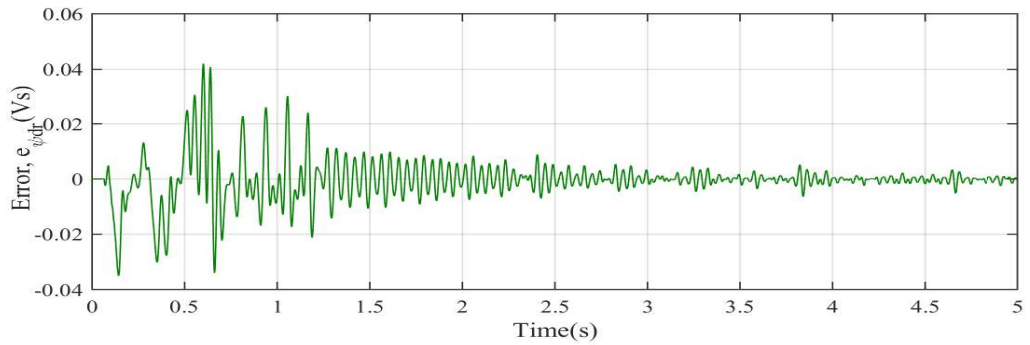
Figure 8.8: Estimation results with a smoothed EKF trained recurrent neural network a) ω_r & $\hat{\omega}_r$ b) ψ_{dr} & $\hat{\psi}_{dr}$ c) ψ_{qr} & $\hat{\psi}_{qr}$

The estimated rotor speed and rotor fluxes for a step reference speed of 75rad/s

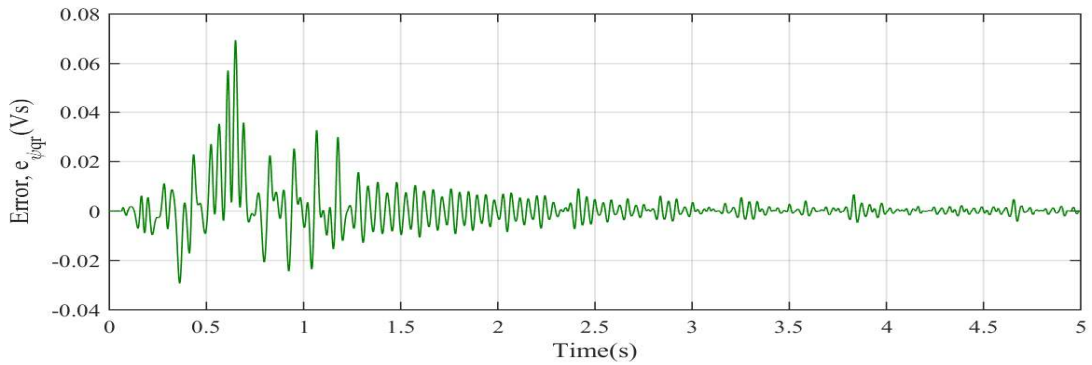
are shown in Fig.8.8. The rotor fluxes are compared with those obtained from the voltage model. These are taken as the true fluxes for error calculation in the EKF algorithm. The corresponding errors are shown in Figs.8.9a, 8.9b and 8.9c.



(a)



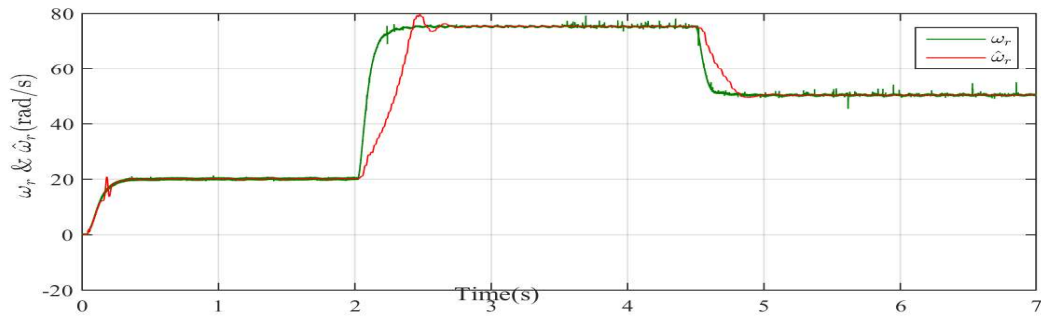
(b)



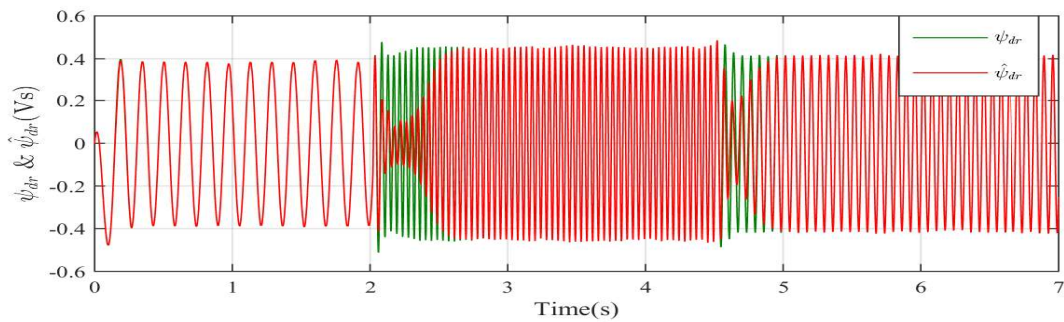
(c)

Figure 8.9: Error in estimation of a) ω_r b) ψ_{dr} and c) ψ_{qr}

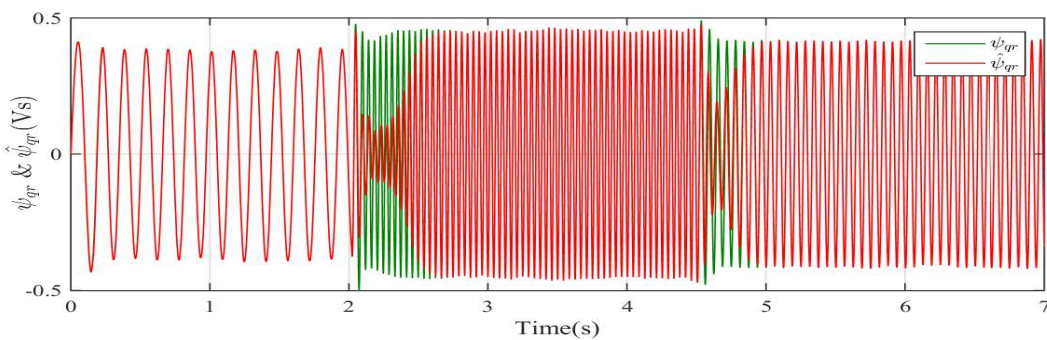
The estimation is performed for a second reference speed also. This reference is the same as that was used in the previous section with conventional EKF. The reference is a varying step- the speed is 20rad/s from 0 to 2s, then the reference value jumps to 75rad/s at t=2s and continues at this speed till t= 4.5s. At t= 4.5s, the reference speed becomes 50rad/s and continues at this speed till t = 7s. The estimation results are shown in Figs. 8.10a, 8.10b and 8.10c.



(a)



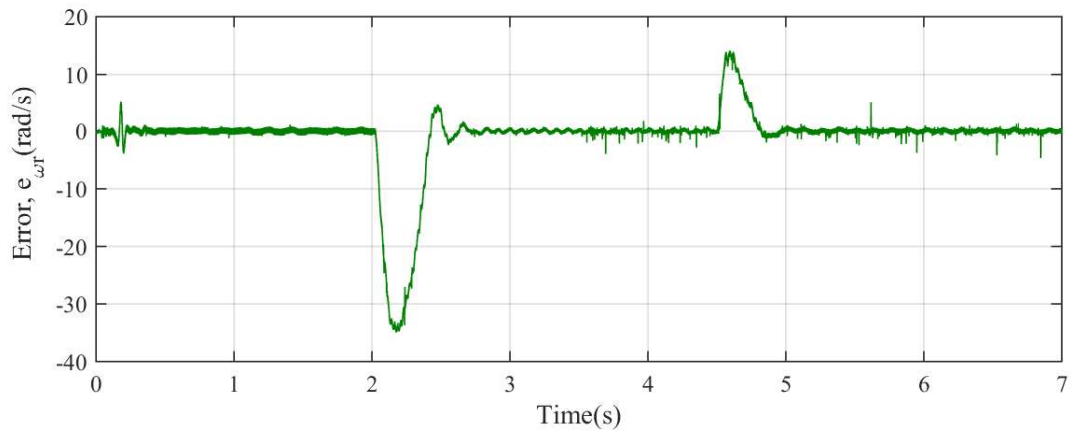
(b)



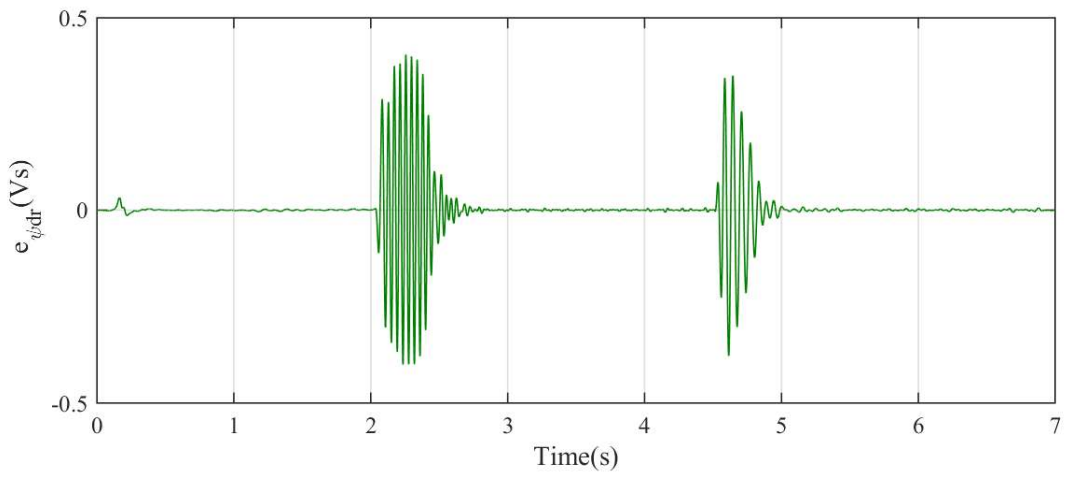
(c)

Figure 8.10: Estimation results with a smoothed EKF trained recurrent neural network a) ω_r & $\hat{\omega}_r$ b) ψ_{dr} & $\hat{\psi}_{dr}$ c) ψ_{qr} & $\hat{\psi}_{qr}$

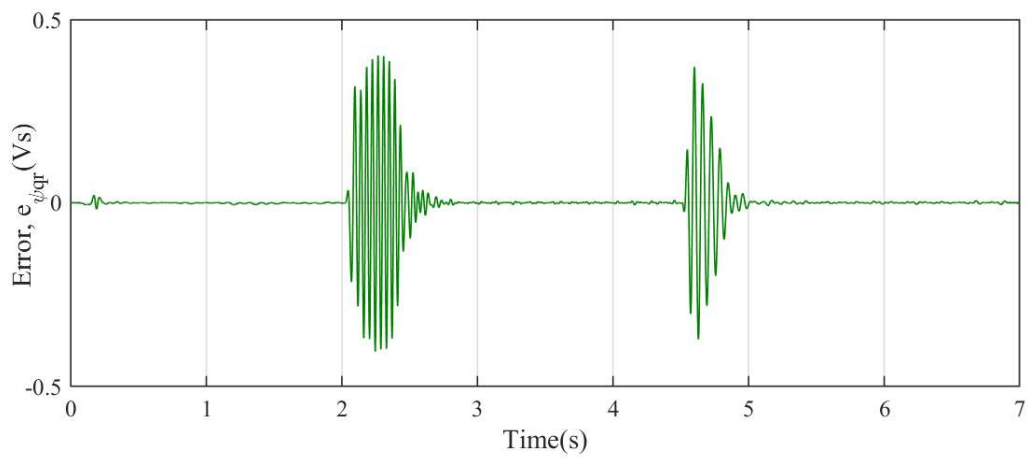
The corresponding errors are shown in Figs.8.11a, 8.11b and 8.11c.



(a)



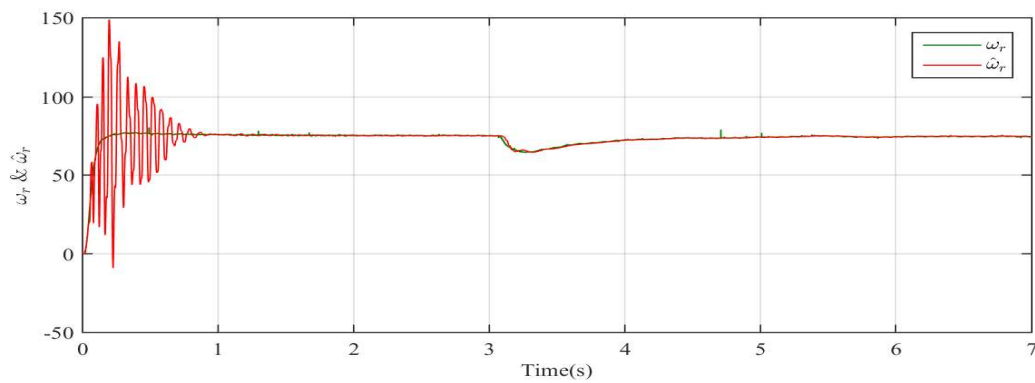
(b)



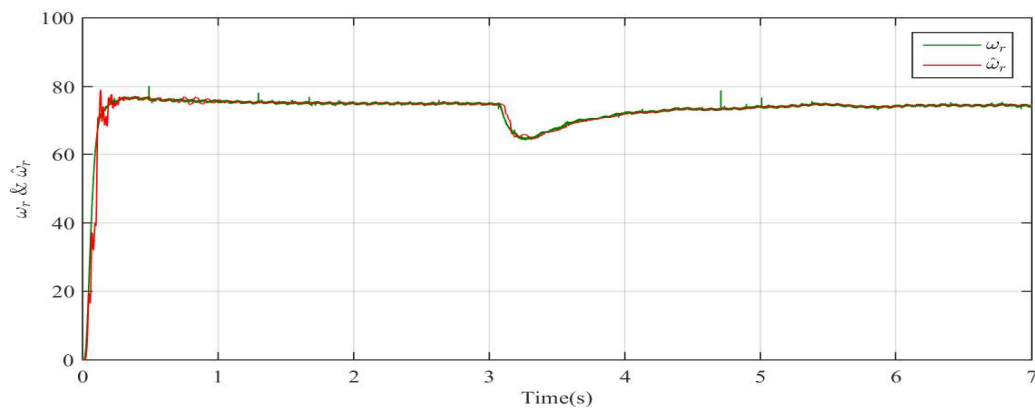
(c)

Figure 8.11: Error in estimation of a) ω_r b) ψ_{dr} and c) ψ_{qr}

Finally, a load was applied to the machine through a resistive load connected to the dc generator coupled to the induction motor. The same load as was applied in the previous cases was used here also. The induction motor is run in closed loop with a reference speed of 75rad/s and the load was applied at 3s. The stator currents measured in this context were applied offline to the conventional and smoothed Kalman observers for speed estimation. Fig.8.12a shows the estimation performance with a conventional Kalman observer and Fig.8.12b shows the improvement in the estimate with a smoothed Kalman observer. As can be seen, the speed estimate with the smoothed Kalman trained RNN based observer is found to give a good tracking performance compared to that with a conventional EKF trained RNN. This also shows the superiority of the smoothing algorithm. The same values of covariance matrices are used in this case as well.



(a)



(b)

Figure 8.12: Speed estimation results when a load is applied at $t=3s$ a)smoothed EKF trained RNN b) conventional EKF trained RNN

8.6 Summary

This chapter presents the performance of offline estimation of an indirect vector controlled induction motor drive using recurrent neural network observer which is trained using a smoothed Kalman filter algorithm. The results are compared with those obtained using a conventional EKF-trained neural network observer. The observer trained using smoothed Kalman filter algorithm is found to give better results, especially in the transient region.

Uma Syamkumar “Smoothed Kalman Observer for Sensorless Field Oriented Control of Induction Motor.” Thesis. Department of Electrical Engineering, Government Engineering College, Trichur, University of Calicut, , 2020.

Chapter 9

Real-time implementation of the smoothed Kalman trained neural observer for IFOC of three phase induction motor

This chapter presents the real-time implementation of the smoothed Kalman filter trained neural observer for indirect field-oriented control of three-phase induction motor. The closed loop observer based system is implemented using the reduced-order model of the machine. The results are compared with those of a conventional EKF trained observer.

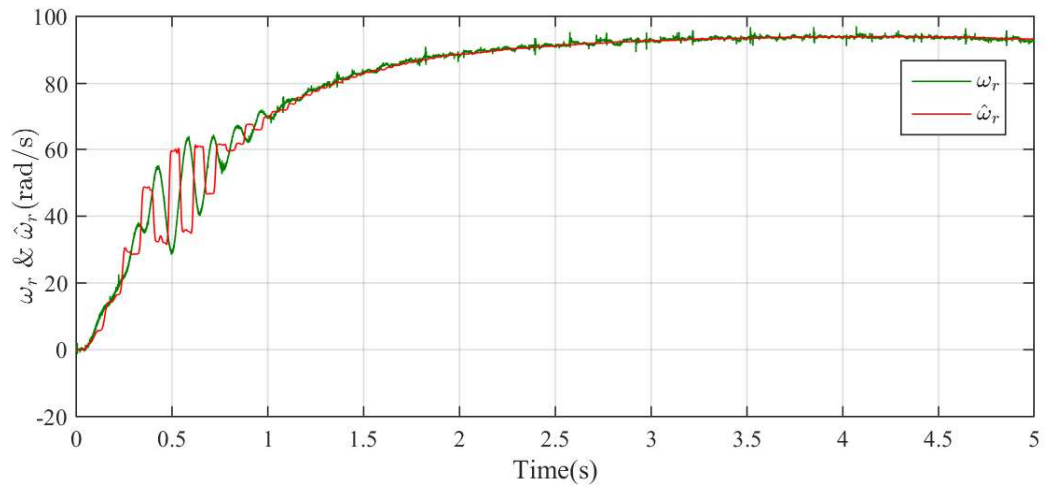
9.1 Introduction

The simulation studies performed in chapter(8) are validated experimentally. The real-time implementations are performed using the hardware set up used in earlier experiments. The algorithm is tested for indirect field-oriented control of induction motor in closed loop. The efficacy of the algorithm is confirmed for various reference speeds, including low and zero speeds.

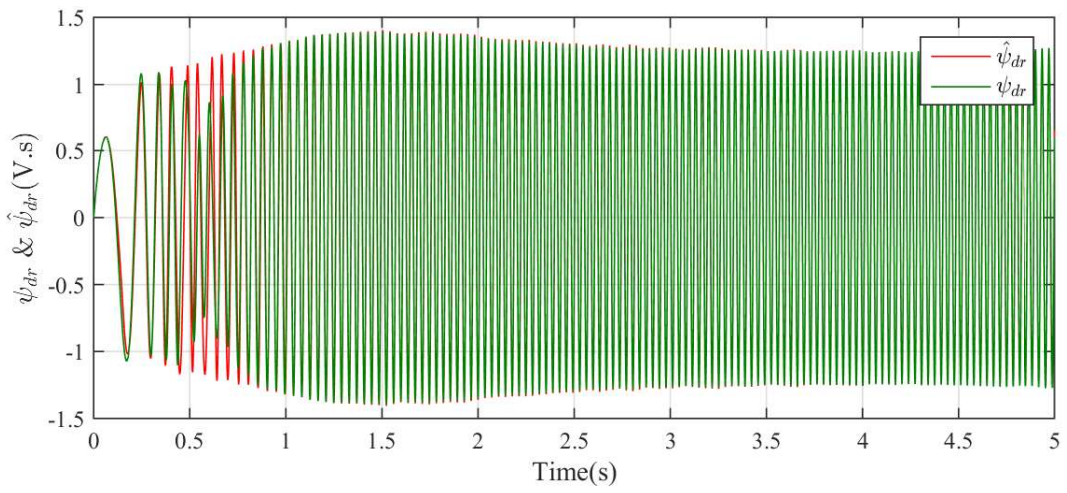
This chapter is organised as follows: Section 9.2 explains the hardware set up of the system, 9.3 shows the results of closed loop performance of the system with a smoothed Kalman trained recurrent neural observer. The performance of the system with a conventional EKF trained observer is elaborated in section 9.4. Section 9.5 summarises the chapter.

9.2 Experimental Setup

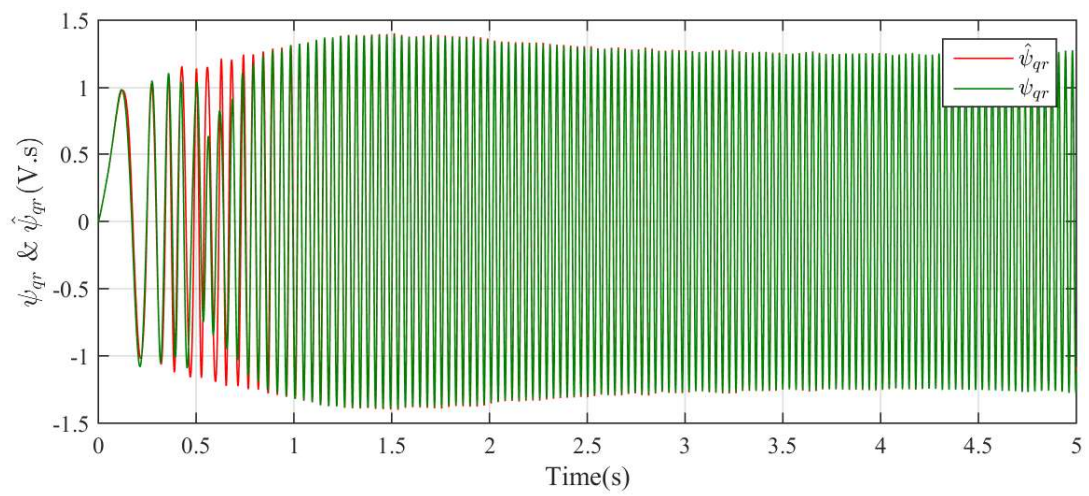
A block diagram of the experimental set up is shown in Fig.9.1. The actual test bed is the same as that used in chapter 5.



(a)

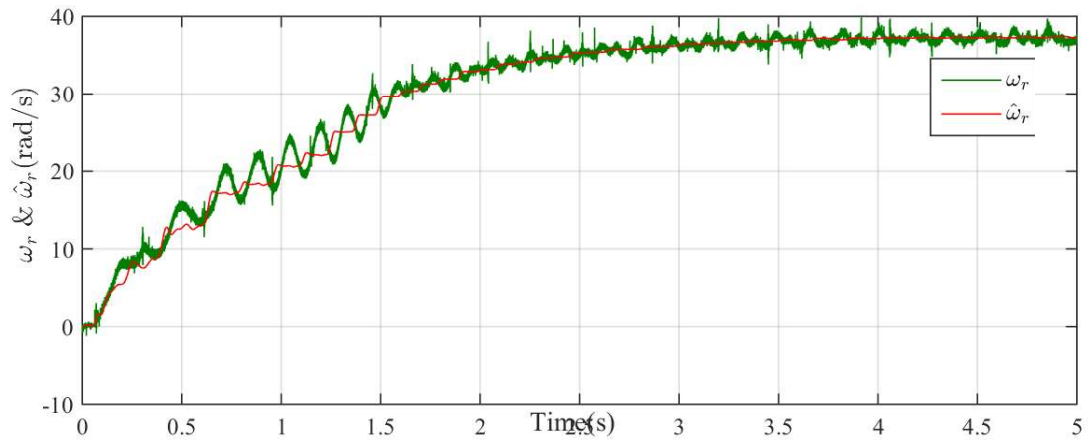


(b)

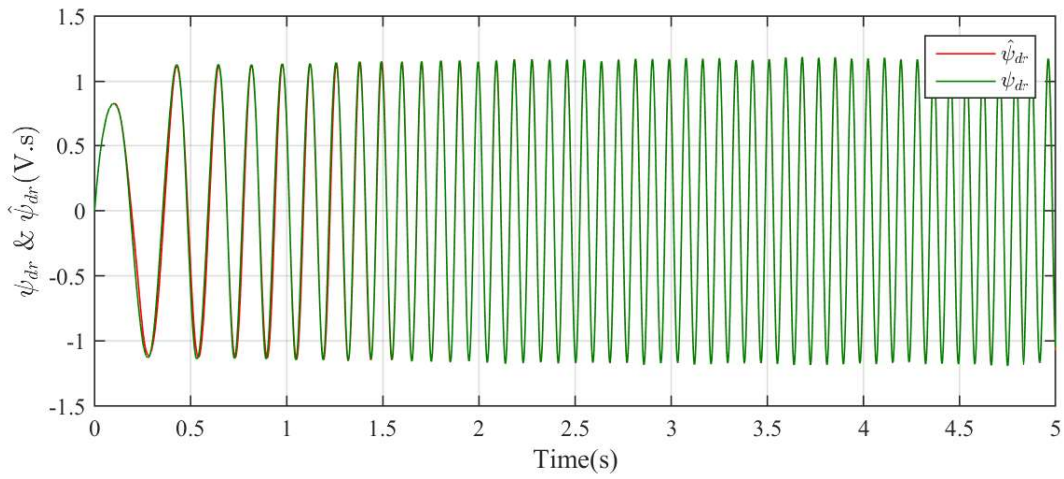


(c)

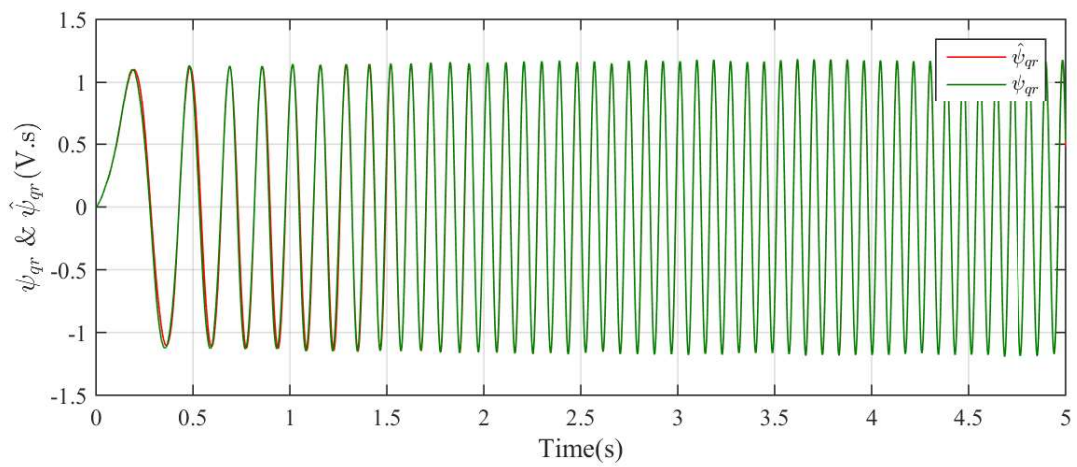
Figure 9.2: Estimation results for a reference speed of 75rad/s a) ω_r b) ψ_{dr} c) ψ_{qr}



(a)

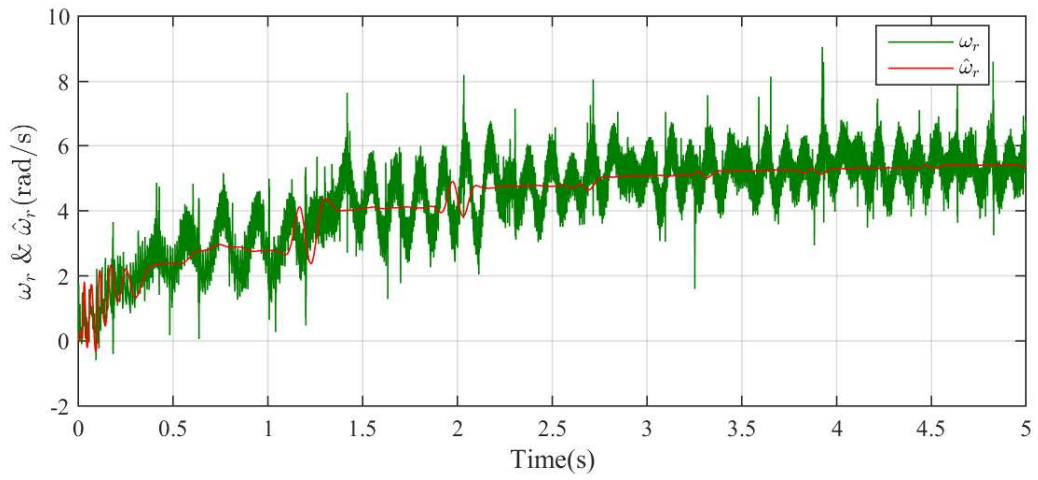


(b)

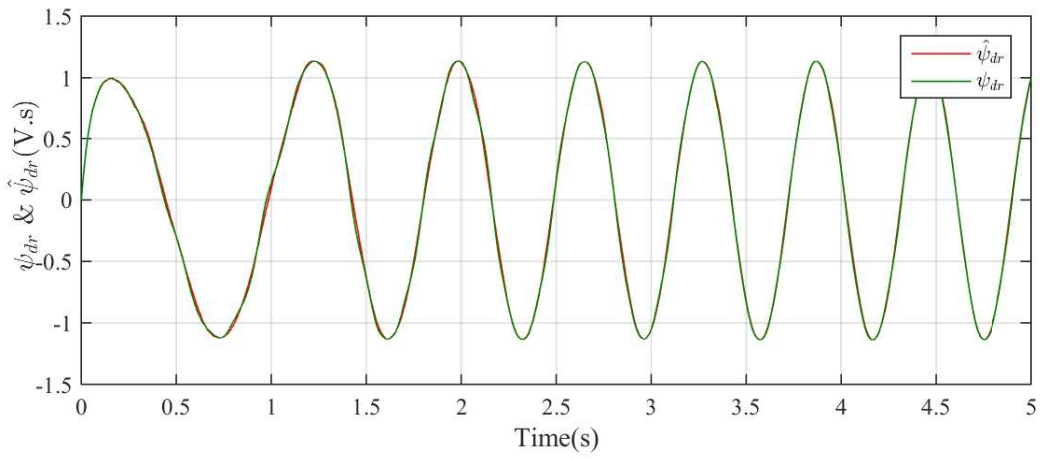


(c)

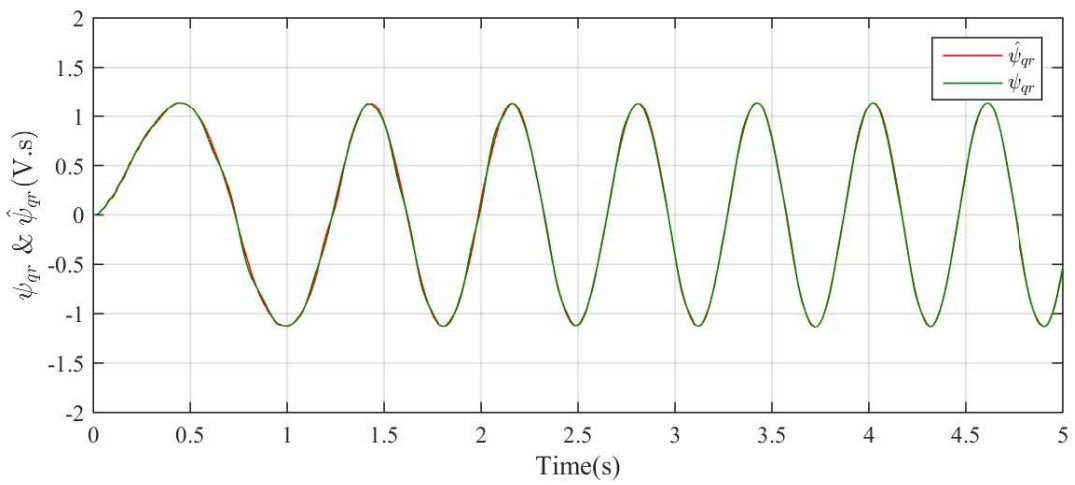
Figure 9.3: Estimation results for a reference speed of 30rad/s a) ω_r b) ψ_{dr} c) ψ_{qr}



(a)

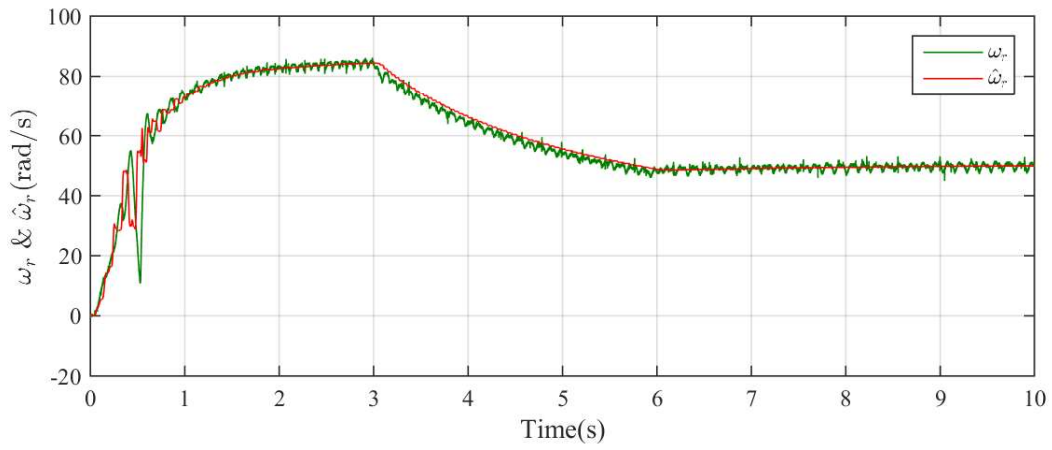


(b)

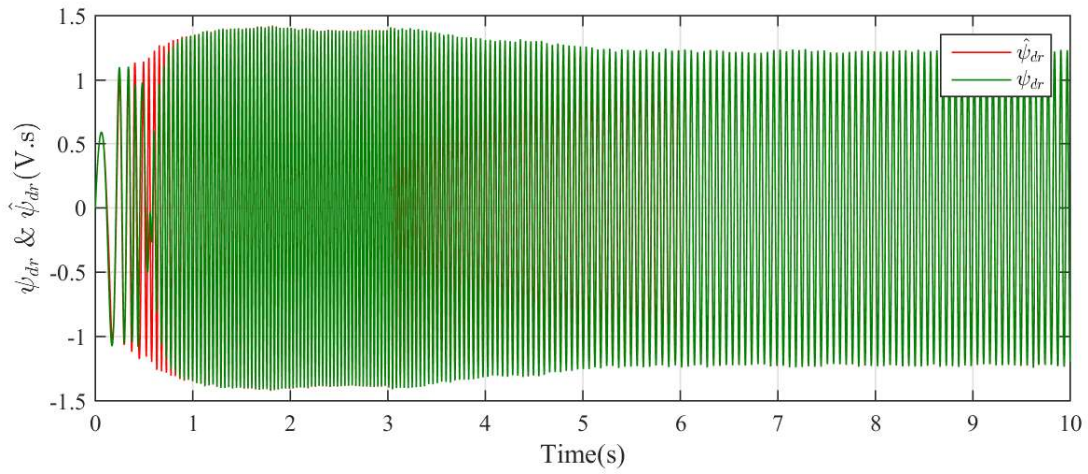


(c)

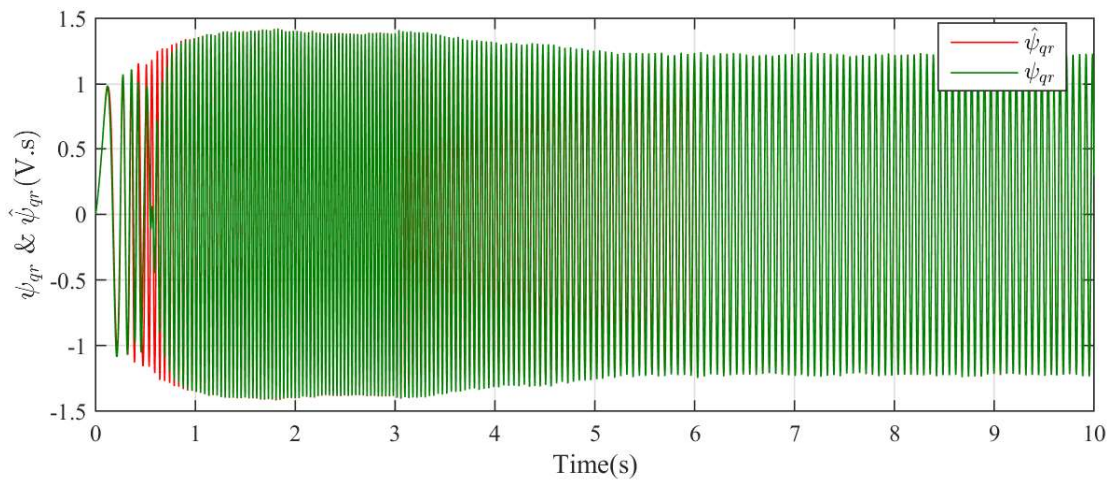
Figure 9.4: Estimation results for a reference speed of 5rad/s a) ω_r b) ψ_{dr} c) ψ_{qr}



(a)

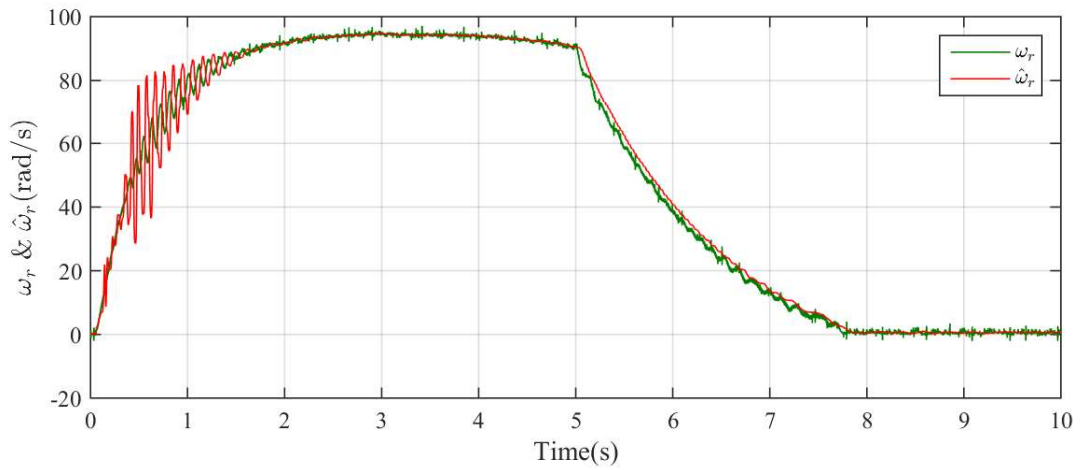


(b)

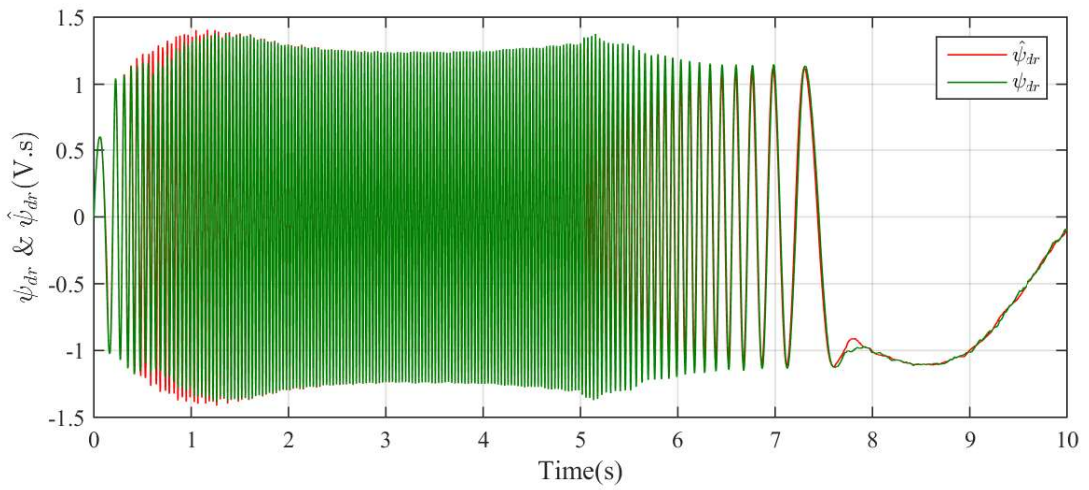


(c)

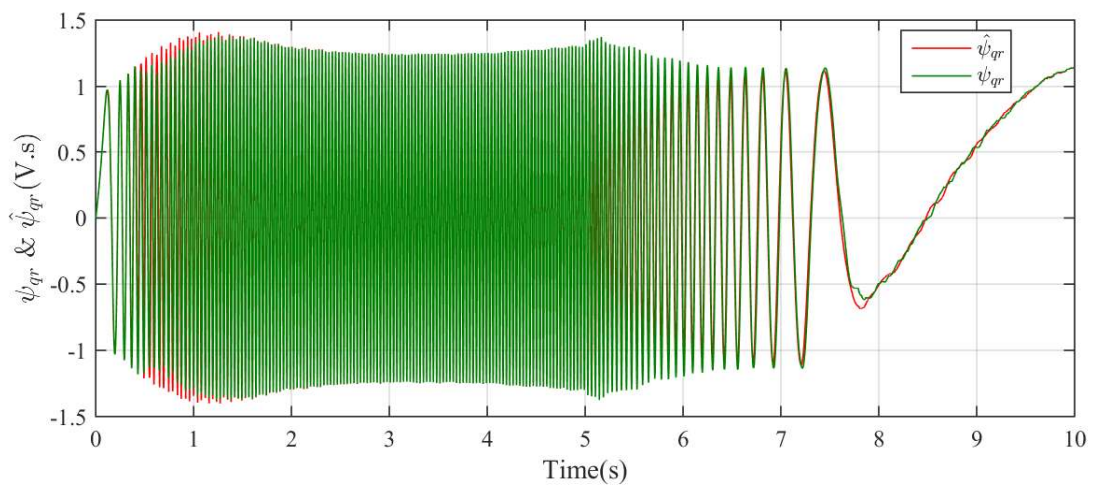
Figure 9.5: Estimation results for a reference speed which changes from 75rad/s to 30rad/s at $t=2.5$ s and then to 50rad/s at $t=5$ s a) ω_r b) ψ_{dr} c) ψ_{qr}



(a)



(b)



(c)

Figure 9.6: Estimation results for a reference speed which changes from 75rad/s to 0 at $t=4.5$ s and continues at zero speed till 7s a) ω_r b) ψ_{dr} c) ψ_{qr}

9.4 Experimental results of field-oriented control based on conventional Kalman filter trained neural network

The estimation results corresponding to the same reference speeds, with a conventional Kalman filter trained recurrent neural network observer are shown in Figs.9.7-9.11. The same process and measurement noise covariance matrices are used here also.

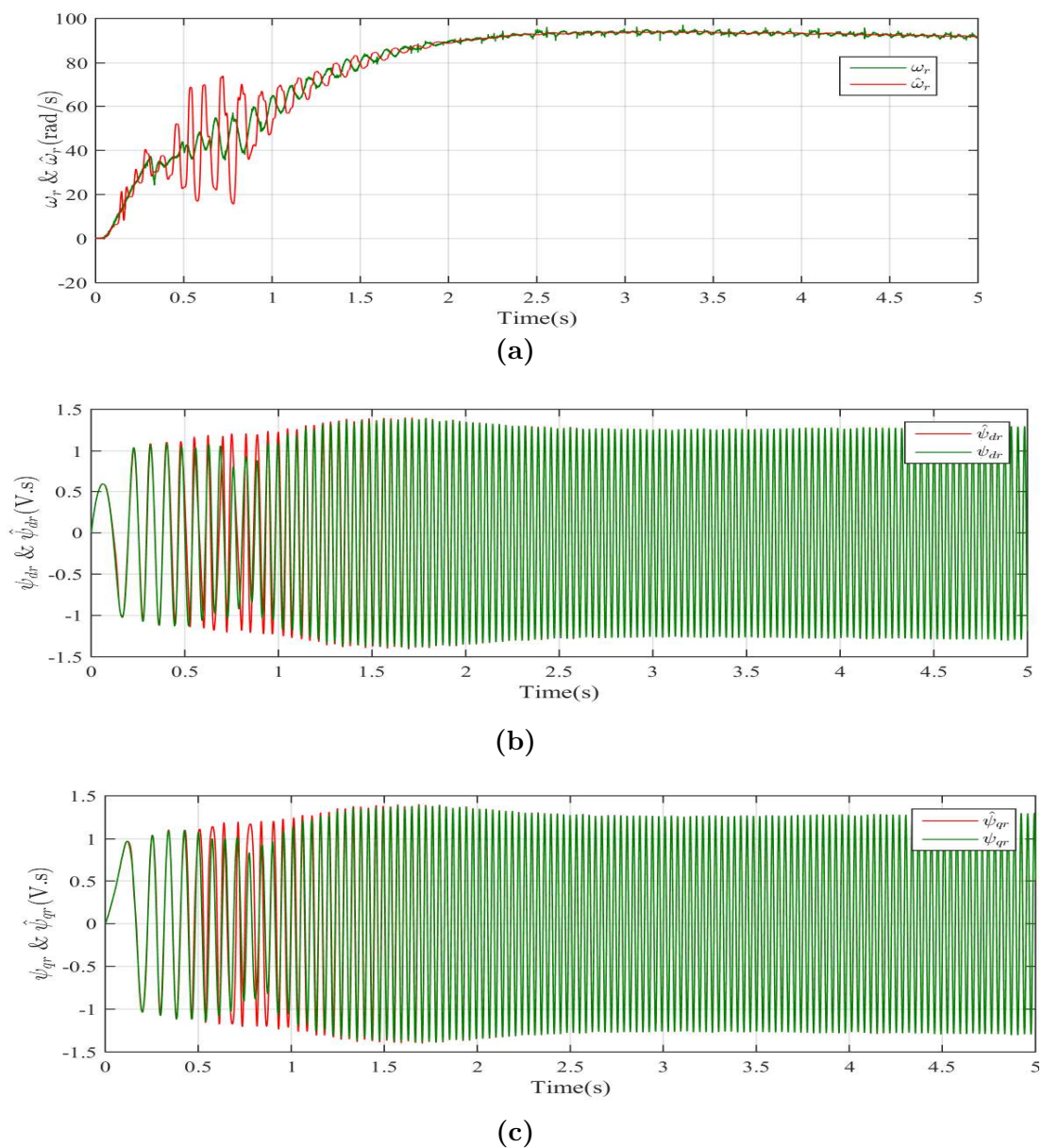
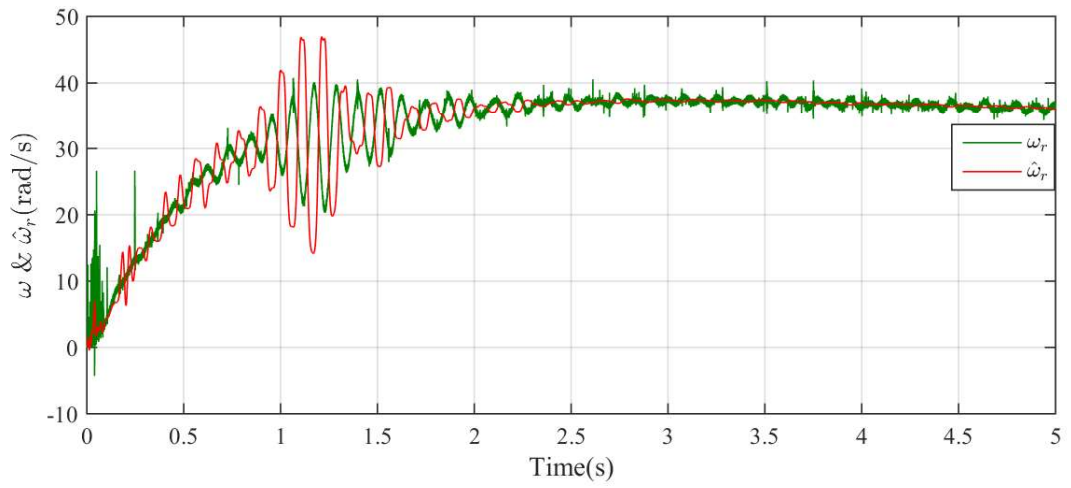
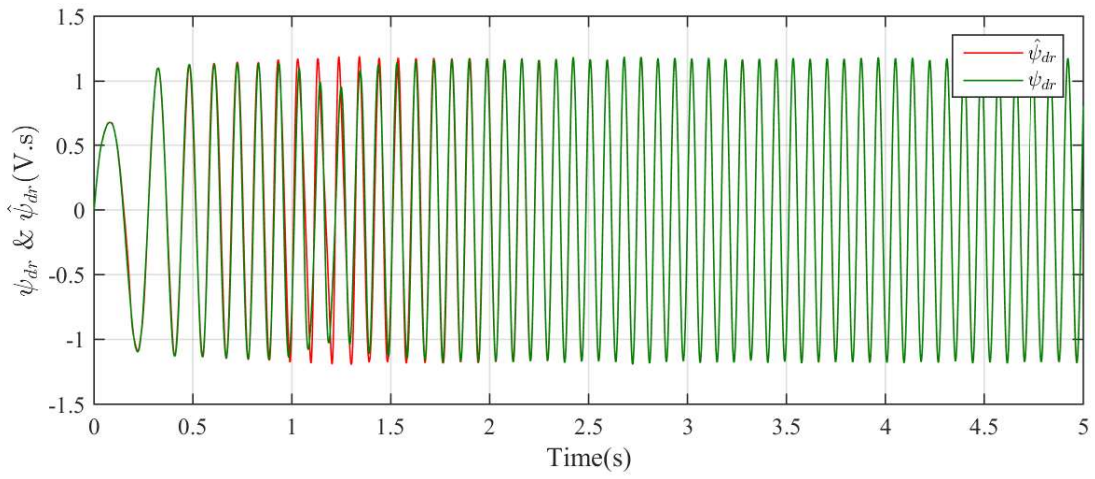


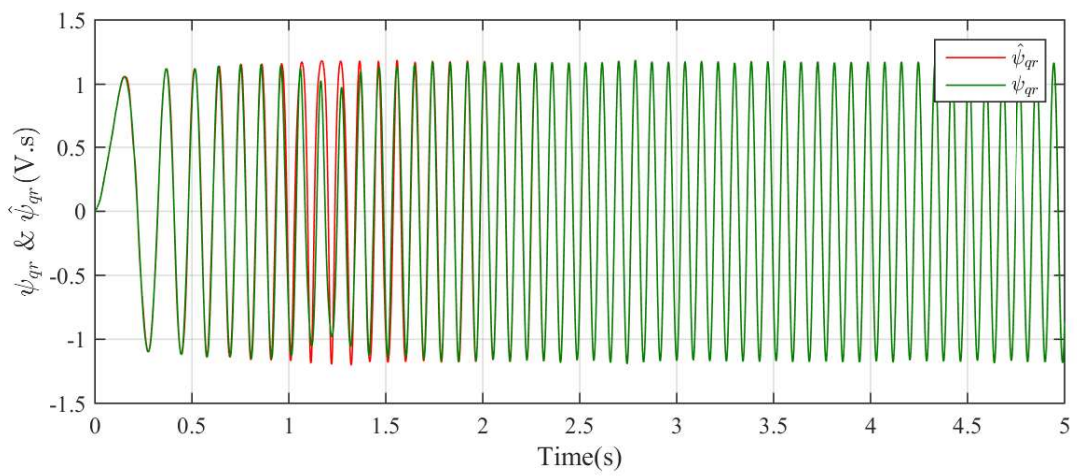
Figure 9.7: Estimation results for a reference speed of 75rad/s a) ω_r b) ψ_{dr} c) ψ_{gr}



(a)

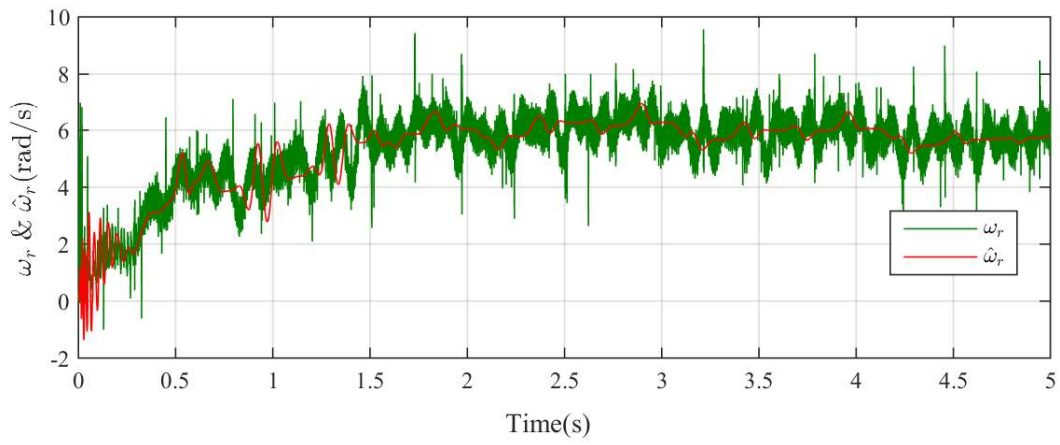


(b)

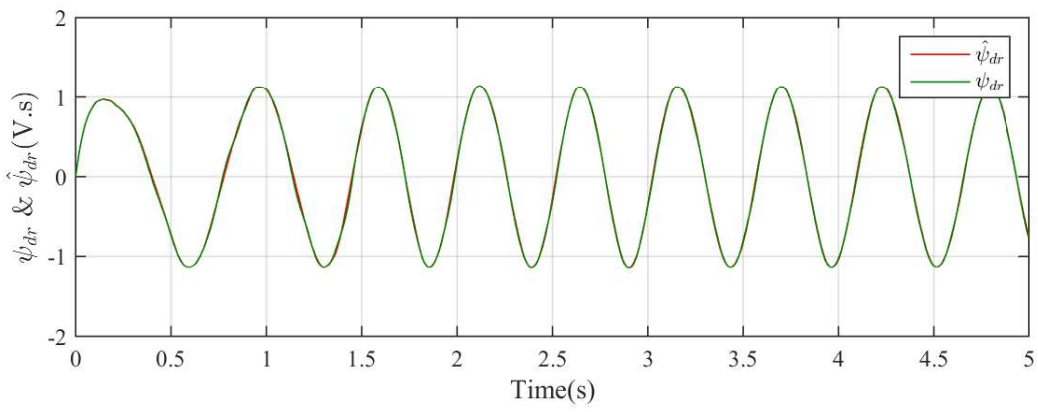


(c)

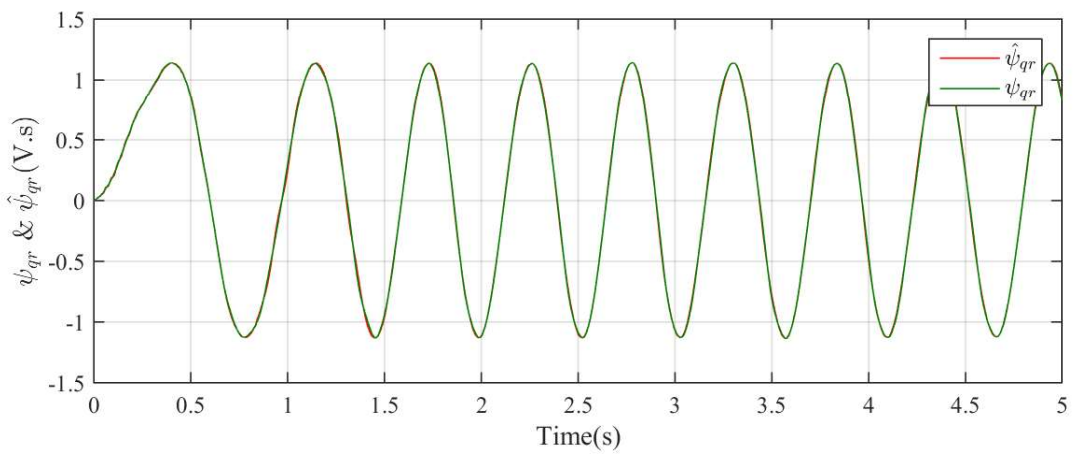
Figure 9.8: Estimation results for a reference speed of 30rad/s a) ω_r b) ψ_{dr} c) ψ_{qr}



(a)

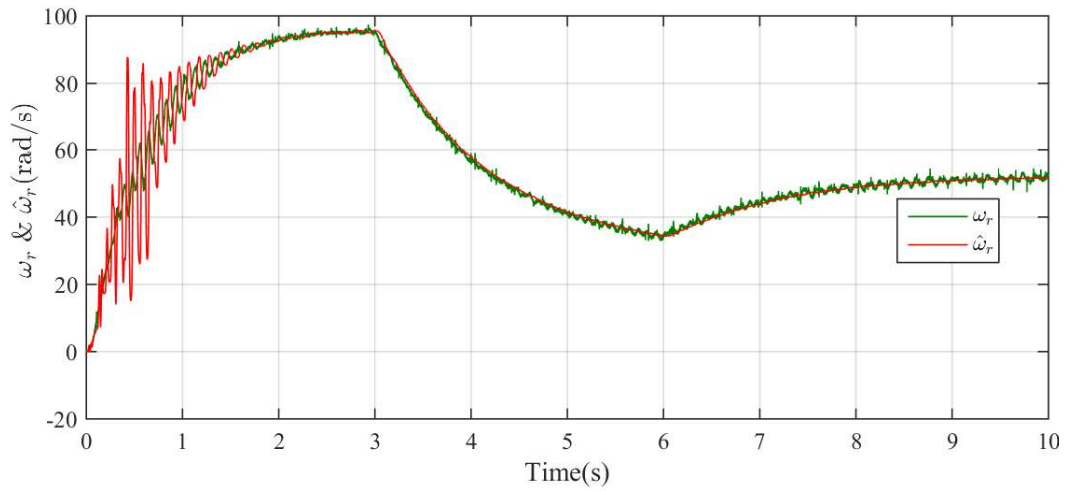


(b)

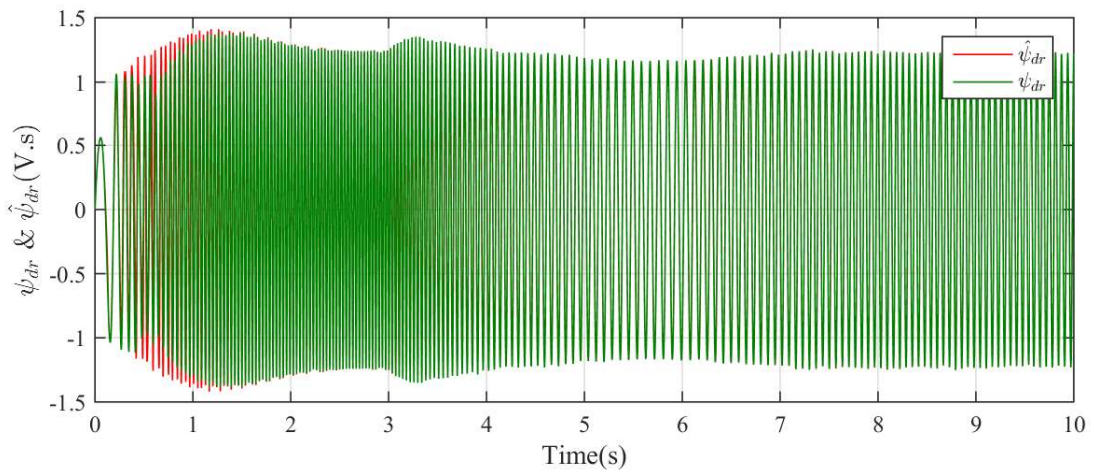


(c)

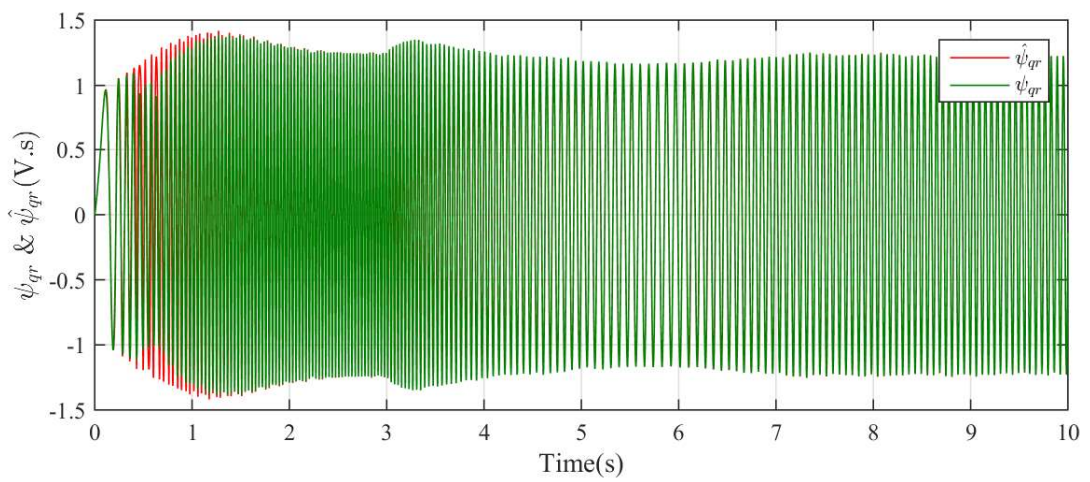
Figure 9.9: Estimation results for a reference speed of 5rad/s a) ω_r b) ψ_{dr} c) ψ_{qr}



(a)

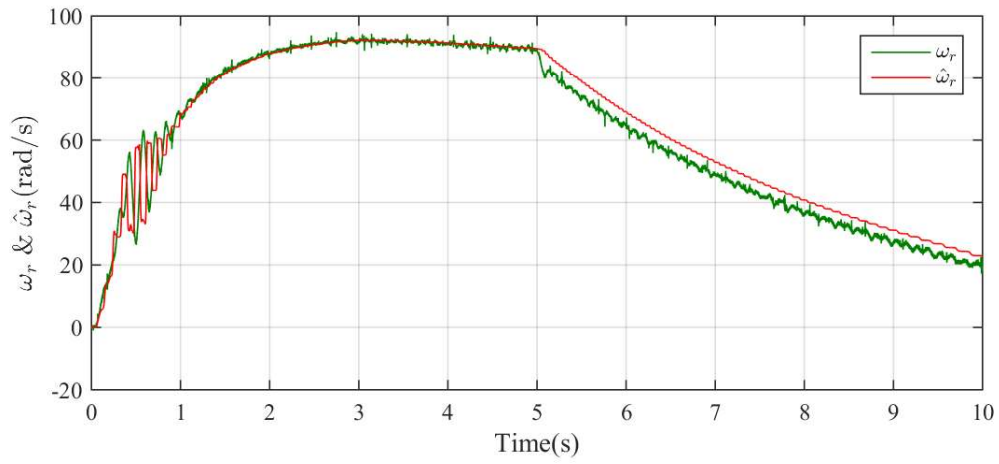


(b)

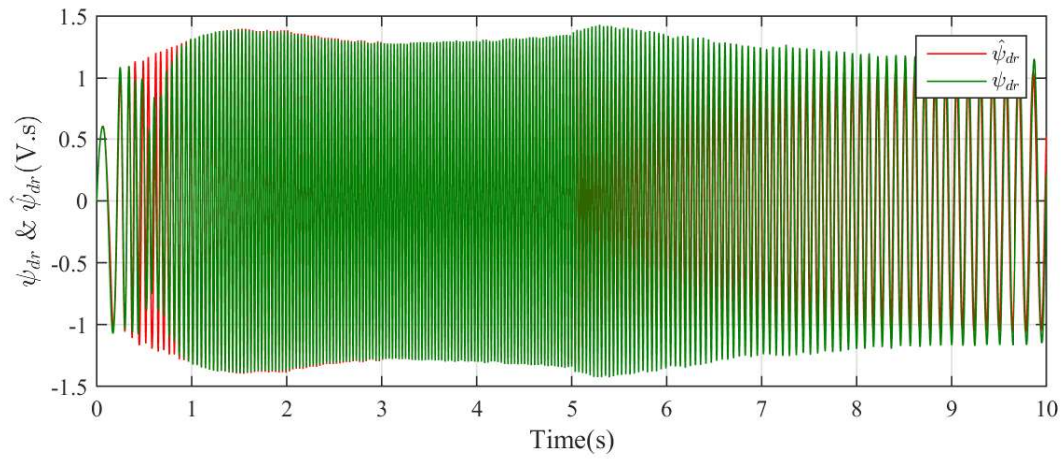


(c)

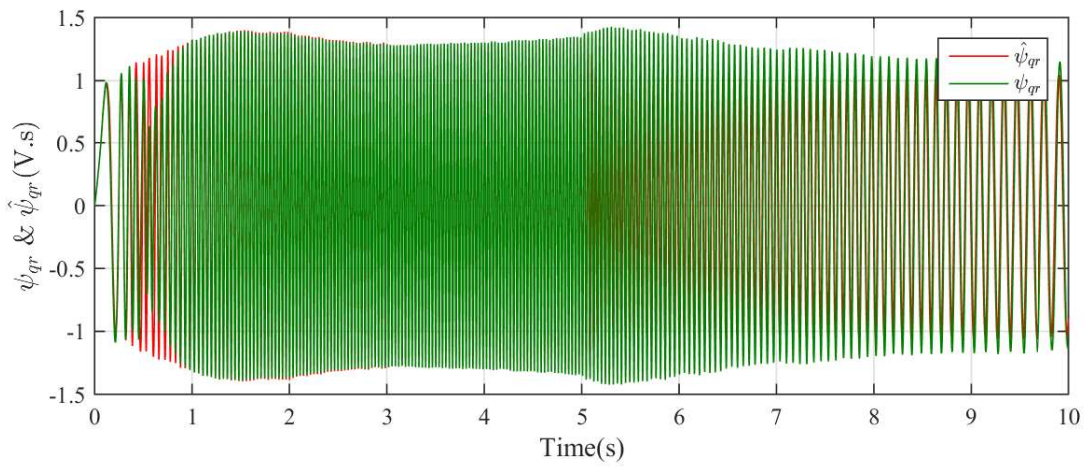
Figure 9.10: Estimation results for a reference speed which changes from 75rad/s to 30rad/s at $t=2.5s$ and then to 50rad/s at $t=5s$ a) ω_r b) ψ_{dr} c) ψ_{qr}



(a)



(b)



(c)

Figure 9.11: Estimation results for a reference speed which changes from 75rad/s to 0 at $t=4.5s$ and continues at zero speed till 7s a) ω_r b) ψ_{dr} c) ψ_{qr}

9.5 Summary

The experimental validation of the smoothed Kalman trained recurrent neural network is done in this chapter. The results are compared with the estimates obtained from a neural network observer trained by a conventional Kalman filter algorithm. The mean square errors of the estimates of rotor speed using both the algorithms are tabulated in Table 9.1. It can be seen that there is a prominent decrease in the mean squared error while using the smoothing algorithm.

Table 9.1: Comparison of estimation results using a smoothed and conventional EKF - trained recurrent neural observer

Ref. Speed(rad/s)	Mean Squared Error(rad/s)		% decrease
	CEKF	SKF	
75rad/s	212.91	104.81	50.77%
30rad/s	99.41	5.86	94.1%
5rad/s	2.15	2.10	5%
75- 0	94.25	72.63	23%
75-30-50	118.02	55.99	52.63%

Uma Syamkumar “Smoothed Kalman Observer for Sensorless Field Oriented Control of Induction Motor.” Thesis. Department of Electrical Engineering, Government Engineering College, Trichur, University of Calicut, , 2020.

Chapter 10

Conclusions and future directions

10.1 Conclusions

The research work embodied in this thesis has addressed the problem of estimating the rotor speed of a three-phase induction motor for use in indirect vector controlled drive. The main aim was to improve the estimates obtained using an extended Kalman filter by incorporating smoothing. A fixed-lag smoothing filter, with a lag of one time instant is used to obtain the improved estimates. The main findings are summarized below.

- An extended Kalman filter with single- stage smoothing is used as an observer for estimating the rotor speed along with rotor currents and fluxes of three phase induction motor.
- The observer is implemented in real-time in a closed loop indirect vector control scheme and estimation is performed for various reference speeds, using two different models of the motor. Initially, a fifth order model is used and results are obtained. As a next step, a reduced order model of the machine is attempted.
- Estimates obtained with the smoothed observer are compared with a conventional EKF keeping the values of process and measurement error covariance matrices same.
- The observer is found to perform well even when the process and measurement error covariance matrices are varied over a wide range.
- The smoothed Kalman algorithm is used to train a real-time recurrent neural network observer for indirect vector controlled drive. In this case also, the results are compared with those of a conventional EKF. The results are found to be better than those with conventional EKF. This is validated using the mean squared errors in both the cases.

- The performance of the observer is satisfactory at very low and near zero speeds also.
- Comparing the mean square errors of the full- order and reduced order models of the motor, mean squared error of rotor speed is more with the reduced order model. This trend is seen for all reference speeds, including very low and zero speeds. This increase may be attributed to the reduction in order of the system, by which some of the pertinent data may be lost. The parameters considered are less in case of the reduced model.
- Comparison of percentage decrease also shows that the full- order observer is more robust compared to the reduced order one, which is evident from the response to sudden changes in reference speeds.
- The MSE of recurrent neural network trained observer is lesser than that with the reduced motor model. This is be due to the inherent capability of neural networks to adapt to non-linearities and sudden changes. The robustness of recurrent neural network is also evident from the percentage decrease in estimation errors.

10.2 Scope for future study

This work was performed by smoothing the estimates using only one data ahead of time.

- The work may be extended to include two stages or rather a fixed time-lag, so as to obtain better results.
- The variations in machine parameters can also be incorporated.

Uma Syamkumar “Smoothed Kalman Observer for Sensorless Field Oriented Control of Induction Motor.” Thesis. Department of Electrical Engineering, Government Engineering College, Trichur, University of Calicut, , 2020.

Bibliography

- [1] Bimal K. Bose. Modern Power Electronics and AC Drives, 2002.
- [2] R-Krishnan. Electric Motor Drives Modeling-Analysis And Control.pdf, 2001.
- [3] J. Holtz. Sensorless control of induction motors - Performance and limitations. In *IEEE International Symposium on Industrial Electronics*, volume 1, 2000.
- [4] Silverio Bolognani, Luca Peretti, and Mauro Zigliotto. Parameter sensitivity analysis of an improved open-loop speed estimate for induction motor drives. *IEEE Transactions on Power Electronics*, 23(4):2127–2135, jul 2008.
- [5] Colin Schauder. Adaptive Speed Identification for Vector Control of Induction Motors without Rotational Transducers. Technical Report 5, 1992.
- [6] Sang Min Kim, Woo Yong Han, and Sung Joong Kim. Design of a new adaptive sliding mode observer for sensorless induction motor drive. *Electric Power Systems Research*, 2004.
- [7] Cristian Lascu, Ion Boldea, and Frede Blaabjerg. A class of speed-sensorless sliding-mode observers for high-performance induction motor drives. *IEEE Transactions on Industrial Electronics*, 56(9):3394–3403, 2009.
- [8] Oscar Barambones, Senior Member, and Patxi Alkorta. Position Control of the Induction Motor Using an Adaptive Sliding-Mode Controller and Observers. *IEEE Transactions on Transactions on Industrial Electronics*, 61(12):6556–6565, 2014.
- [9] X. Sun, L. Chen, Z. Yang, and H. Zhu. Speed-sensorless vector control of a bearingless induction motor with artificial neural network inverse speed observer. *IEEE/ASME Transactions on Mechatronics*, 18(4):1357–1366, Aug 2013.
- [10] Jarosław Guzin, Hamid A Toliyat, and Senior Member. Artificial-Neural-Network-Based Sensorless Nonlinear Control of Induction Motors. *IEEE Transactions on Energy Conversion*, 20(3):520–528, 2005.
- [11] M. Zerikat, A. Mechernene, and S. Chekroun. High-performance sensorless vector control of induction motor drives using artificial intelligent technique. *European Transactions on Electrical Power*, 21(1):787–800, 2011.

- [12] Anup Kumar Panda, Tejavathu Ramesh, and S. Shiva Kumar. Rotor-flux-based MRAS speed estimator for DTFM-SVM of a speed sensorless induction motor drive using Type-1 and Type-2 fuzzy logic controllers over a wide speed range. *International Transactions on Electrical Energy Systems*, 26(9):1863–1881, 2016.
- [13] Mabrouk Jouili, Kamel Jarray, Koubaa Yassine, and Mohamed Boussak. Luenberger state observer for speed sensorless isfoc induction motor drives. *Electric Power Systems Research*, 89:139–147, 08 2012.
- [14] C. Korlinchak and M. Comanescu. Sensorless field orientation of an induction motor drive using a time-varying observer. *IET Electric Power Applications*, 6(6):353–361, 2012.
- [15] Young-Real Kim, Seung-Ki Sul, and Min-Ho Park. Speed sensorless vector control of induction motor using extended kalman filter. *IEEE Transactions on Industry Applications*, 30(5):1225–1233, Sep. 1994.
- [16] Joachim Holtz. Sensorless position control of induction motors - An emerging technology. *IEEE Transactions on Industrial Electronics*, 45(6):840–852, 1998.
- [17] Hisao Kubota and Kouki Matsuse. Speed Sensorless Field-Oriented Control of Induction Motor with Rotor Resistance. *IEEE Transactions on Industry Applications*, 30(5):1219–1224, 1994.
- [18] Joachim Holtz and Juntao Quan. Drift- and Parameter-Compensated Flux Estimator for Persistent Zero-Stator-Frequency Operation of Sensorless-Controlled Induction Motors. *IEEE Transactions on Industry Applications*, 39(4):1052–1060, jul 2003.
- [19] Cedric Caruana, Greg M. Asher, and Mark Sumner. Performance of HF signal injection techniques for zero-low-frequency vector control of induction machines under sensorless conditions, feb 2006.
- [20] Maurizio Cirrincione and Marcello Pucci. An MRAS-based sensorless high-performance induction motor drive with a predictive adaptive model. *IEEE Transactions on Industrial Electronics*, 52(2):532–551, apr 2005.
- [21] Gregor Edelbauer, Karel Jezernik, and Evgen Urlep. Low-speed sensorless control of induction machine. *IEEE Transactions on Industrial Electronics*, 53(1):120–129, feb 2006.

- [22] Joachim Holtz, Jinsheng Jiang, and Hangwen Pan. Identification of rotor position and speed of standard induction motors at low speed including zero stator frequency. *IECON Proceedings (Industrial Electronics Conference)*, 2:971–976, 1997.
- [23] Ibrahim M. Alsofyani and N. R.N. Idris. A review on sensorless techniques for sustainable reliability and efficient variable frequency drives of induction motors, 2013.
- [24] David J. Atkinson, Paul P. Acarnley, and John W. Finch. Observers for Induction Motor State and Parameter Estimation. *IEEE Transactions on Industry Applications*, 27(6):1119–1127, 1991.
- [25] M. Mena, O. Touhami, R. Ibtouen, and M. Fadel. Sensorless direct vector control of an induction motor. *Control Engineering Practice*, 16(1):67–77, 2008.
- [26] François Auger, Senior Member, Mickael Hilairret, Josep M Guerrero, Senior Member, Eric Monmasson, Senior Member, Teresa Orłowska-kowalska, Senior Member, and Seiichiro Katsura. Industrial Applications of the Kalman Filter : A Review. *IEEE Transactions on Industrial Electronics*, 60(12):5458–5471, 2013.
- [27] Hai Peng Liu and Qing Fan Zhang. Research on a modified EKF for speed estimation in induction motor drives. *IEEE ICIT 2007 - 2007 IEEE International Conference on Integration Technology*, (5):432–436, 2007.
- [28] Vishal Tiwari, Sukanta Das, and Abhisek Pal. Sensorless Speed Control of Induction Motor Drive Using Extended Kalman Filter Observer. In *IEEE PES Asia-Pacific Power and Energy Engineering Conference, APPEEC 2017*, pages 2–7, 2017.
- [29] Jongkwang Kim, Yongkeun Lee, and Janghyeon Lee. A sensorless speed estimation for indirect vector control of three-phase induction motor using Extended Kalman Filter. In *IEEE Region 10 Annual International Conference, Proceedings/TENCON*, pages 3087–3090. Institute of Electrical and Electronics Engineers Inc., feb 2017.
- [30] Murat Barut, Student Member, Seta Bogosyan, and Metin Gokasan. Speed-Sensorless Estimation for Induction Motors Using Extended Kalman Filters. *IEEE Transactions on Industrial Electronics*, 54(1):272–280, 2007.

- [31] Murat Barut, Student Member, Seta Bogosyan, Senior Member, and Metin Gokasan. Experimental Evaluation of Braided EKF for Sensorless Control of Induction Motors. *IEEE Transactions on Industrial Electronics*, 55(2):620–632, 2008.
- [32] Emrah Zerdali and Murat Barut. Novel version of bi input-extended Kalman filter for speed-sensorless control of induction motors with estimations of rotor and stator resistances, load torque, and inertia. *Turkish Journal of Electrical Engineering and Computer Sciences*, 24(5):4525–4544, 2016.
- [33] Francesco Alonge, Filippo D Ippolito, Antonino Sferlazza, and Student Member. Sensorless Control of Induction-Motor Drive Based on Robust Kalman Filter and Adaptive Speed Estimation. *IEEE Transactions on Industrial Electronics*, 61(3):1444–1453, 2014.
- [34] Zhonggang Yin, Chang Zhao, Yanru Zhong, and Lidong Li. Speed sensorless vector control of induction motor based on robust extended Kalman filter. In *Proceedings of the 2012 24th Chinese Control and Decision Conference, CCDC 2012*, pages 2989–2993. IEEE, may 2012.
- [35] Zhonggang Yin, Guoyin Li, Xiangdong Sun, Jing Liu, and Yanru Zhong. A speed estimation method for induction motors based on Strong Tracking Extended Kalman Filter. In *2016 IEEE 8th International Power Electronics and Motion Control Conference, IPEMC-ECCE Asia 2016*, pages 798–802. Institute of Electrical and Electronics Engineers Inc., jul 2016.
- [36] Md Habibullah and Dylan Dah Chuan Lu. A Speed-Sensorless FS-PTC of Induction Motors Using Extended Kalman Filters. *IEEE Transactions on Industrial Electronics*, 2015.
- [37] Saeed Jafarzadeh, Cristian Lascu, M Sami Fadali, and Senior Member. State Estimation of Induction Motor Drives Using the Unscented Kalman Filter. *IEEE Transactions on Industrial Electronics*, 59(11):4207–4216, 2012.
- [38] K L Shi, T F Chan, Y K Wong, Senior Member, and S L Ho. Speed Estimation of an Induction Motor Drive Using an Optimized Extended Kalman Filter. *IEEE Transactions on Industrial Electronics*, 49(1):124–133, 2002.
- [39] Emrah Zerdali and Murat Barut. The Comparisons of Optimized Extended Kalman Filters for Speed-Sensorless Control of Induction Motors. *IEEE Transactions on Industrial Electronics*, 64(6), 2017.

- [40] Emrah Zerdali, Recep Yildiz, Remzi Inan, Ridvan Demir, and Murat Barut. Adaptive Fading Extended Kalman Filter Based Speed-Sensorless Induction Motor Drive. *2018 XIII International Conference on Electrical Machines (ICEM)*, pages 1367–1373, 2018.
- [41] Emrah Zerdali. Adaptive Extended Kalman Filter for Speed-Sensorless Control of Induction Motors. *IEEE Transactions on Energy Conversion*, 34(2):789–800, 2019.
- [42] R. Biasco-Giménez. Dynamic performance limitations for MRAS based sensorless induction motor drives. Part 2: Online parameter tuning and dynamic performance studies. *IEE Proceedings: Electric Power Applications*, 143(2):123–134, 1996.
- [43] Fang Zheng Peng and Tadashi Fukao. Robust Speed Identification for Speed-Sensorless Vector Control of Induction Motors. *IEEE Transactions on Industry Applications*, 1994.
- [44] V. V. Vasić and S. N. Vukosavić. Sensorless mras-based induction motor control with parallel speed and stator resistance estimation. *European Transactions on Electrical Power*, 12(2):135–139, 2002.
- [45] Veran Vasić, Slobodan N. Vukosavic, and Emil Levi. A Stator Resistance Estimation Scheme for Speed Sensorless Rotor Flux Oriented Induction Motor Drives. *IEEE Transactions on Energy Conversion*, 18(4):476–483, dec 2003.
- [46] Mateusz Dybkowski and Teresa Orłowska-Kowalska. Application of the stator current-based MRAS speed estimator in the sensorless induction motor drive. In *2008 13th International Power Electronics and Motion Control Conference, EPE-PEMC 2008*, pages 2306–2311, 2008.
- [47] Teresa Orłowska-Kowalska and Mateusz Dybkowski. Stator-current-based MRAS estimator for a wide range speed-sensorless induction-motor drive. *IEEE Transactions on Industrial Electronics*, 57(4):1296–1308, 2010.
- [48] H. Madadi Kojabadi. Simulation and experimental studies of model reference adaptive system for sensorless induction motor drive. *Simulation Modelling Practice and Theory*, 2005.
- [49] Marko Hinkkanen, Lennart Harnefors, and Jorma Luomi. Reduced-order flux observers with stator-resistance adaptation for speed-sensorless induction motor drives. *IEEE Transactions on Power Electronics*, 25(5):1173–1183, 2010.

- [50] Djordje Stojić, Milan Milinković, Slavko Veinović, and Ilija Klasnić. Improved stator flux estimator for speed sensorless induction motor drives. *IEEE Transactions on Power Electronics*, 30(4):2363–2371, 2015.
- [51] Vimlesh Verma and Chandan Chakraborty. New series of MRAS for speed estimation of vector controlled induction motor drive. In *IECON Proceedings (Industrial Electronics Conference)*, 2014.
- [52] A. V. Ravi Teja, V. Verma, and C. Chakraborty. A new formulation of reactive-power-based model reference adaptive system for sensorless induction motor drive. *IEEE Transactions on Industrial Electronics*, 62(11):6797–6808, Nov 2015.
- [53] I. Benlaloui, S. Drid, L. Chrifi-Alaoui, and M. Ouriagli. Implementation of a new mras speed sensorless vector control of induction machine. *IEEE Transactions on Energy Conversion*, 30(2):588–595, June 2015.
- [54] Andrew N. Smith, Shady M. Gadoue, and John W. Finch. Improved rotor flux estimation at low speeds for torque MRAS-based sensorless induction motor drives. *IEEE Transactions on Energy Conversion*, 31(1), 2016.
- [55] Youssef Agrebi Zorgani, Yassine Koubaa, and Mohamed Boussak. MRAS state estimator for speed sensorless ISFOC induction motor drives with Luenberger load torque estimation, 2014.
- [56] Mohamed S. Zaky. Stability analysis of speed and stator resistance estimators for sensorless induction motor drives. *IEEE Transactions on Industrial Electronics*, 59(2):858–870, 2012.
- [57] Marco Tursini, Roberto Petrella, Student Member, and Francesco Parasiliti. Adaptive Sliding-Mode Observer for Speed-Sensorless Control of Induction Motors. *IEEE TRANSACTIONS ON INDUSTRY APPLICATIONS*, 36(5):1380–1387, 2000.
- [58] Cristian Lascu, Ion Boldea, and Frede Blaabjerg. Comparative study of adaptive and inherently sensorless observers for variable-speed induction-motor drives. *IEEE Transactions on Industrial Electronics*, 53(1):57–65, 2006.
- [59] Sea June Oh., Sang Kwun Jeong, Tan Tien Nguyen, Phuc Thinh Doan, and Sang Bong Kim. Sensorless Vector Control of AC Induction Motor Using Sliding-Mode Observer. *International Journal of Science and Engineering*, 4(2):39–43, 2013.

- [60] L. Zhao, J. Huang, H. Liu, B. Li, and W. Kong. Second-order sliding-mode observer with online parameter identification for sensorless induction motor drives. *IEEE Transactions on Industrial Electronics*, 61(10):5280–5289, Oct 2014.
- [61] Mihai Comanescu and Longya Xu. Sliding-mode MRAS speed estimators for sensorless vector control of induction machine. *IEEE Transactions on Industrial Electronics*, 53(1):146–153, 2006.
- [62] Gadoue S ; Giaouris, D ; Finch, J Mras, Sensorless Vector, Shady M Gadoue, Damian Giaouris, and John W Finch. MRAS Sensorless Vector Control of an Induction Motor Using New Sliding-Mode and Fuzzy-Logic Adaptation Mechanisms. *IEEE Transactions on Energy Conversion*, 25(2):394 – 402, 2010.
- [63] Jim Orr, Brandon Murray, and Mihai Comanescu. Design of a second-order sliding mode MRAS speed estimator for the induction motor drive. *2016 IEEE Power and Energy Conference at Illinois, PECE 2016*, 2016.
- [64] Damian Giaouris, J W Finch, S M Gadoue, and D Giaouris. A new fuzzy logic based adaptation mechanism for MRAS sensorless vector control induction motor drives Investigation into the Stability of Complex Power Electronic Converters in Renewable Energy Applications. View project Development of Control Strategies. In *Proceedings of 4th IET International Conference on Power Electronics, Machines and Drives (PEMD 2008), 2008*, pages 179 – 183, 2008.
- [65] Yaman B. Zbede, Shady M. Gadoue, and David J. Atkinson. Model Predictive MRAS Estimator for Sensorless Induction Motor Drives. *IEEE Transactions on Industrial Electronics*, 2016.
- [66] Davood A Khaburi, Ralph Kennel, S Alireza Davari, Davood Arab Khaburi, Fengxiang Wang, and Ralph M Kennel. Using Full Order and Reduced Order Observers for Robust Sensorless Predictive Torque Control of Induction Motors. *IEEE TRANSACTIONS ON POWER ELECTRONICS*, 27(7), 2012.
- [67] Jaroslaw Guzinski and Haitham Abu-Rub. Speed sensorless induction motor drive with predictive current controller. *IEEE Transactions on Industrial Electronics*, 60(2):699–709, feb 2013.
- [68] Youssef Agrebi Zorgani, Yassine Koubaa, and Mohamed Boussak. MRAS state estimator for speed sensorless ISFOC induction motor drives with Luenberger load torque estimation. *ISA Transactions*, 61:308–317, 2016.

- [69] Shuying Yang, Dawei Ding, Xi Li, Zhen Xie, Xing Zhang, and Liuchen Chang. A Novel Online Parameter Estimation Method for Indirect Field Oriented Induction Motor Drives. *IEEE Transactions on Energy Conversion*, 32(4), 2017.
- [70] Ridvan Demir and Murat Barut. Novel hybrid estimator based on model reference adaptive system and extended Kalman filter for speed-sensorless induction motor control. *Transactions of the Institute of Measurement and Control*, 2018.
- [71] Abhisek Pal, Sukanta Das, and Ajit K Chattopadhyay. An Improved Rotor Flux Space Vector Based MRAS for Field-Oriented Control of Induction Motor Drives. *IEEE Transactions on Power Electronics*, 33(6):5131–5141, 2018.
- [72] R. Kumar, S. Das, P. Syam, and A.K. Chattopadhyay. Review on model reference adaptive system for sensorless vector control of induction motor drives. *IET Electric Power Applications*, 9(7):496–511, 2015.
- [73] Kannan Narendra K. S., Parthasarathy. Identification and control of Dynamical Systems Using Neural Networks. *IEEE TRANSACTIONS ON NEURAL NETWORKS*, I(1):4–27, 1990.
- [74] Fu-chuang Chen. Adaptive Control of a Class of Nonlinear Discrete-Time Systems Using Neural Networks. *IEEE Transactions on Automatic Control*, 40(5), 1995.
- [75] M. Godoy Simoes. Neural Network Based Estimation of Feedback Signals for a Vector Controlled Induction Motor Drive. *IEEE Transactions on Industry Applications*, 31(3):620–629, 1995.
- [76] Michael T Wishart and Ronald G Harley. Identification and Control of Induction Machines Using : Artificial Neural Networks. *IEEE Transactions on Industry Applications*, 31(3):612–619, 1995.
- [77] Bimal K Bose and Life Fellow. Neural Network Applications in Power Electronics and Motor Drives — An Introduction and Perspective. *IEEE Transactions on Industrial Electronics*, 54(1):14–33, 2007.
- [78] Azuwien Aida, Wahyu Mulyo, Zainal Alam, Muhd Zin, Sy Yi, and Roslina Mat. Speed Tracking of Indirect Field Oriented Control Induction Motor using Neural Network. *Procedia Technology*, 11(Iceei):141–146, 2013.
- [79] *Neural and Fuzzy Logic Control of Drives and Power Systems*. 2002.

- [80] He Huang, Gang Feng, and Jinde Cao. Robust state estimation for uncertain neural networks with time-varying delay. *IEEE Transactions on Neural Networks*, 19(8):1329–1339, 2008.
- [81] Jinling Liang, Zidong Wang, and Xiaohui Liu. State estimation for coupled uncertain stochastic networks with missing measurements and time-varying delays: The discrete-time case. *IEEE Transactions on Neural Networks*, 20(5):781–793, 2009.
- [82] Dazhi Wang, Renyuan Tang, Hui Jin, and Jie Yang. Sensorless ω -speed control strategy of induction motor based on artificial neural networks. *Proceedings of the World Congress on Intelligent Control and Automation (WCICA)*, 5(6):4467–4471, 2004.
- [83] L. Ben-Brahim and R. Kurosawa. Identification of induction motor speed using neural networks. In *Proceedings of Power Conversion Conference - Yokohama 1993*, pages 689–694. Institute of Electrical and Electronics Engineers Inc., 1993.
- [84] D. Fodor, F. Ionescu, D. Florica, J. P. Six, P. Delarue, D. Diana, and G. Griva. Neural networks applied for induction motor speed sensorless estimation. In *IEEE International Symposium on Industrial Electronics*, volume 1, pages 181–186. IEEE, 1995.
- [85] T J Triggs and Garland Law Publishing. Speed Estimation. *Automotive Engineering and Litigation*, pages p. 95–124, 1996.
- [86] Seong-hwan Kim, Associate Member, Tae-sik Park, and Ji-yoon Yoo. Speed-Sensorless Vector Control of an Induction Motor Using Neural Network Speed Estimation. *IEEE Transactions on Industrial Electronics*, 48(3):609–614, 2001.
- [87] Giribabu D, S.P. Srivastava, and M.K. Pathak. Modified Reference Model for Rotor Flux-Based MRAS Speed Observer Using Neural Network Controller. *IETE Journal of Research*, 65(1):80–95, jan 2019.
- [88] D Giribabu, S P Srivastava, Giribabu Dyanamina, Kumar Pathak, & Satya, Prakesh Srivastava, Mukesh Kumar Pathak, and Satya Prakesh Srivastava. Electric Power Components and Systems. *Electric Power Components and Systems*, 00(00):1–15, 2016.
- [89] Shady M. Gadoue, Damian Giaouris, and John W. Finch. Sensorless control of induction motor drives at very low and zero speeds using neural network flux observers. *IEEE Transactions on Industrial Electronics*, 56(8):3029–3039, 2009.

- [90] Yuksel Oguz and Mehmet Dede. Speed estimation of vector controlled squirrel cage asynchronous motor with artificial neural networks. *Energy Conversion and Management*, 52(1):675–686, 2011.
- [91] Maurizio Cirrincione, Marcello Pucci, Giansalvo Cirrincione, and Gérald André Capolino. An adaptive speed observer based on a new total least-squares neuron for induction machine drives. *IEEE Transactions on Industry Applications*, 42(1):89–104, jan 2006.
- [92] B. Karanayil, M. F. Rahman, and C. Grantham. Investigation of an on-line rotor resistance identification with a new stator resistance observer for induction motor drive using artificial neural networks. *PESC Record - IEEE Annual Power Electronics Specialists Conference*, 4(1):1883–1888, 2003.
- [93] Baburaj Karanayil, Muhammed Fazlur Rahman, and Colin Grantham. Stator and rotor resistance observers for induction motor drive using fuzzy logic and artificial neural networks. *IEEE Transactions on Energy Conversion*, 20(4):771–780, 2005.
- [94] Baburaj Karanayil, Muhammed Fazlur Rahman, Senior Member, and Colin Grantham. Online Stator and Rotor Resistance Estimation Scheme Using Artificial Neural Networks for Vector Controlled Speed Sensorless Induction Motor Drive. 54(1):167–176, 2007.
- [95] E. K. Geetha, T. Thyagarajan, and Vedam Subrahmanyam. Robust speed sensorless induction motor drives. *7th International Conference on Power Electronics, ICPE'07*, 35(2):806–810, 2007.
- [96] Seok Oh Won, Sol Kim, Min Cho Kyu, Gak In Chi, and Eul Yeon Jae. Load variation compensated neural network speed controller for induction motor drives. In *SPEEDAM 2008 - International Symposium on Power Electronics, Electrical Drives, Automation and Motion*, pages 1141–1145. IEEE, jun 2008.
- [97] J. Campbell and M. Sumner. Practical sensorless induction motor drive employing an artificial neural network for online parameter adaptation. *IEE Proceedings: Electric Power Applications*, 149(4):255–260, jul 2002.
- [98] Tien Chi Chen and Tsong Terng Sheu. Model reference robust speed control for induction-motor drive with time delay based on neural network. *IEEE Transactions on Systems, Man, and Cybernetics Part A:Systems and Humans.*, 31(6):746–752, nov 2001.

- [99] Mirosław Wlas, Zbigniew Krzeminski, and Hamid A. Toliyat. Neural-network-based parameter estimations of induction motors. *IEEE Transactions on Industrial Electronics*, 55(4):1783–1794, 2008.
- [100] Besir Dandil. Fuzzy neural network IP controller for robust position control of induction motor drive. *Expert Systems with Applications*, 36(3 PART 1):4528–4534, apr 2009.
- [101] K. Bouhoune, K. Yazid, M. S. Boucherit, and A. Chériti. Hybrid control of the three phase induction machine using artificial neural networks and fuzzy logic. *Applied Soft Computing Journal*, 55:289–301, 2017.
- [102] Oscar Barambones, Aitor J. Garrido, and Izaskun Garrido. Robust speed estimation and control of an induction motor drive based on artificial neural networks. *International Journal of Adaptive Control and Signal Processing*, 22(5):440–464, jun 2008.
- [103] J. S. Meditch. *Stochastic Optimal Linear Estimation and Control*. McGraw Hill Book Company, USA., 1969.
- [104] Dan Simon. Kalman Filtering. *Embedded Systems Programming*, (June):73–79, 2001.
- [105] S. Maiti, C. Chakraborty, Y. Hori, and M. C. Ta. Model reference adaptive controller-based rotor resistance and speed estimation techniques for vector controlled induction motor drive utilizing reactive power. *IEEE Transactions on Industrial Electronics*, 55(2):594–601, Feb 2008.
- [106] A. V. Ravi Teja, Chandan Chakraborty, Suman Maiti, and Yoichi Hori. A new model reference adaptive controller for four quadrant vector controlled induction motor drives. *IEEE Transactions on Industrial Electronics*, 59(10):3757–3767, 2012.
- [107] Vimlesh Verma, Chandan Chakraborty, Suman Maiti, and Yoichi Hori. Speed Sensorless vector controlled induction motor drive using single current sensor. *IEEE Transactions on Energy Conversion*, 28(4):938–950, dec 2013.
- [108] Simon Haykin. *Neural Networks: A Comprehensive Foundation*. Prentice Hall PTR, USA, 1st edition, 1994.